X-Ray Crystallographic Studies of Some Heterocycles and of Cytochrome c_4

Ana Margarida Moreira Leitao de Barros Martins Damas

Doctor of Philosophy
University of Edinburgh
1982

I declare that the work described in this thesis has not been submitted for any other degree and is the original work of the author except where acknowledgement is made by reference. This work was carried out in the Chemistry Department of Edinburgh University under the supervision of Dr. M.M. Harding and Dr. R.O. Gould.

Courses attended include:

Computing (1 week Fortran computing course, given by the staff of the E.R.C.C.)

Introduction to the Cambridge Data Centre, given by Dr. O. Kennard and others.

Chemistry 2h lectures in organic and physical chemistry.

Synchrotron radiation, given by staff of the Daresbury Laboratory of the S.E.R.C.

A new approach to teaching Quantum Mechanics to chemists (5 lectures - Dr. K.P. Lawley)

Electronics and microprocessors (5 lectures - Mr. A. King)

X-Ray Powder Diffraction (10 lectures - Dr. R.O. Gould)

Using the results of crystallography (10 lectures - Dr. R.O. Gould, Dr. A.J. Welch, Dr. M.D. Walkinshaw)

X-Ray Crystallography research seminars (4 years)

ACKNOWLEDGEMENTS

I would like to thank my supervisors, Dr. M.M. Harding and Dr. R.O. Gould, who gave me every help and encouraging enthusiasm in my work. I also thank Dr. M. Walkinshaw, Dr. L. Sawyer, Mr. M. Papiz and Dr. R. Ambler for the very useful discussions we had along this work.

To Dr. C.A. Beevers, always with his joyful and enthusiastic comments on crystallography, I am most grateful.

I am indebted to Dr. M. Paton of the Chemistry Department in Edinburgh for providing the heterocyclic compounds, Dr. H. Watson and Dr. H. Muirhead of the Department of Biochemistry in Bristol and Dr. D. Stuart and Miss R. Todd of the Laboratory of Molecular Biophysics in Oxford for all the help and facilities provided both in collecting and processing the protein data.

Finally, I thank the I.N.I.C. and J.N.I.C.T. in Portugal for their financial support.

Abstract

This study concerns the structure determination by X-ray crystallographic methods of four heterocyclic compounds and Pseudomonas aeruginosa cytochrome c_4 to a resolution of 3.5 Å.

5-Phenyl-2-tricloromethyl-1,3,4-oxathiazole;5-(p-methoxyphenyl)-2-phenyl-2-trifluoromethyl-1,3,4-oxathiazole and 5-(carboxoethyl)-3(methoxyphenyl)isothiazole crystallize in the monoclinic space group $P2_1/c$; 5-(p-methoxyphenyl)-1,3,4-oxathiazol -2-one crystallizes in the triclinic space group $P\bar{1}$.

All these structures were solved using direct methods; nevertheless, for the triclinic crystal, the Patterson function had to be used to get preliminary information. Atomic parameters were refined anisotropically.

The oxathiazole rings are nearly planar with a slight fold across S...O and the bond lengths indicate a localised C=N double bond. The isothiazole ring compared with the oxathiazole ring shows shorter S-C and longer N-C bond lengths and the angle subtended at the S atom is slightly larger.

Cytochrome c_4 crystals belong to the hexagonal space group $P6_522$. $UO_2(NO_3)_2$ and $K_2Pt(NO_2)_4$ heavy atom derivatives were used in this study. The three-dimensional X-ray intensity data for native and derivative crystals were collected on a Nonius CAD-4 diffractometer and on a rotation camera using CuK_α radiation

One electron density map was calculated to a resolution of 5 Å using diffractometer data, and finally another map to a resolution of 3.5 Å was calculated using both diffractometer and rotation camera data. The phases of the Fourier coefficients were determined by the isomorphous replacement method; anomalous dispersion measurements from native and derivative crystals were included in the phase calculations and were also used to find the location of the heavy atom sites.

The probabilistic methods of Chou and Fasman were used to obtain preliminary information on the secondary structure of this molecule; they indicated that it folds in the same way as two small cytochromes c covalently attached to one another. The interpretation of the 5 Å resolution electron density map, has clearly shown cytochrome c_4 as a dimer molecule and the higher resolution electron density map was interpreted using Pseudomonas aeruginosa cytochrome c_{551} as the basic molecular model for each half of the molecule.

Cytochrome c_4 is a di-haem molecule, with 181 amino acids. The overall shape of the molecule is roughly ellipsoidal with dimensions 40 x 52 x 28 Å and the overall "cytochrome fold" has been found twice in this molecule.

CONTENTS

Chapter Two

Cytochrome c_4

Chapter Three

Three Dimensional Structure of Cytochrome c_4 from Pseudomonas aeruginosa at 5 Å resolution

Chapter Four

The cytochrome c_4 three-dimensional structure at 3.5 Å resolution

Reprints: Nitrile Sulphides. Part 1[1]. 1,3-Dipolar cycloaddition to carbonyl groups activated by trihaloalkyl substituents; synthesis and crystal structure of 1,3,4-oxathiazoles.
by A. Margarida Damas, Robert O. Gould, Marjorie M. Harding, R. Michael Paton, John F. Ross and John Crosby
published in J.C.S. Perkin I, 2991-2995, 1981.

Cytochrome c_4 from Pseudomonas aeruginosa.
by L. Sawyer, C.L. Jones, A.M. Damas, M.M. Harding, R.O. Gould and R.P. Ambler,
published in J.Mol.Biol., 153, 831-835, 1981.

CHAPTER ONE

CHAPTER ONE

The Crystal Structure of Some Heterocyclic Compounds

1. The 1,3,4 oxathiazoles

The structures of 5-phenyl-2-trichloromethyl-1,3,4-oxathiazole, 5-(p-methoxyphenyl)-2-phenyl-2-trifluoromethyl-1,3,4-oxathiazole and 5-(p-methoxyphenyl)-1,3,4-oxathiazol-2-one were determined by X-ray analysis.

Several thiazole compounds are already known for their biological activity. They possess mitodepressive , mitostatic, diuretic and schistosomicidal properties[11].

The samples came from Dr. J. Ross and Dr. R.M. Paton who examined the reaction of nitrile sulphides with carbonyl compounds with a view to establishing a new route to 1,3,4-oxathiazole compounds[2].

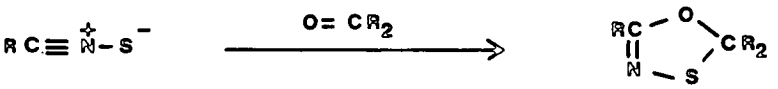

The nitrile sulphides were generated by the thermal decarboxylation of 1,3,4-oxathiazol-2-ones.

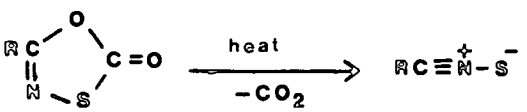

1.1 The crystal structure of 5-phenyl-2-tricloromethyl-1,3,4-oxathiazole (HETCL3)

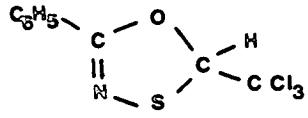

$C_9H_6NOSCl_3$

1.1.1 Preliminary work in the determination of the structure.

The sample was recrystallised by slow cooling, using hexane as solvent.

The shape and reciprocal axes of the crystal are shown below:

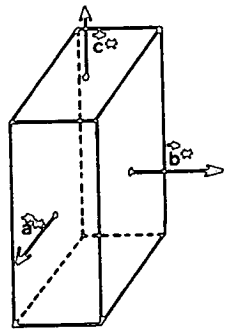

It was birefringent with extinctions oblique to the needle axis.

Oscillation (c and b axes) and Weissenberg (hkO, hk1, and hOl) photographs were taken with CuK_α radiation showing

cell dimensions, crystal system and the space group.

The reflection conditions, indicating the space group $P2_1/a$ (equivalent to $P2_1/c$, no. 14)

(hkl)	none
(hk0)	none
(h0l)	h = 2n
(0kl)	none
(h00)	(h = 2n)
(0k0)	k = 2n
(00l)	none

The density of the crystal, $d_m = 1.55$ g cm^{-3}, was measured by the flotation method, using a mixture of potassium iodide and water. The calculated density based on the molecular weight, cell dimensions and crystal symmetry was $d_c = 1.65$ g cm^{-3}.

Accurate cell dimensions were measured with a Stoë Stadi-2 circle diffractometer using graphite monochromatised MoK_α radiation.

Crystal Data:

Formula: $C_9H_6NOSCl_3$

Molecular Weight: 282.6

Crystal System: monoclinic

Cell Dimensions: a = 11.507 ± 0.008 Å

b = 9.356 ± 0.002 Å

c = 10.560 ± 0.009 Å

$\alpha = \gamma = 90^\circ$; $\beta = 101.460 \pm 0.006^\circ$

Space Group: $P2_1/a$

$Z = 4$

Density: $d_m = 1.55$ g cm^{-3}

$d_c = 1.65$ g cm^{-3}

CuK_α radiation, $\lambda = 1.5418$ Å, $\mu = 88.6$ cm^{-1}

MoK_α radiation, $\lambda = 0.71069$ Å, $\mu = 9.7$ cm^{-1}

1.1.2 Data collection and intensity measurements

For the data collection, a crystal of dimensions 0.2 x 0.2 x 0.7 mm was used.

The intensity data were collected on a Stadi-2 diffractometer, which is controlled by a PDP8 computer. It requires as input: the unit cell dimensions of the crystal, its lattice type, the wavelength of the radiation to be used and the initial orientation of the crystal.

The figure below shows schematically the angles which may be used to bring any defined plane into a reflecting position.

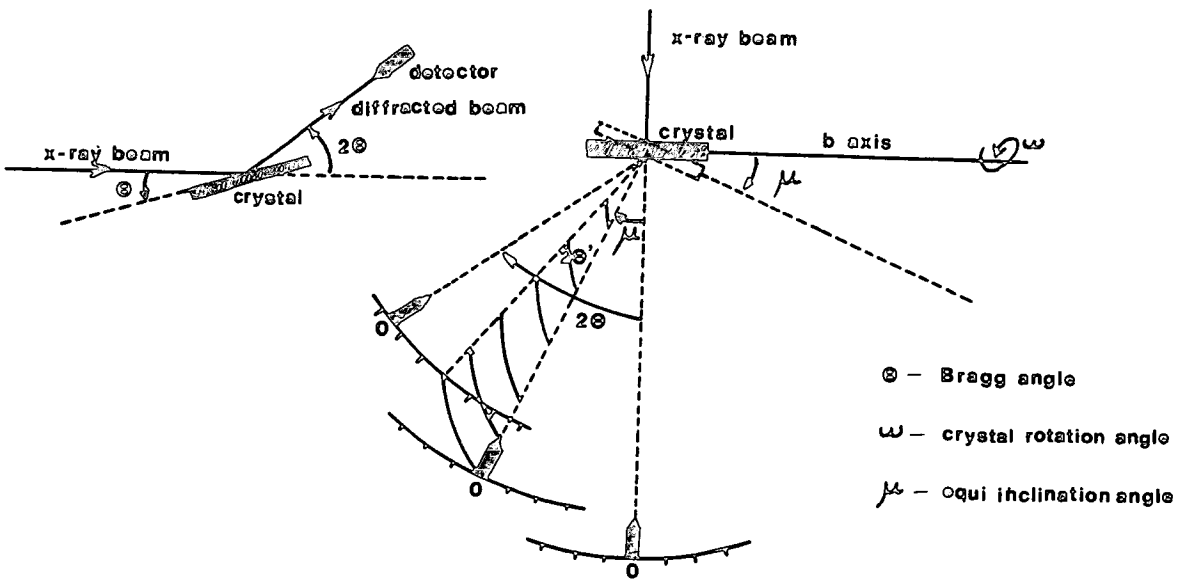

The crystal was mounted along the b axis and the intensities of all (hkl) reflections with positive k and within the range of θ (Bragg angle) from 0 to 25° were measured.

The scan through each peak, consisting of counting the diffracted radiation at intervals of 0.015° in ω was arranged so that half as many counts were made in the background region as in the peak region of each reflection. The scan width was 1.5° in ω and the step scanning time was 0.8 seconds.

The data were obtained from the diffractometer's teletype on paper tape and reduced using a program written by Dr. R.O. Gould. This program subtracts the background measurements from the peak, applies Lorentz and polarization corrections and averages measurements of symmetry equivalent reflections. The net intensity, I, is calculated according to the equation:

$$I = C - \frac{(B_1 + B_2)}{2T_B} T_C$$

where C is the total recorded count in the scan time T_C and B_1, B_2 are background counts for the time T_B each. No absorption corrections were made.

A total number of 3852 reflections were measured. From the agreement of the symmetry equivalent reflections ((hkl)and $(\bar{h}k\bar{l})$), an average relative error in |F| of 0.02 was estimated. The number of unique reflections with $I > 2\sigma(I)$ was 1794.

1.1.3 The solution of the structure

The structure was solved using MULTAN 77 [7], which applies direct methods to the set of normalised structure amplitudes (E's). The observed F values are converted into observed E values according to the formula:

$$E^2(\underline{h}) = F^2(\underline{h})/\langle I \rangle$$

where <I> is the expected intensity for the reflexion $\underline{h}$ and in the case of randomly positioned atoms in the unit cell, the expression for <I> is:

$$\langle I \rangle = K \sum_j f^2(j) \exp(-2B \sin^2\theta/\lambda^2)$$

f(j) being the scattering factor of jth atom, K a scaling factor and B the overall temperature factor.

Using sixteen different starting sets of signs, and generating those of all others with |E| > 1.5, the most consistent set was selected. An electron density map was computed using these signs as coefficients of $E(\underline{h})$. At this stage, the positions of twelve of the fifteen non-hydrogen atoms were found. Then, a difference Fourier was calculated and it showed that the positions of all the atoms, except hydrogens, were nearly right and the residual $R = \frac{\Sigma||F_o| - |F_c||}{\Sigma|F_o|}$ was 0.30. The refinement of the structure was done using the X-RAY 76 system[15]. Three rounds of least squares refinement and one round of three cycles of refinement using isotropic temperature factors brought the R factors down to 0.15.

At this point, the positions of the hydrogen atoms were calculated, and another difference Fourier was computed

to confirm them. With the hydrogen positions and their thermal parameters fixed at U = 0.06 $\AA^2$, another cycle of refinement was computed restricting refinement of hydrogen positions and temperature factors but allowing anisotropic temperature factors for all the Cl, S and C atoms. Other rounds of least squares refinement were computed allowing anisotropic temperature factors for all the atoms except hydrogen and giving each reflection a weight w.

$$w = x \cdot y \ , \ x = 1 \text{ if } \sin\theta > B, \text{ else } x = \sin\theta / B$$

$$y = 1 \text{ if } |F_o| < A, \text{ else } y = A/|F_o|$$

$|F_o|$ is the observed structure factor amplitude; A and B are constants chosen to make the distribution of $w|F_o - F_c|^2$, $|F_c|$ being the calculated structure factor amplitude, nearly constant when analysed in similar sized ranges of $|F_o|$ and $\sin\theta / \lambda$. The values chosen for A and B were 14.0 and 0.4 respectively.

The residual, R, converged to 0.044 for 1588 reflections with $I > 2\sigma(I)$.

The final positional and thermal parameters, bond distances and angles are given in Tables 1.1, 1.2 1.9 and 1.10.

The numbering scheme used in this study is presented in Figure 1.1.

1.1.4 Analysis of the results

Apart from $-CCl_3$ and H(2), the atoms lie almost in two planes. The carbon atoms in the phenyl ring are planar; the maximum deviation of the atoms from the plane being ±0.009 Å. The atoms in the oxathiazole ring are planar within ±0.08 Å; atoms C(21) and H(2) are respectively 1.42 Å and 0.55 Å away from this plane. The acute angle between the two planes is 16.8°.

The C-C bonds in the phenyl ring have a mean of 1.380 Å (mean standard deviation 0.007 Å). The C(2)-C(21) bond length (1.523(6) Å) agrees with the usual value for a single bond length (1.54 Å). The C(6)-C(5) bond length (1.469(6) Å) is shorter than the usual value for a single C-C bond, but agrees with the values found for a single bond between two sp^2 carbons[16]. The C(21)-Cl bond lengths have a mean value of 1.765 Å (mean standard deviation 0.004) which is similar to the values reported by G. Smith *et al* in 1978[14] for the $-CCl_3$ group.

The geometry of the oxathiazole ring is discussed in section 1.4.

The molecular packing in the crystal is illustrated in Figure 1.2. There are no intermolecular contacts less than 3.3 Å involving atoms other than hydrogen.

Figure 1.1 The HETCL3 Molecule

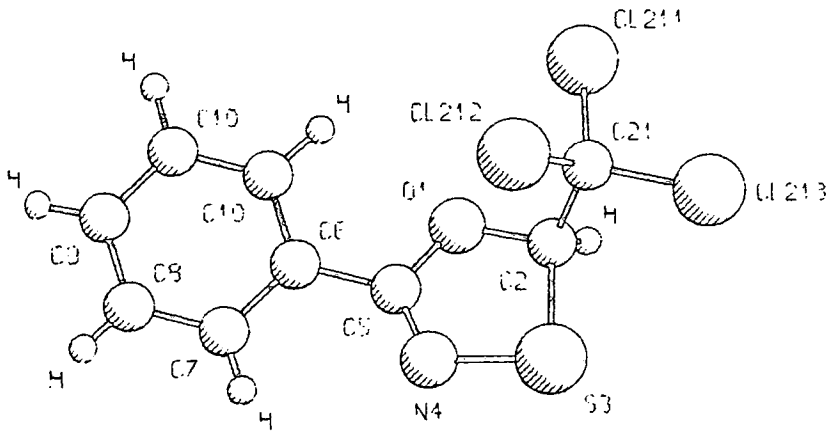

Figure 1.2 The molecular packing in HETCL3

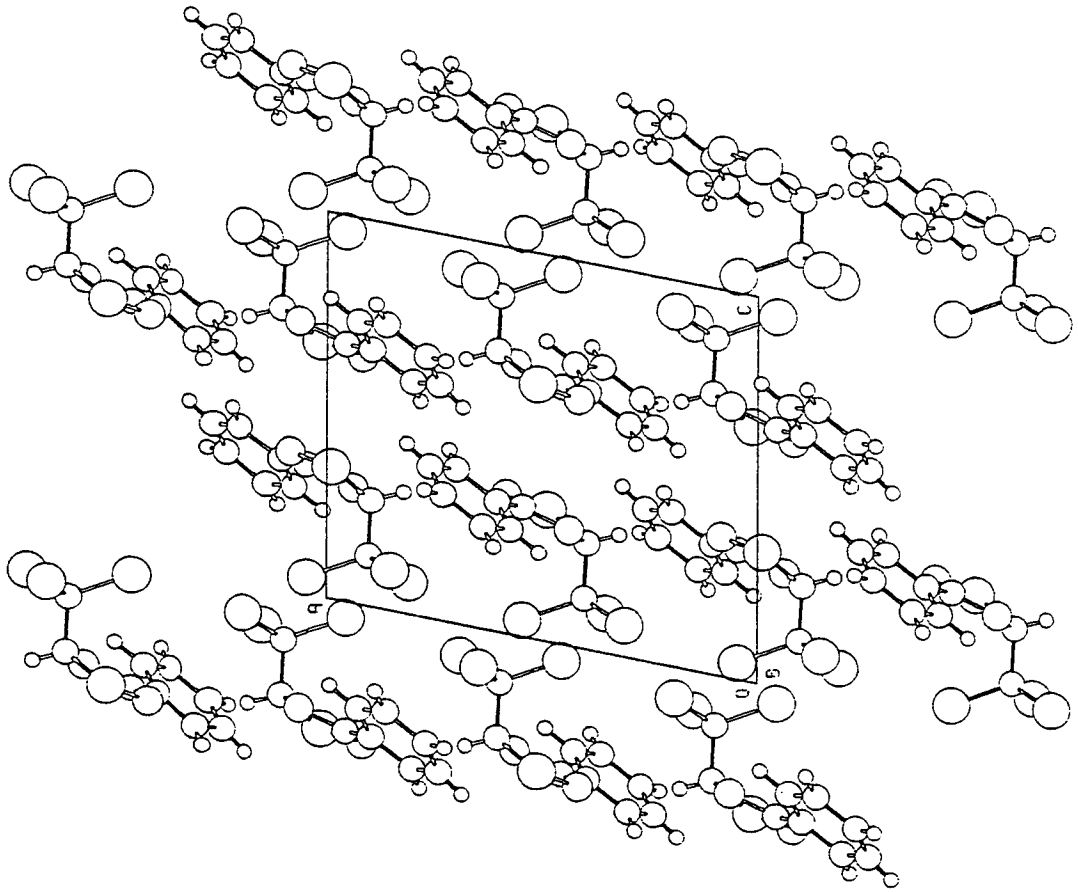

TABLE 1.1 Fractional coordinates for atoms with their standard deviations for HETCL3

Atom	x	y	z
O(1)	0.4381(2)	0.4107(3)	0.2978(3)
C(2)	0.3964(3)	0.2733(4)	0.2736(4)
S(3)	0.4888(1)	0.1488(1)	0.3400(1)
N(4)	0.5838(3)	0.2808(4)	0.3597(4)
C(5)	0.5454(3)	0.4018(4)	0.3344(3)
C(6)	0.6052(3)	0.5394(4)	0.3355(3)
C(7)	0.6999(3)	0.5520(5)	0.3980(4)
C(8)	0.7609(4)	0.6777(7)	0.3920(5)
C(9)	0.7313(5)	0.7922(7)	0.3255(5)
C(10)	0.6382(5)	0.7828(6)	0.2632(5)
C(11)	0.5749(4)	0.6568(5)	0.2700(4)
C(21)	0.4024(3)	0.2550(4)	0.1300(4)
Cl(211)	0.3099(1)	0.3844(1)	0.0806(1)
Cl(212)	0.5457(1)	0.2807(1)	0.0426(1)
Cl(213)	0.3528(1)	0.0820(1)	0.1022(1)
H(2)	0.322 (4)	0.266 (5)	0.311 (4)
H(7)	0.717 (4)	0.477 (5)	0.444 (5)
H(8)	0.815 (4)	0.693 (5)	0.439 (4)
H(9)	0.774 (4)	0.879 (5)	0.329 (5)
H(10)	0.614 (4)	0.867 (5)	0.218 (4)
H(11)	0.509 (4)	0.643 (5)	0.225 (4)

TABLE 1.2 Thermal vibration parameters ($/10^{-3}$ Å^2) for atoms other than hydrogen, with their standard deviations for HETCL3

Atom	U11	U22	U33	U12	U13	U23
O(1)	33(1)	56(1)	65(1)	2(1)	-19(1)	-3(1)
C(2)	31(2)	57(2)	58(2)	-4(1)	-8(1)	3(2)
S(3)	58(1)	57(1)	72(1)	0(1)	-24(1)	14(1)
N(4)	47(1)	70(2)	57(2)	5(2)	-21(2)	5(2)
C(5)	35(2)	65(2)	44(2)	6(2)	-14(2)	-1(2)
C(6)	36(2)	61(2)	46(2)	3(1)	-11(1)	-11(2)
C(7)	49(2)	78(3)	53(2)	5(2)	-22(2)	-13(2)
C(8)	60(2)	102(4)	68(3)	-12(2)	-27(2)	-25(3)
C(9)	75(6)	84(3)	80(3)	-21(3)	-17(2)	-20(3)
C(10)	81(3)	65(3)	75(3)	-10(2)	-19(2)	0(2)
C(11)	52(2)	64(2)	59(2)	-1(2)	-20(2)	-4(2)
C(21)	30(2)	56(2)	59(2)	-5(1)	-13(1)	6(2)
Cl(211)	48(1)	75(1)	83(1)	3(1)	-33(1)	10(1)
Cl(212)	35(1)	85(1)	63(1)	-8(1)	-5(1)	5(1)
Cl(213)	66(1)	61(1)	79(1)	-19(1)	-19(1)	-6(1)

1.2 The crystal structure of 5-(p-methoxyphenyl)-2-phenyl-2-trifluoromethyl-1,3,4-oxathiazole (HETCF3)

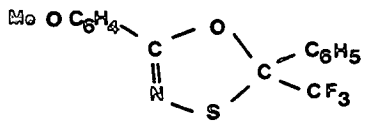

$C_{16}H_{12}NO_2SF_3$

Crystallisation from hexane gave monoclinic prisms showing extinctions parallel to the needle axis when examined with a polarizing microscope.

Similar procedures to the ones described in Section 1.1 were used for solving this structure.

The space group was $P2_1/a$ and a crystal of dimensions 0.15 x 0.20 x 0.25 mm was used for the data collection.

Again, the density was measured by flotation in a mixture of KI/H_2O and it appeared to be in reasonable agreement with the density calculated for Z = 4.

Crystal Data:

Formula:	$C_{16}H_{12}NO_2SF_3$
Molecular weight:	339
Crystal system:	monoclinic
Cell dimensions:	a = 12.282 ± 0.005 Å
	b = 7.311 ± 0.002 Å
	c = 17.181 ± 0.007 Å
	$\alpha = \gamma = 90^\circ$, $\beta = 74.11 \pm 0.03^\circ$
Space group:	$P2_1/a$
Z = 4	

Density: dm = 1.45 g cm^{-3}

dc = 1.52 g cm^{-3}

CuK_α radiation, λ = 1.5418 Å, μ = 23.0 cm^{-1}

MoK_α radiation, λ = 0.71069 Å, μ = 2.6 cm^{-1}

Because the crystals were so small, large errors were introduced in the measured density.

The data was collected on a Stadi-2 diffractometer using MoK_α radiation. The ω-scan method was used with a step width of 1.5° at intervals of 0.015° and a velocity of 3.3 steps sec^{-1}.

The structure was solved by direct methods using the MULTAN system[7]. The largest absolute figure of merit using 200 normalised structure factors indicated the correct solution, and all non-hydrogen atoms could be located in the E-map.

The refinement of the structure was done refining the non-hydrogen atoms with anisotropic temperature factors first and then the hydrogen atoms with isotropic temperature factors. All the reflections were given unit weights.

The R-factor converged to 0.043 for the 1223 reflections with $I > 2\sigma(I)$.

The positional and thermal parameters of the atoms, bond distances and angles are summarized in Tables 1.3, 1.4, 1.9 and 1.10.

Figure 1.3 shows the molecule and the numbering scheme used in this study.

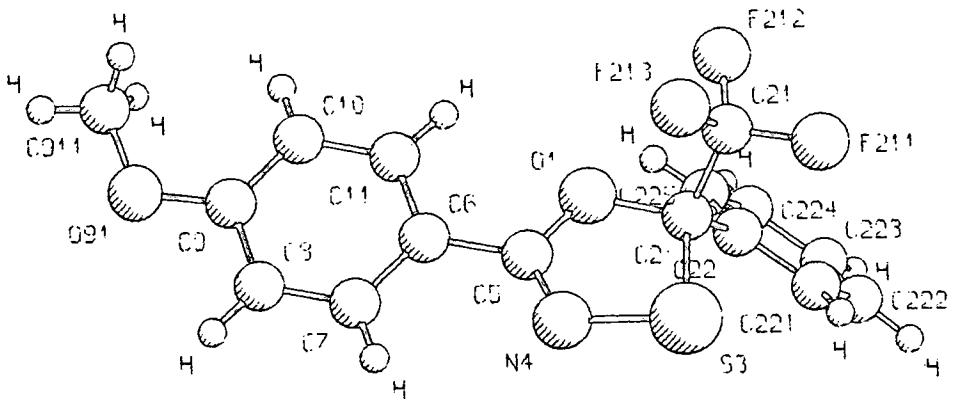

Figure 1.3 The HETCF3 Molecule

The C(21)-F bond lengths have a mean value of 1.327 Å (mean standard deviation 0.007), which agrees with the values reported by O. Didberg *et al*[3] for the $-CF_3$ group.

Analysis of results for the oxathiazole ring is in Section 1.4.

Figure 1.4 shows the molecular packing in the crystal. There are no intermolecular contacts less than 3.3 Å, for non-hydrogen atoms.

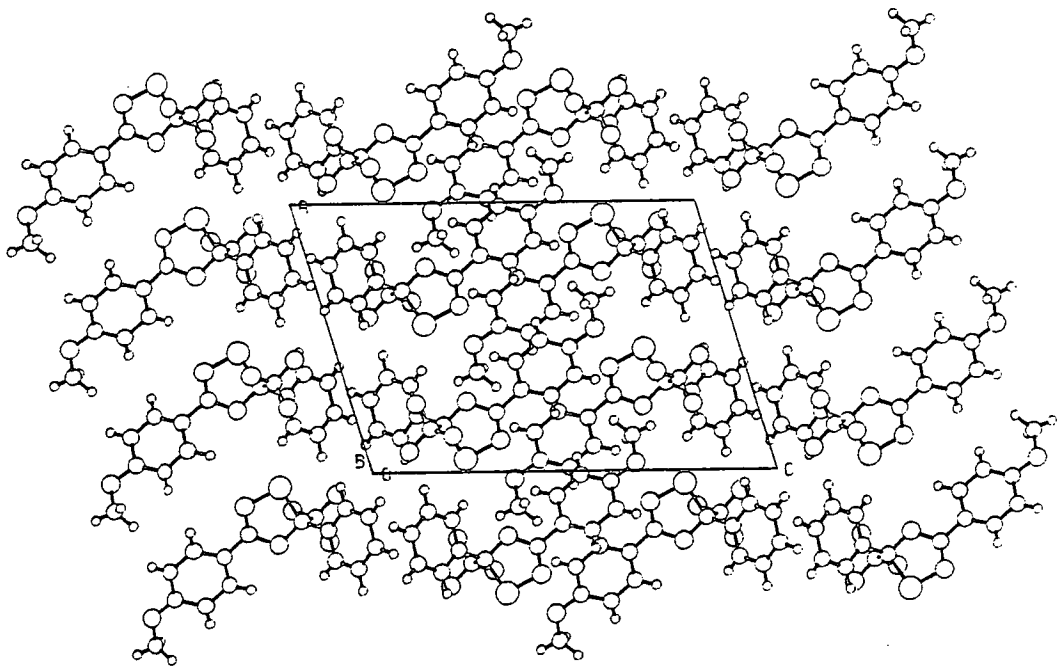

Figure 1.4 The molecular packing in HETCF3

1.2.1 Analysis of the results

The carbon atoms in the phenyl ring bonded to C(2) are planar within ±0.008 Å. Atom C(2) lies 0.02 Å away from this plane.

The maximum deviation of the carbon atoms numbered from C(6) to C(11) from the best plane is 0.01 A°. Atom C(5) is 0.06 Å away from this plane, while O(91) and C(911) are 0.02 Å and 0.13 Å respectively.

The atoms in the oxathiazole ring are planar within ±0.01 Å. Atom C(6) is 0.006 Å away from this plane and C(22) and C(21) are 1.14 Å and 1.32 Å respectively away from the plane.

The angles between the oxathiazole plane and the two planes defined by the phenyl rings are 12.4° and 50.3°.

The C-C bonds in the C(22)...C(225) phenyl ring have a mean value of 1.373 Å (mean deviation 0.009); for the C(6)...C(11) phenyl ring these values are 1.383 Å (0.007).

The C(5)-C(6) bond length (1.458(6) Å) is in agreement with the value found in the previous compound (1.469(6) Å).

TABLE 1.3 Fractional coordinates for atoms with their standard deviations for HETCF3

Atom	x	y	z
O(1)	0.7386(2)	0.3357(5)	0.7154(2)
C(2)	0.8251(4)	0.3504(8)	0.7904(3)
S(3)	0.9512(1)	0.4211(3)	0.7607(1)
N(4)	0.8826(3)	0.4189(7)	0.6614(2)
C(5)	0.7796(4)	0.3743(7)	0.6505(3)
C(6)	0.6960(4)	0.3604(6)	0.5719(3)
C(7)	0.7198(4)	0.4291(7)	0.5028(3)
C(8)	0.6436(4)	0.4114(9)	0.4288(3)
C(9)	0.5408(4)	0.3242(7)	0.4210(3)
C(10)	0.5147(4)	0.2574(7)	0.4892(3)
C(11)	0.5923(4)	0.2776(7)	0.5643(3)
C(21)	0.8387(5)	0.1594(8)	0.8252(3)
F(211)	0.7465(3)	0.0991(5)	0.8415(2)
F(212)	0.8657(3)	0.0400(5)	0.7753(2)
F(213)	0.9230(3)	0.1532(5)	0.8938(2)
C(22)	0.7897(4)	0.4796(7)	0.8472(3)
C(221)	0.8706(5)	0.5705(9)	0.9059(3)
C(222)	0.8387(7)	0.6884(10)	0.9573(4)
C(223)	0.7260(7)	0.7184(9)	0.9508(4)
C(224)	0.6456(6)	0.6279(9)	0.8933(4)
C(225)	0.6772(5)	0.5067(8)	0.8415(3)
O(91)	0.4716(3)	0.3118(5)	0.3445(2)
C(911)	0.3700(6)	0.2127(9)	0.3327(4)

(contd...)

Table 1.3 (contd.)

Atom	x	y	z
H(7)	0.788(4)	0.485(7)	0.508(3)
H(8)	0.663(4)	0.460(3)	0.382(3)
H(10)	0.448(4)	0.205(7)	0.485(3)
H(11)	0.574(4)	0.239(7)	0.614(3)
H(221)	0.950(4)	0.545(7)	0.910(3)
H(222)	0.895(4)	0.757(7)	0.966(3)
H(223)	0.699(4)	0.808(8)	0.990(3)
H(224)	0.564(4)	0.648(7)	0.887(3)
H(225)	0.622(4)	0.452(7)	0.803(3)
H(9111)	0.383(4)	0.089(8)	0.350(3)
H(9112)	0.315(4)	0.271(7)	0.368(3)
H(9113)	0.337(4)	0.207(8)	0.280(3)

TABLE 1.4 Thermal vibration parameters ($/10^{-3}$ Å^2) for atoms other than hydrogen, with their standard deviations for HETCF3

Atom	U11	U22	U33	U12	U13	U23
O(1)	38(2)	70(3)	34(2)	-5(2)	10(2)	2(2)
C(2)	34(3)	58(4)	43(3)	-6(3)	5(2)	6(3)
S(3)	39(1)	109(1)	56(1)	-19(1)	13(1)	-3(1)
N(4)	45(2)	63(3)	52(3)	-3(2)	21(2)	0(2)
C(5)	46(3)	34(3)	46(3)	2(2)	17(2)	1(2)
C(6)	41(2)	29(3)	41(3)	1(2)	16(2)	-1(2)
C(7)	46(3)	41(3)	48(3)	2(3)	23(3)	4(3)
C(8)	55(3)	44(3)	43(3)	3(3)	23(2)	4(3)
C(9)	55(3)	31(3)	43(3)	10(3)	15(2)	0(2)
C(10)	45(3)	32(3)	53(3)	-4(2)	17(3)	1(2)
C(11)	49(3)	33(3)	35(3)	9(2)	17(2)	7(2)
C(21)	55(3)	59(4)	48(3)	7(3)	3(3)	-11(3)
F(211)	74(2)	56(2)	82(2)	-8(2)	21(2)	10(2)
F(212)	100(3)	70(3)	80(2)	19(2)	18(2)	-16(2)
F(213)	77(2)	70(2)	63(2)	14(2)	-10(2)	5(2)
C(22)	48(3)	43(3)	35(3)	-3(3)	11(2)	5(2)
C(221)	53(3)	65(4)	53(3)	-2(2)	3(3)	-7(3)
C(222)	96(5)	63(4)	56(4)	-19(4)	8(4)	-14(4)
C(223)	97(5)	49(4)	65(4)	-5(4)	31(4)	-12(3)
C(224)	69(4)	60(4)	75(4)	3(4)	31(4)	-2(4)
C(225)	48(3)	60(4)	53(3)	-2(3)	11(3)	-5(3)
O(91)	62(2)	55(2)	37(2)	-2(2)	6(2)	5(2)
C(911)	76(4)	46(4)	49(4)	-7(3)	-3(3)	-1(3)

1.3 Structure determination of 5-(p-methoxyphenyl)-1,3,4-oxathiazol -2-one (HETOXY)

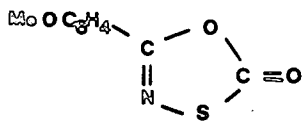

$C_9H_7NO_3S$

A needle-like single crystal elongated along the c axis was examined by X-ray photographic techniques, and shown to be triclinic.

A crystal with dimensions 0.9 x 0.1 x 0.05 mm was used for the data collection.

Crystal Data:

Formula: $C_9H_7NO_3S$

Molecular weight: 209

Crystal System: triclinic

Cell dimensions: $a = 9.856 \pm 0.003$ Å

$b = 10.460 \pm 0.004$ Å

$c = 4.802 \pm 0.002$ Å

$\alpha = 90.82 \pm 0.03^{\circ}$, $\beta = 95.16 \pm 0.03^{\circ}$, $\gamma = 67.16 \pm 0.03^{\circ}$

Space group: $P\bar{1}$ (from solution of structure)

$Z = 2$; $d_c = 1.53$ g cm^{-3}

CuK_α radiation, $\lambda = 1.5418$ Å, $\mu = 29.3$ cm^{-1}

MoK_α radiation, $\lambda = 0.71069$ Å, $\mu = 3.3$ cm^{-1}

The intensities of an hemisphere of the reciprocal lattice with a Bragg angle between 4^{o} and 25^{o} were measured with a Stadi-2 circle diffractometer using graphite-monochromated MoK_{α} radiation.

The ω-scan mode was used with a scan width of 2^{o}, scan speed $0.02^{o}\ s^{-1}$ and background time of 10 s.

The intensities were collected up the c axis and one standard reflection was periodically monitored; no significant change in its intensity was observed.

Lorentz and polarization corrections were applied to 1560 independent reflections. From these reflections, 1187 had a value of $I > 3\sigma(I)$ and 185 reflections were classified as unobserved.

The XRAY system[15] was used to calculate a Patterson map. The location of a S-S vector turned out to be difficult; however, with the geometries of both the oxathiazole and phenyl rings known from the previous two compounds, a model for the molecule was built up in order to help with the interpretation of the map. In this way, it was possible to determine the orientation of a molecule from vectors between the S atom and all the other non-hydrogen atoms of the same molecule.

The whole molecule was input to DIRDIF system[1], assuming one S atom located at the origin and the space group P1. Then, a Fourier input file with all the phases and E values was calculated and input to the MULTAN 77 System[7]

for an improved difference Fourier calculation. The other position of the symmetry related molecule was then clear. The origin was then fixed midway between the two S positions and space group symmetry was used to calculate a new Fourier map.

All atomic coordinates of non-hydrogen atoms were determined and refined by full-matrix least squares methods using the XRAY system[15]. In the later stages of refinement, individual weights, w, were calculated for each reflection, according to the equations:

$$w = (|F_o|/A)^2 \text{ if } |F_o| < A, \qquad \text{else } w = 1$$

where $|F_o|$ is the observed structure factor amplitude and A is a constant set to 9.0. The constant A was adjusted to make the distribution of $w||F_o| - |F_c||^2$, $|F_c|$ being the calculated structure factor amplitude, almost constant with respect to similar sized groups of reflections analysed by ranges of $|F_o|$ and $\sin\theta/\lambda$.

All the hydrogen atoms were assigned isotropic temperature factors fixed at $U = 0.06\ \text{Å}^2$.

The refinement of the scale factor, the coordinates of all the atoms and the anisotropic temperature factors of all non-hydrogen atoms converged to R = 0.041.

Tables 1.5, 1.6, 1.9 and 1.10 show the final positional and thermal parameters, bond lengths and bond angles.

The numbering scheme used in this study is shown in Figure 1.5.

1.3.1 Analysis of the results

Apart from the hydrogen atoms in the methyl group, the molecule is nearly planar. The carbon atoms in the phenyl ring define a plane from which the maximum deviation is ±0.007 Å; atoms O(91), C(911) and C(5) lie respectively 0.01 Å, 0.06 Å and 0.01 Å away from this plane. The atoms in the oxathiazole ring are planar within ±0.005 Å; atoms O(21) and C(6) lie respectively 0.01 Å and 0.02 Å away from it. The acute angle between the two planes is 3.8°.

The mean value for the C-C bond lengths in the phenyl ring is 1.386 Å (mean deviation 0.004). The C(5)-C(6) bond length has a value of 1.457(4) Å, which is in good agreement with the other values found for this bond (1.458(6) Å and 1.469(6) Å). The angles and bond lengths for the methoxyphenyl group are close to the ones found in the previous and similar compounds.

The analysis of the results for the oxathiazole ring is in Section 1.4.

Figure 1.6 shows the molecular packing in the crystal. The only intermolecular contacts involving non-hydrogen atoms less than 3.3 Å are S...O contacts. The intermolecular distance S(3)...O(21') is 3.038(3) Å. Clearly there is no covalent bond between these oxygen and sulphur atoms, since the sum of the covalent radii of sulphur and oxygen is 1.70 Å[12]. However, this contact is less than the sum of the Van der Waals radii[13] of sulphur and oxygen which is 3.25 Å. This suggests that there is probably a weak electrostatic attraction between S(3) and O(21').

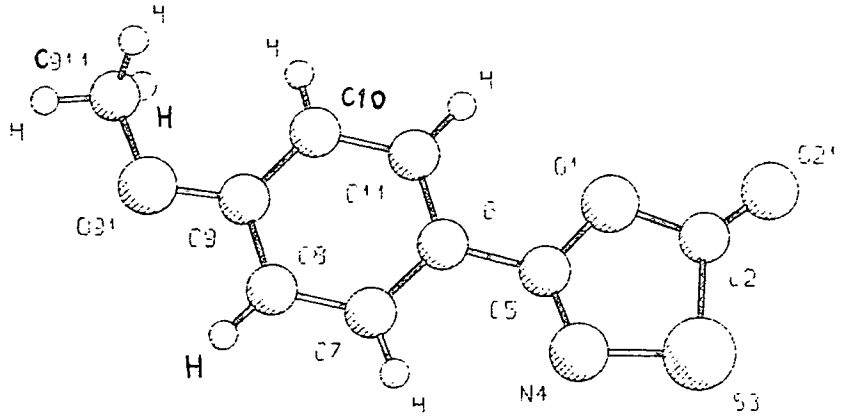

Figure 1.5 The HETOXY molecule

Figure 1.6 The molecular packing in HETOXY

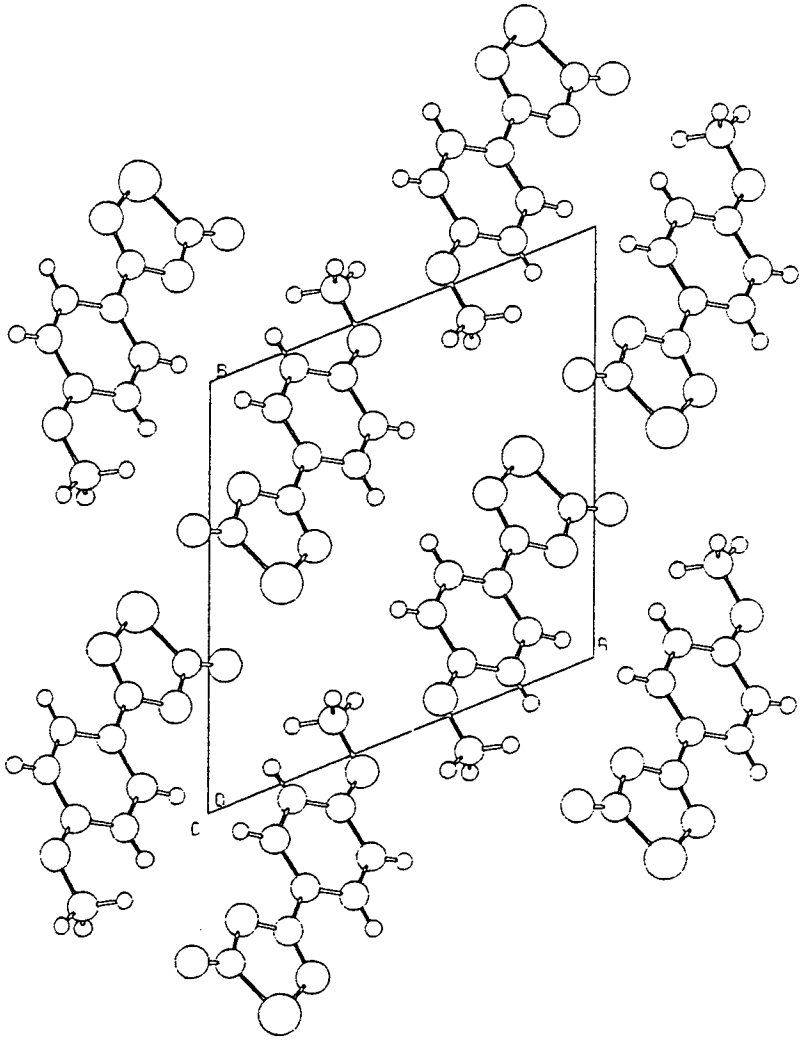

TABLE 1.5 Fractional coordinates for atoms with their standard deviations for HETOXY

Atom	x	y	z
O(1)	0.0876(2)	0.7216(2)	0.1024(4)
C(2)	0.0580(3)	0.6317(3)	0.2725(6)
S(3)	0.1882(1)	0.4653(1)	0.2225(2)
N(4)	0.2728(3)	0.5209(2)	-0.0086(5)
C(5)	0.2084(3)	0.6523(3)	-0.0440(5)
C(6)	0.2527(3)	0.7364(3)	-0.2264(5)
C(7)	0.3795(3)	0.6719(3)	-0.3656(6)
C(8)	0.4235(3)	0.7467(3)	-0.5430(6)
C(9)	0.3435(3)	0.8891(3)	-0.5824(5)
C(10)	0.2178(3)	0.9547(3)	-0.4450(6)
C(11)	0.1727(3)	0.8777(3)	-0.2690(6)
O(21)	-0.0412(2)	0.6712(2)	0.4188(5)
O(91)	0.3987(2)	0.9529(2)	-0.7591(4)
C(911)	0.3234(4)	1.0997(3)	-0.8012(8)
H(7)	0.433 (4)	0.576 (3)	-0.323 (7)
H(8)	0.509 (4)	0.705 (3)	-0.637 (7)
H(10)	0.163 (4)	1.048 (3)	-0.469 (7)
H(11)	0.083 (4)	0.929 (3)	-0.179 (7)
H(9111)	0.321 (4)	1.150 (3)	-0.628 (8)
H(9112)	0.379 (4)	1.124 (3)	-0.931 (7)
H(9113)	0.216 (4)	1.125 (3)	-0.891 (7)

TABLE 1.6 Thermal vibration parameters ($/10^{-3}$ Å^2) for atoms other than hydrogen, with their standard deviations for HETOXY

Atom	U11	U22	U33	U12	U13	U23
O(1)	41(1)	37(1)	46(2)	-9(1)	11(1)	-2(1)
C(2)	44(2)	43(2)	44(2)	-15(2)	8(2)	-3(2)
S(3)	49(1)	37(1)	55(1)	-11(1)	13(1)	3(1)
N(4)	44(2)	37(2)	53(2)	-8(1)	10(2)	2(2)
C(5)	34(2)	39(2)	36(2)	-10(2)	2(2)	-4(2)
C(6)	35(2)	36(2)	36(2)	-9(2)	2(2)	-3(2)
C(7)	38(2)	33(2)	44(2)	-6(2)	6(2)	-1(2)
C(8)	36(2)	41(2)	49(2)	-8(2)	9(2)	-4(2)
C(9)	40(2)	39(2)	38(2)	-14(2)	2(2)	-2(2)
C(10)	40(2)	32(2)	48(2)	-5(2)	3(2)	-2(2)
C(11)	37(2)	39(2)	44(2)	-7(2)	11(2)	-5(2)
O(21)	60(2)	52(2)	13(2)	-15(2)	32(2)	-3(2)
O(91)	41(2)	42(2)	58(2)	-13(1)	14(1)	4(1)

1.4 Discussion and analyses of results

These are probably the first crystal structure determinations of the 1,3,4-oxathiazole ring. In this section, the structure of the oxathiazole ring in compounds HETCL3, HETCF3 and HETOXY (Figure 1.7) is compared and discussed.

Comparison of the bond lengths in the oxathiazole ring (Figure 1.8) in the three compounds with the expected length of single and double bonds, suggests the bond orders given in the last column of Table 1.11.

There are no significant differences in the oxathiazole ring between compounds HETCL3 and HETCF3. Compound HETOXY shows different values for the atoms bonded to C(2) which is now double bonded to an oxygen atom; the C(2)-O(1) bond length is now similar to C(5)-O(1) in all compounds and the S(3)-C(2) bond length (1.744(2) Å) compares well with 1.78 Å found in phenylthiazolidinedione sodium salt (Figure 1.9) by B.W. Matthews[8].

In compounds HETCL3 and HETCF3, the atom C(2) is pyramidal and sp^3 hybridized; the bond angles around the C atom have a mean value of 109°. For the HETOXY compound, the C(2) atom is planar and sp^2 hybridized and the angles around the carbon atom are 107.2°, 122.0° and 130.8°.

Figure 1.7 The 5-phenyl-2-tricloromethyl-1,3,4-oxathiazole (HETCL3), 5-(p-methoxyphenyl)-2-phenyl-2-trifluoromethyl-1,3,4-oxathiazole (HETCF3) and 5-(p-methoxyphenyl)-1,3,4-oxathiazole-2-ones (HETOXY) molecules

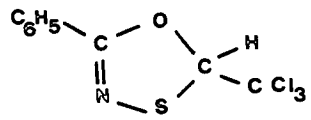

HETCL3

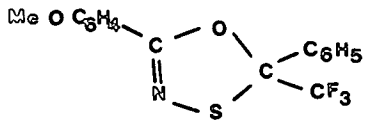

HETCF3

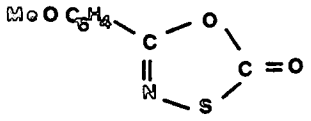

HETOXY

Figure 1.9 The phenylthiazolidinedione sodium salt

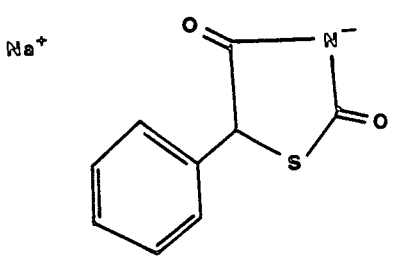

Figure 1.8 The oxathiazole ring

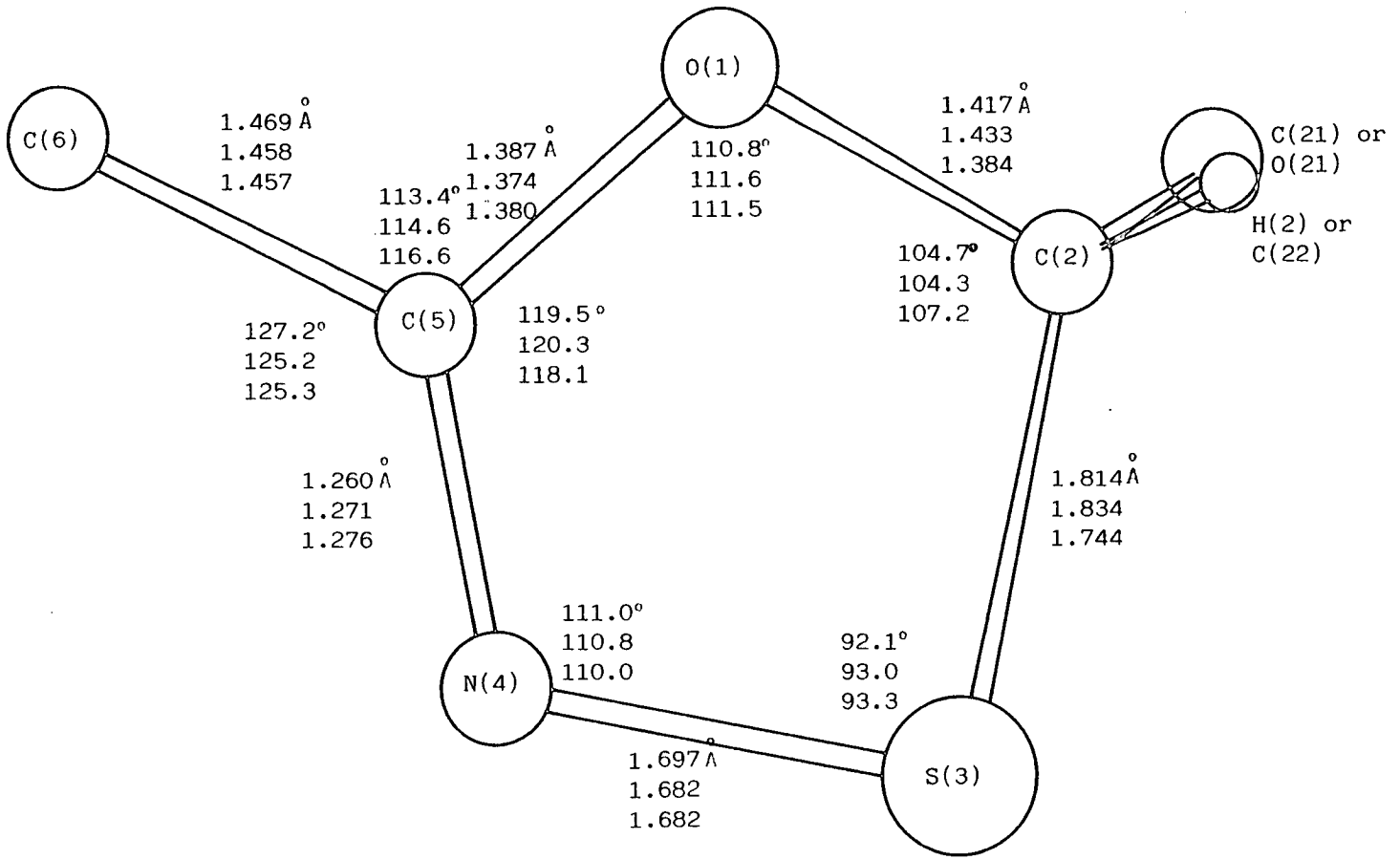

Table 1.11 Comparison of the observed and expected bond lengths in the 1,3,4-oxathiazole ring

Compound	Observed Bond Lengths			Estimated Bond Lengths		Approximate Bond Order		
	HETCL3	HETCF3	HETOXY	Single bond	Double bond	HETCL3	HETCF3	HETOXY
O(1)-C(5)	1.387(4)	1.374(6)	1.380(3)	1.41*	1.22	1	1	1
C(2)-O(1)	1.417(5)	1.433(5)	1.384(4)	1.41*	1.22	1	1	1
S(3)-C(2)	1.814(4)	1.834(6)	1.744(2)	1.83	1.65	1	1	1∿2
N(4)-S(3)	1.697(4)	1.682(4)	1.682(3)	1.66		1	1	1
C(5)-N(4)	1.260(6)	1.271(6)	1.276(3)	1.47	1.28	2	2	2

* Generally this bond is shorter when the C atom is double bonded to another atom.

The bond lengths are consistent with a localised C=N double bond.

The oxathiazole rings are nearly planar with a very slight fold across S...O. In compound HETCL3 the maximum deviation from the best plane of the five ring atoms is 0.08 Å, in compound HETCF3 is 0.01 Å and in HETOXY is 0.005 Å. Figure 1.10 shows the deviations from the best plane of atoms O(1), C(2), S(3), N(4) andC(5).

Figure 1.10 Deviations of the oxathiazole ring atoms from the best plane.

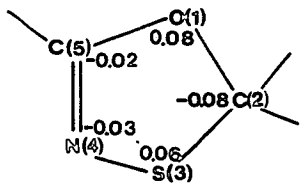

HETCL3

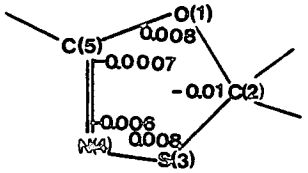

HETCF3

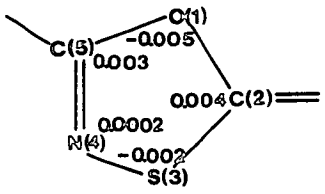

HETOXY

The phenyl ring is not coplanar with the five membered ring; the torsion angle C(7)-C(6)-C(5)-N(4) is respectively 16.7°, 12.0° and 3.3° for HETCL3, HETCF3 and HETOXY.

2. Structure determination of 5-(carboxoethyl)-3(methoxyphenyl) isothiazole (HETCET)

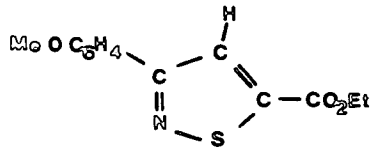

$C_{13}H_{13}NO_3S$

The structure of this compound was determined by X-ray diffraction in order to know the bond lengths and orientation of the five membered ring.

The crystals were obtained from Dr. J.F. Ross and Dr. R.M. Paton and a needle-like single crystal was examined by X-ray photographic techniques.

The space group was $P2_1/c$ and the intensity data were collected on a CAD-4 diffractometer with CuK_α radiation using a crystal with dimensions 1.1 x 0.2 x 0.04 mm.

I would like to thank the Physics Department of the University of Edinburgh for all the facilities provided for the data collection.

Crystal Data:

Formula: $C_{13}H_{13}NO_3S$

Molecular weight: 263

Crystal system: monoclinic

Cell dimensions: a = 13.803 ± 0.005 Å

b = 8.156 ± 0.007 Å

c = 12.380 ± 0.002 Å

$\alpha = \gamma = 90^{\circ}$, $\beta = 67.63 \pm 0.002$ Å

Space group: $P2_1/c$

Z = 4

Density: dm = 1.23 g cm^{-3}

dc = 1.36 g cm^{-3}

CuK_α radiation , $\lambda = 1.5418$ Å, $\mu = 21.8$ cm^{-1}

MoK_α radiation, $\lambda = 0.71069$ Å, $\mu = 2.5$ cm^{-1}

A total number of 1178 independent reflections were recorded within the range $2^{\circ} < 2\theta < 42^{\circ}$, but only 766 of these had $I > 2\sigma(I)$. The data were corrected for Lorentz and polarization effects but not for absorption.

The structure was solved using the MULTAN system[7]. The solution of the structure was based on 250 reflections with the largest E-values. The E-map corresponding to the solution with the best figure of merit revealed all non-hydrogen atoms.

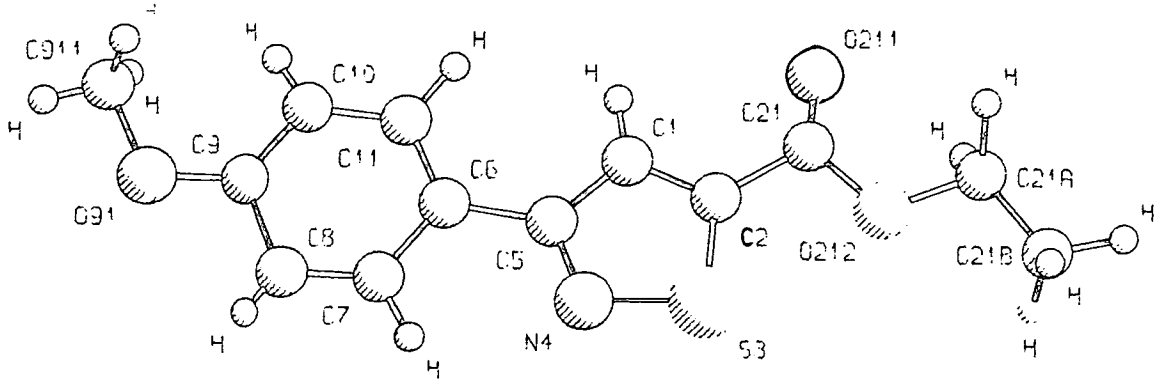

Figure 1.11 The HETCET molecule

The refinement of the structure was carried out using the XRAY system[15]. Reflections with very large structure factor amplitudes were weighted down and isotropic thermal parameters for all hydrogen atoms were fixed at U = 0.06 $\AA^2$, while non-hydrogen atoms were allowed to vibrate anisotropically. The refinement converged to a final R = 0.053.

Tables 1.7, 1.8, 1.9 and 1.10 show the final atomic positions, thermal parameters, bond lengths and bond angles.

Figure 1.11 shows the molecule and the numbering scheme used in this study. This was chosen in order to permit an easy comparison with the previous crystal structures.

2.1 Analysis and discussion of results

The carbon atoms of the phenyl ring define a plane within ±0.002 $\AA$. The mean value for the C-C bond lengths in this ring is 1.380 $\AA$ with a mean standard deviation of 0.020 $\AA$.

Another plane making an angle of 6.3° with the latter is defined by the five membered ring. Figure 1.12 shows the deviations of each atom from the plane; a slight bend is noticed through N(4)...C(2).

Figure 1.12 The deviations of the isothiazole ring atoms

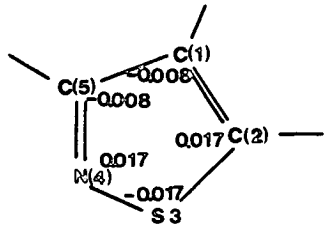

The bond lengths and angles in the isothiazole ring are presented in Figure 1.13.

Figure 1.13 Bond lengths and angles in the isothiazole ring

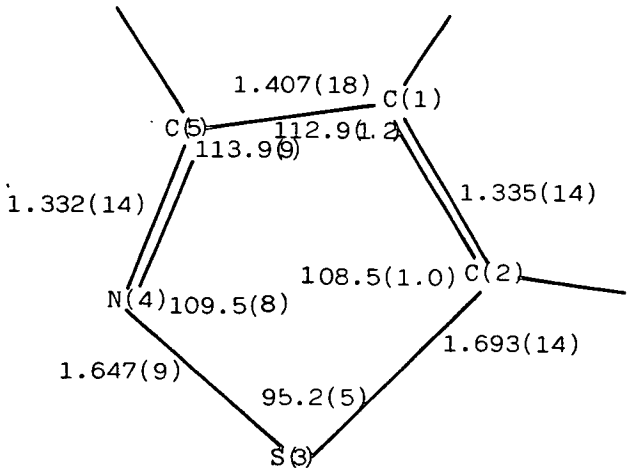

Table 1.12 gives a comparison of these bond lengths and the angle subtended at the sulphur atom with the values for the oxathiazole ring and the values reported for the 3-hydroxy-5-(methyl-sulphonyl)-4-phenylisothiazole (A)[9] and 4-hydroxymethylisothiazole-3-carboxylic acid (B)[6]. These two compounds are presented in Figure 1.14.

Figure 1.14 The 3-hydroxy-5-(methyl-sulphonyl)-4-phenyl-isothiazole (A) and 4-hydroxymethylisothiazole-3-carboxylic acid (B) molecules

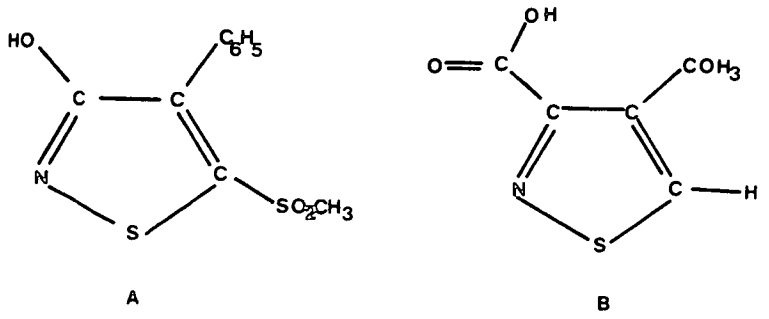

Table 1.12 Bond lengths (Å) and sulphur angle of the isothiazole ring and comparison with values in the oxathiazole ring

Bond	Present Work	(A)	(B)	oxathiazole ring (mean)
S(3)-N(4)	1.647(9)	1.661(7)	1.655(2)	1.687
S(3)-C(2)	1.693(14)	1.715(8)	1.704(2)	1.799
N(4)-C(5)	1.332(14)	1.316(10)	1.303(3)	1.269
C(5)-C(1)	1.407(18)	1.397(11)	1.435(3)	
C(1)-C(2)	1.335(14)	1.380(11)	1.350(3)	
[N(4)-S(3)-C(2)]	95.2(5)°	93.3°	95.5°	92.7°

A good agreement is found between the values reported for the isothiazole ring system and it is noticeable a longer S-C bond length and a shorter N-C bond length in the oxathiazole ring system.

Considerations of the ring geometry (Figure 1.13) and comparison of the bond lengths with the usual values for single and double-bond lengths (C-C 1.54 Å; C=C 1.33 Å; C-N 1.47 Å; C=N 1.28 Å; C-S 1.83 Å; C=S 1.65 Å; S-N 1.66 Å) suggests that considerable π-electron delocalization is found through the ring system.

Figure 1.15 shows the molecular packing in the crystal. No intermolecular distances not involving H-atoms less than 3.2 Å were found.

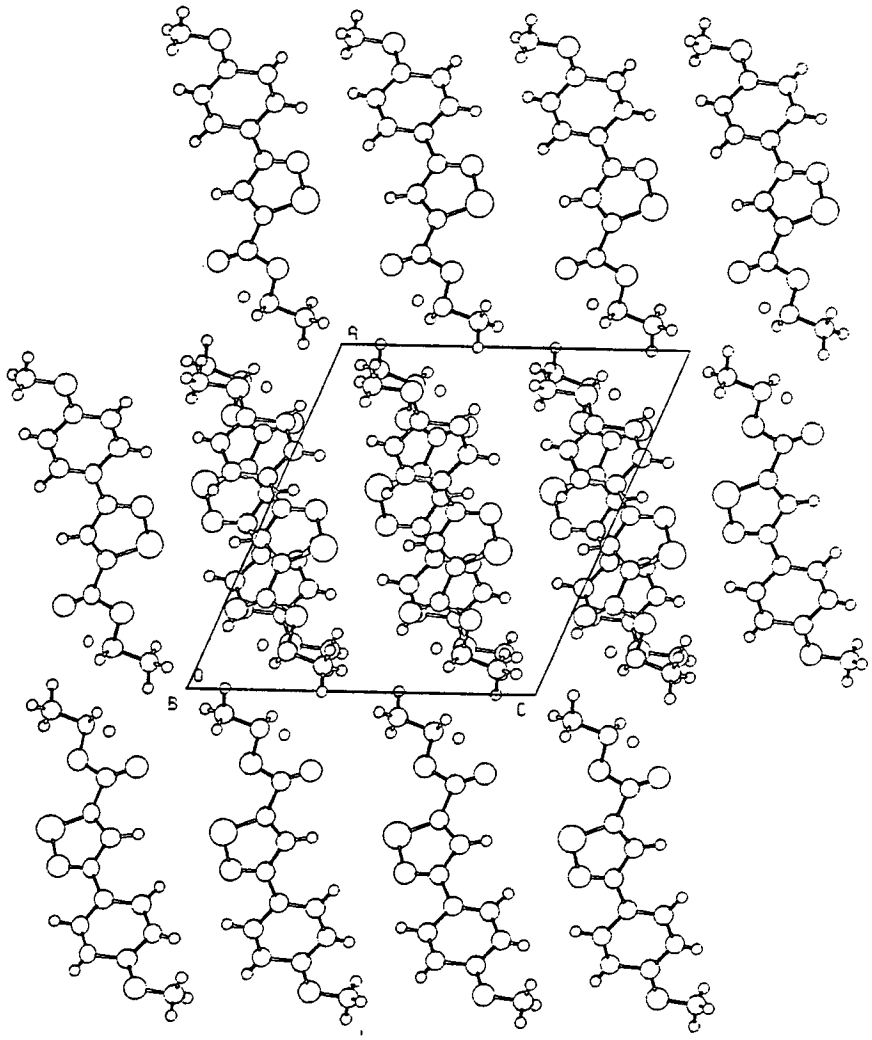

Figure 1.15 The molecular packing in HETCET

TABLE 1.7 Fractional coordinates for atoms with their standard deviations for HETCET

Atom	x	y	z
C(1)	0.5651(9)	0.1965(16)	0.9882(10)
C(2)	0.6354(9)	0.1152(15)	0.8991(9)
S(3)	0.5884(3)	0.0972(5)	0.7917(3)
N(4)	0.4809(7)	0.2036(12)	0.8601(7)
C(5)	0.4772(8)	0.2466(14)	0.9654(9)
C(6)	0.3881(9)	0.3467(12)	1.0402(9)
C(7)	0.3108(10)	0.3975(17)	1.0002(10)
C(8)	0.2296(10)	0.4930(18)	1.0691(9)
C(9)	0.2176(9)	0.5328(15)	1.1816(9)
C(10)	0.2920(10)	0.4801(15)	1.2244(10)
C(11)	0.3744(9)	0.3840(15)	1.1537(9)
C(21)	0.7373(8)	0.0451(15)	0.8916(11)
O(211)	0.7696(6)	0.0519(12)	0.9690(7)
O(212)	0.7872(6)	-0.0224(11)	0.7864(7)
C(21A)	0.8879(10)	-0.1035(20)	0.7684(12)
C(21B)	0.9277(10)	-0.1616(21)	0.6487(11)
O(91)	0.1336(7)	0.6293(11)	1.2443(7)
C(911)	0.1182(12)	0.6636(23)	1.3602(12)
H(1)	0.577(7)	0.215(12)	1.055(8)
H(7)	0.323(7)	0.364(12)	0.921(8)
H(8)	0.181(7)	0.511(12)	1.041(8)
H(10)	0.278(7)	0.518(12)	1.299(8)
H(11)	0.428(7)	0.336(11)	1.189(8)
H(21A1)	0.923(8)	0.002(13)	0.783(8)
H(21A2)	0.871(7)	-0.187(12)	0.847(8)

(contd..)

Table 1.7 (contd..)

Atom	x	y	x
H(21B1)	0.941(7)	-0.067(13)	0.588(8)
H(21B2)	1.002(8)	-0.227(12)	0.620(8)
H(21B3)	0.882(8)	-0.249(12)	0.643(8)
H(9111)	0.108(8)	0.552(13)	1.406(8)
H(9112)	0.166(8)	0.727(13)	1.369(9)
H(9113)	0.057(8)	0.714(12)	1.387(9)

TABLE 1.8 Thermal vibration parameters ($/10^{-3}$ Å^2) for atoms other than hydrogen, with their standard deviations for HETCET

Atom	U11	U22	U33	U12	U13	U23
C(1)	47(11)	72(13)	41(10)	-16(9)	-14(9)	14(9)
C(2)	52(10)	70(12)	43(9)	2(10)	-19(8)	2(9)
S(3)	78(4)	105(4)	43(3)	12(3)	-30(2)	-14(3)
N(4)	71(9)	79(10)	52(9)	18(8)	-33(8)	-21(7)
C(5)	47(9)	73(12)	38(9)	-7(8)	-22(7)	3(8)
C(6)	58(9)	40(11)	46(9)	-12(8)	-26(7)	3(7)
C(7)	66(11)	93(14)	43(10)	-2(12)	-23(10)	-18(12)
C(8)	69(12)	110(17)	42(10)	-16(12)	-35(10)	6(11)
C(9)	43(10)	69(12)	55(10)	0(9)	-18(9)	2(10)
C(10)	69(12)	64(13)	40(9)	-4(11)	-14(10)	-9(10)
C(11)	61(11)	74(13)	32(8)	0(10)	-24(8)	6(9)
C(21)	47(11)	78(14)	54(11)	-10(10)	-16(9)	0(10)
O(211)	67(7)	121(11)	61(7)	8(7)	-29(6)	-5(8)
O(212)	57(7)	94(9)	58(7)	-1(7)	-19(6)	-5(7)
C(21A)	55(12)	86(16)	76(13)	5(13)	-15(10)	4(14)
C(21B)	47(12)	107(18)	61(12)	7(11)	6(10)	-17(13)
O(91)	78(8)	114(11)	52(7)	21(8)	-26(6)	-7(7)
C(911)	69(17)	123(25)	63(15)	8(17)	-13(13)	-14(16)

TABLE 1.9 Interatomic distances and their standard deviations for compounds HETCL3, HETCF3, HETOXY and HETCET. (In this Table, X is Cl in HETCL3 and F in HETCF3)

Bond	Bond Length/Å			
	HETCL3	HETCF3	HETOXY	HETCET
O(1)-C(2)	1.417(5)	1.433(5)	1.384(4)	
C(1)-C(2)				1.335(15)
C(2)-S(3)	1.814(4)	1.834(6)	1.744(2)	1.693(14)
S(3)-N(4)	1.697(4)	1.682(4)	1.682(3)	1.648(9)
N(4)-C(5)	1.260(5)	1.271(6)	1.276(3)	1.332(15)
C(5)-O(1)	1.387(4)	1.374(6)	1.380(3)	
C(5)-C(1)				1.408(18)
C(5)-C(6)	1.469(6)	1.458(6)	1.457(4)	1.472(14)
C(6)-C(7)	1.400(6)	1.392(7)	1.395(4)	1.399(20)
C(7)-C(8)	1.369(8)	1.363(6)	1.369(5)	1.365(17)
C(8)-C(9)	1.364(9)	1.388(7)	1.395(4)	1.377(17)
C(9)-C(10)	1.380(9)	1.386(8)	1.384(4)	1.391(20)
C(10)-C(11)	1.385(7)	1.386(6)	1.388(5)	1.384(16)
C(11)-C(6)	1.383(6)	1.384(7)	1.386(3)	1.379(16)
C(2)-C(21)	1.523(6)	1.510(8)		1.488(18)
C(2)-O(21)			1.193(4)	
C(21)-X(211)	1.774(4)	1.339(6)		
C(21)-X(212)	1.759(3)	1.315(7)		
C(21)-X(213)	1.762(4)	1.328(7)		
C(21)-O(211)				1.203(18)
C(21)-O(212)				1.338(14)

Table 1.9 (contd..)

	HETCL3	HETCF3	HETOXY	HETCET
O(212)-C(21A)				1.478(17)
C(21A)-C(21B)				1.449(19)
C(2)-C(22)		1.506(8)		
C(22)-C(221)		1.377(7)		
C(221)-C(222)		1.366(10)		
C(222)-C(223)		1.375(12)		
C(223)-C(224)		1.362(9)		
C(224)-C(225)		1.385(10)		
C(225)-C(22)		1.373(8)		
C(9)-O(91)		1.359(5)	1.358(4)	1.371(13)
O(91)-C(911)		1.408(8)	1.431(4)	1.396(18)
C(1)-H(1)				0.91(11)
C(2)-H(2)	0.88(5)			
C(7)-H(7)	0.90(5)	0.91(5)	0.95(3)	0.97(10)
C(8)-H(8)	0.88(5)	0.96(5)	0.94(3)	0.88(11)
C(9)-H(9)	0.96(5)			
C(10)-H(10)	1.01(5)	0.89(5)	0.91(3)	0.92(10)
C(11)-H(11)	1.00(5)	0.98(6)	0.97(3)	1.06(11)
C(21A)-H(21A1)				1.04(11)
C(21A)-H(21A2)				1.14(10)
C(21B)-H(21B1)				1.04(10)
C(21B)-H(21B2)				1.09(10)
C(21B)-H(21B3)				0.97(11)
C(221)-H(221)		0.98(5)		
C(222)-H(222)		0.95(5)		
C(223)-H(223)		1.05(6)		
C(224)-H(224)		0.99(5)		
C(225)-H(225)		0.90(5)		
C(911)-H(911)		0.95(6)	0.98(4)	1.05(11)
C(911)-H(9112)		1.11(6)	0.96(4)	0.87(12)
C(911)-H(9113)		0.89(5)	1.04(4)	0.88(10)

TABLE 1.10 Bond angles between non-hydrogen atoms and their standard deviations for HETCL3, HETCF3, HETOXY and HETCET compounds (Here X is Cl in HETCL3 and F in HETCF3)

Angle	Bond Angles/degrees			
	HETCL3	HETCF3	HETOXY	HETCET
C(5)-O(1)-C(2)	110.8(3)	111.6(3)	111.5(2)	
C(5)-C(1)-C(2)				112.9(1.2)
O(1)-C(2)-S(3)	104.7(3)	104.3(3)	107.2(2)	
C(1)-C(2)-S(3)				108.5(1.0)
C(2)-S(3)-N(4)	92.1(2)	93.0(2)	93.3(1)	95.2(5)
S(3)-N(4)-C(5)	111.0(3)	110.8(4)	110.0(2)	109.5(8)
N(4)-C(5)-O(1)	119.5(3)	120.3(4)	118.1(3)	
N(4)-C(5)-C(1)				113.9(9)
N(4)-C(5)-C(6)	127.2(3)	125.2(5)	125.3(2)	118.3(1.1)
C(6)-C(5)-O(1)	113.4(3)	114.6(4)	116.6(2)	
C(6)-C(5)-C(1)				127.7(1.1)
C(5)-C(6)-C(7)	119.9(4)	120.3(4)	118.6(2)	
C(5)-C(6)-C(11)	121.6(3)	120.9(4)	122.4(2)	
C(7)-C(6)-C(11)	118.4(4)	118.8(4)	118.9(3)	117.9(1.0)
C(6)-C(7)-C(8)	120.0(4)	120.7(5)	120.6(2)	120.3(1.2)
C(7)-C(8)-C(9)	121.1(5)	120.5(5)	120.2(3)	121.3(1.4)
C(8)-C(9)-C(10)	120.1(5)	119.7(4)	119.9(3)	119.4(1.0)
C(8)-C(9)-O(91)		115.8(5)	115.2(2)	117.3(1.2)
C(10)-C(9)-O(91)		124.5(5)	124.9(2)	123.3(1.0)
C(9)-C(10)-C(11)	119.4(5)	119.4(5)	119.4(2)	118.8(1.1)
C(10)-C(11)-C(6)	121.0(4)	120.9(5)	120.9(2)	122.1(1.3)
O(1)-C(2)-C(21)	110.1(3)	105.1(4)		
O(1)-C(2)-O(21)			122.0(2)	
C(1)-C(2)-C(21)				127.9(1.2)

Table 1.10 (contd..)

	HETCL3	HETCF3	HETOXY	HETCET
O(1)-C(2)-C(22)		110.8(4)		
S(3)-C(2)-C(21)	113.8(3)	111.3(4)		123.6(8)
S(3)-C(2)-O(21)			130.8(3)	
S(3)-C(2)-C(22)		114.7(4)		
C(21)-C(2)-C(22)		110.1(4)		
C(2)-C(21)-X(211)	108.0(2)	110.8(4)		
C(2)-C(21)-X(212)	111.4(3)	112.7(5)		
C(2)-C(21)-X(213)	108.6(3)	111.9(5)		
X(211)-C(21)-X(212)	109.0(2)	107.7(5)		
X(211)-C(21)-X(213)	109.6(2)	106.1(5)		
X(212)-C(21)-X(213)	110.2(2)	107.4(5)		
C(2)-C(21)-O(211)				124.2(1.0)
C(2)-C(21)-O(212)				110.0(1.2)
O(211)-C(21)-O(212)				125.8(1.1)
C(21)-O(212)-C(21A)				115.9(1.1)
O(212)-C(21A)-C(21B)				105.6(1.3)
C(2)-C(22)-C(221)		119.9(5)		
C(2)-C(22)-C(225)		120.5(4)		
C(221)-C(22)-C(225)		119.5(5)		
C(22)-C(221)-C(222)		120.1(6)		
C(221)-C(222)-C(223)		120.6(6)		
C(222)-C(223)-C(224)		119.7(7)		
C(223)-C(224)-C(225)		120.1(6)		
C(224)-C(225)-C(22)		120.0(5)		
C(9)-O(91)-C(911)		117.9(4)	117.6(2)	117.6(1.1)

REFERENCES

1. Beurskens, P.T., Bosman, W.P., Doesburg, H.M., Gould, R.O., van den Hark, T.E.M., Prick, P.A.Y., Beursken, G., and Parthasarathi, V., "Dirdif, Direct Methods for Difference Structure Factors", Technical Report 1981/82, Crystallography Laboratory, University of Nijmegen.

2. Damas, A.M., Gould, R.O., Harding, M.M., Paton, R.M., Ross, J.F., J.C.S. Perkin I, 2991-2995, 1981.

3. Didberg O., Campsteyn, H., Spirlet, M.R., Dupont, L., Lamotte, J., Vermeire, M., Acta Cryst., B35, 1496-1497, 1979.

4. Germain, G., Main, P., Woolfson, M.M., Acta Cryst., A27, 368-376, 1971.

5. Hudson, P., Robertson, J.H., Acta Cryst., 17, 1497-1505, 1964.

6. Koster, W.H., Dolfini, J.E., Toeplitz, B., Gougoutas, J.Z., J.Org.Chem., 43, 79-82, 1978.

7. Main, P., Lessinger, L., Woolfson, M.M., Germain, G., Declercq , J.P., "MULTAN. A System of Computer Programs for the automatic solution of crystal structures from X-ray diffraction data", University of York, England, and Louvain, Belgium, 1977.

8. Matthews, B.W., Acta Cryst., 17, 1413-1420, 1964.

9. McVicars, J.L., MacKay, M.F., Davis, M., J.C.S. Perkin II, 1332-1334, 1977.

10. Motherwell, W.D.S., "Pluto. A program for plotting molecular and crystal structures", University Chemical Laboratory, Cambridge, England.

11. "Organic compounds of sulphur, selenium and tellurium" The Chemical Society, Burlington House, London, 1973, Vol. 2, pp. 613.

12. Pauling, L., "The nature of chemical bond", 3rd Ed., Cornell University Press, Ithaca, N.Y., 1960, pp. 224.

13. Pauling, L., Ref.12, pp. 260.

14. Smith, G., Kennard, C.H., White, A.H., Acta Cryst., B34, 3113-3115, 1978.

15. Stewart, J.M., Machin, P.A., Dickinson, C., Ammon, H.L., Heck, H., Flack, H., "The XRAY 76 system", Tech.Rep. TR-446. Computer Science Center, University of Maryland, U.S.A., 1976.

16. Sundaralingam, M., Jensen, L.H., Acta Cryst., 18, 1053-1058, 1965.

CHAPTER TWO

CHAPTER TWO

Cytochrome c_4

1 Introduction

Cytochromes c are proteins very widely distributed among living organisms. They are important parts of the respiratory systems and several cytochromes are believed to pass on electrons to cytochrome oxidase in aerobic respiration or to cytochrome reductase in nitrate or sulphate respiration[2].

Respiration is a process in which an organic molecule is oxidized with hydrogen atoms being removed and transferred to an oxidant (molecular oxygen, nitrate or sulphate). In any case, electrons must flow and proteins must be present to accept the electrons and pass them along the chain[21,22,24].

Cytochromes c contain one or more haem groups covalently attached to the protein by thioether linkages (Figure 2.1). In all those whose structures have been determined, the haem group sits in a crevice which is lined with side chains of apolar amino acids. The two vinyl groups are bound to two cysteine residues; one charged propionate group is at the surface of the molecule and the other one is hydrogen bonded to the interior of the molecule.

Figure 2.1 The haem group in Cytochromes c

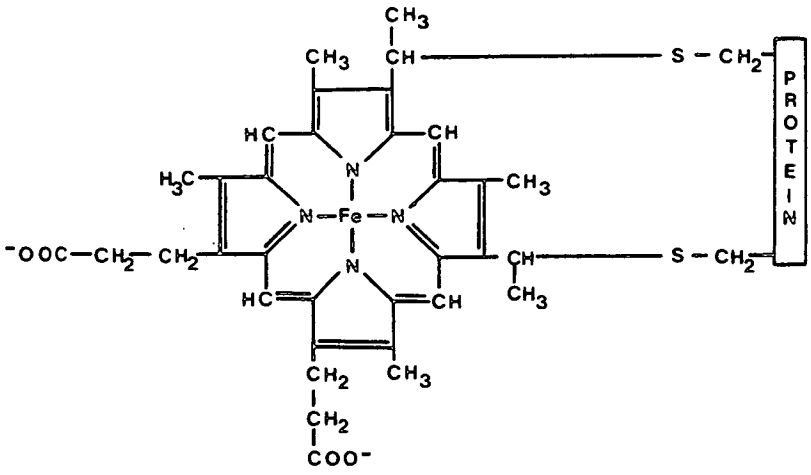

The arrangement of the electron transport chain seen in mitochondria appears to be paralleled in the bacterial membrane system[14,15,20]. Knowledge of the mechanism of action of the bacterial respiratory systems is therefore an important way of obtaining a better understanding of the mitochondrial system and furthermore, will give information about the evolutionary history of the organisms that contain them[19,27].

Considerable amino acid sequence data and crystallographic data exist showing similarities between the protein chains and suggesting that all c-type cytochromes are descendents of a common evolutionary ancestor[2,7,10]. Evidence for similarity between cytochromes c in different classes of organisms has been found if the deletion of some residues is assumed[8]. Nevertheless, the need for assuming deletion in the chains without stringent criteria is doubtful, and only the knowledge of the tertiary structure will give complete and unambiguous answers.

This study is concerned with cytochrome c_4 from Pseudomonas aeruginosa. Cytochrome c_4 is characterized by two haem groups covalently attached to each sub-unit near its N-terminus. It is thus double the size of many cytochromes c. The molecular weight based on amino acid composition is 19,000. It has been isolated from Azotobacter vinelandii[16,23,25], Pseudomonas stutzeri[13], Pseudomonas aeruginosa and Pseudomonas mendocina[1].

Pseudomonas aeruginosa is a bacterium with nitrate respiration, so it is able to use a nitrate ion as an electron acceptor in the respiratory chain when cultivated under anaerobic conditions.

The reduction of oxides of nitrogen is a process of respiration coupling the reduction of nitrogen compounds as terminal acceptors to the storage of energy. The different steps which are believed to occur *in vivo* in the reduction

of nitrate to molecular nitrogen and the corresponding catalysts are:

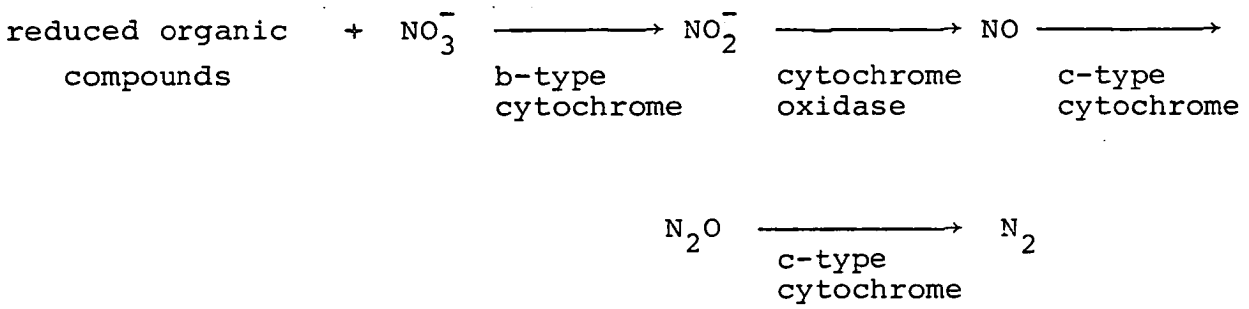

$$2NO_3^- + 4H^+ + 4e^- \longrightarrow 2NO_2^- + 2H_2O$$

$$2NO_2^- + 4H^+ + 2e^- \longrightarrow 2NO + 2H_2O$$

$$2NO + 2H^+ + 2e^- \longrightarrow N_2O + H_2O$$

$$N_2O + 2H^+ + 2e^- \longrightarrow N_2 + H_2O$$

Although the exact function of c_4 is unknown, it is produced in significant but variable quantities together with c_{551} and azurin when Pseudomonas aeruginosa is grown anaerobically. These observations led us to wonder if there is some subtle yet significant difference between the c_4 and c_{551} structures, between the two halves and if there was some interaction between the two haems. Both proteins are acidic and they have similar redox potentials. Cytochrome c_4 has an oxidation/reduction potential of 280 mV and an isoelectric point of approximately 5[1].

The study of the crystal structure of cytochrome c_4 was begun in order to answer the previous questions and also because the three dimensional structure should help in the search for the mechanism of electron transfer.

2 Amino acid sequence. Comparison with other cytochromes c.

Most cytochromes c, with known amino acid sequence, contain at least once in the molecule the characteristic sequence cysteine-x-y-cysteine-histidine. Two bonds connect the edges of the haem group to sulphur in the cysteines, one bond connects the iron to a nitrogen of the histidine and one more connects the iron to a sulphur atom in a methionine much further along the protein chain.

The amino acid sequence of 181 residues has been reported by Dr. R.P. Ambler[3] for Pseudomonas aeruginosa cytochrome c_4. From this sequence the protein appears to be two "short"[10] molecules joined end to end.

The cytochrome c_4 from Pseudomonas aeruginosa is closely related to that from Azotobacter vinelandii[4]. A comparison of the amino acid sequences of cytochrome c_{554} from the halotolerant bacterium Paracoccus ATCC12084 [10] with each "half" of cytochrome c_4 shows that they are closely related, and there is, indeed, more homology between them than between the two halves of cytochrome c_4.

The amino acid sequences of Pseudomonas aeruginosa and Azotobacter vinelandii cytochromes c_4, Haloterant Micrococcus c_{554}, Pseudomonas aeruginosa c_{551} and Tuna c are presented in Table 2.1. In Figure 2.2, the twenty different amino

Table 2.1 The amino acid sequences for four bacterial cytochromes c and for the mitochondrial cytochrome c of Tuna. In this Table, B means asparagine or aspartic acid and Z means glutamine or glutamic acid. The amino acids which are bonded to the haem group are in bold letters and the amino acids which have similar positions in the chain are underlined.

Pseudomonas aeruginosa c_4, 1st half

AGDAAAGQAKAAV**C**GA**CH**GABGBASPPNFPKLAGQGERYLLKQMHDIK---------DGKRTVLEMTGLLTBLSBZDIADLAAYFASQKMSVGMABPBLVZAGEA

Azotobacter vinelandii c_4, 1st half

AGDAAAGQGKAAV**C**GA**CH**GPDGNSAAPNFPKLAGQGERYLLKQMQDIKAGTKPGAPEGSGRKVLEMTGMLDNFSDQDLADLAAYFTSQKPTVGAADPQLVEAGET

Pseudomonas aeruginosa c_4, 2nd half

LFRGGKIAEGMPA**C**TG**CH**GSSPVGIATAGFPHLGGQHATYVAKQLTDFREGTRTNDGDTKIMQSIAAKLSNKDIAAISSYIQGLH

Azotobacter vinelandii c_4, 2nd half

LYRGGKLADGMPA**C**TG**CH**SPNGEGNTPAAYPRLSGQHAQYVAKQLTDFREGARTNDGDNMIMRSIAAKLSNKDIAAISSYIQGLH

Halotolerant micrococcus c_{554}

AGDAAAGEDKIGT**C**VA**CH**GTDGQGLAPIYPNLTGQSATYLESSIKAYRDGQRKGGNAALMTPMAQGLSDEDIADIAAYYSSQE

Pseudomonas aeruginosa c_{551}

EDPEVLFKNKG**C**VA**CH**AIDTKMVGPAYKDVAAKFAGQAGAEAELAQRIKMGSQGVWGPIPMPPNAVSDDEAQTLAKWVLSQK

Tuna c

CDVAKGKKTFVQK**C**AQ**CH**TVENGGKHKVGPNLWGLFGRKTGQAEGYSYTDANKTKGIVWNNDTLMEYLENPKKYIPGTKMIFAGIKKKGERQDLVAYLKSATS

Figure 2.2 The twenty amino acid side chains

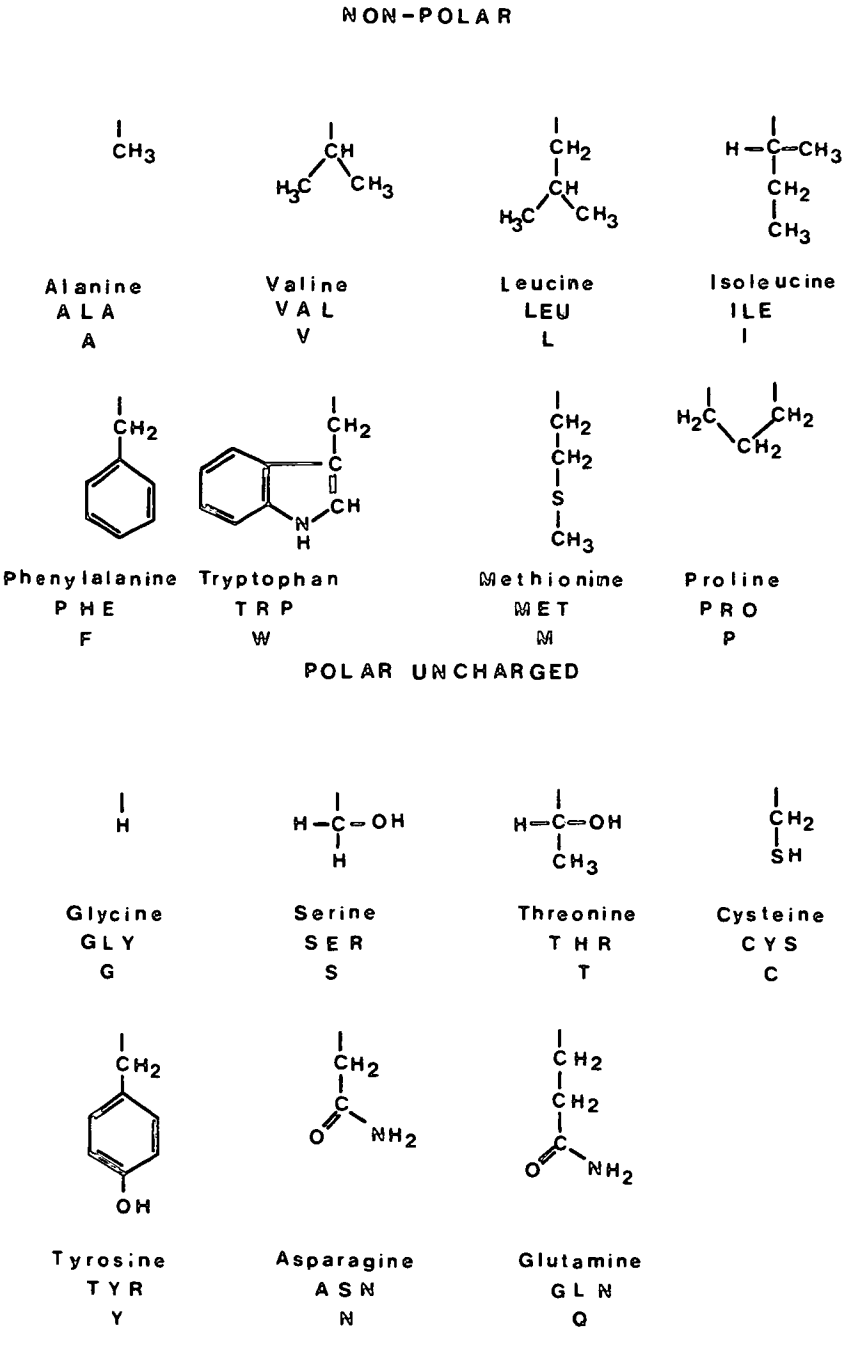

Figure 2.2 (contd.)

ACIDIC

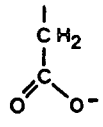

Aspartate
ASP
D

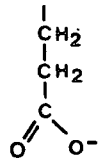

Glutamate
GLU
E

BASIC

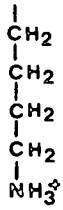

Lysine
LYS
K

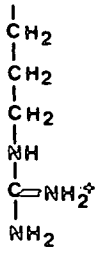

Arginine
ARG
R

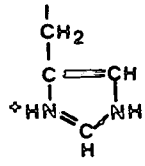

Histidine
HIS
H

acid side chains are illustrated together with their respective 3-letter and 1-letter abbreviations and their classification as non-polar, polar uncharged, acidic or basic groups.

In Table 2.1, the four amino acids which are bonded to the haem group are in bold letters and the amino acids which have similar positions in the different chains are underlined.

Cytochrome c_4 in Azotobacter vinelandii shows an insertion of nine residues in relation to the one in Pseudomonas aeruginosa. Tuna c shows the sequence F----GQ---Y and the tyrosine amino acid sixteen residues away from the methionine ligand as in cytochromes c_{554} and c_4. These similarities in the amino acid sequences point to similarities in functional importance as well as regions in the three dimensional structure.

The three dimensional structures of cytochrome c from Tuna, Pseudomonas c_{551}, Paracoccus c_{550}, Chlorobium c_{555} and Rhodospirillum c_2 show that although very little structural similarity could be seen from the amino acid sequence data[10], all five proteins fold in the same general way and in fact the sequence of the small cytochrome c_{551} has been aligned with the longer sequence of Tuna c in a structurally meaningful way. It is apparent that the three dimensional structure is much better conserved than the primary structure (Figure 2.3, taken from reference 10).

Figure 2.3 The protein chain of four bacterial cytochromes along with that of Tuna, a typical mitochondrial cytochrome c.

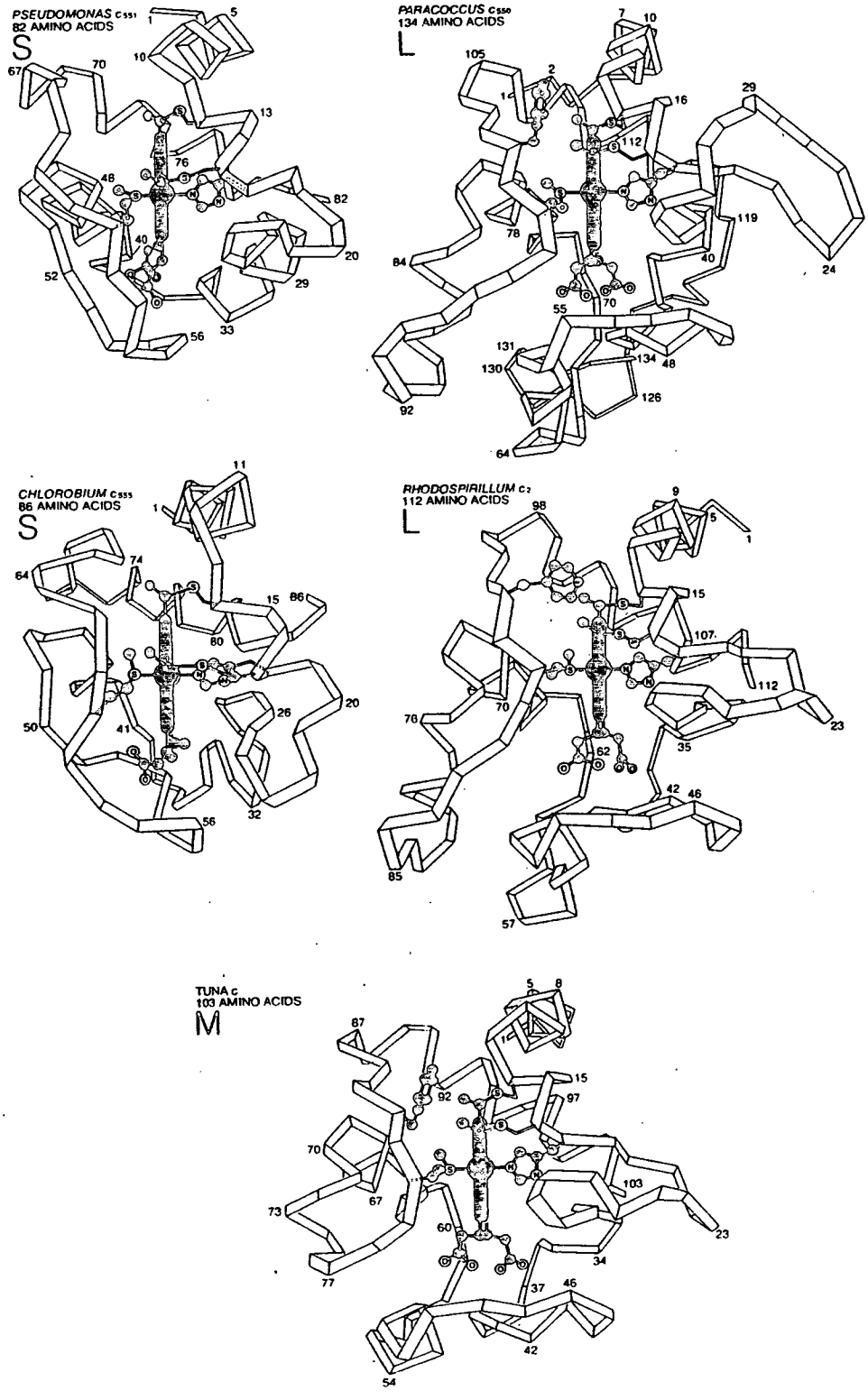

3 Prediction of the secondary structure from the amino acid sequence

Many attempts have been made to predict protein structures from their primary sequence.

The earlier prediction models classified amino acids qualitatively as helix breakers[11], helix formers[19] or helical and antihelical[18]. However, these models are poor since they are based on a small number of known three-dimensional protein structures.

Here, the predictions of Chou and Fasman[5,6] are applied to Tuna cytochrome c and the calculated structure is compared with the real one. Finally, the same method is applied to predict the secondary structure of cytochrome c_4.

3.1 The right-handed alpha helix and the beta pleated sheet

In 1951 Pauling and Corey[17] proposed two periodic polypeptide structures called the α-helix and the β-pleated sheet.

A polypeptide chain may be defined in terms of three torsion angles ϕ, Ψ, and ω, as shown in Figure 2.4. If these are regularly repeated, a helical structure results, which is stabilized by hydrogen bonds between peptide amide and carbonyl groups. In practice, $\omega \approx 180^{\circ}$ and variations need normally be considered only in ϕ and Ψ.

Figure 2.4 Definition of the dihedral angles in a polypeptide chain

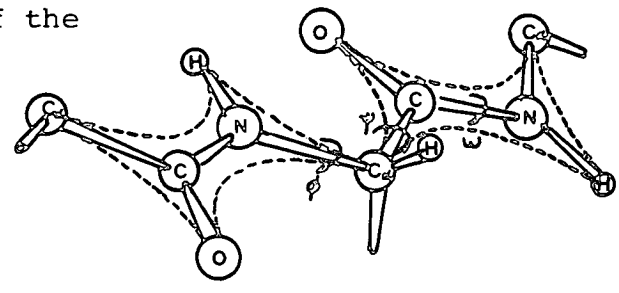

The right handed α-helix (Figure 2.5) is characterized by 3.6 amino acid residues per turn of the helix and each residue is related to the next one by a translation of 1.5 Å along the helix axis and a rotation of 100°. The carbonyl group of residue i is hydrogen bonded to the amide group of residue i + 4 (Figure 2.6).

Figure 2.5 An α-helix with each residue represented by its C_α atoms.

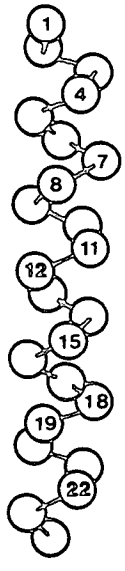

Figure 2.6 The hydrogen bonds in a right handed α-helix

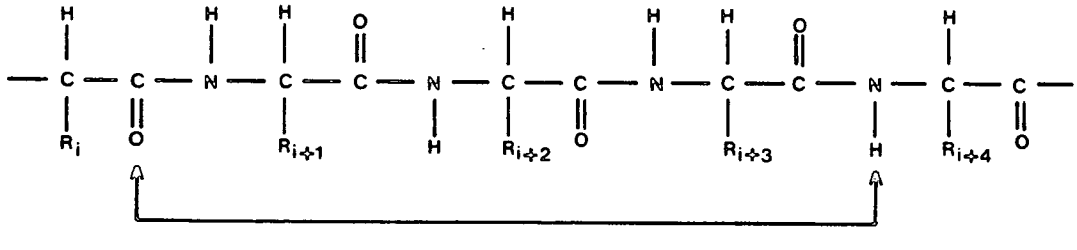

The α-helix structure has been found in many proteins. All cytochromes c of known three dimensional structure show α-helices at the beginning and at the end of the polypeptide chain.

The parallel and antiparallel β-pleated sheets as postulated by Pauling and Corey[17] are regular hydrogen-bonded structures as shown in Figure 2.7.

These extended configurations have the CO and NH groups pointing in directions perpendicular to that of the polypeptide chain; therefore, although they are not available for hydrogen bonding within the polypeptide chain, they form hydrogen bonds to neighbouring chains.

A Ramachandran plot[22] for a polypeptide chain of L-alanines is shown in Figure 2.8. It is apparent from the figure that the β-pleated sheet and the right-handed α-helix are both in allowed regions.

3.2 Reverse Turns

Reverse turns are defined[26] as an arrangement of four consecutive peptide units (C_α^i to C_α^{i+3}) in which the distance between C_α^i and C_α^{i+3} is less than 7 Å without there being an α-helix.

In reverse turns of type I and II (Figure 2.9) there is a hydrogen bond between O_i and N_{i+3}. Reverse turns of type II are found almost exclusively with glycine in position (i+2).

Figure 2.7 The antiparallel and parallel three-stranded β-sheets. The hydrogen bonds are indicated by dashed lines, the chain directions by arrows and the C_α atoms are marked by dots.

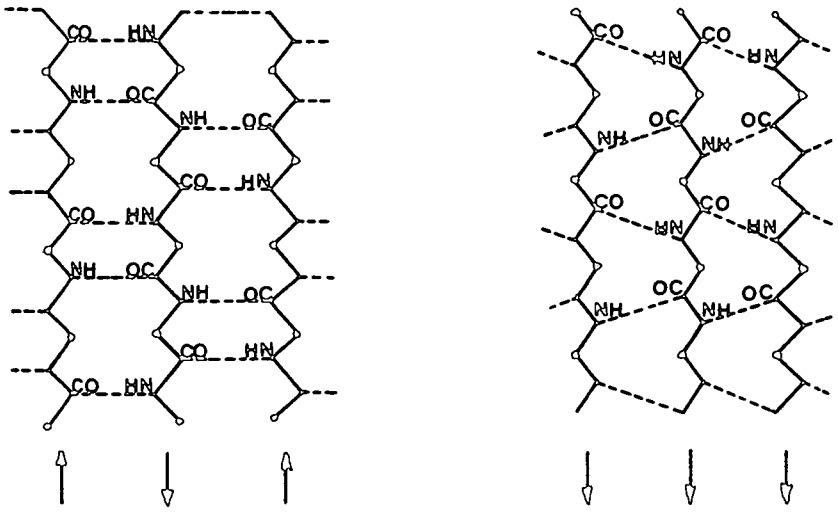

Figure 2.8 A Ramachandran plot for a polypeptide chain of L-alanines. Continuous lines define allowed conformations and dashed lines define partially allowed conformations. The regions defining the β-pleated sheet, left and right-handed α-helix and the 3_{10} and π helices have been indicated.

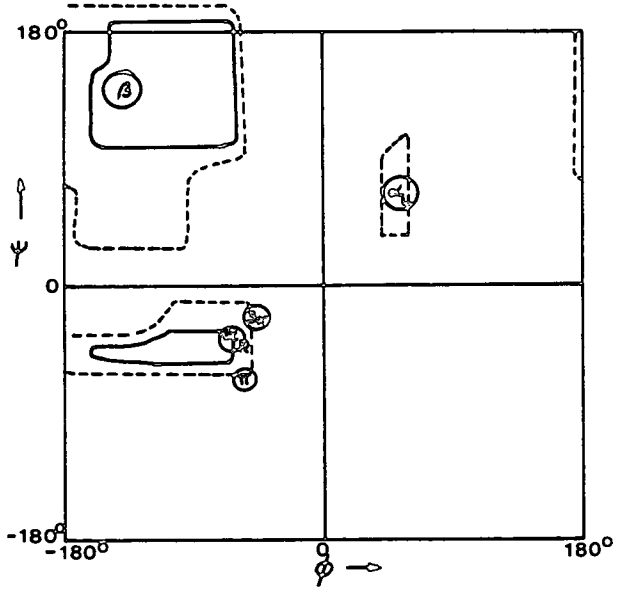

A survey of the location of reverse turns in proteins[13] shows that they are concentrated at the surface of the molecule and they contain mostly hydrophilic residues.

Figure 2.9 Type I and II β-bends

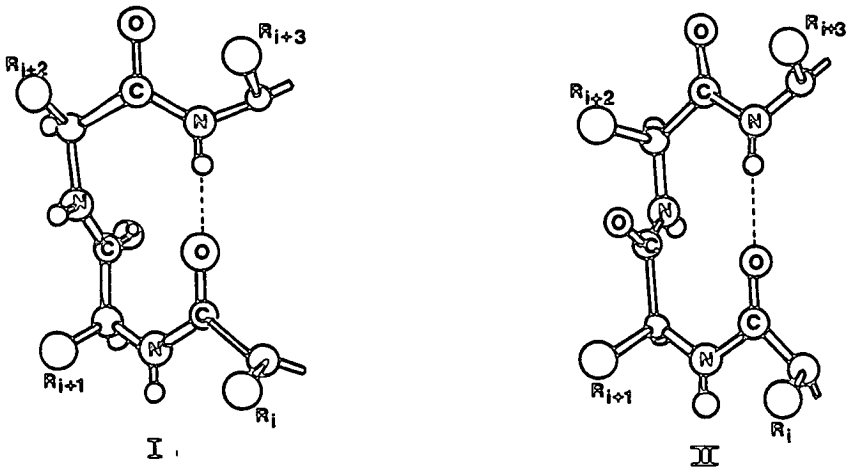

3.3 Chou and Fasman predictions

A survey was made on fifteen proteins with known amino acid sequences[5,6]. For each amino acid, its frequency in helical (f_α), β-sheet (f_β) and coil (f_c) regions together with its propensity P were calculated. In an helical region these terms may be defined thus:

$$f_\alpha = n_\alpha/n \quad \text{for any amino acid}$$

$$\langle f_\alpha \rangle = \Sigma n_\alpha/\Sigma n \quad \text{for all amino acids}$$

$$P_\alpha = f_\alpha/\langle f_\alpha \rangle$$

where n is the total number of residues of a particular amino acid and n_α is the number of those residues which are in a helical region.

The results show that Glu and Ala are found most frequently in helical regions; Met, Val and Ile appear to be the amino acids with larger β-sheet propensities; Pro, Gly, Asn and Ser are the most frequent random coil residues in proteins.

The frequency of occurrence of amino acids in positions i to i+3 in reverse turns of type I and II was also calculated.

Based on this information each residue has been assigned with symbols H($P \geqslant 1.30$), h($1.30 > P \geqslant 1.10$), I($1.10 > P \geqslant 0.98$), i($0.98 > P \geqslant 0.75$), b($0.75 > P \geqslant 0.60$) and B($0.60 > P$). In Table 2.2 the twenty amino acids are listed with the respective classifications for helix, β-sheet, coil and reverse turn regions.

The secondary structure is predicted on the basis of each amino acid's propensity for appearing in the different regions.

Table 2.3 shows a comparison between the predicted and observed structures for Tuna cytochrome c.

TABLE 2.2 The α-helical, β-sheet, coil and reverse turn propensities.

Amino Acid	Helical	β-sheet	coil	reverse turn
ALA	H	I	b	B
ARG	i	i	h	I
ASN	b	b	H	H
ASP	I	i	I	h
CYS	i	H	I	h
GLN	h	h	i	B
GLU	H	B	i	B
GLY	B	i	H	H
HIS	h	b	i	b
ILE	I	H	i	B
LEU	H	h	b	B
LYS	I	b	I	I
MET	h	H	b	b
PHE	h	h	i	i
PRO	B	b	H	H
SER	i	b	h	H
THR	I	h	I	I
TRP	h	h	i	h
TYR	b	h	h	h
VAL	h	H	b	B

The results of the Chou and Fasman prediction for secondary structure of cytochrome c_4 are tabulated in Table 2.4. According to this, helical regions are predicted near both ends of the polypeptide chain and at the end of the first half and beginning of the second half of cytochrome c_4. These α-helices at the beginning and end of the polypeptide chain are constant features in all cytochromes c whose structure has been determined.

These predictions, together with the well established geometry about the haem group, provide an excellent starting point for the structural analysis of cytochrome c_4.

TABLE 2.3 Comparison of experimental and predicted helical and reverse turn regions for Tuna cytochrome c.

Helical regions		Reverse turn regions	
X-ray	Predicted	X-ray	Predicted
2 - 13	2 - 8	21 - 24	22 - 25
14 - 18	10 - 18	-	29 - 32
49 - 55	-	32 - 35	-
62 - 70	62 - 74	35 - 38	-
71 - 75		39 - 42	39 - 42
87 - 102	82 - 103	43 - 46	-
		-	46 - 49
		-	54 - 57
		75 - 78	75 - 78

TABLE 2.4 Predicted secondary structure for cytochrome c_4

Helical regions	Reverse turns	β-sheet
1 - 13	26 - 29	119 - 126
16 - 24	48 - 51	
37 - 47	98 - 101	
54 - 61	110 - 113	
63 - 81	113 - 116	
85 - 93	151 - 154	
102 - 107	174 - 177	
137 - 146		
156 - 173		

REFERENCES

1. Ambler, R.P. and Murray, S., Biochemical Society Transactions, 531st Meeting, Lancaster, 1973.

2. Ambler, R.P., Bacterial cytochromes c and molecular evolution, Syst.Zool., 22, 554-565, 1974.

3. Ambler, R.P., Fron cyclotrons to cytochromes, Robinson A.B. and Kaplan, N.O. Eds., Academic Press, New York, in press, 1981.

4. Ambler, R.P., unpublished results.

5. Chou, P.Y. and Fasman, G.D., Biochemistry, 13, 211-245, 1974.

6. Chou, P.Y. and Fasman, G.D., Adv.Enzymol., 47, 145-148, 1978.

7. Cookson, D.J., Moore, G.R., Pitt, R.C., Williams, J.P., Campbell, I.D., Ambler, R.P., Bruschi, M., Le Gall, J. Eur. J. Biochem., 83, 261-275, 1978.

8. Dickerson, R.E., J.Mol.Biol., 57, 1-15, 1971.

9. Dickerson, R.E., Timkovich, R., Almassy, R.J., J.Mol.Biol., 100, 473-491, 1976.

10. Dickerson, R.E., Scientific American, (March), 99-110, 1980.

11. Guzzo, A.V., Biophys.J., 5, 809-822, 1965.

12. Kodama, T., and Shidara, S., J.Biochem.(Tokyo), 65, 351-360, 1969.

13. Kuntz, I.D., J.Amer.Chem.Soc., 94, 4009-4012, 1972.

14. Lemberg, R. and Barrett, J., Cytochromes, Academic Press, London, 1973.

15. Nachbar, M.S. and Salton, M.R.J., Biochim. and Biophys. Acta., 223, 309-320, 1970.

16. Neumann, N.P. and Burris, R.H., J.Biol.Chem., 234, 3286-3290, 1959.

17. Pauling, L., Corey, R.B., Branson, H.R., Proc.Nat.Acad.Sci., USA, 37, 205-211, 1951.

18. Periti, P.F., Gvagliarotti, G., Liquori, A.M., J.Mol.Biol., 24, 313-322, 1967.

19. Prothero, J.W., Biophys.J., 5, 809-922, 1966.

20. Rothfield, C.M. and Endo, A., Membrane proteins, pg. 27, Little Brown and Co., Boston, 1969.

21. Salemme, F.R., Ann.Rev.Biochem., 46, 299-329, 1977.

22. Stryer, L., Biochemistry, W.H. Freeman and Company, San Francisco, 1975.

23. Swank, R.T. and Burris, R.H., Biochim,Biophys.Acta., 180, 473-489, 1969.

24. The Enzymes, P.D. Boyer Ed., Vol. XI, Chapter VII, Academic Press, New York.

25. Tissieres, A., Biochem.J., 64, 582-589, 1956.

26. Venkatachalam, C.M., Biopolymers, 6, 1425-1436, 1968.

27. Yamanaka, T., Advan. in Biophys., 3, 227-276, 1972.

CHAPTER THREE

CHAPTER THREE

Three Dimensional Structure of Cytochrome c_4 from Pseudomonas aeruginosa at 5 Å resolution

1. Preliminary work in the determination of the structure

X-ray studies of this cytochrome c_4 were started by Dr. L. Sawyer and Mr. L. Jones in Edinburgh. Space group, cell dimensions and 5 Å intensity data sets that have been used in this study were previously determined by them.

The amino acid sequence was obtained from Dr. R. Ambler[1].

The predicted secondary structure (Table 2.4) suggests an appreciable amount of helix which coincides fairly well with the position for helices in the other small cytochromes c. In particular, the helices at the start and end of the structures appear to be the only absolutely constant features (Figure 2.3), the former running parallel to and the latter perpendicular to the plane of the haem.

1.1 The Crystals

The crystals were supplied by Dr. A.F.W. Coulson[7]. They were grown by precipitating a concentrated solution of the protein in 80% saturated ammonium sulphate solution at pH 6.0 and resuspending the precipitate in a minimum quantity of 50 mM ammonium acetate at pH 6.0. The crystals

grew at a temperature of 4°C over a period of one to three days. The crystals were then stabilised by transferring them to a solution of 2M ammonium sulphate and 50 mM ammonium acetate, pH 6, in which they are quite stable at temperatures from 4 to 22°C.

The protein crystallises as long hexagonal bipyramids.

1.2 Crystal mounting

Crystals with the longest dimension about 0.4 mm were mounted in thin glass walled capillaries for the X-ray studies.

The crystals were first introduced into the capillaries by drawing them up by capillary action; then the mother liquor was removed using thin strips of filter paper. In order to keep the crystal always moist, a very small quantity of mother liquor is left around the crystal. Using thin strips of filter paper, the capillary inner surface was dried and a few drops of mother liquor or filter paper soaked in it were placed at each end of the capillary which was finally sealed with wax. Figure 3.1 illustrates this procedure.

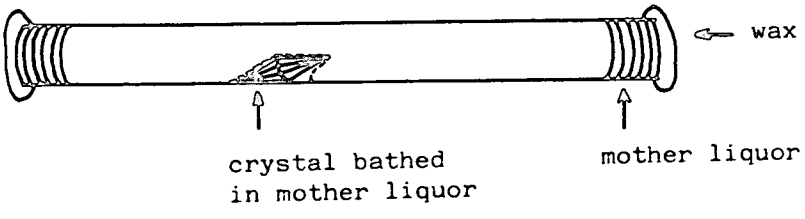

Figure 3.1 Cytochrome c_4 crystal mounting

For the data collection, it is desirable to have the crystal rotating around the six-fold axis, so before sealing the capillary that axis was made approximately parallel to the tube using strips of filter paper.

1.3 Symmetry and space group

Precession photographs were taken with CuK_α radiation (λ = 1.5418 Å).

The intensity relationships and the reflection conditions indicated that the crystals have space group $P6_122$ or $P6_522$, (l = 6n for 0001 reflection).

The approximate cell dimensions were a = b = 62.4 Å and c = 174.2 Å.

The measured crystal density is 1.22 g cm^{-3} and the molecular weight based on amino acid composition is 19,000. Assuming that there are twelve molecules in the unit cell, in the absence of solvent the density should be 0.65 g cm^{-3} and the corresponding average crystal volume per unit weight is:

$$V_m = \frac{\text{volume of asymetric unit}}{\text{molecular weight}} = 2.58 \text{ Å}^3 \text{ dalton}^{-1}$$

which is well within the usually observed range[19]. Supposing that the solvent has a density of 1.1 g cm^{-3}, the fraction of crystal volume occupied by solvent is 52%, which is again within the observed range of 27-65%.

1.3.1 Space groups $P6_122$ and $P6_522$

The intensity relationships indicating that the crystal belongs to the Laue group 6/ mmm are:

$$\begin{aligned} I(hkil) &= I(\bar{h}\,\bar{k}\,\bar{i}\,\bar{l}) \quad \text{(Friedel inversion)} \\ &= I(\bar{i}\,\bar{h}\,\bar{k}\,l) \quad \text{(6-fold axis } \parallel c^*) \\ &= I(h\,i\,k\,\bar{l}) \quad \text{(2-fold axis } \parallel a^*) \end{aligned}$$

and relationships derived from these, giving general reflections, $h \neq k \neq i \neq 0$, $l \neq 0$, a multiplicity of 24. The reciprocal axes a^* and b^* are at 60° to each other and perpendicular to the unique axis, c^* and i is defined as $i = -(h+k)$.

The reflection conditions indicating the space group $P6_122$ or $P6_522$ were:

(h k i l)	none
(0 0 0 l)	l = 6n

In class 622, there are three independent special zones: (h k i 0), (h 0 $\bar{h}$ l) and (h h $2\bar{h}$ l). For these zones, the structure factor phases are restricted to two values ϕ and $\pi+\phi$, where $\phi = n\pi/6$ with n being an integer between 0 and 12. For other reflections, phases may have any value, and I(h k i l) may differ from I($\bar{h}\,\bar{k}\,\bar{i}\,\bar{l}$) because of anomalous scattering.

The equivalent positions for the atoms in a unit cell with symmetry $P6_122$ or $P6_522$ are:

$P6_122$	$P6_522$
(x, y, z)	(x, y, z)
$(\bar{x}, \bar{y}, \frac{1}{2}+z)$	$(\bar{x}, \bar{y}, \frac{1}{2}+z)$
$(\bar{y}, x-y, \frac{1}{3}+z)$	$(\bar{y}, x-y, \frac{2}{3}+z)$
$(y, y-x, \frac{5}{6}+z)$	$(y, y-x, \frac{1}{6}+z)$
$(y-x, \bar{x}, \frac{2}{3}+z)$	$(y-x, \bar{x}, \frac{1}{3}+z)$
$(x-y, x, \frac{1}{6}+z)$	$(x-y, x, \frac{5}{6}+z)$
$(y, x, \frac{1}{3}-z)$	$(y, x, \frac{2}{3}-z)$
$(\bar{y}, \bar{x}, \frac{5}{6}-z)$	$(\bar{y}, \bar{x}, \frac{1}{6}-z)$
$(\bar{x}, y-x, \frac{2}{3}-z)$	$(\bar{x}, y-x, \frac{1}{3}-z)$
$(x, x-y, \frac{1}{6}-z)$	$(x, x-y, \frac{5}{6}-z)$
$(x-y, \bar{y}, \bar{z})$	$(x-y, \bar{y}, \bar{z})$
$(y-x, y, \frac{1}{2}-z)$	$(y-x, y, \frac{1}{2}-z)$

1.3.2 Patterson with symmetry P6/mmm

The space groups $P6_122$ and $P6_522$ lead to a Patterson map with symmetry P6/mmm. In this map the symmetry related vectors are:

(u, v, w)	$(\bar{v}, u-v, w)$	$(v-u, \bar{u}, w)$
$(\bar{u}, \bar{v}, w)$	$(v, v-u, w)$	$(u-v, u, w)$
$(\bar{u}, \bar{v}, \bar{w})$	$(v, v-u, \bar{w})$	$(u-v, u, \bar{w})$
$(u, v, \bar{w})$	$(\bar{v}, u-v, \bar{w})$	$(v-u, \bar{u}, \bar{w})$
(v, u, w)	$(\bar{u}, v-u, w)$	$(u-v, \bar{v}, w)$
$(\bar{v}, \bar{u}, w)$	$(u, u-v, w)$	$(v-u, v, w)$
$(\bar{v}, \bar{u}, \bar{w})$	$(u, u-v, \bar{w})$	$(v-u, v, \bar{w})$
$(v, u, \bar{w})$	$(\bar{u}, v-u, \bar{w})$	$(u-v, \bar{v}, \bar{w})$

The Patterson vectors for a single atom in a general position (x, y, z) are:

$(x, y, \frac{1}{6})$	$(0, x-2y, \frac{1}{6} -2z)$	$(-y, y, 2z)$
$(-x-y, x-2y, \frac{1}{3})$	$(0, x+y, \frac{1}{6} +2z)$	$(y-x, x-y, \frac{1}{3} -2z)$
$(2x, 2y, \frac{1}{2})$	$(0, y-2x, \frac{1}{2} +2z)$	$(-x, x, \frac{1}{3} +2z)$
$(0, 0, 0)$		

and symmetry related positions. All peaks have a multiplicity of one except the origin peak which has a multiplicity of 12.

From the Patterson vectors, we conclude that the three Harker sections at $z = \frac{1}{2}, \frac{1}{3}$ and $\frac{1}{6}$ give the x and y atomic coordinates and the interpretation of the other two Harker sections will give the z coordinate.

1.4 Data Collection

Two derivatives with $UO_2(NO_3)_2$ and $K_2Pt(NO_2)_4$ were prepared by soaking native crystals in 2.0M ammonium sulphate solution at pH 6.0 in 1 mM solution of heavy atom for 24 hours.

Intensity data, for native and derivative crystals, were collected on the NONIUS CAD-4 diffractometer in the Edinburgh University Physics Department, with a He-flushed tube fitted between the crystal and the detector.

Accurate cell dimensions were obtained by refinement of the angle settings for 10 to 15 intense reflections distributed about reciprocal space (Table 3.1).

Crystal	cell dimenstions a(Å)	b(Å)	c(Å)
Native	62.39(6)	62.37(3)	174.19(7)
$UO_2(NO_3)_2$	62.31(4)	62.23(4)	174.62(5)
$K_2Pt(NO_2)_4$	62.31(7)	62.30(5)	174.63(6)

Table 3.1 Cell dimensions for native and derivative crystals.

Lorentz polarization and absorption corrections were applied to the intensity data. The absorption corrections were done using the semi-empirical method of North et al[20]; an absorption curve was obtained from the variation in intensity of a strong (001) reflection as the crystal was rotating about the c axis at intervals of 5^{o}. Figure 3.2 shows the absorption curve used for the native data absorption corrections.

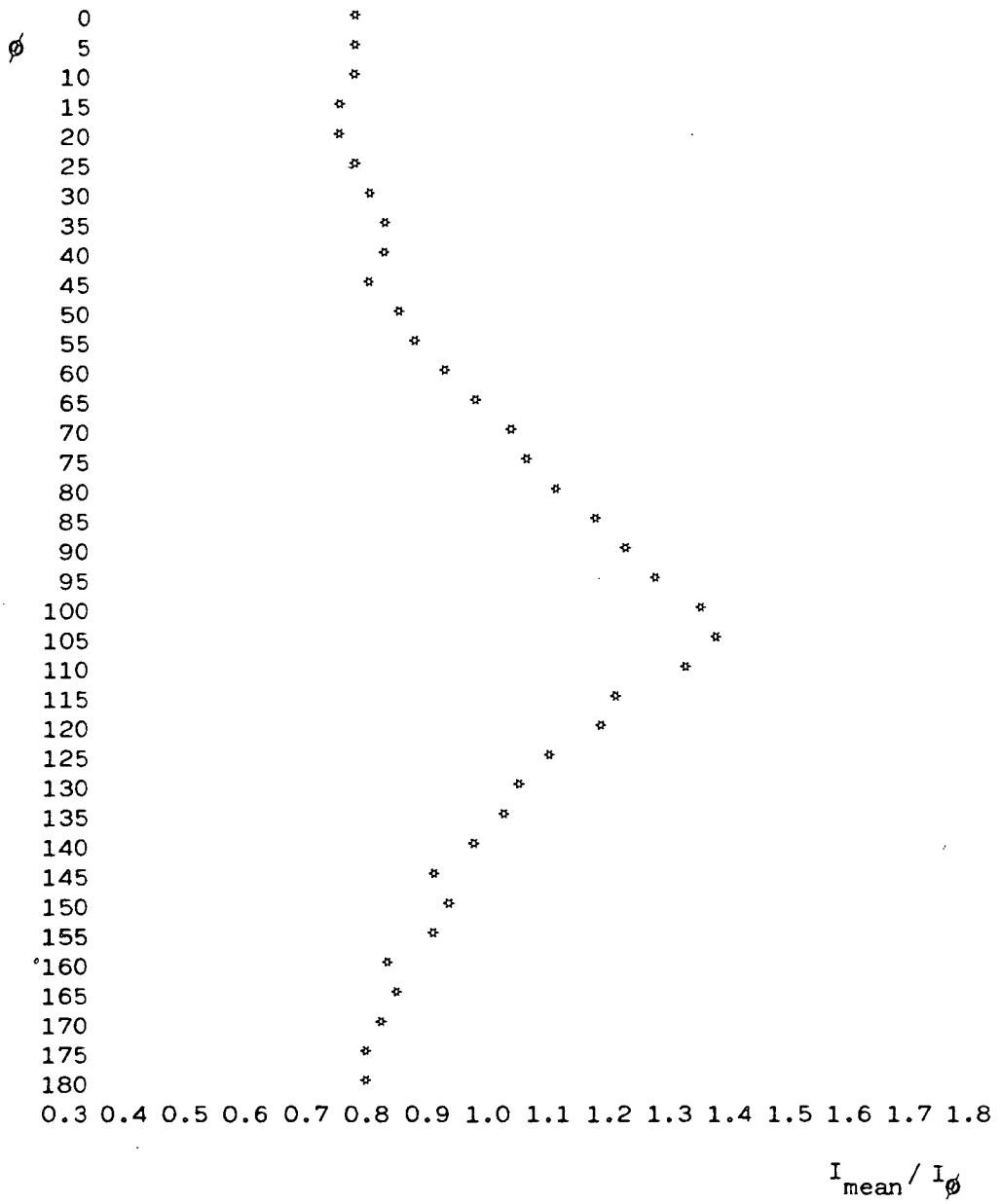

Figure 3.2 Absorption curve for the native cytochrome c_4 crystal

1.5 Resolution and the number of reflections

Diffraction data were collected to a resolution of 5 Å for the derivative crystals and 3 Å for the native crystal. These resolutions correspond to $\theta_{max} = 9^{o}$ (5 Å) or 15^{o} (3 Å), for copper K_{α} radiation.

To obtain an estimate of the number of reflections to be measured, the volume of the sphere in reciprocal space corresponding to a resolution of dm is divided by the volume of the reciprocal unit cell. Hence the number of reflections to be measured in a primitive lattice is given by

$$N = \frac{(4/3)\pi \quad (\lambda/dm)^3}{(\lambda^3/V)} \quad = \quad \frac{4}{3} \times \frac{\pi V}{dm^3}$$

$$dm = \lambda / \ 2\sin\theta_{max}$$

N must be divided by the multiplicity factor of the general reflections (h k l) to give an estimate of the number of unique reflections. Considering that the number of symmetry equivalent reflections in the hexagonal lattice is 24, the number of unique reflections to be measured for the 5 Å data set is about 800 and 3800 for the 3 Å set. This is an under-estimate, since it does not take into accound the lower multiplicities of many reflections.

In a similar way, we can predict the number of centric and acentric reflections in both data sets. Table 3.2 gives these values.

Table 3.2 Calculated number of unique reflections to be measured in the 5 Å and 3 Å data sets

	Number of reflections		
	centric	acentric	total
5 Å data set	470	590	1060
3 Å data set	1470	3090	4560

The total number of reflections measured was 4141 for $0 \leq h \leq k$, $0 \leq l$ to a resolution of 3 Å. Of these reflections, 1264 were centric and 2877 were acentric and Friedel related intensities were measured for these. A total of 3701 reflections had a structure factor amplitude F greater than its standard deviation σ. For each reflection, F and σ values were calculated according to the equations:

$$F = \frac{[|F(hkl)|/\sigma^2(hkl)] + [|F(hk\bar{l})|/\sigma^2(hk\bar{l})]}{[1/\sigma^2(hkl)] + [1/\sigma^2(hk\bar{l})]}$$

$$\sigma = \max\{\sigma_A, \sigma_B\}$$

$$1/\sigma_A^2 = [1/\sigma^2(hkl)] + (1/\sigma^2(hk\bar{l})]$$

$$\sigma_B^2 = \frac{\{[F-|F(hkl)|]^2/\sigma^2(hkl)\} + \{[F-|F(hk\bar{l})|]^2/\sigma^2(hk\bar{l}]\}}{[1/\sigma^2(hkl)] + [1/\sigma^2(hk\bar{l})]}$$

$|F(hkl)|$ is the structure factor amplitude for the reflection (hkl).

The number of reflections collected for both derivative data sets and their total number of unique reflections with the structure factor amplitude greater than the standard deviation is tabulated in Table 3.3.

Table 3.3 Number of reflections collected for the $UO_2(NO_3)_2$ and $K_2Pt(NO_2)_4$ derivative data sets

	Number of unique reflections collected			
	centric	acentric	total	total with F > σ
$UO_2(NO_3)_2$	829	1031	1860	1751
$K_2Pt(NO_2)_4$	829	1031	1860	1514

In both derivative data sets there were some reflections with higher resolution than 5 Å.

2. Studies on the Structure

2.1 Approximate absolute scale and scaling of derivatives to native data

An approximate value of the absolute scale of the native data was derived from a Wilson plot.

Assuming a randomly distributed structure with a large number of atoms, Wilson has proved that:

$$\ln \frac{\langle I \rangle}{\Sigma f_j^2} = -\ln K - 2B \frac{\sin^2\theta}{\lambda^2}$$

$\langle I \rangle$ intensity mean value for a Bragg angle θ

f_j atomic scattering factor

B isotropic temperature factor

K scale factor

Σ is extended to all the atoms in the unit cell

Because we do not have a random structure, this equation is approximate and a plot of $\ln(\langle I \rangle / \Sigma f_j^2)$ versus $\sin^2\theta / \lambda^2$ for the cytochrome c_4 native data shows that there are indeed large deviations from the predicted straight line. Figure 3.3 shows the Wilson plot and the best straight line fitted to the experimental points. According to this, the overall isotropic temperature factor for the protein is $B = 7.5$ Å^2 and the scale factor K is 1.2.

The scaling of derivatives to native data was done using the program ANSC[12].

A scale factor of the form $K.\exp(B_{ov}\sin^2\theta / \lambda^2)$ was found by equating

$$\frac{\Sigma K \, F_{PH}^2(\underline{h}) \, \exp(-B_{ov}.\sin^2\theta / \lambda^2)}{\Sigma \, F_p^2(\underline{h})} = 1$$

where the sums are extended to all the reflections within the same $(\sin^2\theta/\lambda^2)$ range and $F_{PH}(\underline{h})$ and $F_p(\underline{h})$ represent respectively the structure factors of the $(\underline{h})$ reflection for derivative and native data. This equation implies a trivial overall contribution by the heavy atoms.

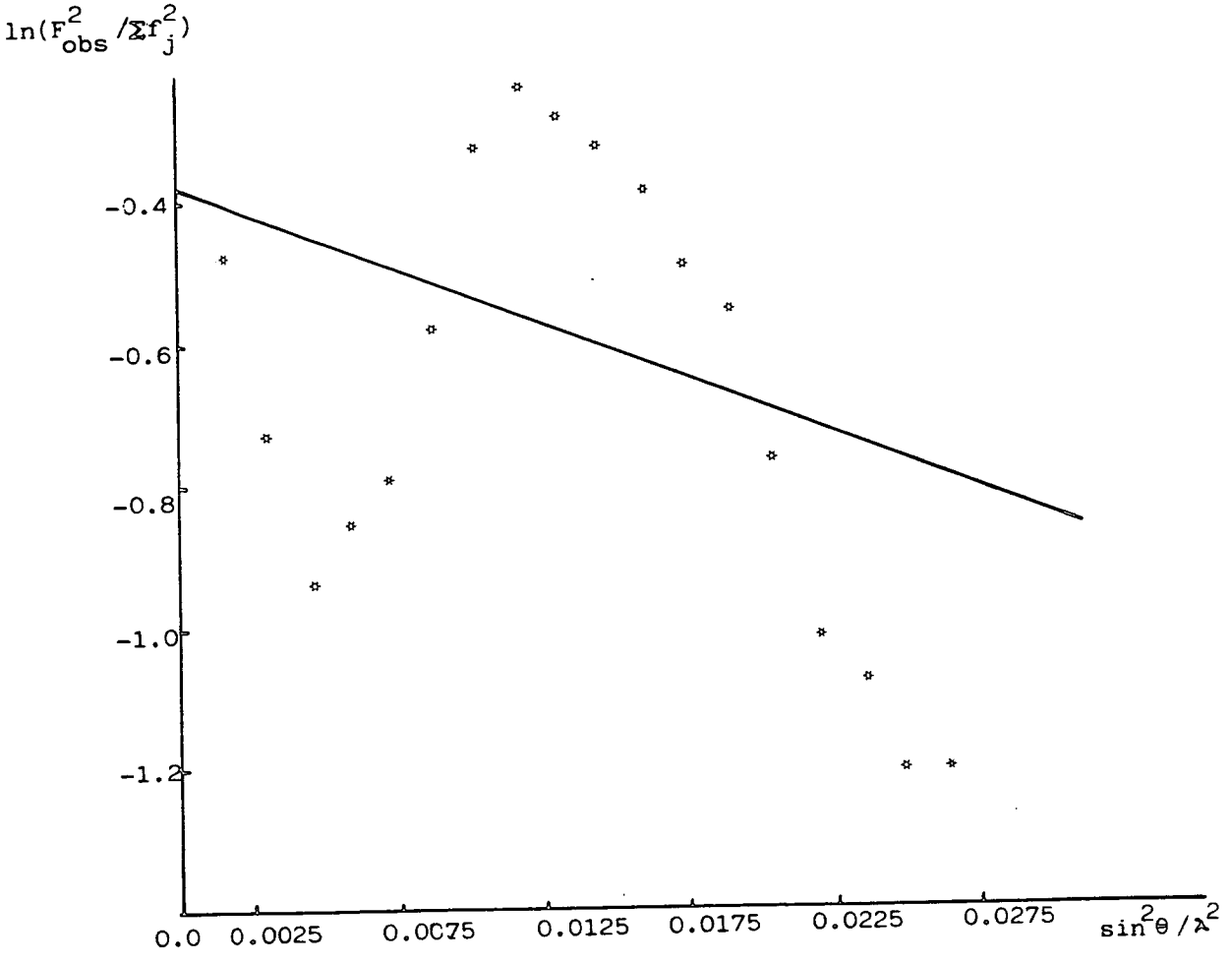

Figure 3.3 Wilson plot for cytochrome c_4

Figure 3.4 The scaling of the $UO_2(NO_3)_2$ derivative data to the native data

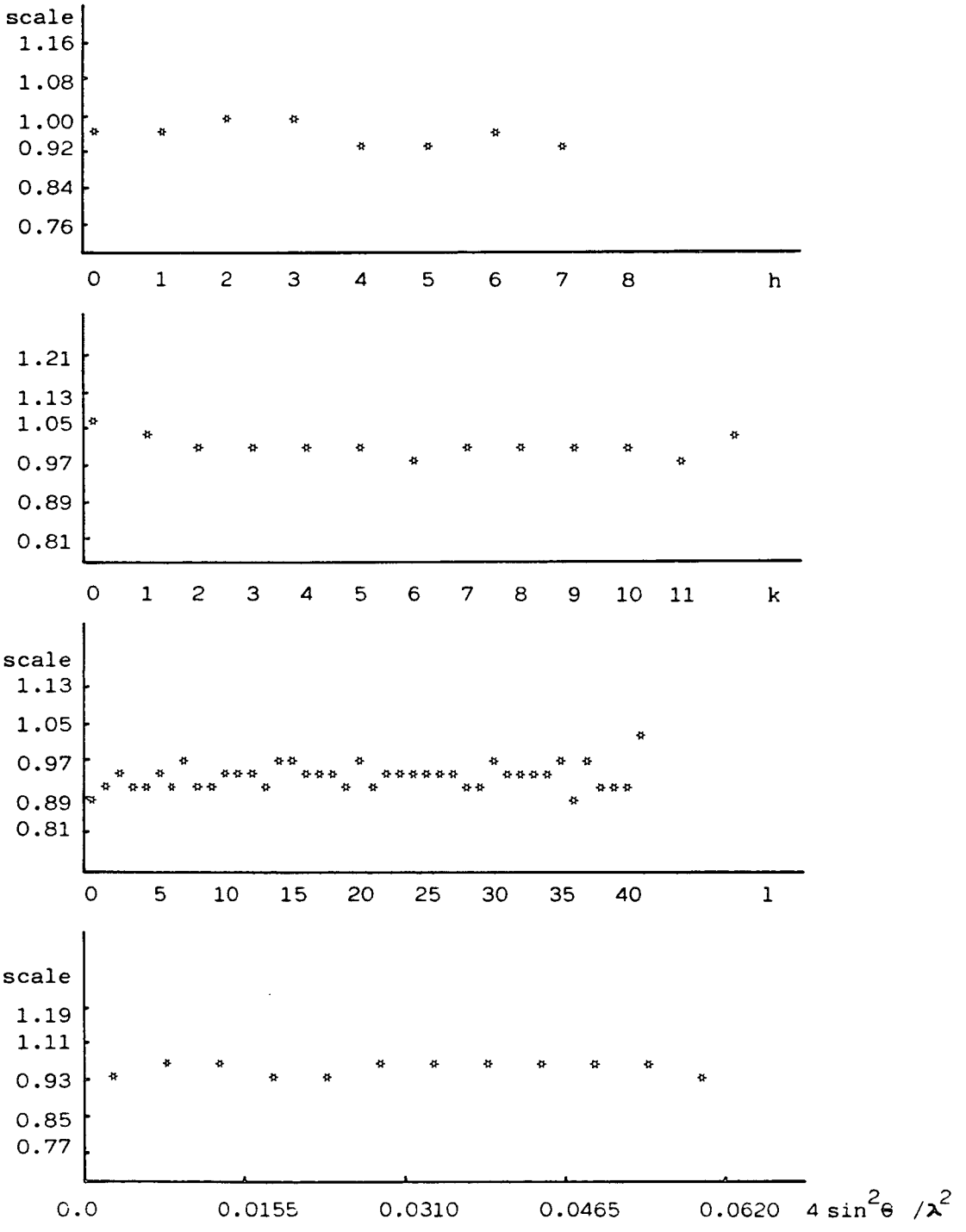

Figure 3.5 The scaling of the $K_2Pt(NO_2)_4$ derivative data to the native data

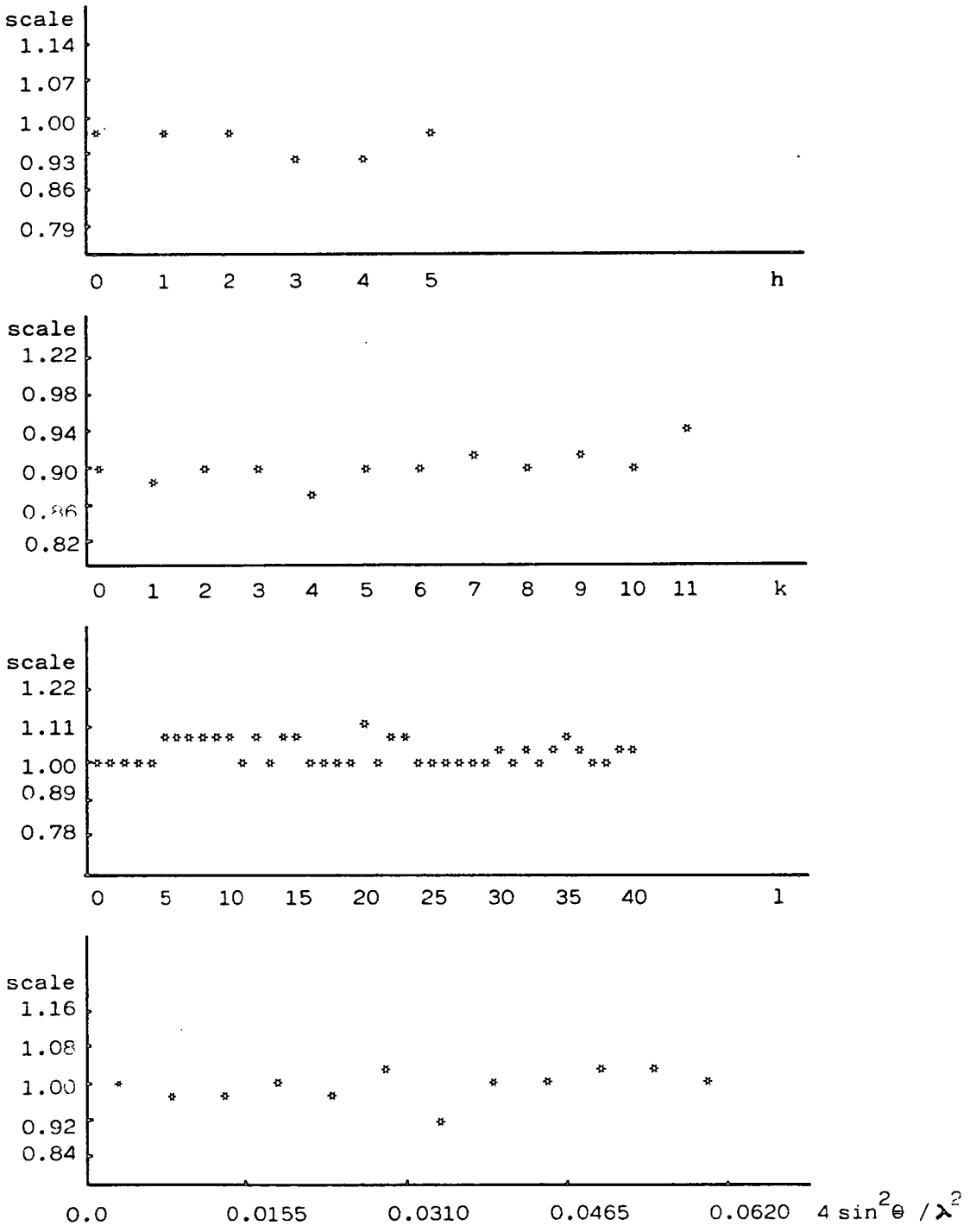

Figures 3.4 and 3.5 show the analyses of derivative structure factors against native ones in ranges of h, k, l and $4(\sin\theta/\lambda)^2$ for both derivatives.

It is apparent from the plots that the scale factor remains relatively constant for all the analyses.

The values for K and B_{ov} are listed in Table 3.4.

Table 3.4 The derivative to native scale factors

Crystal	K	B_{ov} ($\AA^{-2}$)
Native	-	-
$UO_2(NO_3)_2$	0.986(9)	1.1(1.2)
$K_2Pt(NO_2)_4$	0.986(7)	-2.0(0.9)

The large errors in B_{ov} were to be expected considering the low resolution of the data set.

2.2 F_{HLE} calculation for $UO_2(NO_3)_2$ and $K_2Pt(NO_2)_4$ derivatives

Approximate values for the heavy atom contribution which take into account both isomorphous ($\Delta iso = |F_{PH}(\underline{h})| - |F_P(\underline{h})|$) and anomalous ($\Delta an = |F_{PH}(\underline{h})| - |F_{PH}(\bar{\underline{h}})|$) contributions are the heavy atom lower estimate F_{HLE} [13,16,18,22].

$$F^2_{HLE} = F^2_{PH} + F^2_P - \sqrt{1 - \left(\frac{K\Delta an}{2|F_P|}\right)^2} \cdot 2|F_P| \; |F_{PH}|$$

with $K = \frac{f_H}{f''_H}$

where f_H represents the real part of the heavy atom structure factor and f''_H, the imaginary one.

A file with $|F_P|$, $|F_{PH}|$, Δan and the corresponding standard deviations (σ_P, σ_{PH}, σ_a) was input to the FHLE program[25] in order to get the F_{HLE} values according to the above equation.

The $|F_{PH}|$ values had previously been calculated as the mean value between the Friedel pairs of reflections ($|F_{PH}(\underline{h})|$ and $|F_{PH}(\bar{\underline{h}})|$) and σ_a was $2.\sigma_{PH}$.

The input value for K was not the theoretical K but the empirical value K_{emp}.

$$K_{emp} = 2\langle||F_{PH}| - |F_P||\rangle / \langle||F_{PH}(\underline{h})| - |F_{PH}(\bar{\underline{h}})||\rangle$$

The use of K_{emp} in the F_{HLE} expression gives a relative weighting for the combination of the anomalous and isomorphous differences and has been used successfully in several analyses[2,4,18].

Figures 3.6 and 3.7 show the plots of K_{emp} against $4\sin^2\theta/\lambda^2$ for both derivatives as well as the theoretical value.

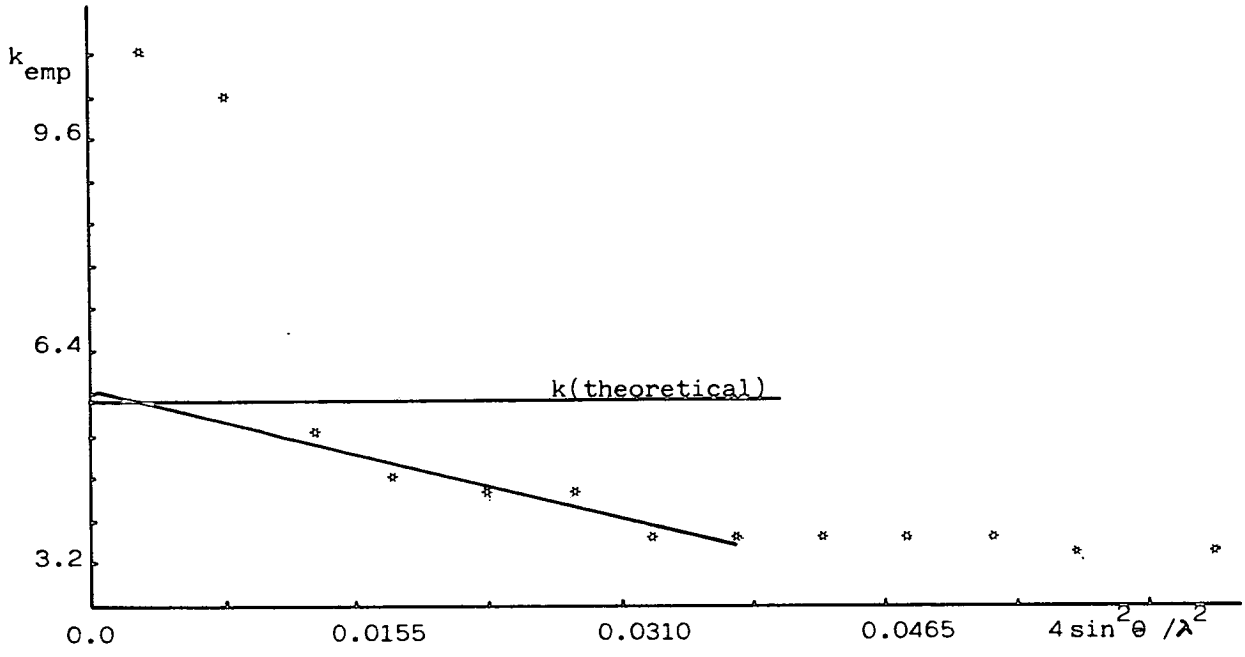

Figure 3.6 Analysis of K_{emp} in ranges of $4\sin^2\theta/\lambda^2$ for the $UO_2(NO_3)_2$ derivative

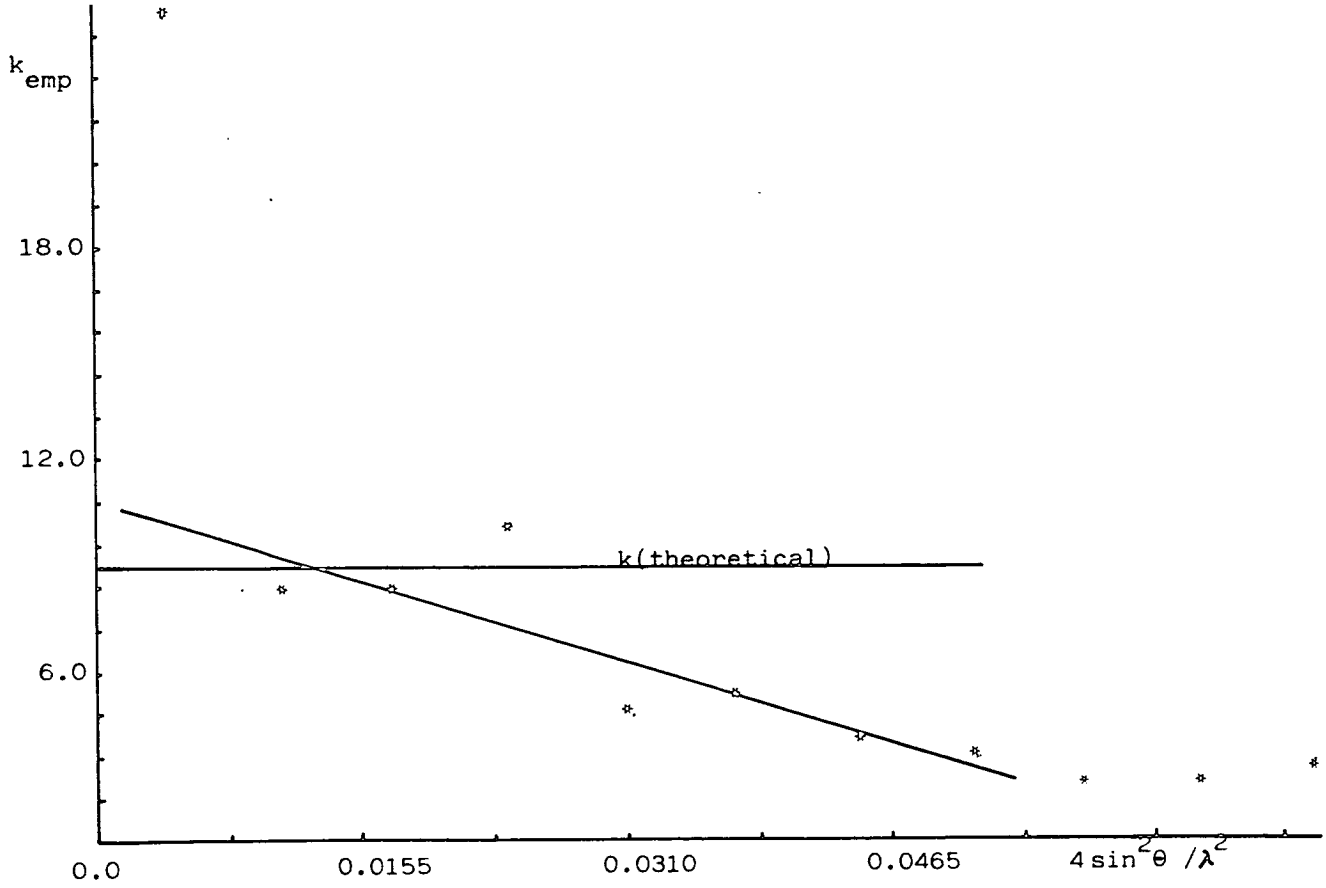

Figure 3.7 Analysis of K_{emp} in ranges of $4\sin^2\theta/\lambda^2$ for the $K_2Pt(NO_2)_4$ derivative

In both derivatives, K_{emp} is less than K indicating that the anomalous differences have been over-estimated.

The values of K_{emp} input to the F_{HLE} calculation were estimated from a line drawn through the averaged values. The reflections were used only when

$$|F_H|\sin(\alpha_{PH} - \alpha_H) \leqslant |F_P|$$

and $$|F_{HLE}| \leqslant ||F_{PH}| - |F_P||_{maxim} \leqslant |F_{HUE}|$$

(F_{HUE} is the heavy atom upper estimate)

and $$|F_P| \gg 0.25 \langle|F_P|\rangle$$

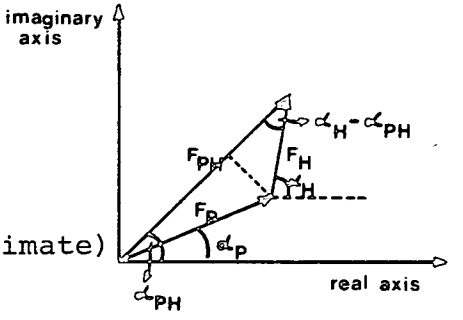

Table 3.5 shows the number of reflections input and output from the F_{HLE} program, the mean value for F_{HLE} and the maximum isomorphous differences for both derivatives.

Table 3.5 Summary of the F_{HLE} calculation

	$UO_2(NO_3)_2$	$Pt(NO_2)_4^=$
Total number of input reflections	1671	1672
Number of output reflections { centric	328	345
Number of output reflections { acentric	500	487
Mean $\|F_{HLE}\|$	80	100
Maximum $\|\|F_{PH}\| - \|F_P\|\|$	370	324

The errors in F_{HLE} were calculated in the following way:

$$\Delta(|F_{HLE}|) = -|F_{HLE}| + \sqrt{F_{HLE}^2 + \sqrt{\sigma^2(F_{HLE}^2)}}$$

where $$\sigma^2(F_{HLE}^2) = \left(\frac{K}{2}\right)^4 (2.\Delta an \,.\, \sigma_a + \sigma_a^2)^2$$

$$+ (2\sqrt{\sigma^2_P + \sigma^2_{PH}}\,||F_{PH}| - |F_P||) + \sigma^2_P + \sigma^2_{PH})^2$$

The expression used for the calculation of the standard deviation is similar to the one suggested by Dodson et al[11].

2.3 The heavy atom positions

The direct methods program MULTAN was used with F_{HLE} values on both derivatives. Unfortunately this did not lead to sites which refined convincingly by the method of Hart[15].

The Patterson Synthesis and Difference Fourier maps were used to get heavy atom coordinates.

2.3.1 Patterson Synthesis

Solutions for the heavy atom coordinates of the uranyl derivative were found using F_{HLE}, isomorphous and anomalous difference Patterson maps. Although the three maps were calculated at the same time, the isomorphous and anomalous Pattersons were used just to check whether the uranium vector peaks were present in all of them.

These maps revealed one single binding site per molecule, close to a special position of the type (2x, x, 1/12) in $P6_122$ or (2x, x, 11/12) in $P6_522$.

Figure 3.8 shows the three Harker sections (w = 1/6, 1/3, 1/2) for the three difference Pattersons calculated for this derivative. Although all of them contain the expected heavy atom vector peaks, the anomalous map is much more noisy than the other ones.

A comparison of the ratios of each heavy atom vector peak to the origin peak in the three different Patterson syntheses has shown that for the isomorphous and anomalous Pattersons, they are approximately 1.3 and 0.8 times those in the F_{HLE} Patterson.

The $K_2Pt(NO_2)_4$ derivative was interpretable in terms of three binding sites found from a difference Fourier map as described in Section 2.4. None of these sites were the same as the uranium site. The Figure 3.9 shows the three Harker sections for this derivative. In this case, the Patterson maps are not so clear as the uranium ones and there are some peaks which have not been explained.

All the maps are to the same arbitrary scale. The height of the origin peak and the contour intervals are marked on the maps.

The Patterson syntheses were calculated using a program written by Dr. M.M. Harding.[14]

Figure 3.8 Heavy atom Patterson functions for the $UO_2(NO_3)_2$ derivative

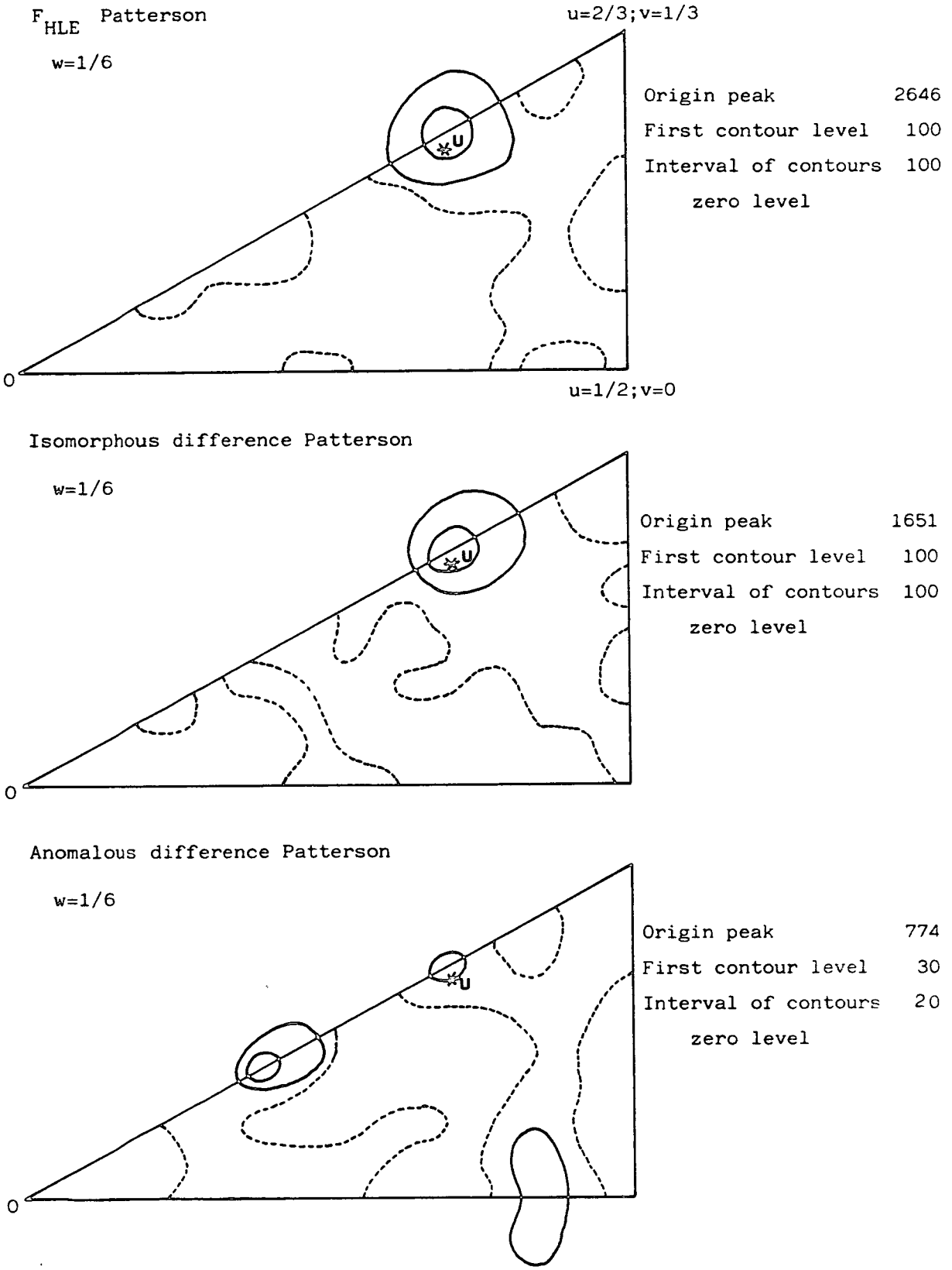

Figure 3.8 (contd.)

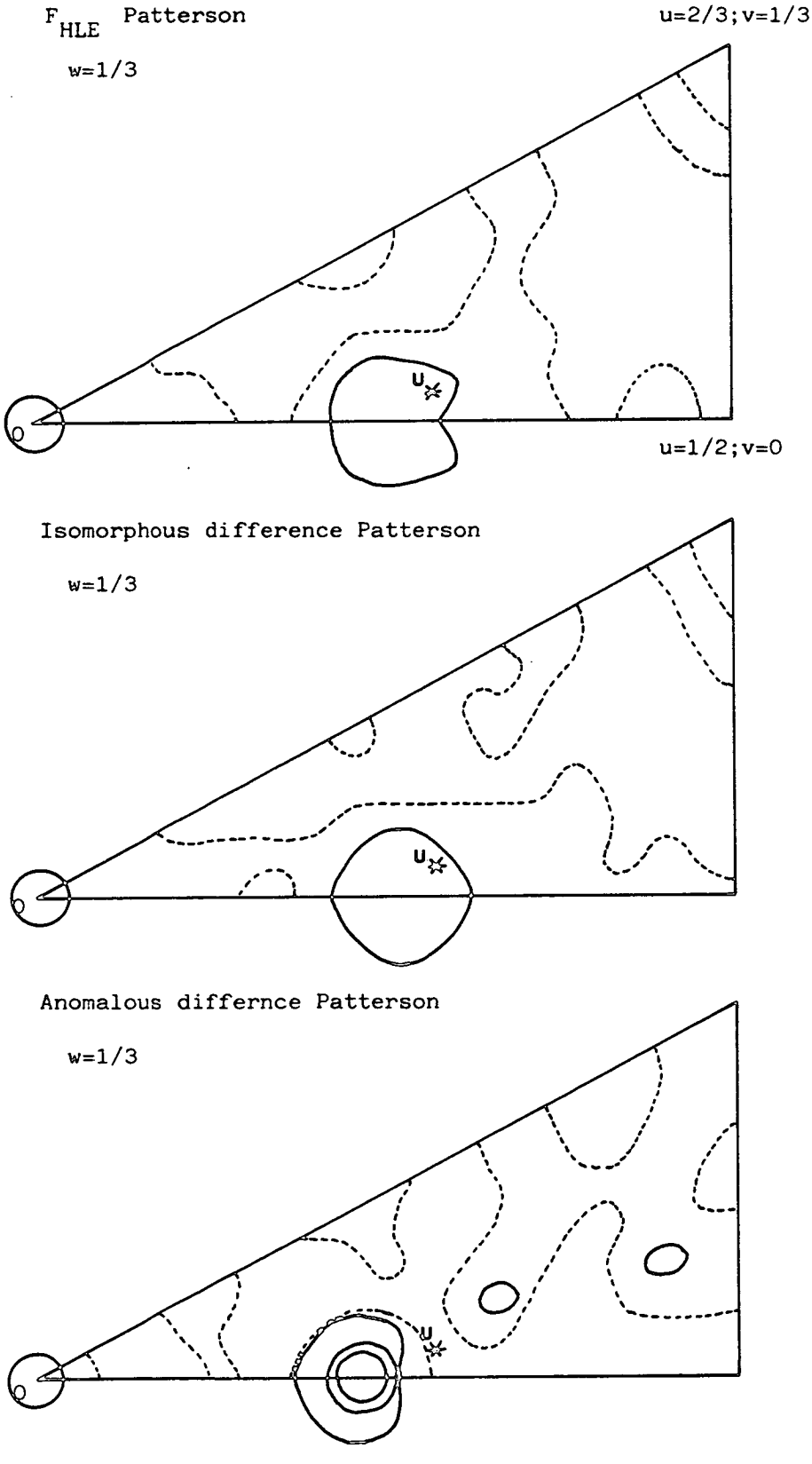

Figure 3.8 (contd.)

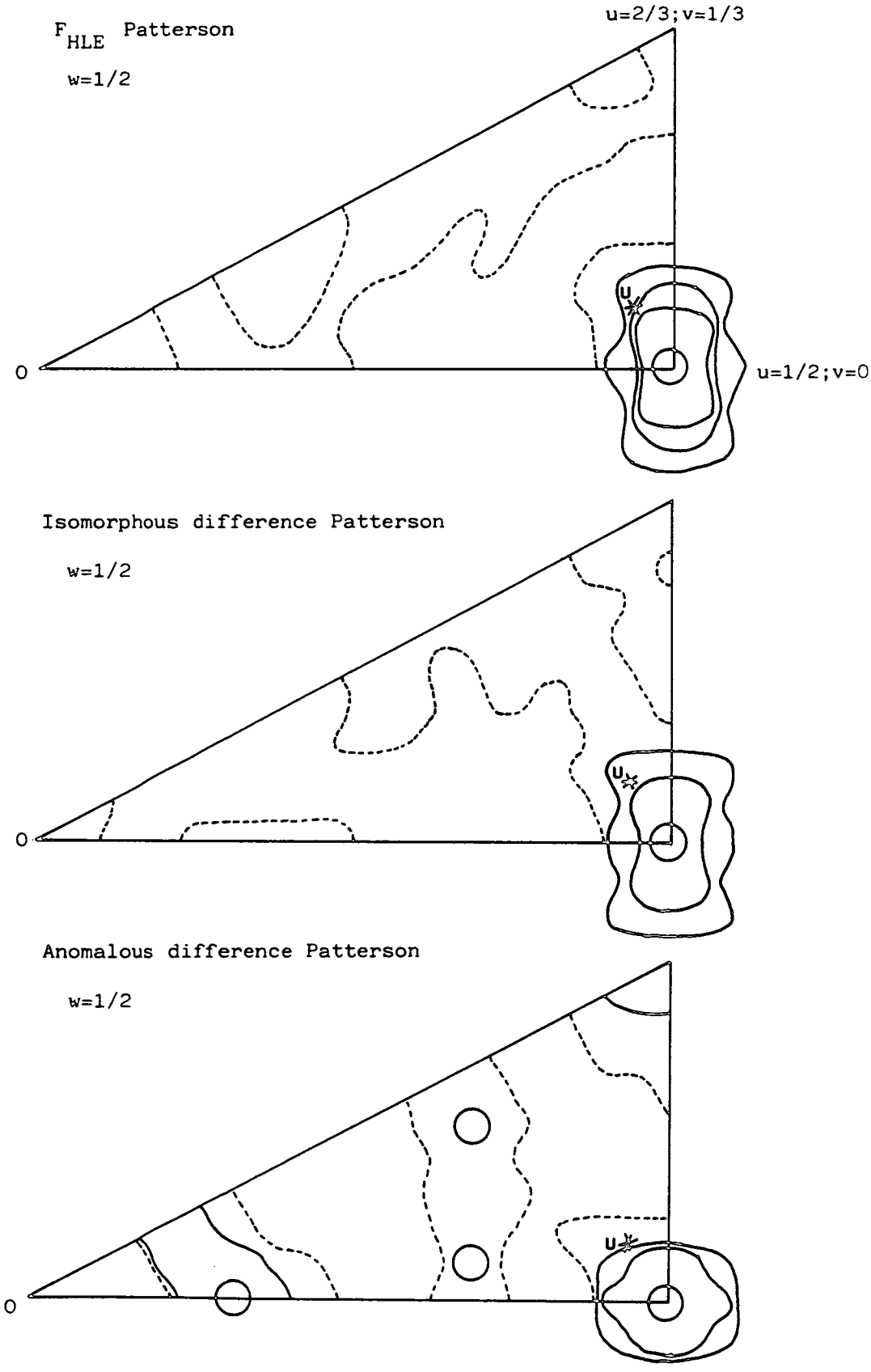

Figure 3.9 Heavy atom Patterson functions for the $K_2Pt(NO_2)_4$ derivative

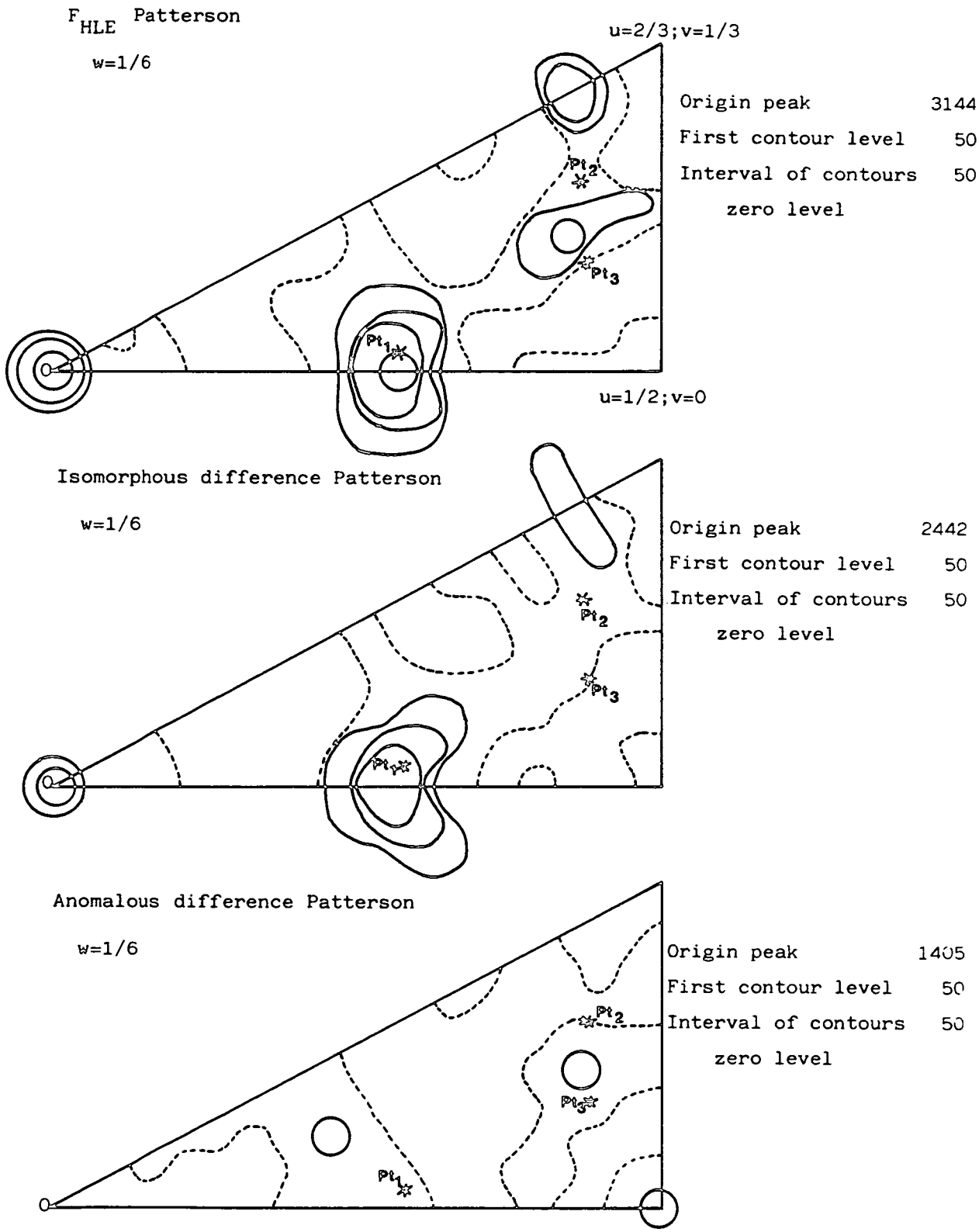

Figure 3.9 (contd.)

F_{HLE} Patterson

w=1/3

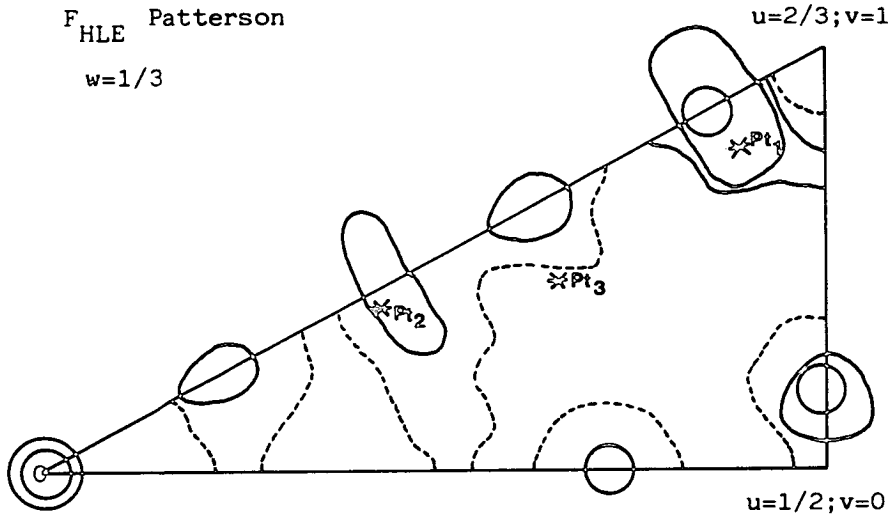

Isomorphous difference Patterson

w=1/3

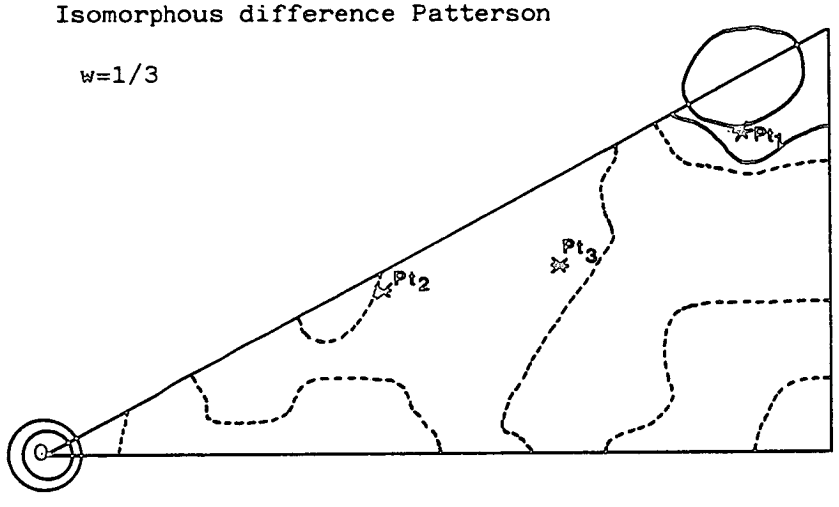

Anomalous difference Patterson

w=1/3

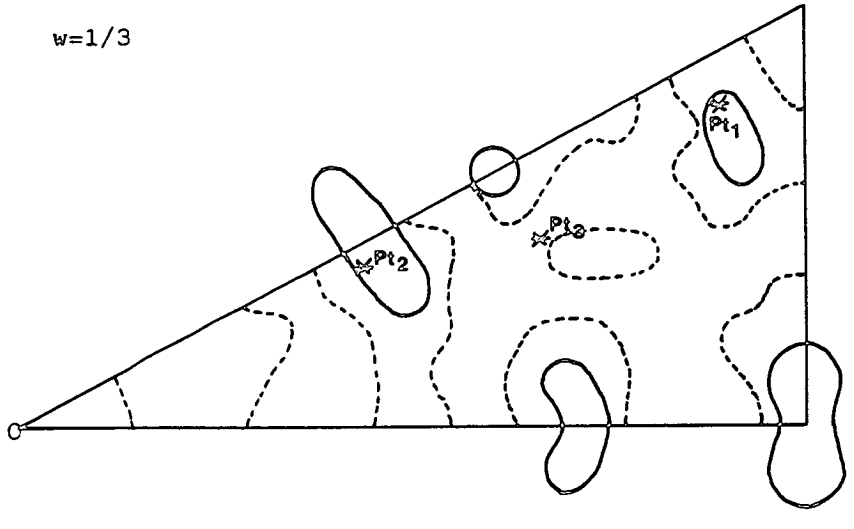

Figure 3.9 (contd.)

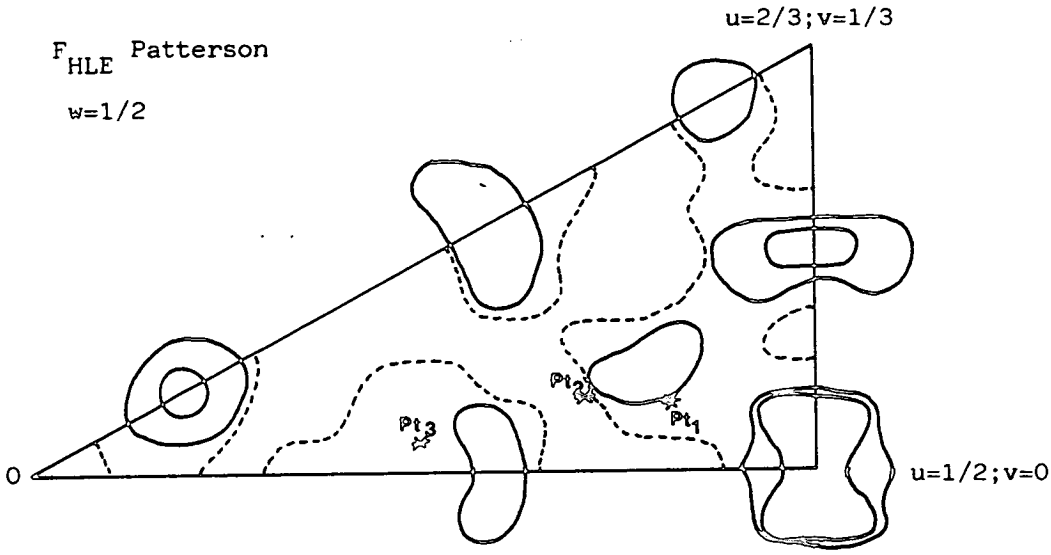

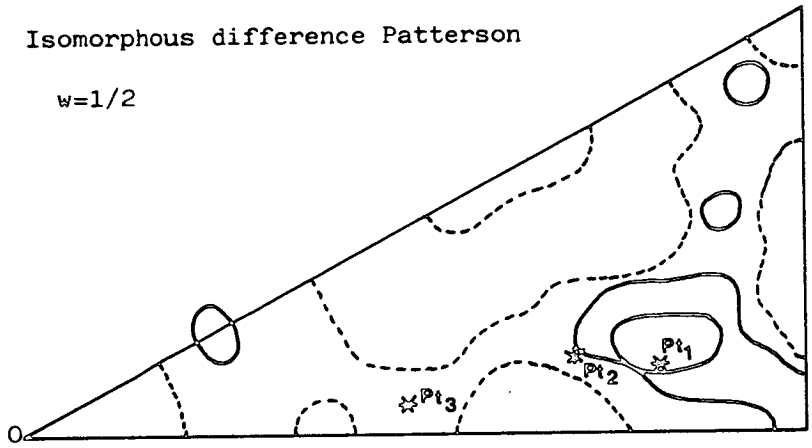

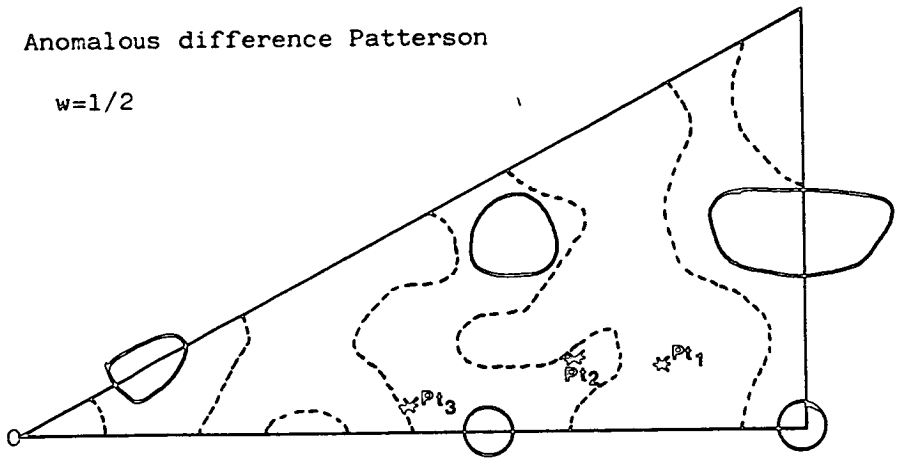

2.4 Difference Fourier Maps

The platinum derivative was solved by calculation of a difference Fourier with coefficients[23]

$$m(|F_{PH}| - |F_P|) \exp(i\alpha_p)$$

where m is the figure of merit associated with the protein phase, α_p (see section 2.6) and $|F_p|$ and $|F_{PH}|$ are the native and derivative structure factor amplitudes.

After refining the uranium site, an estimate of the protein phases was obtained based on the phases for the uranyl derivative alone.

Because there was an ambiguity in the space group, two difference Fourier syntheses were calculated. One based on protein phases calculated from the uranyl derivative with one site at (2x, x, 1/12) and phase relationships based on $P6_122$ space group; the other with protein phases based on one site at (2x, x, 11/12) and phase relationships from $P6_522$ space group.

The $P6_122$ difference Fourier map, revealed several peaks, from which only the coordinates of the largest one, A (about 2.2 $e\text{Å}^{-3}$) refined well. The second highest peak (1.3 $e\text{Å}^{-3}$) corresponds to the uranium input position and was to be expected since the phases were calculated based on that site. All the other peaks had an electron density less than a half of A peak and did not refine.

The $P6_522$ difference Fourier map, shows four big peaks:

	electron density
A (equivalent to A peak in $P6_122$)	2.7 $e\text{Å}^{-3}$
B	1.1
C	1.2
D	1.0

Peaks A, B, C refined well; D did not refine and is at the uranium atom position.

2.5 Refinement of heavy atom parameters

Heavy atom positions and occupancy were refined using all the data and minimizing the quantity M

$$M = \Sigma W(|F_{HLE}| - |F_H \text{ calc}|)^2$$

where the sum is extended to all the reflections and W was assigned as:

$$W = \frac{1}{\sigma(F^2_{HLE})}$$

During the refinement, x, y and z coordinates were allowed to vary as well as the site occupancies. The derivative to native scale factor and the overall temperature factor were fixed.

The agreement between F_{HLE} and F_H calc. values was monitored using:

$$\text{(i)} \quad R(F_{HLE}) = \frac{\Sigma\{||F_{HLE}| - |F_H \text{ calc}||\}}{\Sigma|F_{HLE}|}$$

$$\text{(ii)} \quad WR(F_{HLE}) = \frac{\Sigma\{W(|F_{HLE}| - |F_H \text{ calc}|)\}^2}{\Sigma F_{HLE}^2}$$

(iii) The slope of $\sqrt{\langle|F_H \text{ calc}|\rangle^2}$ against $\langle|F_{HLE}|\rangle$, where the mean values were calculated in different ranges of $\sin^2\theta$.

Table 3.6 shows the parameters (i), (ii) and (iii) at the end of refinement.

Table 3.6 The agreement between F_{HLE} and F_H calc

Refinement index		Uranium	Platinum		
		1 site	1 site	2 sites	3 sites
R		53.9%	58.2%	57.4%	56.5%
WR		38.1%	44.4%	40.9%	39.1%
slope		0.32	0.25	0.25	0.27
Number of reflections	centric	339		361	
	acentric	479		470	

These values are in good agreement with the ones used for other protein structure studies[10].

The final parameters from the refinement are given in Table 3.7.

Table 3.7 The heavy atom sites after the F_{HLE} refinement

	B_{ov}	site	x	y	z	occu-pancy	B($\AA^{-2}$)
$UO_2(NO_3)_2$	1.13	1	0.4797(8)	0.2248(10)	-0.0771(2)	0.32(1)	15
$Pt(NO_2)_4^{=}$	-2.0	1	0.7011(10)	-0.9765(11)	0.0217(3)	0.42(1)	15
		2	0.8069(31)	0.3379(29)	0.0367(6)	0.15(1)	15
		3	0.3833(40)	0.4889(41)	0.0272(8)	0.11(1)	15

The uranium site was not treated as being on the two-fold axis and the occupancy is as for a general position (two symmetry related U atoms would be 2.9 $\AA$ apart).

2.6 Phasing

After finding the phases of the heavy-atom contribution, α_H, it is possible to estimate the protein phases using the expressions[5]

$$\sin(\alpha_{PH} - \alpha_H) \simeq \frac{|F_{PH}(\underline{h})| - |F_{PH}(\bar{\underline{h}})|}{2f''_H}$$

$$\text{and } \cos(\alpha_{PH} - \alpha_H) = \frac{-F_P^2 + F_{PH}^2 + F_H^2}{2|F_{PH}|.|F_H|}$$

Combining both expressions, $(\alpha_{PH} - \alpha_H)$ is determined and the angle α_P can be found from the vector triangle defined by $F_P(\underline{h})$, $F_{PH}(\underline{h})$ and $F_H(\underline{h})$.

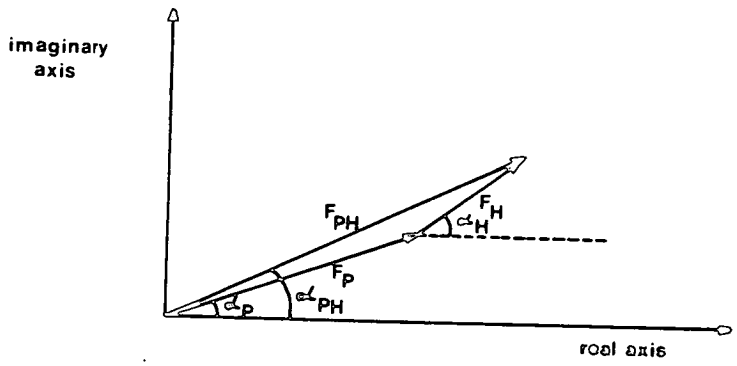

The errors in the protein phases, α_P, are expressed by the figure of merit m and by the Dickerson factor (m.r.e.).

$$m = \frac{\int_{\alpha=0}^{2\pi} P(\alpha)\ \exp(i\alpha)\ d\alpha}{\int_{\alpha=0}^{2\pi} P(\alpha)\ d\alpha}$$

where $P(\alpha)$ is the probability that a phase angle α for the protein structure is correct[6].

$$P(\alpha) = \exp(-\Sigma_j\ \epsilon_j^2(\alpha)/2\ E_j^2),$$

the sum being extended to all the derivatives

$$\epsilon_j = |F_{PH}(\text{obs.})| - |F_{PH}(\text{calc.})|$$

E_j is the total error resulting from inaccuracies in the determination of F_P and F_{PH} amplitudes; the errors in positional, occupancy and thermal parameters attributed to the heavy atoms as well as the lack of isomorphism.

This error can be estimated from a centrosymmetric projection by the expression[3]

$$\langle E_j^2 \rangle = \langle (||F_{PH}| \pm |F_P|| - |F_H|)^2 \rangle$$

Hence, m is the mean value of the cosine of the error in phase angle for a reflection.

The Dickerson factor[8] is defined as

$$\text{m.r.e.} = \sum_j \frac{\epsilon_j^2}{2E_j^2}$$

where the summation is for all derivatives. If E_j values were correctly estimated then $\langle \epsilon_j^2 \rangle = E_j^2$ and m.r.e. = n · 0.5, where n represents the total number of derivatives.

Phase sets based on the uranium site, on the platinum sites and both platinum and uranium were calculated using the phase relationships for the space groups $P6_122$ and $P6_522$.

Mean figures of merit and Dickerson factors divided by the number of derivatives, for these calculations are compared in Table 3.8.

Table 3.8 The mean figures of merit and Dickerson factors for the native data when phased on the uranyl, platinum or both sites.

	U $P6_522$	U $P6_122$	Pt $P6_522$	Pt $P6_122$	U+Pt $P6_522$	U+Pt $P6_122$
M	0.667	0.667	0.525	0.525	0.744	0.735
m.r.e./n	0.27	0.28	0.25	0.25	0.72	0.69

The mean figure of merit for phases calculated from both derivatives is slightly better in $P6_522$ than $P6_122$, although the difference is not significant.

The variation of m with the m.r.e. in a two derivative refinement[8] is shown in Table 3.9.

Table 3.9 The variation of the mean figure of merit with the Dickerson factor.

	m	m.r.e./n
E_j chosen properly	0.46	0.56
$2.E_j$	0.26	0.14
$E_j/2$	0.59	2.18

Figure 3.10 show the variation of m with $|F_P|$ and $4(\sin\theta/\lambda)^2$ for the (U+Pt) $P6_522$ phase set, indicating that the larger protein structure amplitudes and the smaller $\sin\theta$ values tend to have a larger value of m.

2.7 The space group ambiguity

In order to decide in which space group cytochrome c_4 crystallizes, several difference Fourier maps with coefficients $m(|F_{PH}| - |F_P|) \exp(i\alpha_P)$ were calculated.

Protein phases were calculated based on each derivative and Fourier maps were computed for $P6_122$ and $P6_522$.

Figure 3.10 The mean figure of merit for the protein phases when the data was phased on both derivatives

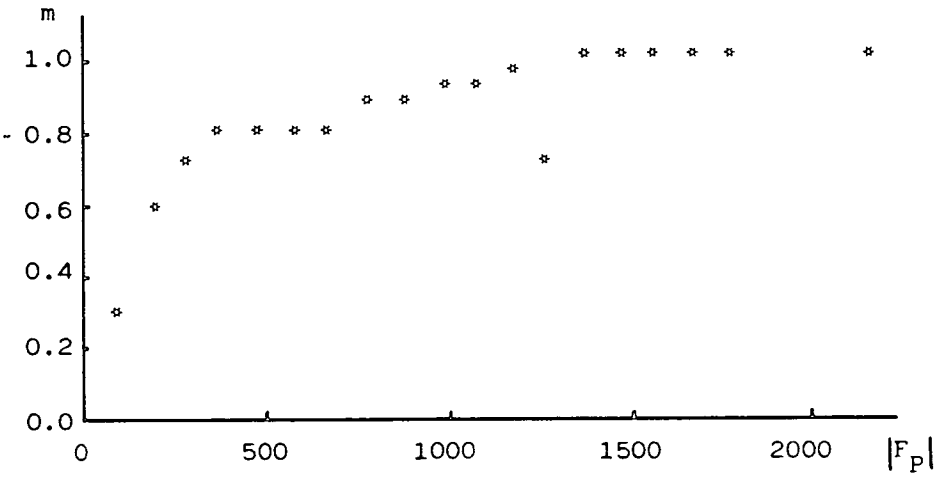

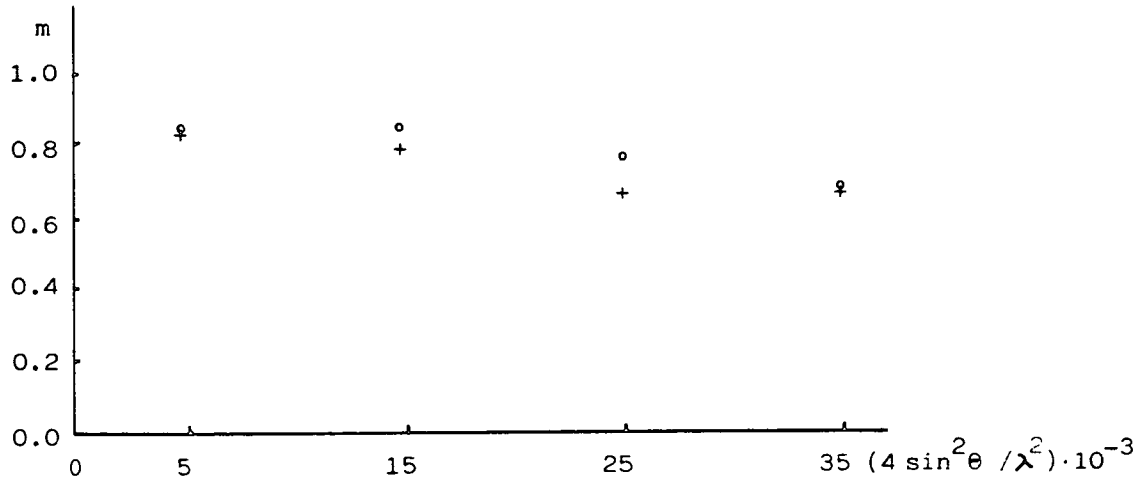

o centric reflections

\+ acentric reflections

Apart from obtaining the uranium positions from phases based on the platinum sites and vice-versa, these maps gave a clear indication of $P6_522$ as being the correct space group.

Table 3.10 gives a summary of the peak heights for the four heavy atom sites in the difference Fourier syntheses.

Table 3.10 The heavy atom sites in different difference Fouriers.

Difference Fourier $m(\|F_{PH}\| - \|F_P\|) \exp(i\alpha_P)$				Observed peak heights (e. Å^{-3} units)		
F_{PH},	α_P,	space group	U	Pt_1	Pt_2	Pt_3
$K_2Pt(NO_2)_4$,	U,	$P6_522$	-	2.7	1.1	1.2
$K_2Pt(NO_2)_4$,	U,	$P6_122$	-	2.2	0.9	0.7
$UO_2(NO_3)_2$,	Pt,	$P6_522$	2.3	-	-	-
$UO_2(NO_3)_2$,	Pt,	$P6_122$	2.1	-	-	-
$UO_2(NO_3)_2$,	U,	$P6_522$	3.7	-	-	-
$UO_2(NO_3)_2$,	U,	$P6_122$	3.3	-	-	-

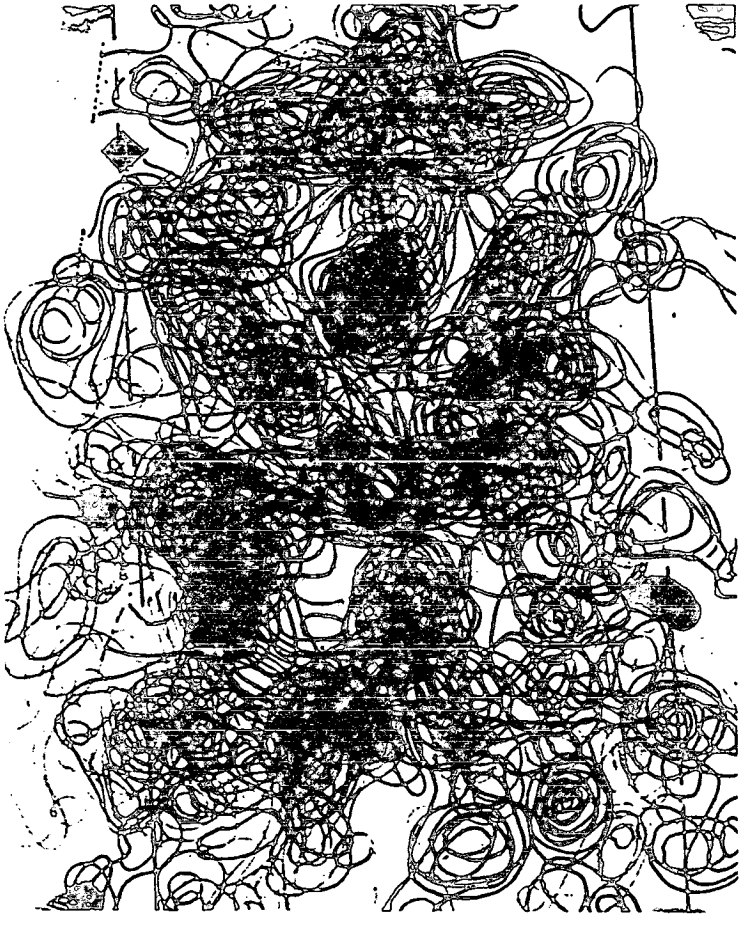

Figure 3.11 The electron density map at 5 Å resolution of cytochrome c_4 showing the 2 "halves" of the molecule. The parallel lines represent the dyad axes at z = 1/12, which are 31.2 Å apart (a/2). The 6_5 screw axis is seen as a series of circules to the right. One UO_2^{2+} site is shown as a square on the dyad. Only 1 asymmetric unit has been plotted in order to emphasize the molecular boundary which, for the most part, is well-defined. The electron density contours are at equal, arbitrary intervals.

3. The 5 Å electron density map

An electron density map for the native protein in space group $P6_522$ was calculated using terms $m|F_p|\exp(i\alpha_p)$. Ten sections of spacing $\Delta Z = 174.2/120$ Å along the c axis were output, with an interval of 62.4/30 Å along a and b.

The map reveals a bi-lobed structure with dimensions about 60 x 30 x 35 Å which compares well with the dimensions already found for other small cytochromes c - 30 x 35 x 35 Å [9,17,21,24,26].

The molecular boundary is fairly clear for most of the molecule which is shown in Figure 3.11.

The haem groups can be seen to the upper left and lower right of the molecule but, surprisingly, a third dense region is close by one of them.

The haem group is flanked by rods of density, which by comparison with other cytochromes c are most probably helix.

4. The iron positions

Since one of the Fe positions was not clear it was decided to attempt to use the anomalous scattering of Fe to find these positions. For CuK_α radiation the imaginary component of the atomic scattering factor for iron is 3.4 ($\sin\theta/\lambda = 0$) and 3.3 ($\sin\theta/\lambda = 0.4$); for sulphur these values are 0.6. So, it is expected that the Fe atoms will be the major contributors for the anomalous differences which were measured in the native data.

To measure the amount of the anomalous contribution in the native data set relative to experimental error, an R-factor defined as

$$R = \frac{\Sigma_{\underline{h}} |\Delta an|}{\Sigma_{\underline{h}} |F(\underline{h})|}$$

was calculated. For the centric reflections, where Δan should be 0, R = 0.113 and for the acentric reflections R = 0.147.

A Fourier synthesis with coefficients

$$|\Delta an| \exp i(\alpha_p \pm 90^o)$$

was calculated, where α_p are the calculated protein phases. The positive sign was applied when Δan was negative and vice-versa. This procedure was based on the assumption that the anomalous differences are significant only when the Fe atoms are scattering nearly 90^o out of phase with the protein. The map had several peaks of the same height and led to no conclusions about the Fe positions.

A Patterson synthesis based on the native anomalous data for the non-centric reflections appeared to be very noisy and no explanation was found for all the peaks. These results suggest that the native anomalous data is not sufficiently accurate, and no more work was done with it.

Finally a new 5 Å map was calculated with phases based on three $K_2Pt(NO_2)_4$ sites and two instead of one $UO_2(NO_3)_2$ sites. The new $UO_2(NO_3)_2$ site was found using 3 Å data for

both native and derivative. Details of data collection and refinement are given in Chapter 4.

After the phase calculation, for the 851 input reflections, the mean figure of merit was 0.797 and there were 411 reflections with a figure of merit ≥ 0.9. Table 3.11 shows the number of reflections and the mean figure of merit in ranges of 0.02 Å^{-2} in $4\sin^2\theta/\lambda^2$.

Table 3.11 The number of reflections and the mean figure of merit in ranges of $4\sin^2\theta/\lambda^2$.

Range of $4\sin^2\theta/\lambda^2$	Reflections					
	centric		acentric		total	
	Fig. merit	number	Fig. merit	number	Fig. merit	number
0.0 - 0.02	0.912	168	0.857	150	0.886	318
0.02 - 0.04	0.814	180	0.709	353	0.745	533

Figure 3.12 shows the variation of the figure of merit with the structure factor amplitude $|F_p|$. As expected, reflections with large $|F_p|$ and small $\sin\theta$ values have larger figures of merit.

The electron density map was calculated in sections along the $\underline{c}$ axis showing the whole $\underline{a}$ and $\underline{b}$ axes. The intervals were $|\underline{a}|/60$ Å, $|\underline{b}|/60$ Å and $|\underline{c}|/180$ Å.

This map was more clear than the previous one and this time the Fe positions could be confidently assigned to the two largest peaks in the map. Their positions are:

(32.5/60; 32.5/60; 3/180)

(32.5/60; 54/60; 15/180)

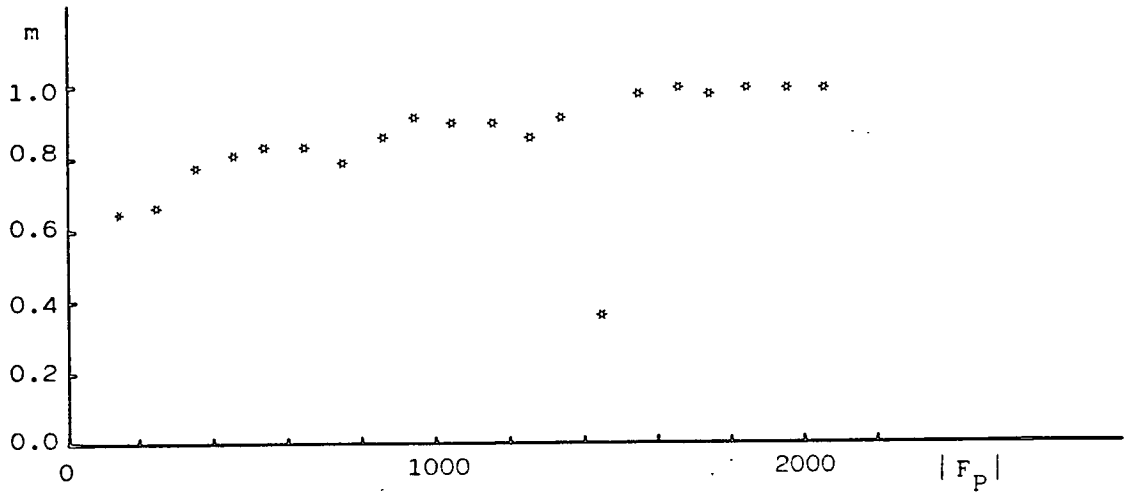

Figure 3.12 The variation of the figure of merit with the structure factor amplitude

References

1. Ambler, R.P., Murray, S., Biochemical Society Transactions, 531st Meeting, Lancaster, 1973.

2. Arnone, A., Bier, C.J., Cotton, F.A., Day, V.W., Hazen, E.E., Richardson, J.S., Yonath, A., J.Biol.Chem., 246, 2302-2316, 1971.

3. Blow, D.M., Crick, F.H.C., Acta Cryst., 12, 794-802, 1959.

4. Blundell, T.L., Dodson, E.J., Dodson, G.G., Hodgkin, D.C., Vijayan, M., Comtemporary Phys., 12, 209, 1971.

5. Blundell, T.L., Johnson, L.N., "Protein Crystallography", pg.364, Academic Press, London, 1976.

6. Blundell, T.L., Johnson, L.N., Reference 5, pg.368.

7. Coulson, A.F.W., Oliver, R.K., Biochem.J., 181, 159-169, 1979.

8. Dickerson, R.E., Weinzierl, J.E., Palmer, R.A., Acta Cryst., B24, 997-1003, 1968.

9. Dickerson, R.E., Takano, T., Eisenberg, D., Kallai, O.B., Samson, L., Cooper, A., Margoliash, E., J.Biol.Chem., 246, 1511-1535, 1971.

10. Dodson, E.J., A comparison of different methods of refinement, "Computing methods for crystallography", Ahmed, F. Munksgaard, 1975.

11. Dodson, E.J., Evan, P.R., French, S., "Anomalous scattering", pg. 423, Ramasesham and S.C. Abrahams, Munksgaard, Copenhagen, 1975.

12. Evans, P., "ANSC. Derivative scale analyser and scaler", 1977.

13. Harding, M.M., D.Phil. Thesis, Oxford University, 1962.

14. Harding, M.M., "P6/MMM PATTERSON".

15. Hart, R.G., Acta Cryst., 14, 1194-1195, 1961.

16. Kartha, G., Parthasarathy, R., Acta Cryst., 18, 745-749, 1965.

17. Korzun, Z.R., Salemme, F.R., Proc.Natl. Acadm.Sci., U.S.A., 74, 5241-5247, 1977.

18. Matthews, B.W., Acta Cryst., 20, 230-239, 1966.

19. Matthews, B.W., J.Mol.Biol., 33, 491-497, 1968.

20. North, A.C.T., Phillips, D.C., Mathews, F.S., Acta Cryst., A24, 351-355, 1968.

21. Salemme, F.R., Freer, S.T., Xuong, N.G.H., Alden, R.A., Kraut, J., J.Biol.Chem., 248, 3910-3921, 1973.

22. Singh, A.K., Ramasesham, S., Acta Cryst., 21, 279-280, 1966.

23. Stryer, L., Kendrew, J.C., Watson, H.C., J.Molec.Biol., 8, 96-104, 1964.

24. Takano, T., Trus, B.L., Mandel, N., Mandel, G., Kallai, O.B., Swanson, R., Dickerson, R.E., J.Biol.Chem., 252, 776-785, 1977.

25. Tickle, I., "FHLE program", 1977.

26. Timkovich, R., Dickerson, R.E., J.Biol.Chem., 13, 4033-4046, 1976.

CHAPTER FOUR

CHAPTER FOUR

The Cytochrome c_4 three-dimensional structure at 3.5 Å resolution

1. Data collection to a resolution of 3 Å

Derivatives of $UO_2(NO_3)_2$ and $K_2Pt(NO_2)_4$ were prepared for the data collection using the procedures described in Chapter Three.

Native and $UO_2(NO_3)_2$ derivative data sets were recorded on the Enraf-Nonius rotation camera at the Department of Biochemistry of Bristol University. The camera was fitted with a graphite monochromator and supplied by a 40 mA, 40 kV high intensity x-ray tube (λ = 1.54182 Å).

The $K_2Pt(NO_2)_4$ derivative data were collected by Dr. L. Sawyer in the Biochemistry Department of the University of Alberta in Canada. The data were recorded on a Ni-filtered rotating anode tube run at 40 mA, 40 kV.

Figures 4.1 and 4.2 show the geometry of the rotation camera. The crystal rotates about one axis normal to the X-ray beam in order to bring the reciprocal lattice points into a reflection position (Figure 4.1). The reflections which cut the sphere of reflection are recorded on a flat film (Figure 4.2). Three-dimensional data are collected by taking a series of oscillation photographs with small angular range until the whole unique volume of the reciprocal lattice is recorded.

Figure 4.1 Geometry of the rotation camera. The reciprocal lattice points are brought into a reflecting position by a rotation about the rotation axis

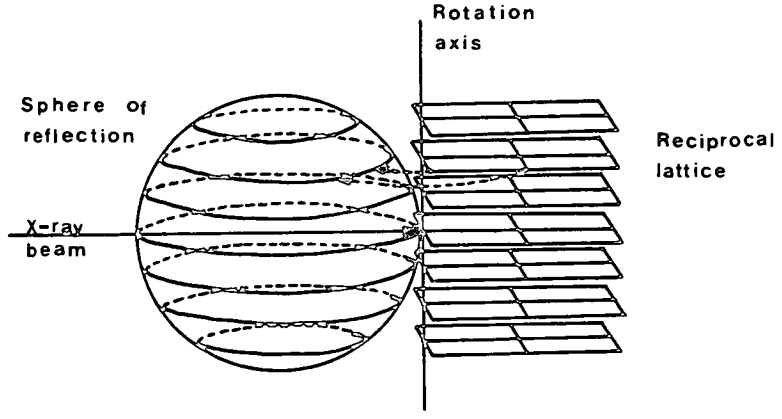

Figure 4.2 The reflections are recorded onto a flat film

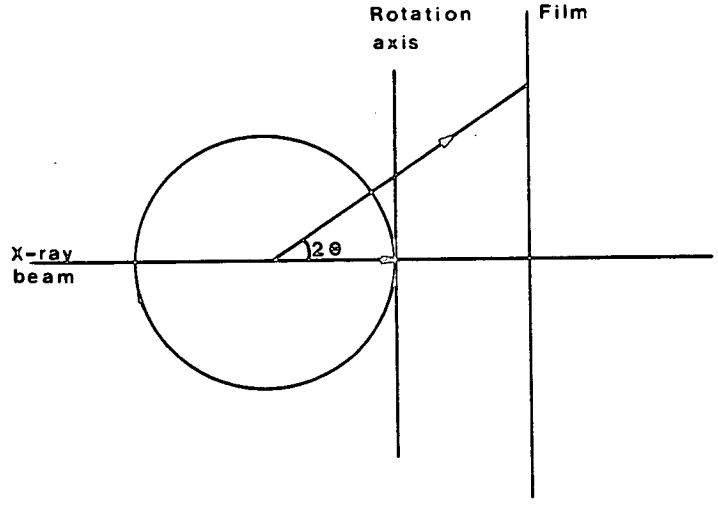

A graphical estimate of the rotation angle necessary to record one unique set of data from one crystal of class 622 mounted along the six-fold axis is shown in Figure 4.3. The figure representing the (hkiO) zone shows the area of reciprocal space which will pass through a reflecting position as the Ewald sphere rotates through an angle of 21^{o}. Reflections (hkil) and its Friedel related ($hki\bar{l}$) are recorded on the same film as shown in Figure 4.4. Then, a rotation of 21^{o} is enough to record one unique set of data with a resolution of 3 Å.

Using equivalent constructions, the calculated rotation angles for different resolutions are:

Resolution	Rotation angle
5.0 Å	16^{o}
4.0 Å	18^{o}
3.0 Å	21^{o}

The rotation angle for each film was chosen so that a maximum number of reflections was recorded on each film with a small amount of overlap.

According to Blundell and Johnson[5] and Arndt and Wonacott[3] the maximum angle which avoids overlap is given by:

$$\Delta\phi = \frac{p^*}{dm^*} - \Delta$$

where p* is the reciprocal lattice spacing which is likely to cause overlap, dm*is the maximum resolution in reciprocal space and Δ is the angular range over which a crystal diffracts when rotated through the Bragg position ($\Delta \approx 0.7^{o}$).

Figure 4.3 Projection down the six-fold axis showing the area of reciprocal space swept out as the crystal is rotated through 21°

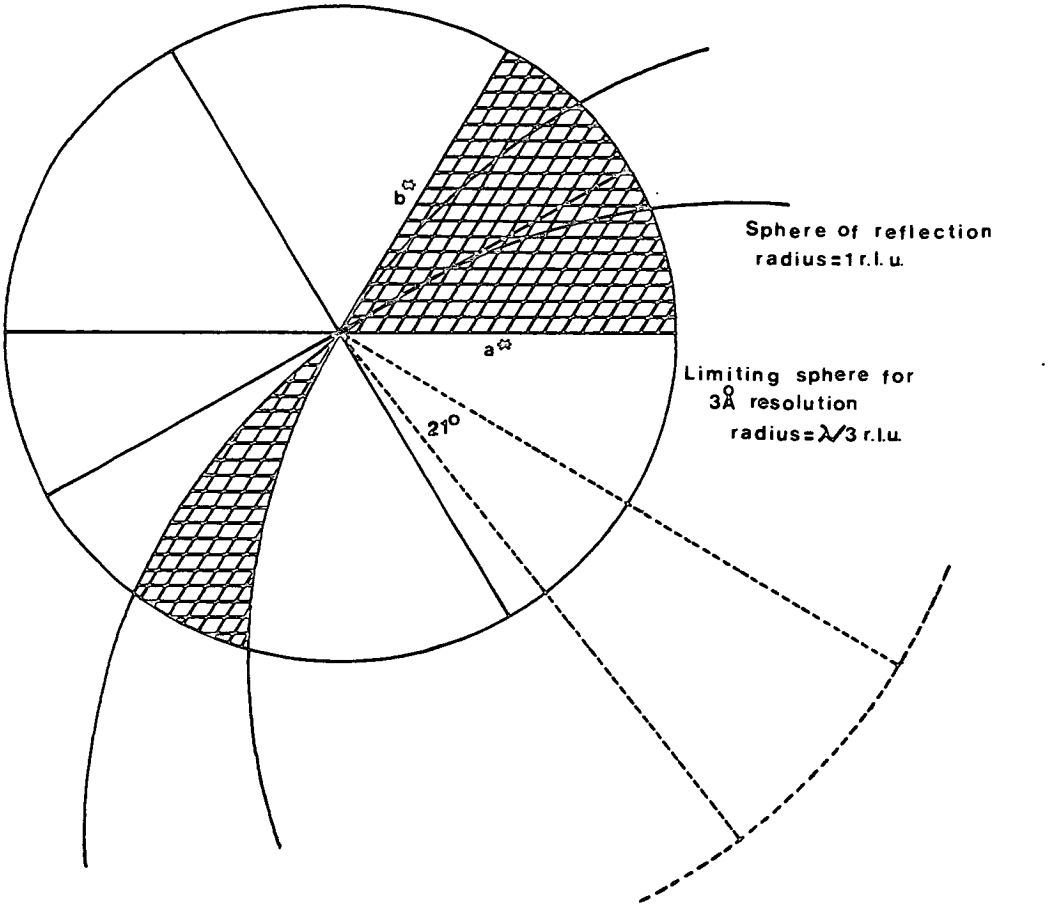

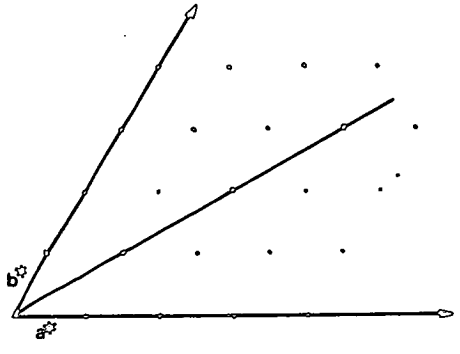

$(h0\bar{h}l)$, $(0k\bar{k}l)$, $(hh2\bar{h}l)$ are mirror planes in the diffraction pattern

In our case, these values are:

$$p^* = a^* = \frac{\lambda}{62.4 \cdot \sin 60^\circ}$$

$$dm^* = \frac{\lambda}{3}$$

$$\Delta\phi = 3.18 - 0.7 = 2.48^\circ$$

All the data were collected in 3.0° intervals of the rotation angle on two film packs.

The choice of a distance from crystal to film, F, was based on the two following criteria:

(i) The film radius, given by $F \tan 2\theta_{max}$ should not be greater than 55 mm. Since the resolution dm and the maximum Bragg angle θ_{max} are related by

$$dm = \frac{\lambda}{2\sin\theta_{max}}$$

to obtain a resolution of at least 3 Å at the edge of the film, $\theta_{max} = 15^\circ$ and F should be at most 95 mm.

(ii) The distance between the centres of adjacent spots along $\underline{c}^*$ should be at least 0.7 mm. According to the equations

$$2\,\frac{\sin\theta}{\lambda} = 1\,c^*$$

$$\tan 2\theta = \frac{R_f}{F}$$

where R_f is the distance between one spot and the centre of the film, the distance F should be at least 76 mm.

From the above results, it was decided that the crystal to film distances should be approximately 90 mm. The crystal to film distances used for the collection of the three data sets were as follows:

native	90.3(5) mm
$K_2Pt(NO_2)_4$ derivative	88.0(1) mm
$UO_2(NO_3)_2$ derivative	90.0(1) mm

All the data sets were collected over an oscillation range of 21 degrees. In the $UO_2(NO_3)_2$ derivative, as the crystal was accidentally mounted along an axis 30° away from c^*, some data were lost and the Friedel pairs were not recorded on the same film, greatly increasing the errors in the anomalous differences.

Figures 4.4, 4.5 and 4.6 show graphic representations of three rotation photographs from the native and derivative crystals.

2. Data Processing

2.1 The positions of reflected spots on the film

It is convenient to refer the reciprocal lattice axes to an orthogonal system (X, Y, Z), where Z is parallel to the rotation axis and X is parallel to the X-ray beam (Figure 4.7).

Figure 4.4 A graphic plot of a rotation photograph of the native crystal. The rotation axis c is horizontal and the lower region of the photograph shows part of the (hh2$\bar{h}$l) zone

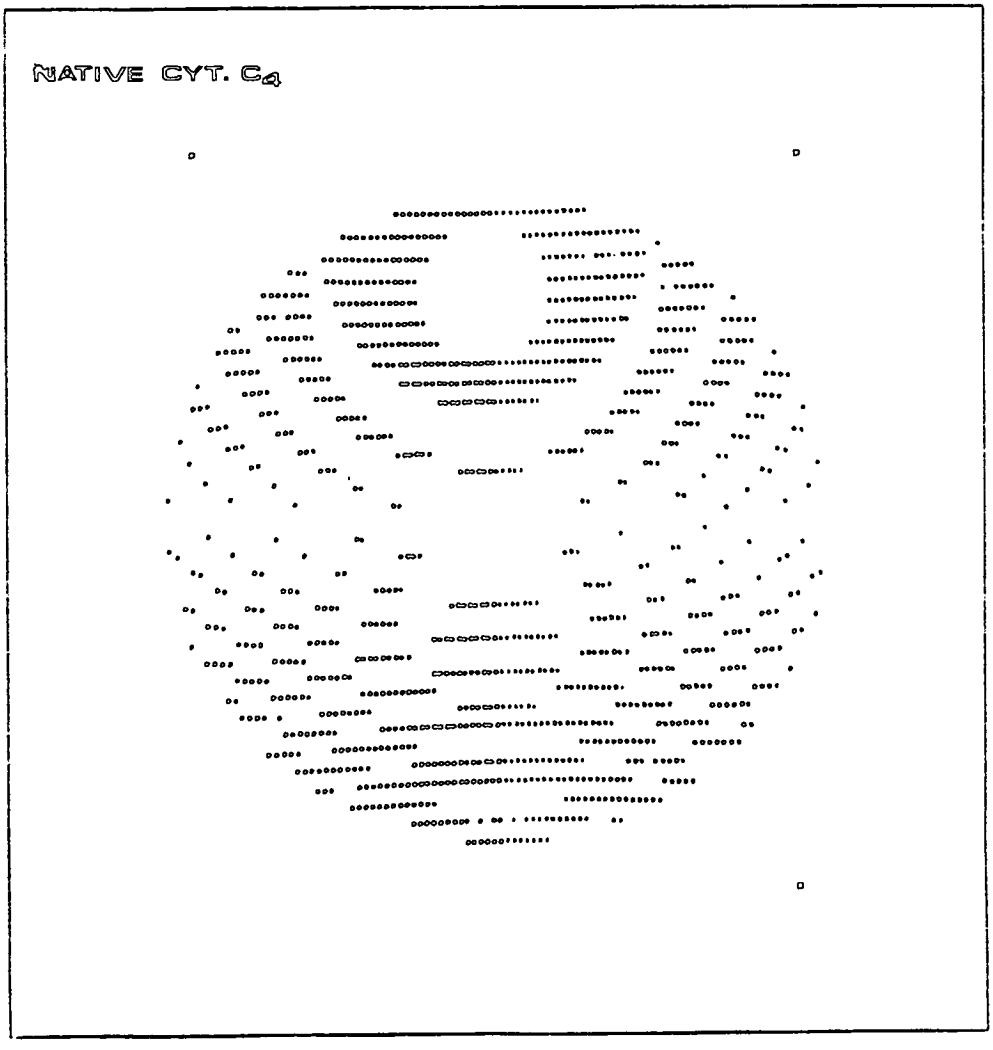

Figure 4.5 A graphic plot of a rotation photograph of the $UO_2(NO_3)_2$ derivative crystal

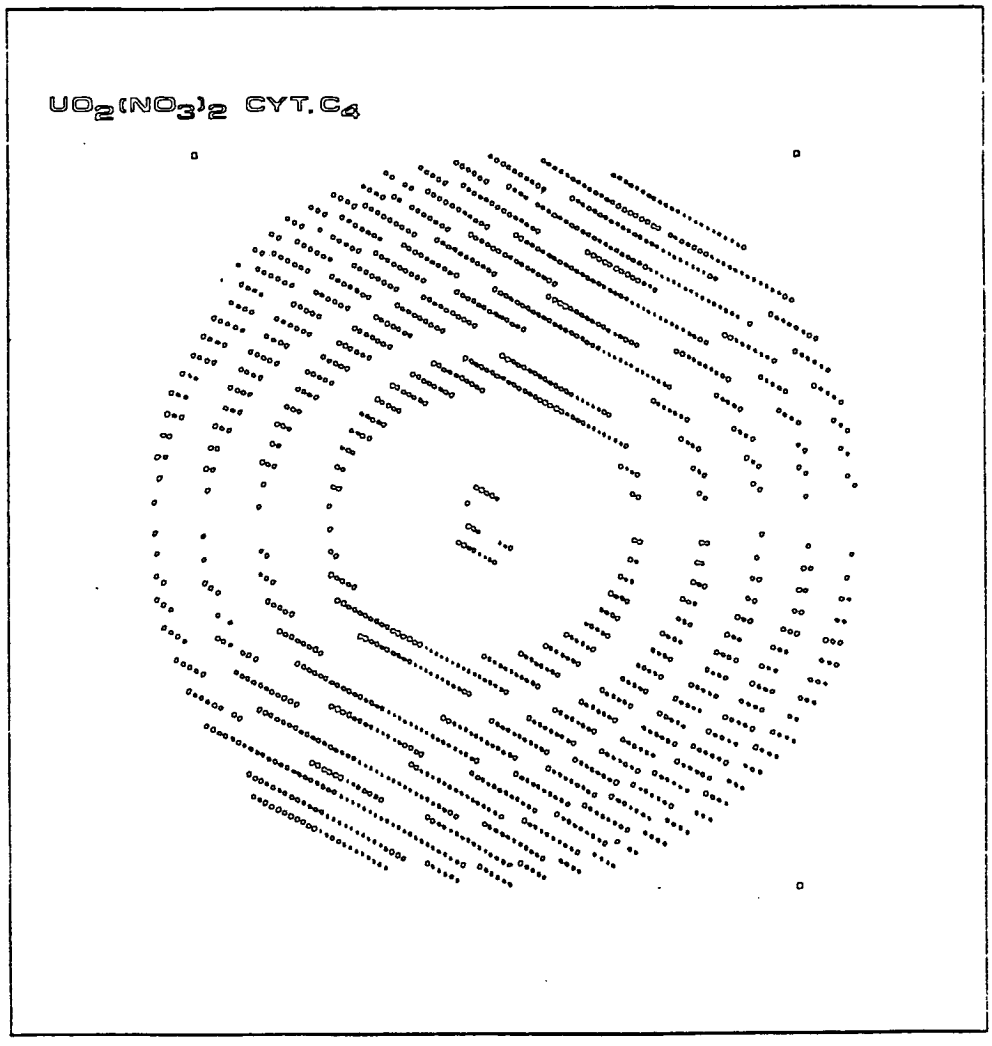

Figure 4.6 A graphic plot of a rotation photograph of the $K_2Pt(NO_2)_4$ derivative crystal

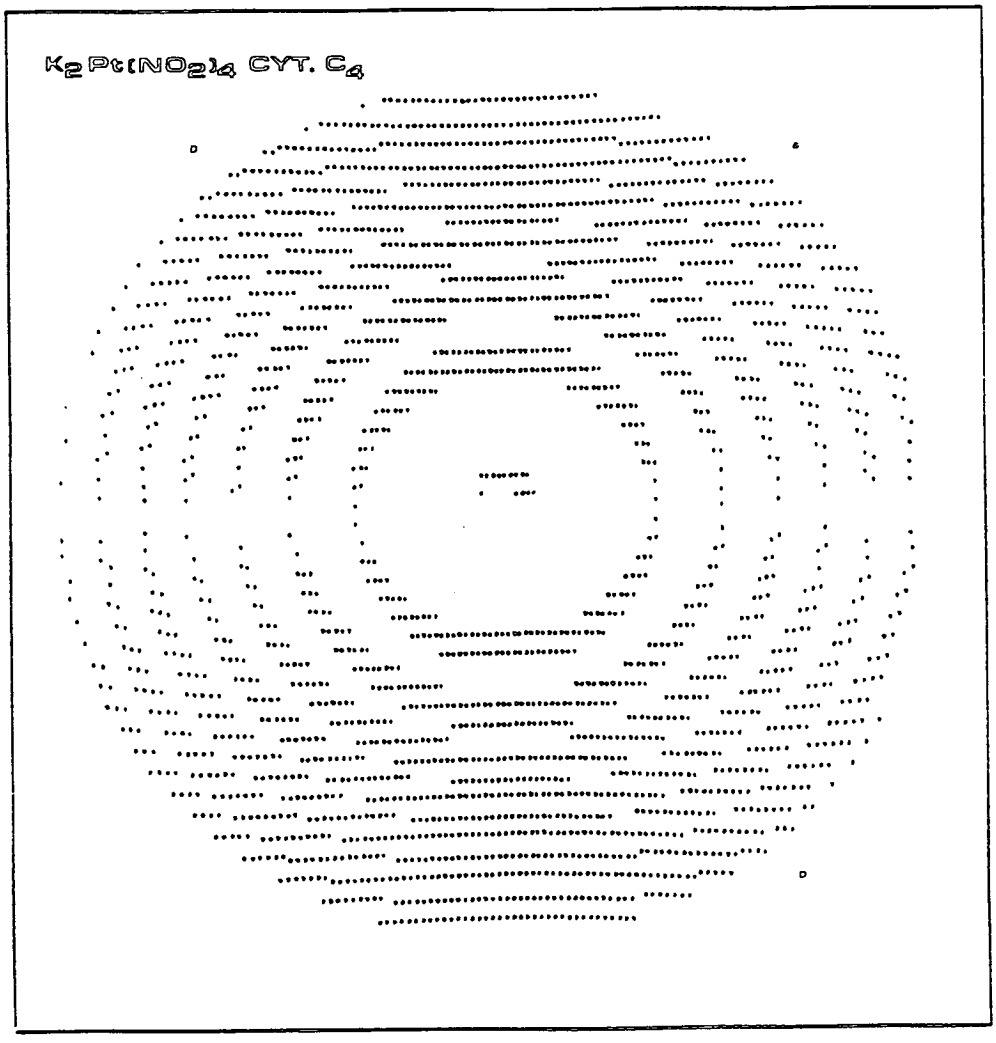

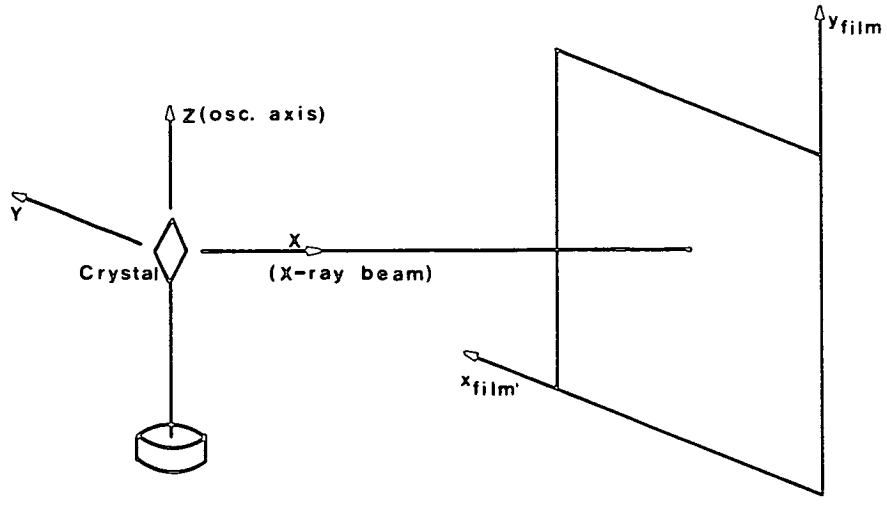

Figure 4.7 The relationship between the film co-ordinate system and the orthogonal system in relation to which the orientation of the crystal is defined.

To find the coordinates of a reflection on the film, an orthogonal coordinate system (x_{film}, y_{film}) with origin at the point where the main beam strikes the film is defined.

Let us consider a reflection cutting the Ewald sphere at a point P (Figure 4.8). It will be recorded on a flat film at a distance F from the crystal, at a position Q.

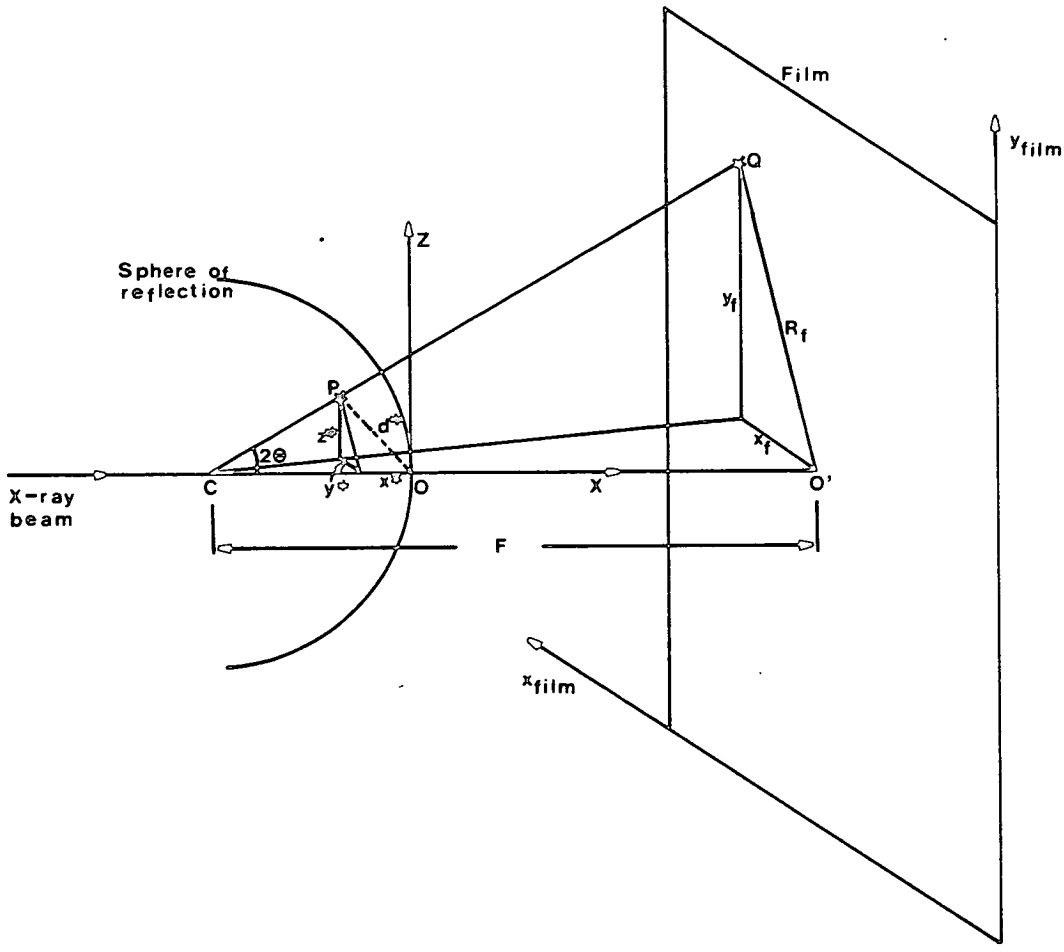

Figure 4.8 The relationship between a reciprocal lattice point in a reflecting position and the position where this reflection is recorded on the film

The reciprocal lattice vector $d^*(x^*, y^*, z^*)$ is related to the film coordinates (x_f, y_f) by the expressions:

$$x^* = 1 - \cos 2\theta$$

$$y^* = x_f \frac{\sin 2\theta}{R_f}$$

$$z^* = y_f \frac{\sin 2\theta}{R_f}$$

where $2\theta = \tan^{-1} \frac{R_f}{F}$

The initial orientation for the native and $K_2Pt(NO_2)_4$ derivative crystals, which is in fact the ideal orientation for cytochrome c_4 crystals, is shown in Figure 4.9. Native data collection was started at this position, while the derivative data collection started 90^o away from it.

Figure 4.9 The orientation of the native and $K_2Pt(NO_2)_4$ derivative crystals when the rotation angle was 0^o

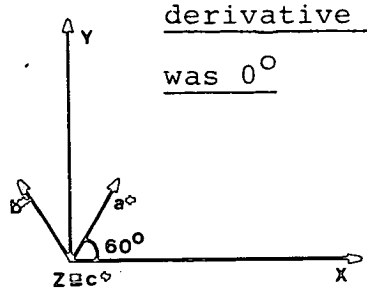

The orientation matrix associated with this orientation was:

$$A = \begin{pmatrix} a^*_x & b^*_x & c^*_x \\ a^*_y & b^*_y & c^*_y \\ a^*_z & b^*_z & c^*_z \end{pmatrix} = \begin{pmatrix} a^*\cos 60^o & -a^*\cos 60^o & 0 \\ a^*\sin 60^o & a^*\sin 60^o & 0 \\ 0 & 0 & c^* \end{pmatrix}$$

In the case of $UO_2(NO_3)_2$ derivative, the crystal orientation is shown in Figure 4.10 and the respective orientation matrix was:

$$A^* = \begin{pmatrix} a^*\sin 60^o & 0 & o \\ a^*(\cos 60^o \cdot \cos 29.6^o) & a^*\cos 29.6^o & c^*\sin 29.6^o \\ -a^*(\cos 60^o \cdot \sin 29.6^o) & -a^*\sin 29.6^o & c^*\cos 29.6^o \end{pmatrix}$$

Although the crystals are first set with still photographs, the orientation matrix is usually mis-set in relation to the ideal (a^*, b^*, c^*) positions.

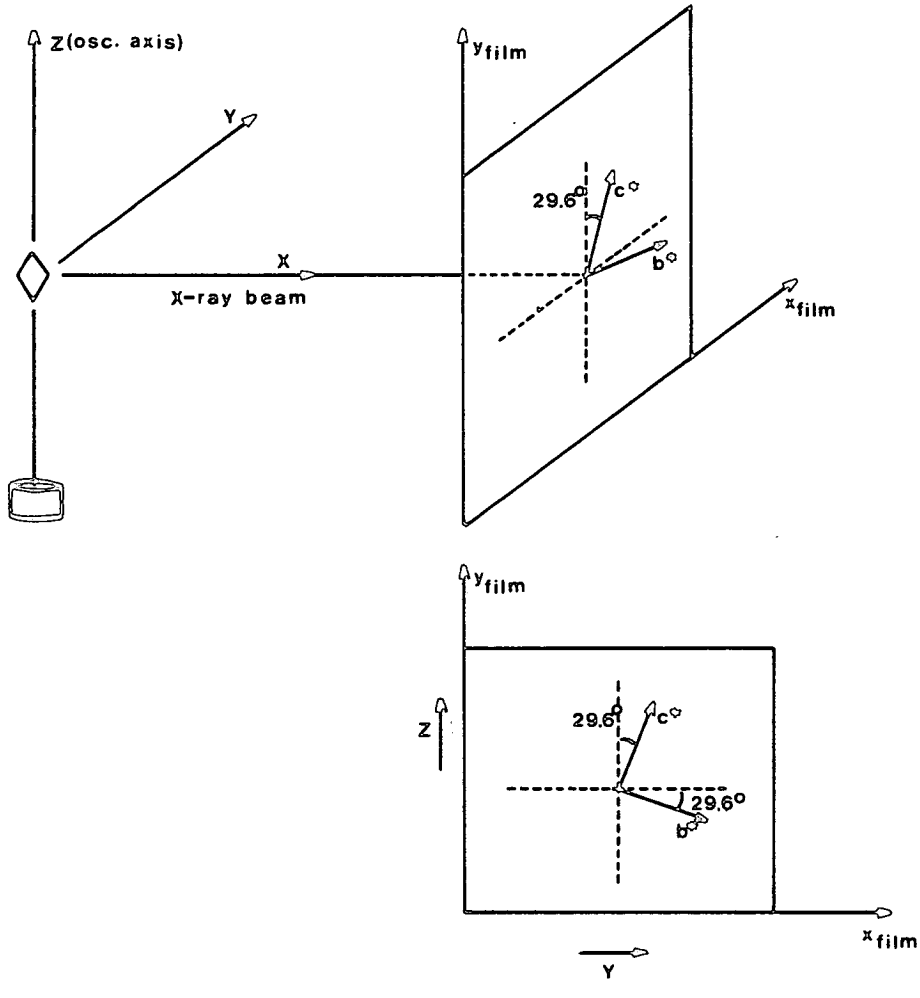

Figure 4.10 The orientation of the $UO_2(NO_3)_2$ derivative crystal when the rotation angle was 0°

We define (ψ_X, ψ_Y, ψ_Z) as being the misorientation angles of the real positions of (a^*, b^*, c^*) in relation to (X, Y, Z) with the ones used to build up the orientation matrix (a^*, b^*, c^*) ideal.

The values for (ψ_X, ψ_Y, ψ_Z) are obtained using two still photographs 90^o apart.

Reflections from the still photographs are indexed using the orientation matrix and the relation between any reflection and its film coordinates. Then, as all these reflections must lie on the Ewald sphere, the indices are forced to be integers.

Refinement of (ψ_X, ψ_Y, ψ_Z), F, a^* and c^* was done minimizing the residual Res,

$$\text{Res} = \sum_{i=1}^{N} \left(\frac{R_o^i - R_c^i}{d^*} \right)^2$$

where R_o^i and R_c^i are the observed and calculated distances of the reflection i from the Ewald sphere.

$$R_c^i = [(1 - x_i^*)^2 + y_i^{*2} + z_i^{*2}]^{\frac{1}{2}}$$

$$R_o^i = 1 + \frac{x}{2} d^*(1 - m)$$

m being the degree of partiality of the reflection i and x is the angle over which the reflection diffracts (beam divergence).

The refinement procedure was carried out over a total of 30, 96 and 75 reflections respectively for native, $UO_2(NO_3)_2$ and $K_2Pt(NO_2)_4$ derivative data sets. All the reflections were assumed to be 50% recorded.

In all the cases, camera constants and misorientation angles were refined first alone and then together with the cell parameters.

Table 4.1 gives the values for Res and the r.m.s. deviation of observed from calculated Bragg angle at the end of both refinements.

Table 4.1 The residual, Res, and the r.m.s. deviation of the Bragg angle for native and derivatives data sets

	Native	$UO_2(NO_3)_2$	$K_2Pt(NO_2)_4$
Res	0.000162	0.000156	0.000064
r.m.s. (deg.)	0.143	0.075	0.054
Res	0.000015	0.000074	0.000054
r.m.s. (deg.)	0.044	0.051	0.049

Final values from refinement for a^*, c^*, ψ_X, ψ_Y, ψ_Z are listed in Table 4.2.

Table 4.2 The reciprocal cell dimensions and the mis-orientation angles at the end of refinement

	Native	$UO_2(NO_3)_2$	$K_2Pt(NO_2)_4$
a^* (r.l.u.)	0.028594(95)	0.028641(22)	0.028532(29)
c^* (r.l.u.)	0.008848(12)	0.008833(5)	0.008845(5)
ψ_X (deg.)	2.158(95)	0.081(18)	-0.582(13)
ψ_Y (deg.)	0.366(20)	1.093(11)	-0.671(10)
ψ_Z (deg.)	-0.978(22)	-0.207(8)	-0.250(9)

With these new constants, a list of indexed film coordinates was generated for each film pack.

2.2 The intensity measurements

Native and $UO_2(NO_3)_2$ derivative films were scanned on an off-line OPTRONICS scanner in the Biochemistry Department at Bristol University.

The $K_2Pt(NO_2)_4$ derivative films were scanned and processed in the Laboratory of Molecular Biophysics in Oxford. In this case, the film intensities were measured using a SCANDIG 3 microdensitometer.

In every case, the raster size was 100 μm and the optical densities were scaled to lie in the range $0 \rightarrow 255$.

The absolute optical density is determined by the ratio of transmitted (I_T) to incident (I_o) light when white light is incident on the film. It is defined by the relation

$$I_T = I_o \, 10^{-D}$$

$$\underline{\text{or}} \quad D = -\log \frac{I_T}{I_o}$$

Both native and $UO_2(NO_3)_2$ films were scanned on an optical density range of 0 → 2 OD units, however the $K_2Pt(NO_2)_4$ films were unusually dark and had to be scanned on an optical density range of 0 → 3 OD units.

Using standard optical densities in the 0 → 2 OD range, it is found that Kodirex films have an almost linear response, meaning that the intensity of the scattered X-ray beam corresponds to the observed optical densities. For the 0 → 3 OD units range the optical densities had to be corrected according to the curve shown in Figure 4.11.

For each film, the scanner coordinates are related to the film coordinates by a translation along both axes and a tilt angle. These values are calculated and refined using 18 reflections from different parts of the film and minimizing the quantity:

$$\sum_{i=1}^{18} (y_i - u_i)^2 + (z_i - v_i)^2$$

where (u_1, v_i) are the centres of gravity for the scanner observed reflections and (y_i, z_i) are the calculated ones

Figure 4.11 The correction of the optical densities used for the $K_2Pt(NO_2)_4$ derivative films

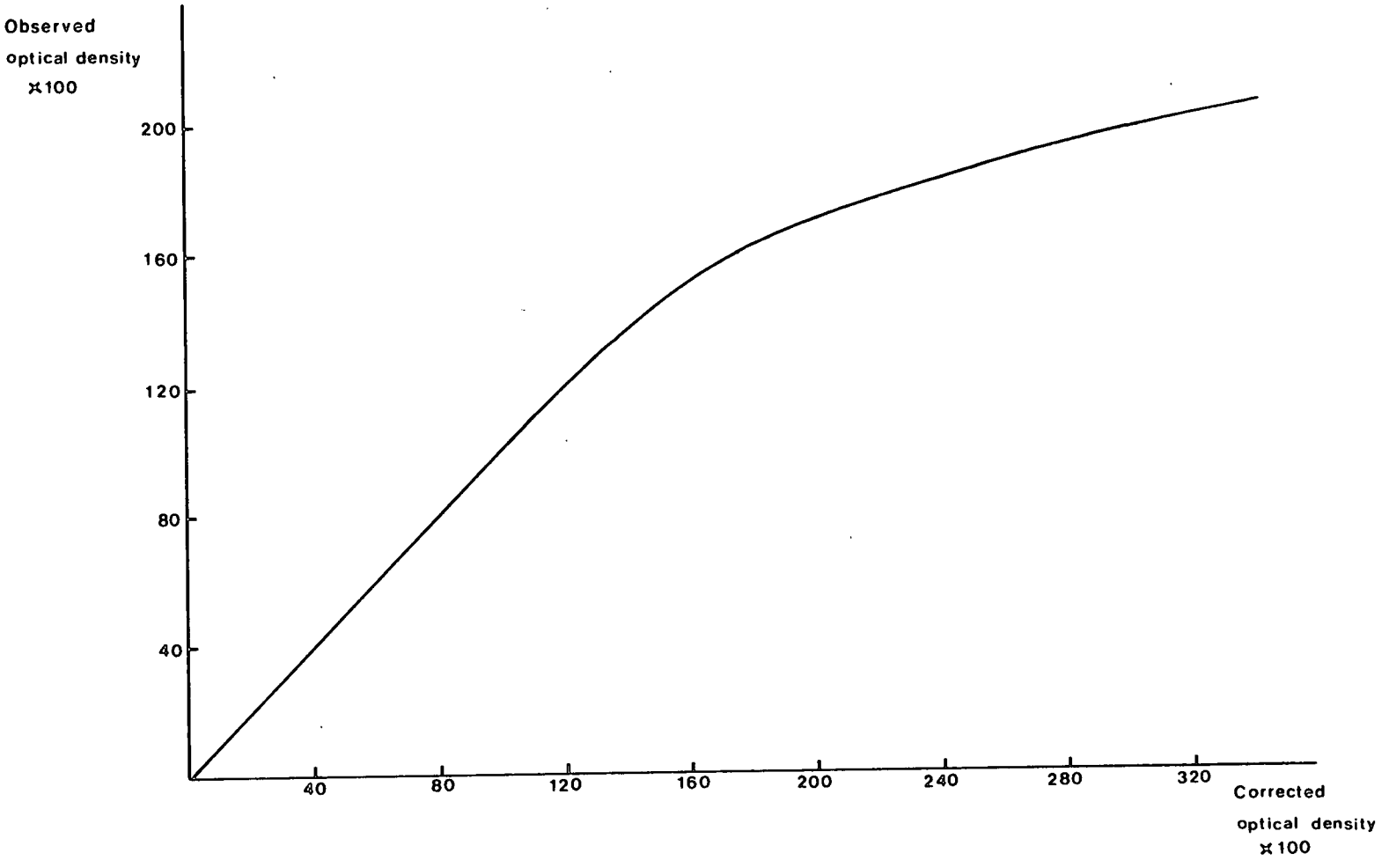

for the same reflection. Then, all the reflections on the film are processed.

Because of the difference in crystal alignment, different options for background measurement were used for the three data sets. Figures 4.12 and 4.13 show the spot and background areas chosen for each set of films.

Figure 4.12 The spot and background areas chosen for the native and $K_2Pt(NO_2)_4$ derivative data processing

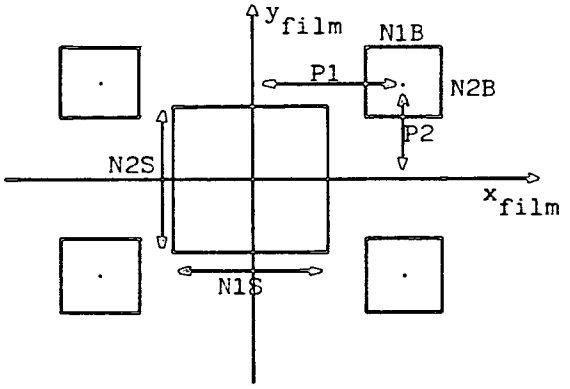

	Native	$K_2Pt(NO_2)_4$
N1S	70 units	70 units
N2S	70 "	90 "
P1	70 "	80 "
P2	30 "	40 "
N1B	50 "	50 "
N2B	50 "	50 "

1 unit=50 μm

Figure 4.13 The spot and background areas chosen for the $UO_2(NO_3)_2$ derivative data processing.

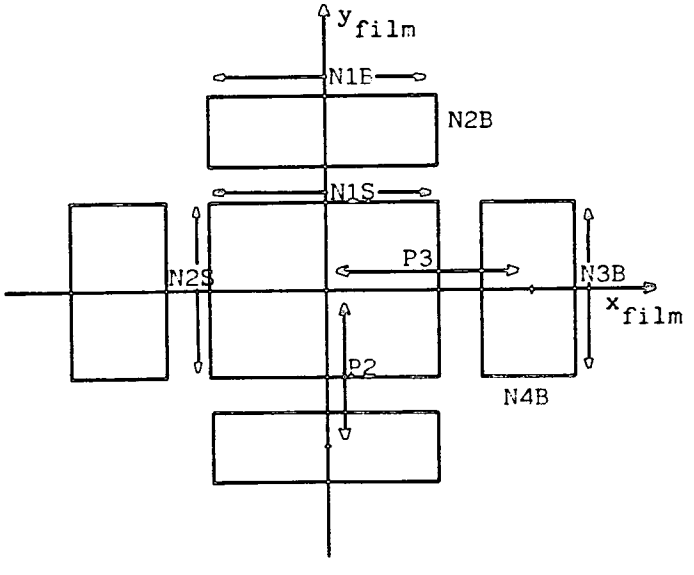

	$UO_2(NO_3)_2$
N1S	90 units
N2S	70 "
P2	70 "
P3	80 "
N1B	90 "
N2B	50 "
N3B	50 "
N4B	30 "

1 unit=50 μm

The films were processed on a DEC PDP 11/45 computer using the "PDP 11 Oxford" suite of programmes for processing Arndt-Wonacott oscillation camera data[19].

2.3 Scaling of the films within a pack, Lorentz, polarization, parabolic and oblique incidence corrections

Lorentz and polarization factors were applied to the integrated intensities. They are of the form[4] :

$$LP^{-1} = (\sin^2 2\theta - \zeta^2)^{\frac{1}{2}} \cdot \frac{(1 + \cos 2\phi)}{(\zeta^2 (1 - \cos 2\phi) + \cos^2 2\theta + \cos 2\phi)}$$

where ζ is the reciprocal lattice distance, in cylindrical polar coordinates, of a point on the Ewald sphere to the plane perpendicular to the rotation axis; 2ϕ is the diffraction angle of the (002) reflection of the graphite monochromator crystal (26° approximately) and 2θ is the diffraction angle of the reflection.

Because of the non-linear relationship between optical density and exposure time, a parabolic correction[14] of the form:

$$I = D + BD^2$$

I = intensity

D = optical density

B = constant to be determined from common reflections in both films

was done.

The oblique incidence "Cox and Shaw" factor[21] compensates for the change in absorption of X-ray beam by the film at different angles of incidence 2θ

$$I_{corr}(2\theta) = \frac{I(2\theta)[\exp(-\alpha-(N-1)\beta) - \exp(-\alpha-NB)]}{\exp((-\alpha-(N-1)\beta)\sec 2\theta) - \exp((-\alpha-NB).\sec 2\theta)}$$

$I(2\theta)$ = observed intensity at 2θ

$I_{corr}(2\theta)$ = corrected intensity

$\alpha = 0.04$, $\beta = 1.1$ } film constants

N = number of the film in the pack

Tables 4.3, 4.4 and 4.5 give the scale factors for films within a pack, the overall agreement between both films and the total number of reflections on each film.

Table 4.3 The scale between films of the same pack for the native data

	Pack Number					
	1	2	3	4	5	6
Scale factor	3.73(4)	3.33(3)	3.46(3)	3.42(3)	3.74(4)	3.47(5)
R	0.076	0.069	0.066	0.060	0.069	0.086
N°. refl. on 1st film	1333	1300	1317	1268	1345	1229
N°. refl. on 2nd film	132	126	122	94	105	96

$$R = \sum_{hkl} \sum_{i=1}^{N} |\langle I\rangle - I_i| / \sum_{hkl} N\langle I\rangle$$

N = number of common reflections with indices (hkl)

$\langle I\rangle$ = mean intensity of common reflections

Table 4.4 The scale between films of the same pack for the $UO_2(NO_3)_2$ data

	Pack Number 1	2	3	4	5
Scale factor	2.28(2)	2.43(2)	2.19(2)	2.40(2)	2.39(2)
R	0.054	0.054	0.055	0.066	0.068
N°. refl. on 1st film	1054	1059	488	479	384
N°. refl. on 2nd film	120	164	161	168	152

Table 4.5 The scale between films of the same pack for the $K_2Pt(NO_2)_4$ data

	Pack Number 1	2	3	4	5	6	7
Scale factor	6.63(10)	6.96(10)	6.54(10)	6.39(9)	6.09(9)	6.86(10)	6.46(9)
R	0.108	0.121	0.109	0.105	0.105	0.105	0.099
N°. refl. on 1st film	1690	1502	1648	1539	1555	1630	1539
N°. refl. on 2nd film	398	571	494	499	456	527	428

In the $UO_2(NO_3)_2$ derivative the second film of pack number six could not be used since the refinement of the differences between the centres of the gravity of the scanner observed reflections and the calculated ones did not converge. Unfortunately, the same happened with the first films of packs number seven for both native and $UO_2(NO_3)_2$ derivative; this meant that all the data collected in these last 3 degrees oscillation were lost.

A surprisingly high scale factor was found between films of the $K_2Pt(NO_2)_4$ derivative data. This was probably a result of the unusual darkness on the top films. As these films were relatively intense, the number of reflections recorded on the second films is approximately three times as much for the $K_2Pt(NO_2)_4$ data set as for the other two data sets.

In the case of the $UO_2(NO_3)_2$ derivative data set, the program GENERT[19] was unable in some cases to cope with the crystal misorientation and the generation of film coordinates for previously indexed reflections, mainly for the high angle data.

2.4 Final scaling and average of the recorded data

Scale and temperature factors between over-lapping batches of data were calculated by the method of Fox & Holmes[10].

Initial scale and temperature factors were determined from a plot of $\langle I \rangle$ against $(\sin^2\theta/\lambda^2)$ for each pack. Then, scale factors of the form:

$$K(i) = C(i) \exp(-2B(i) \frac{\sin^2\theta}{\lambda^2})$$

were calculated. Pack number one was arbitrarily set to C(1) = 1 and B(1) = 0 and all the others are calculated relative to this.

Table 4.6 shows the scale factors C(i) for native and derivative data sets.

Table 4.6 The scale factors between overlapping batches of data

Native							
Pack No.	1	2	3	4	5	6	
C(i)	1.0	1.08	1.10	1.03	1.16	1.22	
$UO_2(NO_3)_2$ Derivative							
Pack No.	1	2	3	4	5	6	
C(i)	1.0	0.81	0.70	0.64	0.76	0.58	
$K_2Pt(NO_2)_4$ Derivative							
Pack No.	1	2	3	4	5	6	7
C(i)	1.0	0.77	0.86	0.81	0.80	0.80	0.91

Finally, these scale factors were applied, partially recorded reflections were added together and repeated measurements of symmetry equivalent reflections were averaged.

Common reflections with an intensity which deviated by more than three times the standard deviation from the mean value were rejected.

Table 4.7 shows the total number of centric and acentric independent reflections together with the number of reflections with anomalous measurements.

Table 4.7 The total number of reflections which have been collected

	centric	acentric	with anomalous measurements
Native	962	2193	1750
$UO_2(NO_3)_2$	742	1520	865
$K_2Pt(NO_2)_4$	984	3702	3033

The native centric data set has most of the (hhl) reflections since we have started the data collection at this zone but with data only up to 18 degrees on the rotation angle, many (hol) reflections were lost.

The $K_2Pt(NO_2)_4$ data set contains reflections to a resolution of 2.7 Å but many low resolution data were lost due to the extreme darkness of the films in the middle.

The accuracy of the intensity data sets described here leaves much to be desired. The native films were weak, the platinum derivative had high background and the uranium derivative crystal was misset. Had equipment been available in or near the Department, we should have repeated all of these photographs in order to improve the accuracy, but this was unfortunately not possible at the time.

Since most of the large crystals were used to get the diffractometer data, only small crystals were left to get high resolution data. An application was successfully made to the SERC Laboratory in Daresbury to record new data sets using the synchrotron radiation source and the Arndt Wonacott camera there.

3. Comparison of the rotation camera and diffractometer data sets

3.1 The native data

Figures 4.14 and 4.15 show a comparison of both native data sets in terms of F^2 and $4 \sin^2\theta/\lambda^2$ for the 5 Å resolution data set and for the data between 5 Å and 3 Å resolution.

There are 1191 common independent reflections in the region 5 Å < dm < ∞ and 1740 in the region 3 Å < dm < 5 Å.

The analysis of both data sets in terms of F^2 shows that the rotation camera structure factor amplitudes (F_{RC}) are higher than the diffractometer ones (F_D) when the diffractometer value is less than 305 which is approximately 1/3 of the largest F value . There are 470 reflections of this type in the region 5 Å < dm < ∞ and 742 in the region 3 Å < dm < 5 Å.

In general the film intensity reflections were very weak, giving large errors mainly for the less intense reflections. Because of these anomalies it was decided to use the diffractometer data instead of the rotation camera data.

Figure 4.14 Comparison of the rotation camera and diffractometer native data sets at 5 Å resolution

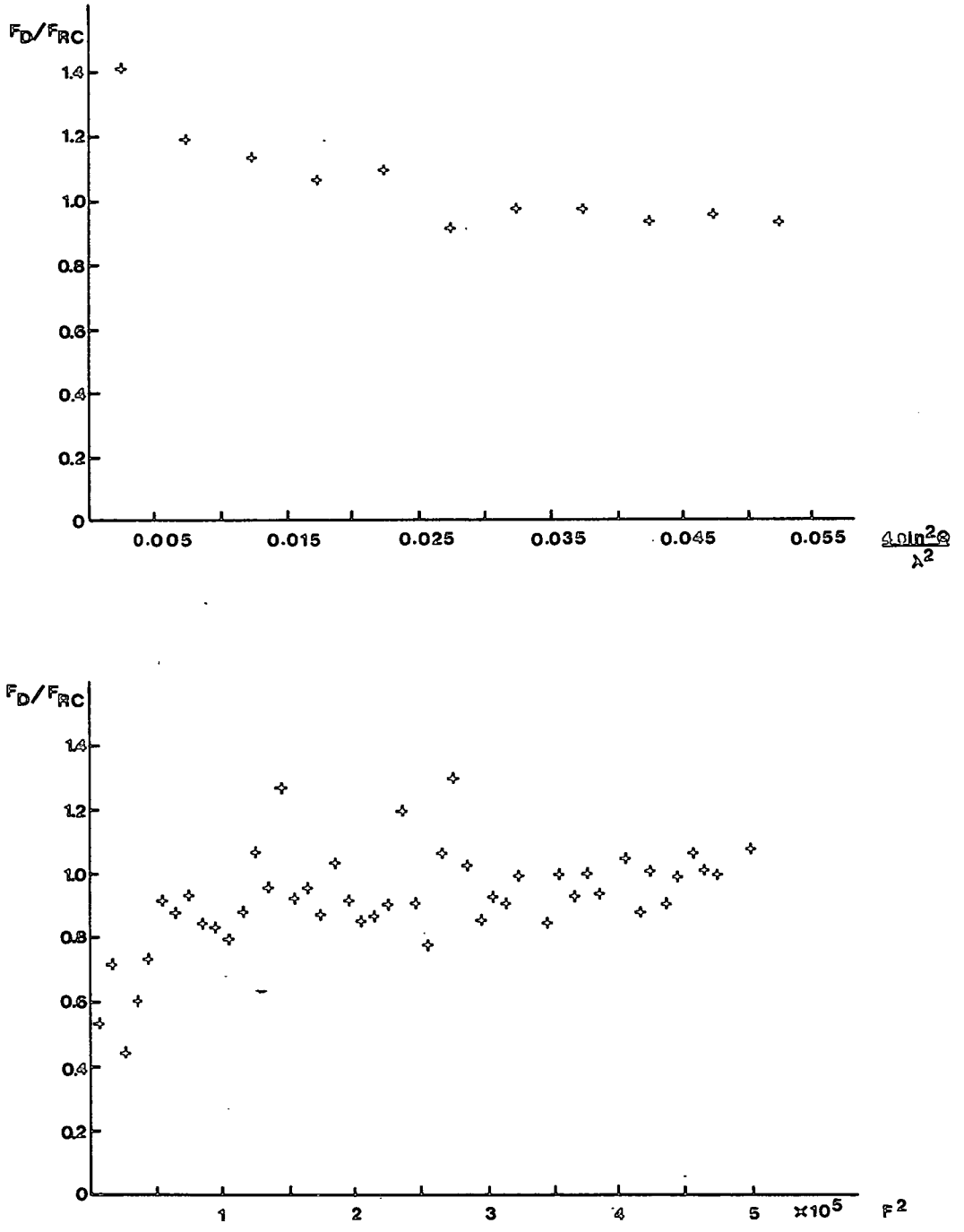

Figure 4.15 Comparison of the rotation camera and diffractometer native data sets at a resolution between 5 Å and 3 Å

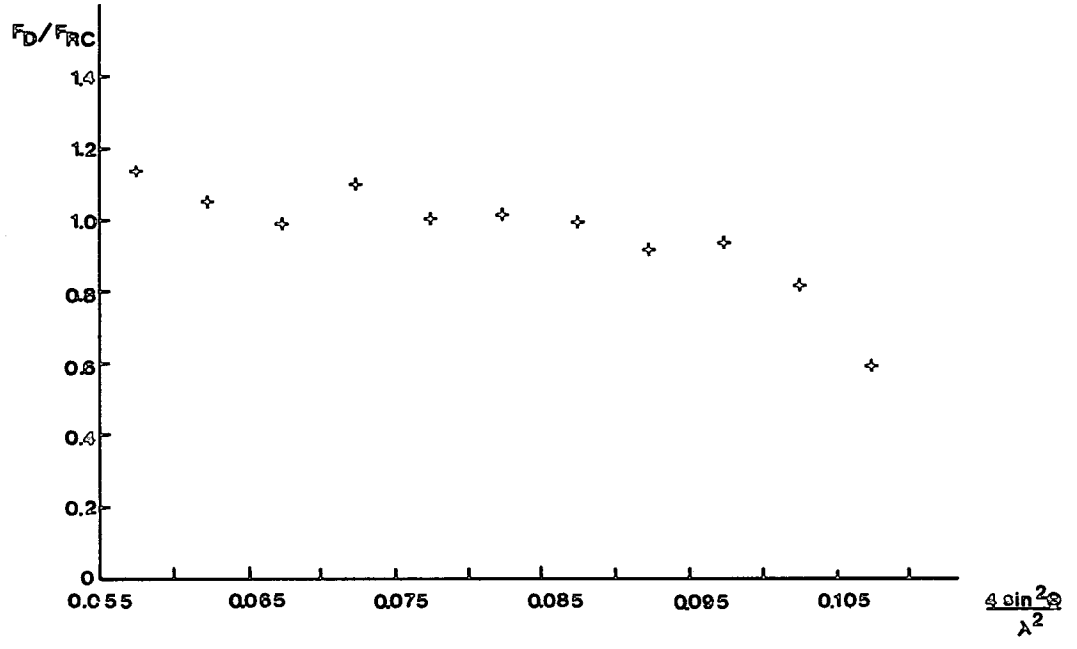

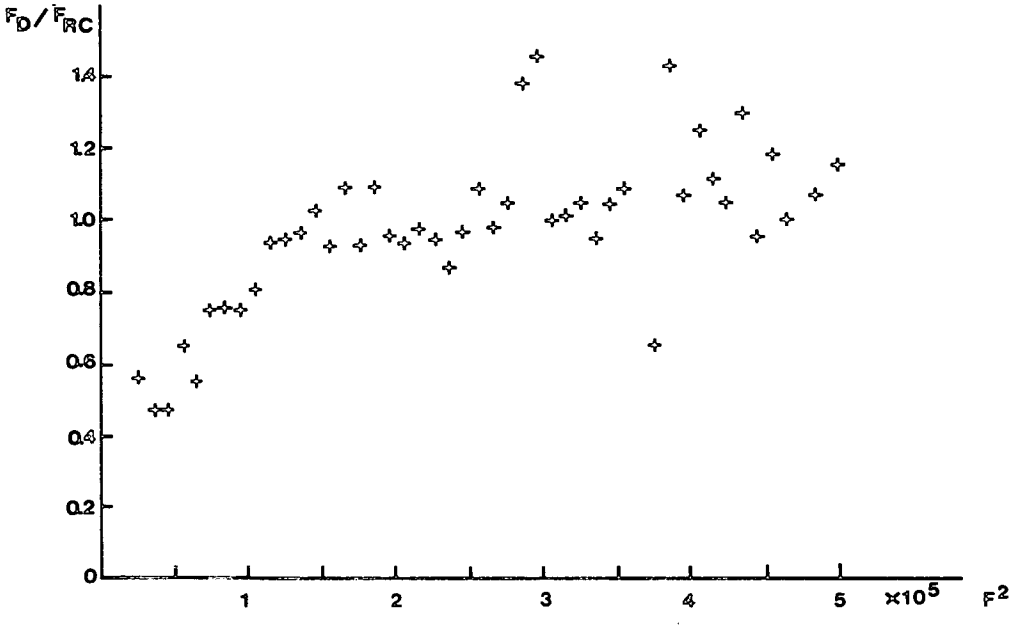

3.2 The $UO_2(NO_3)_2$ derivative data

There were 1151 common independent reflections when the rotation camera and diffractometer data sets were compared. In this case, the common reflections correspond mainly to the 5 Å resolution data set.

Figure 4.16 shows an analysis of both data sets in terms of F^2 and $4\sin^2\theta/\lambda^2$. Although for small F values the agreement is not very good, both data sets compare well in ranges of $4\sin^2\theta/\lambda^2$.

As the crystal was not properly orientated when these intensity data were collected on the rotation camera some high and low θ angle reflections were not recorded and a new data set was generated by merging both rotation camera and diffractometer data sets.

Before merging the data sets, the anomalous data were compared, but a poor agreement was found. This was to be expected since most of the Friedel reflections were recorded on different films. In view of this, only anomalous differences from the diffractometer data set were included on the new data set.

The structure factor amplitudes for the new data set were calculated in the following way when both measurements were available:

Figure 4.16 Comparison of the rotation camera and diffractometer $UO_2(NO_3)_2$ derivative data sets

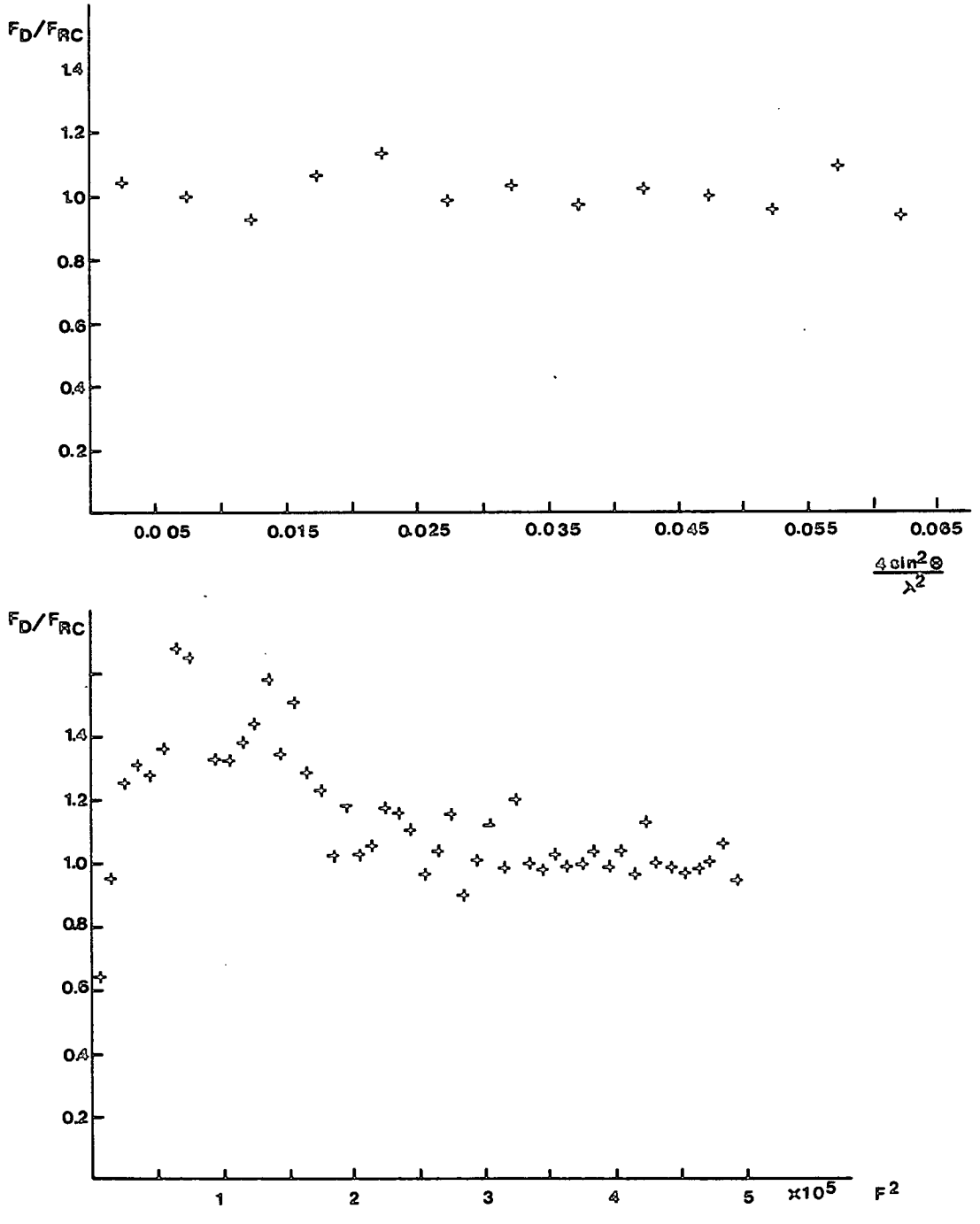

(i) $F_{RC} < 380$ (small F)

$$F_M = F_D$$

$$\sigma_M = \sigma_D$$

(ii) $F_{RC} \geqslant 380$

$$F_M = \frac{F_{RC}/\sigma^2_{RC} + F_D/\sigma^2_D}{1/\sigma^2_{RC} + 1/\sigma^2_D}$$

$$\sigma_M = \max\{\sigma_A, \sigma_B\}$$

$$1/\sigma^2_A = 1/\sigma^2_{RC} + 1/\sigma^2_D$$

$$\sigma^2_B = \frac{(\Delta_{RC}/\sigma_{RC})^2 + (\Delta_D/\sigma_D)^2}{1/\sigma^2_{RC} + 1/\sigma^2_D}$$

$$\Delta_{RC} = F_M - F_{RC}$$

$$\Delta_D = F_M - F_D$$

where the indices RC, D and M stand for rotation camera, diffractometer and merged data respectively.

The merged data set gave better results when a F_{HLE} Patterson maps with F_{HLE} values calculated from the diffractometer native data set and the merged or rotation camera $UO_2(NO_3)_2$ derivative data sets were compared. Also when the one site available from the 5 Å data was refined, the R factors were significantly better for this new data set:

(i) F_{HLE} refinement using $UO_2(NO_3)_2$ rotation camera data.

R = 67.3%

WR = 63.4%

(ii) F_{HLE} refinement using $UO_2(NO_3)_2$ merged data

R = 64.2%

WR = 48.3%

3.3 The $K_2Pt(NO_2)_4$ derivative data

There were 795 independent reflections present in both data sets. A comparison of the structure factor amplitudes for these common reflections was made in terms of F^2 and $4\sin^2\theta/\lambda^2$ and is presented in Figure 4.17.

The agreement in $4\sin^2\theta/\lambda^2$ shows that for the inner reflections the rotation camera structure factor amplitudes are less than the diffractometer ones. These reflections were recorded on the central part of the films which were very dark on the centre getting lighter towards the edge. So these reflections were the ones with the higher optical densities and bigger corrections between the observed and corrected optical densities. This tendency also shows when we plot F_D/F_{RC} in ranges of F^2; for F^2 greater than 50×10^4 the quotient F_D/F_{RC} has a mean value higher than the mean value for smaller F^2.

Because of low consistency, only the rotation camera data were used for the calculation of the new Fourier map for cytochrome c_4.

Figure 4.17 Comparison of the rotation camera and diffractometer $K_2Pt(NO_2)_4$ derivative data sets

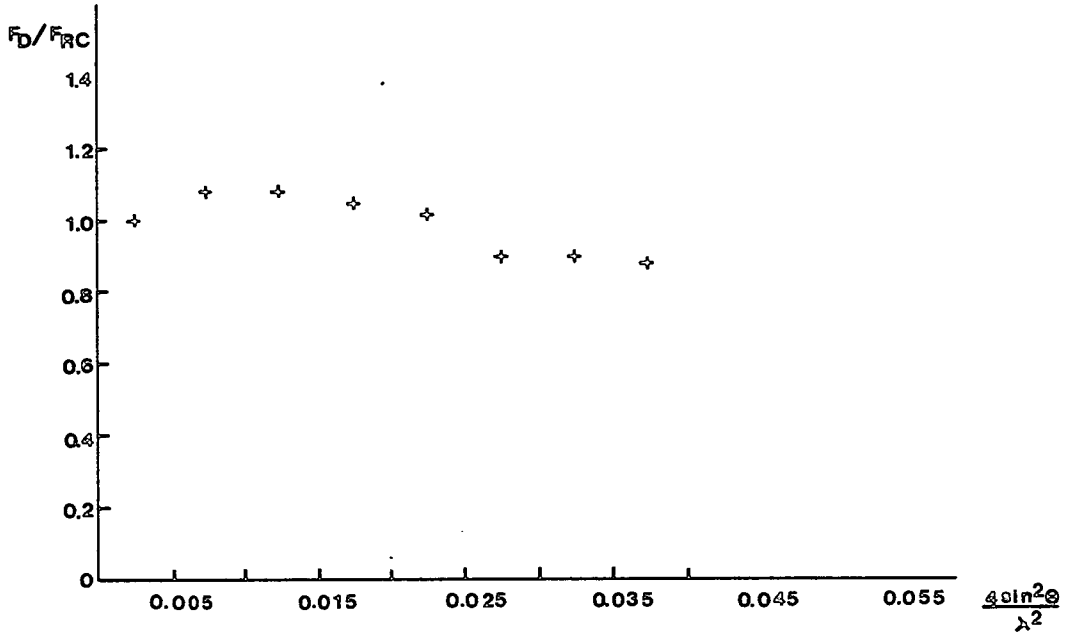

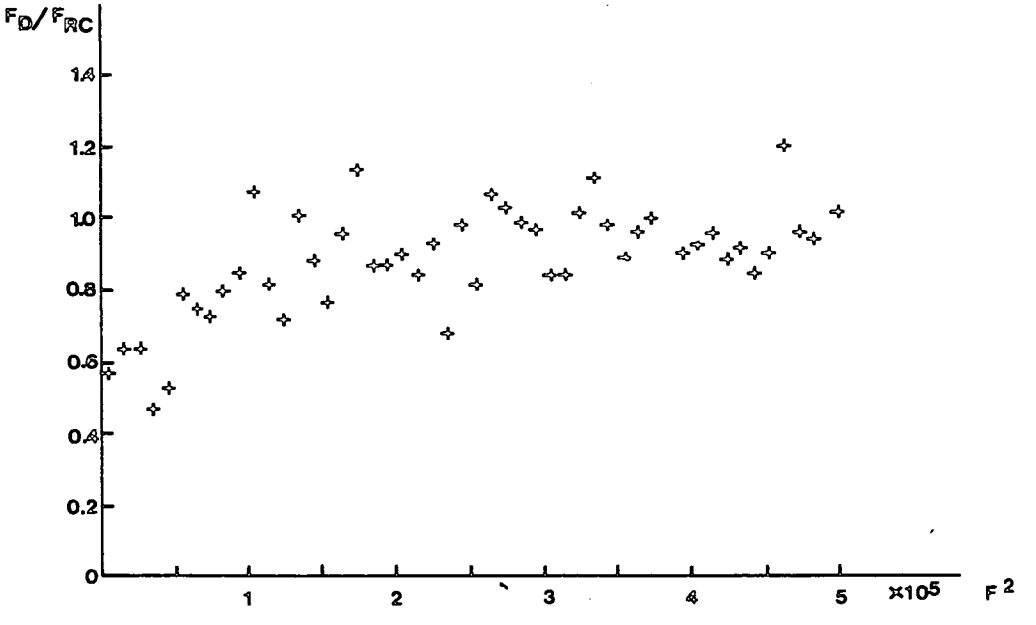

4. Fourier map calculation

In this section are described the stages leading to the higher resolution electron density map, at approximately 3.5 Å resolution. Ideally, the same procedures should have been used to record intensity data for the native protein and derivatives; this was not possible, and consequently some extra problems arose in scaling the data sets together (4.1). F_{HLE} values were calculated (4.2) and the heavy atom positions were refined using those values (4.3), and then phases were calculated for the map (4.4). Finally, the electron density map was calculated (4.5) and interpreted (4.6).

4.1 Scaling of derivative to native data sets

The data sets used in the Fourier map calculation were as follows:

(i) Native data set collected on the diffractometer.

(ii) $K_2Pt(NO_2)_4$ derivative data set collected on the rotation camera.

(iii) $UO_2(NO_3)_2$ derivative data set merged in the way described in Section 3.2.

The scaling procedure was done as described in Chapter Three. Figures 4.18 and 4.19 show the analyses of the quotient $(\Sigma|F_P|/\Sigma|F_{PH}|)$ in terms of $(4 \sin^2\theta/\lambda^2)$ and F_P^2 for both derivatives. The sums are extended to all the reflections within the same $(4 \sin^2\theta/\lambda^2)$ range in the first case and all the reflections within the same F_P^2 range in the other case.

Figure 4.18 Scaling of $UO_2(NO_3)_2$ derivative to native data sets

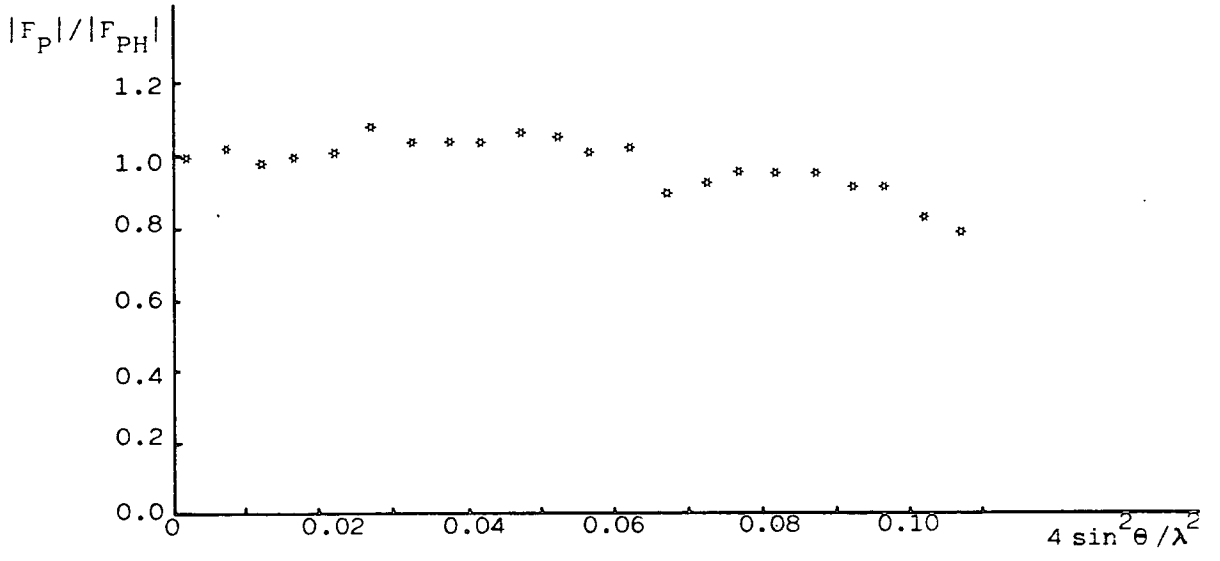

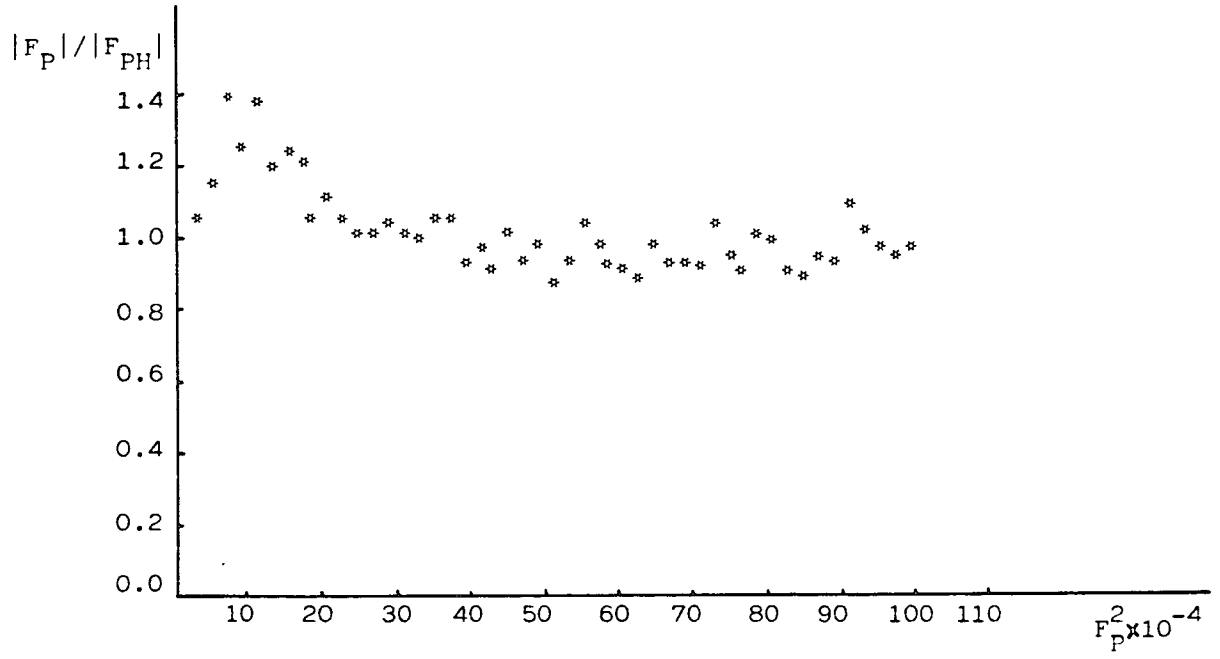

Figure 4.19 Scaling of $K_2Pt(NO_2)_4$ derivative to native data sets

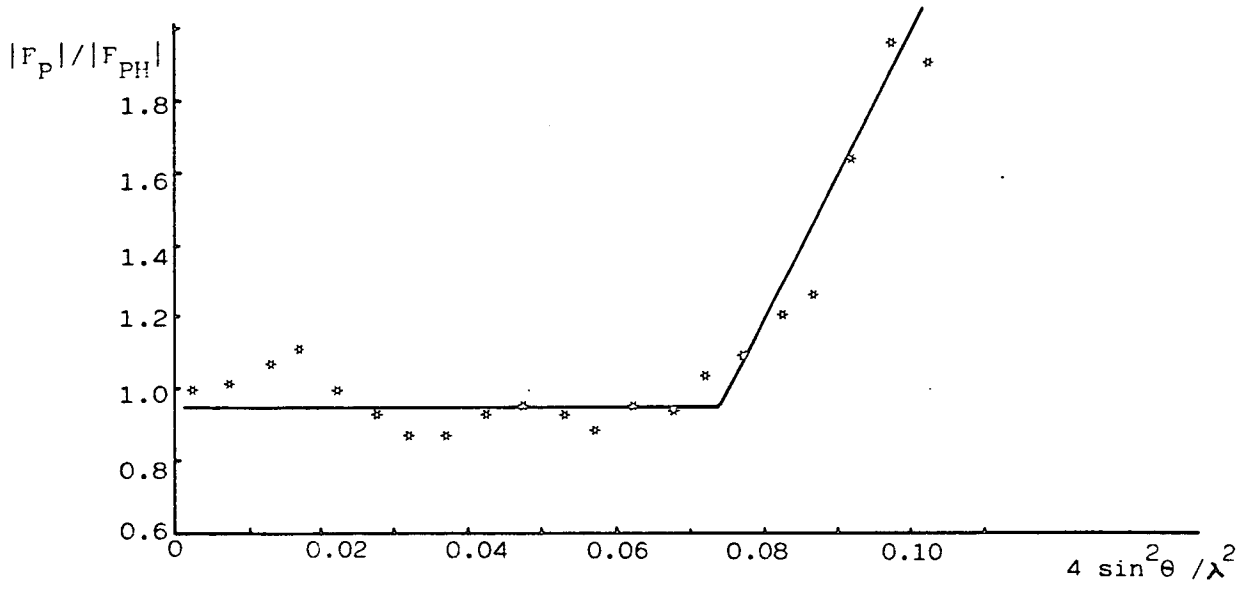

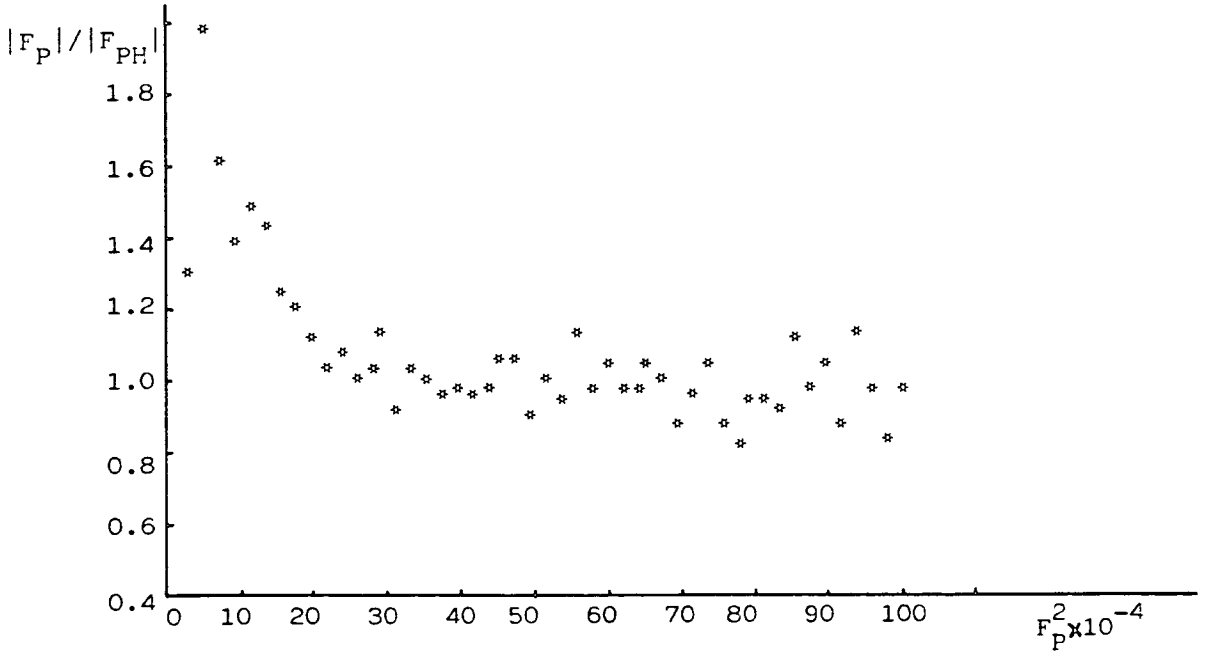

The scaling of $UO_2(NO_3)_2$ derivative data to native is particularly bad for small F_P values, showing large errors in the less intense reflections. As a result, only reflections with both native and derivative structure factor amplitudes greater than 300 electrons were considered for the F_{HLE} calculation.

The analysis of $(\Sigma|F_P|/\Sigma|F_{PH}|)$ in ranges of $(4 \sin^2\theta/\lambda^2)$ for $K_2Pt(NO_2)_4$ derivative points to a different scale for the high angle data. Apparently this derivative's intensities should be higher for high angle data and this must be a result of the very high background intensity, particularly at low angles, on these films.

The new scale was calculated tracing a line through the points between $(4 \sin^2\theta/\lambda^2) = 0.076$ Å^{-2} and 0.12 Å^{-2} as shown in Figure 4.19 and forcing it to be horizontal.

Figure 4.20 shows the agreement between native and derivative data after the new scale has been applied.

Table 4.8 shows the values of K and B_{ov} applied to both derivatives.

Table 4.8 Scale factors between derivative and native data sets

	K	B_{ov} (Å^{-2})
Native	-	-
$UO_2(NO_3)_2$	1.001 ± 0.013	0.067 ± 1.62
$K_2Pt(NO_2)_4$	1.001 ± 0.029	0.062 ± 2.40

Figure 4.20 Scaling of $K_2Pt(NO_2)_4$ derivative to native data sets after correcting the high angle data

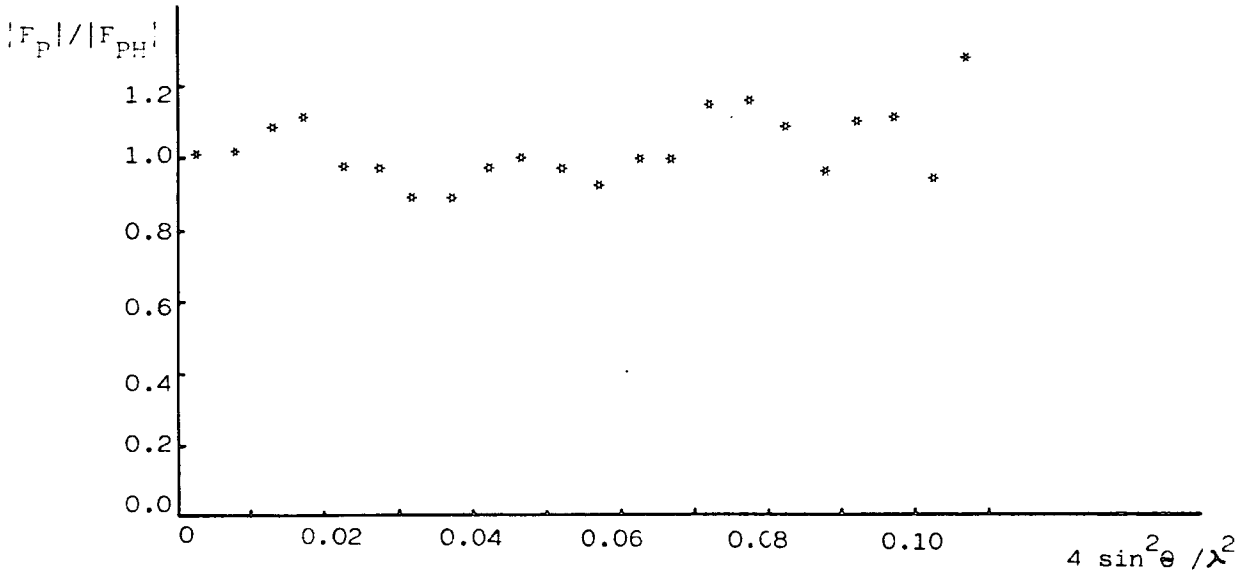

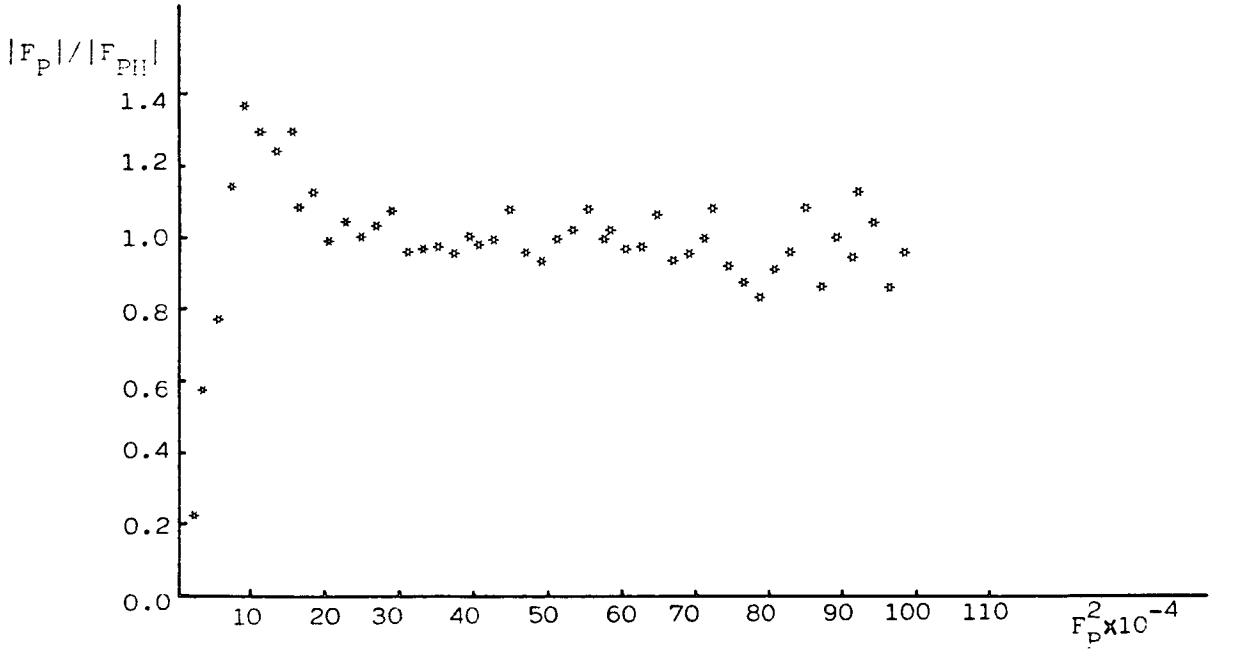

4.2 F_{HLE} Calculation

An analysis of the isomorphous differences for both data sets shows that their mean value is between 100 and 150 electrons and their maximum value is around 400 electrons. Thus, reflections were left out of the heavy atom refinement when $|F_{HLE}|$ values were greater than 400 electrons or $|F_{HUE}|$ was less than 400 electrons.

The reflections were also rejected when

$$K_{emp}\left|\frac{\Delta an}{2}\right| > |F_p|$$

and as K_{emp} was calculated using the equation

$$K_{emp} = \frac{2<|\Delta iso|>}{<|\Delta an|>}$$

over different ranges of $\sin^2\theta$, it meant for most of the reflections that the F_{HLE} values were not calculated when

$$|\Delta iso| > |F_p| \quad (||F_{PH}| - |F_p|| > |F_p|)$$

In the uranyl nitrate derivative, the anomalous differences recorded on the rotation camera were included in the F_{HLE} calculation when diffractometer data were not available.

The values for the empirical K (K_{emp}) were input at intervals of 0.016 Å^{-2} in 4 $\sin^2\theta/\lambda^2$ and were defined by the line drawn through the points (K_{emp}, 4 $\sin^2\theta/\lambda^2$) when K_{emp} was calculated at smaller intervals of $4\sin^2\theta/\lambda^2$.

Figures 4.21 and 4.22 show these plots. These curves show an abnormal increase of K_{emp} at low θ angles. It is possible that some of the heavy atom sites were occupied by $UO_2(NO_3)_2$ or $K_2Pt(NO_2)_4$ and not by the ions UO_2^{2+} or $Pt(NO_2)_4^{2-}$; at low angles, those groups would contribute to the real part of the scattering amplitude, but not to the imaginary one. Furthermore, at low Bragg angles the intensities are highly dependent on solvent and consequently are likely to cause bigger errors in the isomorphous differences. The uranyl nitrate derivative shows an abrupt increase in the value of K_{emp} at about 4 Å resolution which is expected since the anomalous data from this derivative are rather inaccurate from this resolution onwards.

Table 4.9 shows the number of reflections input and output from the F_{HLE} program and the mean F_{HLE} value for both derivatives.

Table 4.9 Summary of the F_{HLE} calculation

	$UO_2(NO_3)_2$	$K_2Pt(NO_2)_4$
Total number of input reflections	2894	4011
Number of output reflections {centric	711	670
Number of output reflections {acentric	1700	2312
Mean $\|F_{HLE}\|$	102	98
Mean overall isomorphous contribution	106	106
Mean anomalous contribution	95	88

Figure 4.21 Analysis of K_{emp} for the $UO_2(NO_3)_2$ derivative data

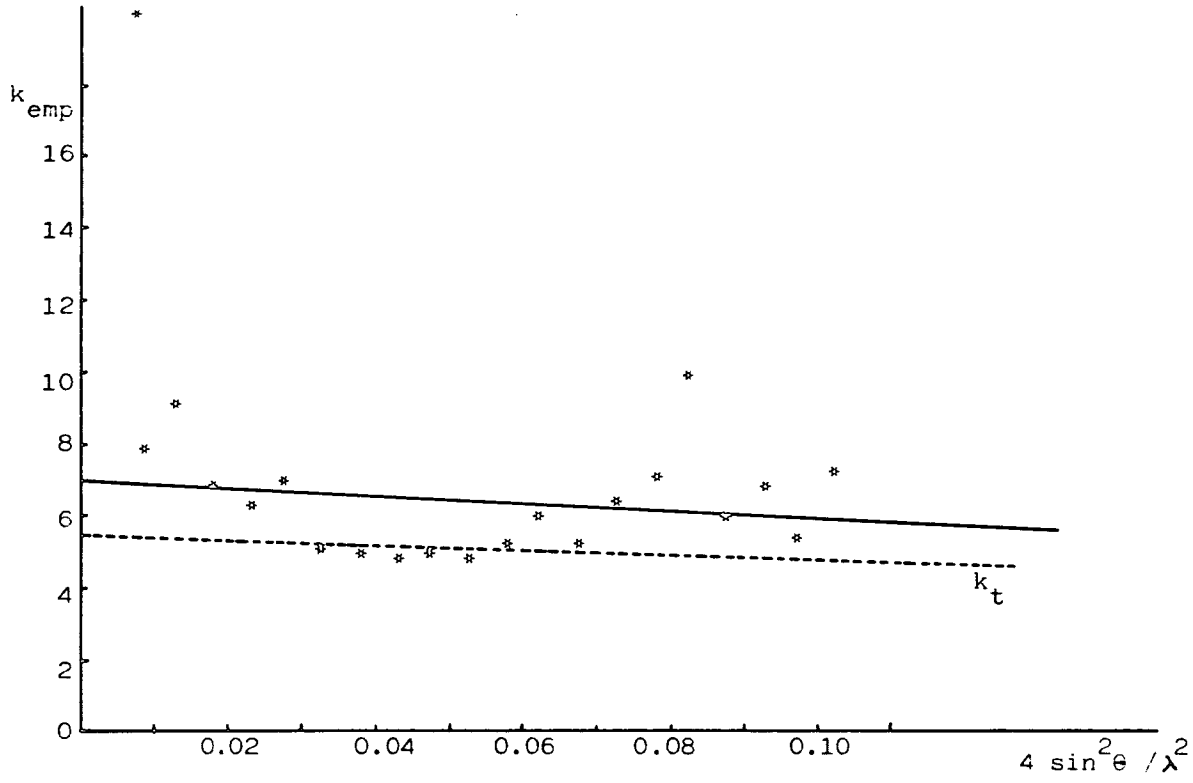

Figure 4.22 Analysis of K_{emp} for the $K_2Pt(NO_2)_4$ derivative data

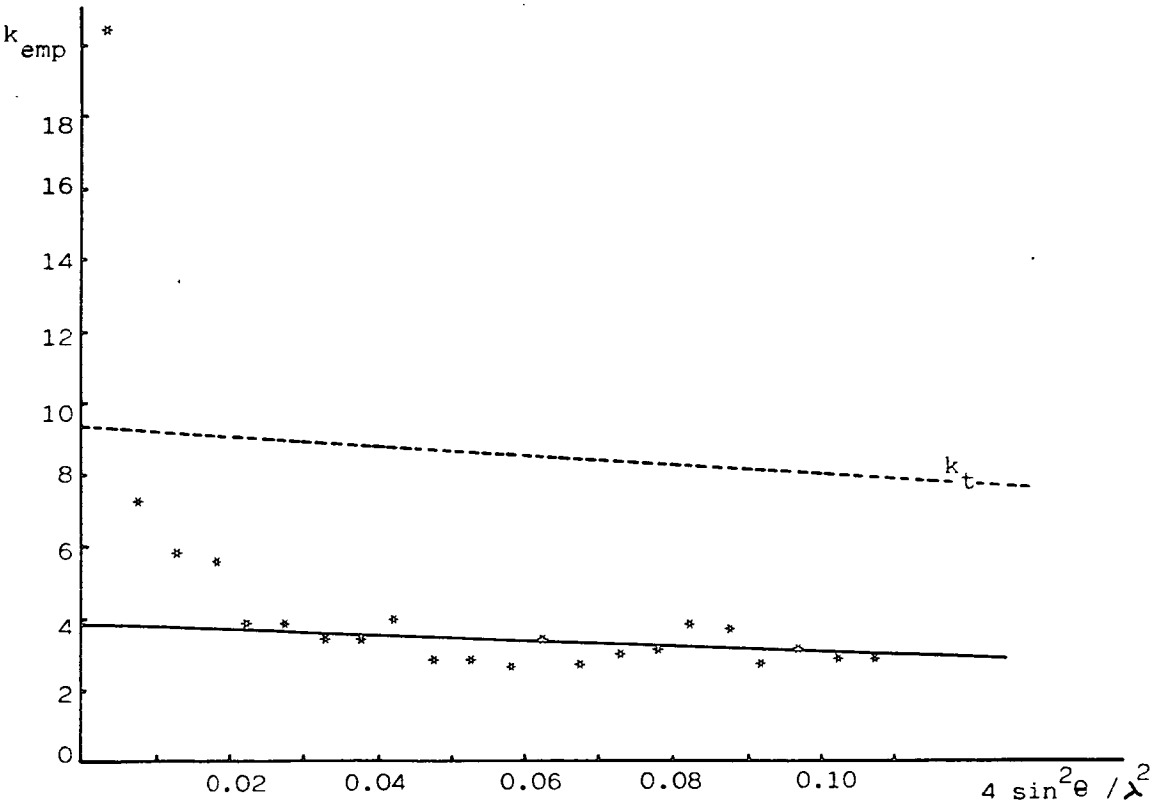

The empirical K was again calculated for every reflection for which a F_{HLE} value had been calculated and Table 4.10 compares this value with the theoretical one in different ranges of $(4\sin^2\theta/\lambda^2)$.

Table 4.10 Theoretical and empirical K averaged over different ranges of $(4\sin^2\theta/\lambda^2)$.

	$UO_2(NO_3)_2$		$K_2Pt(NO_2)_4$	
$4\sin^2\theta/\lambda^2$	K_{emp}	K_t	K_{emp}	K_t
0.000-0.016	5.1	5.5	4.8	9.3
0.016-0.032	3.7		3.1	
0.032-0.048	2.9	5.2	3.1	8.6
0.048-0.064	4.7		2.9	
0.064-0.080	8.0		2.5	
0.080-0.096	8.2	4.9	2.6	8.1
0.096-0.112	7.6		2.5	

Table 4.10 shows that in the case of $K_2Pt(NO_2)_4$ cytochrome c_4 derivative the anomalous differences have been over-estimated and the isomorphous differences under-estimated. Nevertheless there is a decrease in the K_{emp} values at high angles. This is probably related to the errors in the data on anomalous differences since the intensities were weaker at high angles and as a result subject to higher errors.

4.3 The heavy atom positions

Refinement of the 5 Å heavy atom sites was done using the new F_{HLE} values. Their occupancies remained high showing that in both derivative cytochrome c_4 molecules the heavy atom molecules were bonded to the protein at the same positions as before.

After five cycles of least squares refinement of the occupancy and positional parameters of the remaining uranium site, all the parameters converged.

The positions and occupancies of the platinum sites were refined until all the parameters became nearly constant. Then, isotropic temperature factors were refined alternating three cycles of least squares refinement of the occupancies with three cycles of temperature factor refinement.

A Fourier map with coefficients $F_{HLE} \exp(i\alpha)$ was calculated for each derivative. For each of them, the input phases were based on the previous heavy atom sites. The platinum map revealed several small possible sites, but when refined, their occupancy went below 0.09 so they were not considered to be significant heavy atom sites. The uranium Fourier map revealed a new site which refined well. Tables 4.11 and 4.12 give a summary of the position, occupancy, temperature factors and refinement indeces at the end of the F_{HLE} refinement. The refinement of the isotropic temperature factors for the two uranium sites was done as described for the platinum sites.

In both derivatives only F_{HLE} values greater than one standard deviation and weighted by $1/\sigma^2$ were used in the refinement.

Table 4.11 Summary of F_{HLE} refinement for the heavy atom sites

Refinement index		Uranium 1 site	Uranium 2 sites	Platinum 3 sites
R		54.9%	51%	47.0%
WR		46.0%	45.4%	54.0%
slope		0.13	0.19	0.13
Number of reflections	centric	380	380	379
	acentric	759	759	1007

Table 4.12 Position, occupancy and temperature factor for the heavy atom sites at the end of the refinements

	site	x	y	z	occupancy	B($Å^2$)
$UO_2(NO_3)_2$ (one site)	1	0.4807(8)	0.2178(8)	-0.0764(2)	0.43(1)	15
$UO_2(NO_3)_2$ (two sites)	1	0.4801(8)	0.2229(8)	-0.0746(2)	0.39(1)	2(3)
	2	0.1544(21)	-0.3015(23)	0.0630(5)	0.16(1)	2(4)
$K_2Pt(NO_2)_4$	1	0.7185(9)	0.0266(9)	0.0187(2)	0.35(1)	4(3)
	2	0.8184(20)	0.3336(19)	0.0324(4)	0.26(1)	18(5)
	3	0.4036(12)	0.5092(11)	0.0243(3)	0.30(1)	1(3)

After two uranium sites had been refined, protein phases were calculated based on the 5 Å diffractometer $K_2Pt(NO_2)_4$ data and $UO_2(NO_3)_2$ merged data to a resolution of 5 Å. These phases were used for the calculation of a protein Fourier map with 5 Å resolution. Details of this map and its calculation have been given in Chapter Three.

4.4 Phases for the higher resolution electron density map

After refining the heavy atom parameters for both derivatives, protein phases were calculated according to the procedures described in Chapter Three.

The mean figure of merit (m) for the 3858 reflections which were processed was 0.665 and the Dickerson factor (m.r.e.) was 0.64. Table 4.13 gives an analysis of the figure of merit in ranges of $(4\sin^2\theta/\lambda^2)$ and the number of reflections observed and theoretically predicted for each range.

A comparison of these data with those used for the 5 Å resolution map calculation shows that these data in the 5 Å region are poorer than before. A Fourier map calculated with these phases proved to be very poor; the haem groups were not very clear and there were other regions with the same electron density as the haem groups.

In order to improve the map, it was decided to merge the phases from the 5 Å map with the ones which had just been calculated.

Table 4.13 The number of reflections and the mean figure of merit in ranges of $4\sin^2\theta/\lambda^2$

Range of $4\sin^2\theta/\lambda^2$	Reflections								
	Centric			Acentric			Total		
	m	Number of reflections		m	Number of reflections		m	Number of reflections	
		obs.	theor.		obs.	theor.		obs.	theor.
0.00-0.02	0.829	211	230	0.770	175	176	0.802	386	406
0.02-0.04	0.705	231	242	0.652	406	410	0.670	637	652
0.04-0.06	0.689	221	250	0.856	561	569	0.773	782	819
0.06-0.08	0.671	210	238	0.702	668	692	0.686	878	930
0.08-0.10	0.616	199	245	0.673	717	796	0.664	916	1041
0.10-0.12	0.456	44	248	0.539	215	895	0.497	259	1143

For a reflection whose phase had first been calculated using the 5 Å resolution derivative data sets and finally the 3 Å resolution derivative data, there were two different phase probability distributions $P(\alpha)$. The probability for having a phase angle α for the protein structure factor is:

$$P(\alpha) = \exp[-\Sigma_j(\epsilon_j^2(\alpha)/2\ E_j^2)]$$

where the sum is extended to both derivatives and

$$\epsilon_j = (|F_{PH}(obs)| - |F_{PH}(calc)|),$$

$$|F_{PH}(calc)| = |F_P + F_H(calc)|$$

$$E_j^2 = (|F_{HLE}| - |F_H(calc)|)^2$$

Hendrickson and Lattman[12] have shown that the probability curve $P(\alpha)$ can be expressed in the form:

$$P(\alpha) = \exp(K + A\cos\alpha + B\sin\alpha + C\cos2\alpha + D\sin2\alpha)$$

For a protein reflection within the 5 Å resolution sphere, the two phase probability distributions were expressed in the following way:

$$P_1(\alpha) = \exp(K_1 + A_1\cos\alpha + B_1\sin\alpha + C_1\cos2\alpha + D_1\sin2\alpha)$$

$$P_2(\alpha) = \exp(K_2 + A_2\cos\alpha + B_2\sin\alpha + C_2\cos2\alpha + D_2\sin2\alpha)$$

and a new phase distribution was assigned to the reflection as being:

$$P(\alpha) = \exp[(K_1+K_2) + (A_1+A_2)\cos\alpha + (B_1+B_2)\sin\alpha + (C_1+C_2)\cos2\alpha + (D_1+D_2)\sin2\alpha]$$

The merging of the phases was done using the program MERGPHA written by Mr. M. Papiz[15]. Table 4.14 shows an analysis of the overall mean figure of merit before and after merging the phases.

Table 4.14 Analysis of the mean figure of merit after merging the phases

	Reflections			
	Centric		Acentric	
	m	number	m	number
Protein phases calculated from the 5 Å derivative data sets.	0.871	400	0.765	557
Protein phases calculated from the 3 Å derivative data sets.	0.771	400	0.703	557
Protein phases merged	0.930	400	0.788	557

The mean figure of merit for the 3858 unique reflections which made up the 3 Å resolution native data set was then 0.735.

Figure 4.23 shows an analysis of the mean figure of merit in ranges of $|F_p|$.

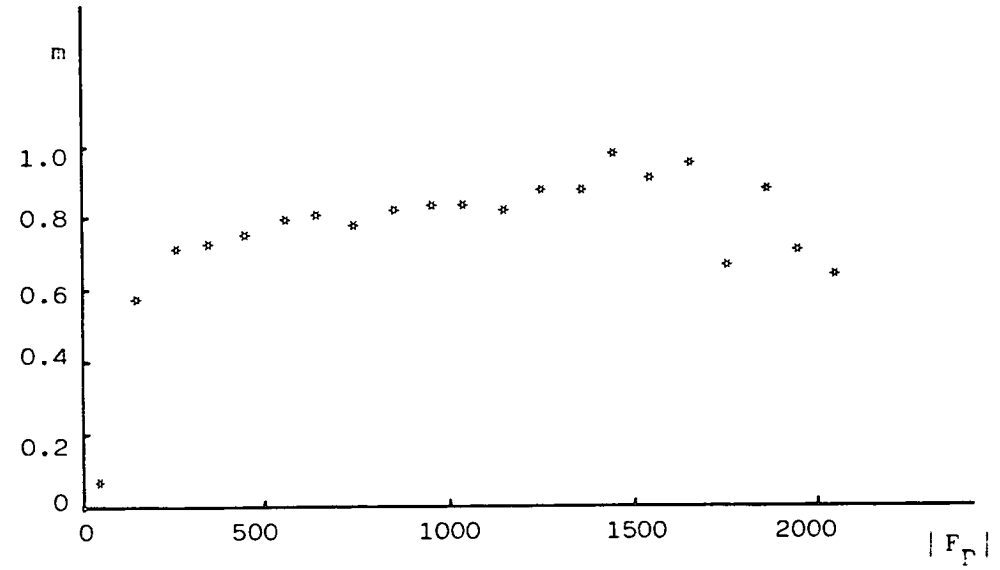

Figure 4.23 The mean figure of merit in ranges of $|F_p|$

Figure 4.24 The variation of the mean figure of merit with the protein structure factor amplitude

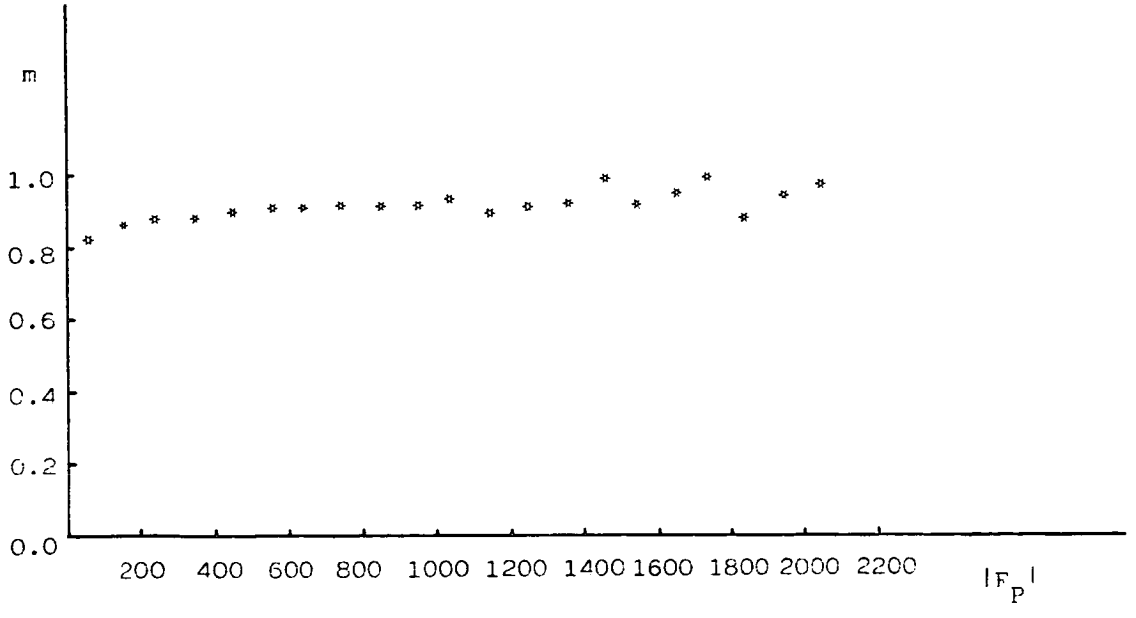

4.5 The Electron Density Map

The three-dimensional electron density map of cytochrome c_4 was calculated using 2873 of the 3858 measured reflections, whose figure of merit was greater than 0.55. This meant that the overall mean figure of merit for the reflections included in the calculation was 0.90 and the nominal resolution is 3 Å.

Figure 4.24 shows the distribution of the mean figure of merit with $|F_p|$ and Table 4.15 gives the same analysis together with the number of reflections in ranges of $(4\sin^2\theta/\lambda^2)$.

A comparison of the number of reflections used in the electron density map calculation with the number of predicted reflections shows that nearly all the reflections within the 4 Å resolution sphere have been included in the map, but the number of reflections within a resolution of 4.1 Å to 3.2 Å is approximately 2/3 of the predicted one.

The Fourier syntheses had coefficients

$$m|F_p| \exp(i\alpha_p)$$

where $|F_p|$ is the protein structure factor amplitude for a given reflection with a phase α_p to which the figure of merit m has been associated. The Fourier program FRP65[11] has been used. The a, b and c axes were divided into 60, 60 and 180 intervals, respectively, giving a grid dimension of approximately 1 Å. A contour plotting program[9] was used to display each section of the map with constant z and the whole of the a and b axes. The number of sections

Table 4.15 Analysis of the mean figure of merit and the number of reflections in ranges of $4\sin^2\theta/\lambda^2$. For each range, the corresponding resolution and the number of theoretically predicted reflections is given in brackets.

$4\sin^2\theta/\lambda^2$ ($\AA^{-2}$)	Reflections					
	Centric		Acentric		Total	
	m	number	m	number	m	number
0.00-0.02 (∞-7.1 Å)	0.986	195(230)	0.785	154(176)	0.897	349(406)
0.02-0.04 (7.1-5.0 Å)	0.973	202(242)	0.871	349(410)	0.908	551(652)
0.04-0.06 (5.0-4.1 Å)	0.932	151(250)	0.945	484(569)	0.942	635(819)
0.06-0.08 (4.1-3.5 Å)	0.905	143(238)	0.901	462(692)	0.902	605(930)
0.08-0.10 (3.5-3.2 Å)	0.881	123(245)	0.871	479(796)	0.873	602(1041)
0.10-0.12 (3.2-2.9 Å)	0.842	17(248)	0.869	115(895)	0.866	132(1143)

calculated was 16 (z = 0 to z = 1/12) since all the other sections could be reproduced using the two-fold axes present at z = 0 and z = 1/12. The map was contoured at a minimum level of 0.3 $e\text{Å}^{-3}$ and at 0.2 $e\text{Å}^{-3}$ thereafter (approximate absolute scale).

The electron density map is presented in Appendix 2. Thirty sections of constant z are presented. Based on what was found at 5 Å, in each section, x goes from -50/60 to 10/60 and y from -44/60 to 16/60 in order to have one whole molecule included in these sections.

4.6 Interpretation of the electron density map

The electron density map was plotted on transparent sheets at a scale of 0.5 cm Å^{-1}.

The highest features on the map were the centres of the iron atoms with an electron density of 1.5 and 1.3 $e\text{Å}^{-3}$. These were at sections z = 3/180 and z = 16/180.

The sulphurs of residues cysteines 14, 17, 110 and 113 and methionines 57 and 158 were identified as being the highest peaks around the haem groups; another peak of comparable height was later identified as residue 25.

After identifying the iron and the sulphur haem-binding amino acid positions, two main features became apparent: one α-helix in sections 9 to 15 and two strands of β-sheet in sections 19 to 21.

Given the quality of the map, although in many regions the c_4 polypeptide chain could be traced unambiguously from the electron density map alone, there were several ambiguities when an attempt was made to fit the whole polypeptide chain.

Since Pseudomonas aeruginosa cytochrome c_{551} has approximately the same number of residues as each half of cytochrome c_4, an attempt was made to fit its polypeptide chain to the cytochrome c_4 electron density map.

For this purpose, the section of α-helix was tentatively associated with the haem group at section 3 and the β-sheet with the other haem group. These were later identified as residues 169-180 and 48-59 respectively.

At that stage, for one half of the molecule, the iron position (z = 16/180), three possible haem ligands (Cys 14, Cys17, Met57) and one anti-parallel β-sheet (residues 48 to 59) had been identified. For the other half of the molecule, there were the iron position (z = 3/180), three haem ligands (Cys110, Cys113, Met158) and some α-helix (residues 169 to 180) which seemed to be near the carboxy-terminus, as no further continuous density could be traced.

Coordinates for the iron, haem group ligands and α-carbons of cytochrome c_{551} were taken from the Protein Data Bank [16] and a small program was written in order to get an orientation matrix which would superimpose the iron positions and one previously defined vector for both cytochromes. The iron positions and vectors defining the direction of one β-sheet strand and the direction of the α-helix were input to that program.

With these orientations of the c_{551} molecules defined, the α-carbon positions of cytochrome c_{551} were marked onto the map and where there were ambiguities before, a continuous path, corresponding to that found in the c_{551} molecule, was found. If the c_{551} α-carbon positions coincided with some electron density on the map it was assumed that cytochrome c_4 had an α-carbon at the same position; when the electron density did not coincide but was close by, the α-carbon was moved into that region. Nevertheless, there are two regions (residue 21 to 35 and residue 120 to 135) where the fitting of cytochrome c_{551} to c_4 looked very poor and most of the polypeptide chain would be in regions with zero electron density while many peaks in the map would have no explanation. In these cases the fitting of the polypeptide chain appeared to have little or no relation with the cytochrome c_{551} chain.

The orientation of the cytochrome c_{551} molecule which was related to one iron position at z = 3/180, coincides with one of the orientations found by Dr. L. Sawyer [18] when the rotation function was applied to the Patterson functions of both cytochromes. This was encouraging although the other orientation was not found among the rotation function results.

4.6.1 The molecular conformation

There were only four regions, all on the surface of the molecule, in which it was impossible to match the electron density map to the c_{551} models. They consist of residues 21 to 35, 41 to 45, 63 to 70 (α-helix near the carboxy -terminus in c_{551}) and 120-135.

Connecting the first and second half of the c_4 molecule, there are two α-helices (corresponding to the beginning and end of two different c_{551} molecules) connected by 15 residues with random coil secondary structure.

The direction of the α-helix present at the end of the first half of the c_4 molecule is approximately 40° away from the direction of the corresponding one in the c_{551} molecule.

Sections 15 to 19 in the electron density map show the haem group of the first half of the c_4 molecule with strong density at the thioether cysteine 14 and 17 residues and the methionine 57. The first α-helix, at the amino-terminus, is seen in sections 2 to 11 as a lumpy mass of density going from residues 1 to 11.

The chain pathway from residues 21 to 35 is not very clear and can only be determined unambiguously with data at higher resolution. It resembles a loop folding up to residues 24 to 25 bringing Ser25 near the top of the haem group, then it goes underneath to pick up the c_{551} folding again near residue 35. Phe29 is clearly seen extending to the inside of the crevice contributing to a hydrophobic region around the haem group.

A globular side chain extends to the inside of the molecule from residue Tyr39 as well as His45. Lys48 is seen extending to the outside of the molecule.

The α-helix starting at residue 41 (c_4 numbering) in the c_{551} molecule is not very clear in the map and we seem to have only one turn of an α-helix.

Sections 19 to 21 show clearly one anti-parallel β-sheet running from residues 48 to 59. The methionine ligand to the haem, Met57 is shown in section 17.

After the β-sheet, the polypeptide chain goes down and then forms an α-helix going from residue 68 to 82 (sections 2 to 6) and after two extended strands of polypeptide chain, another α-helix is present at the beginning of the second half of the molecule (residues 97 to 104).

The two cysteine 110 and 113 residues are clearly seen as two large masses of density near the haem group.

Once again the folding of the molecule after residue 120 to 135 does not resemble the one found in c_{551}. The chain goes up to the side of the molecule, folding down again and bringing Phe126 to the interior of the molecule. An extended chain goes from residues 128 to 135, then there is an α-helix from residue 138 to 146. After this helix there is one two-stranded β-sheet at the same position found in c_{551} and the first half of the c_4 molecule. Finally there is the carboxy-terminus α-helix which runs in sections 10 to 14 (residues 169-180).

Approximate coordinates for the C_α atoms were taken from the electron density map. Then, a program was written in order to set all the distances between the C_α atoms equal to 3.80 Å minimizing the sum of the squares of all the deviations and at the same time not allowing the distance between each C_α atom to any other, except its neighbours, to be less than 4.5 Å. The maximum shifts were of 2 Å for residues 12, 13, 28, 172 and 173. Table 4.16 shows the new coordinates in an orthogonal Å system with x along $\underline{a}$, y along $\underline{b}^*$ and z along $\underline{c}$.

Figure 4.25 shows the folding of the c_4 molecule and two c_{551} molecules in the same orientation as each half of the c_4 molecule. A has x running horizontal and y vertical, B has y horizontal and z vertical. Figure 4.26 shows one ribbon drawing of the polypeptide chain in cytochrome c_4.

The structure determinations of Tuna cytochrome c[8], Rhodospirillum rubrum bacterium cytochrome c_2 [17], Pseudomonas denifricans c_{550} [20], Chlorobium thiosulfatophilium bacterium c_{555} [13] and Pseudomonas aeruginosa c_{551} [2] were used by E. Adman[1] to show how different c cytochromes compare with one another. From this comparison, it is believed that the essential parts are the N- and C-terminal helices, the Cys, His and Met ligands, the helix near residue 40 (c_{551} numbering), a couple of aromatic residues near one another at the interface between the N- and C-terminal helix and enough additional protein to complete the wrapping of the haem group leaving one edge exposed.

The common structural features in c_{551} and both halves of c_4, in addition to those for the other cytochromes, are the β-sheets near residue 50 (and 150 in c_4).

Table 4.16 Coordinates for the C_α atoms of the c_4 molecule. The distances between non-neighbouring C_α atoms which are less than 5 Å have been indicated at the end of the table.

Residue	x	y	z	Residue	x	y	z
Ala1	10.93	59.79	1.81	Lys51	-3.77	44.02	18.67
Gly2	14.13	61.82	2.16	Arg52	-5.02	42.28	15.53
Asp3	12.04	63.89	4.57	Thr53	-3.90	38.80	16.56
Ala4	8.30	63.62	3.97	Val54	-1.16	39.57	19.08
Ala5	8.00	60.22	5.64	Leu55	1.78	41.82	19.95
Ala6	11.32	59.34	7.25	Glu56	0.69	45.37	20.74
Gly7	10.69	62.38	9.43	Met57	1.55	48.88	19.56
Gln8	7.20	61.33	10.50	Thr58	1.11	52.22	21.32
Ala9	6.93	58.81	13.33	Gly59	0.80	55.91	20.47
Lys10	10.71	59.02	13.02	Leu60	-0.78	59.36	20.42
Ala11	10.09	62.52	14.37	Leu61	-1.47	61.95	17.73
Ala12	11.54	62.64	17.88	Thr62	1.59	62.53	15.55
Val13	12.72	59.03	17.76	Asn/Asp63	2.60	58.95	16.32
Cys14	11.52	55.53	16.91	Leu64	-0.26	58.09	13.97
Gly15	14.95	55.22	15.32	Ser65	-0.28	59.27	10.36
Ala16	15.56	52.72	18.11	Asn/Asp66	-2.47	56.42	9.13
Cys17	13.31	49.73	17.46	Glu/Gln67	-1.34	53.90	6.51
His18	11.14	49.11	14.40	Asp68	0.05	52.30	3.36
Gly19	13.96	48.50	11.92	Ile69	2.50	55.07	2.49
Ala20	13.58	48.90	8.16	Ala70	3.72	54.79	6.08
Asn/Asp21	12.91	45.45	6.71	Asp71	4.97	51.23	5.63
Gly22	10.88	44.71	9.84	Leu72	6.56	50.26	2.32
Asn/Asp23	11.19	44.03	13.57	Ala73	7.42	53.89	1.61
Ala24	9.71	43.11	16.95	Ala74	8.59	55.18	4.99
Ser25	5.92	43.29	16.90	Tyr75	10.09	51.80	5.85
Pro26	4.27	40.83	14.51	Phe76	11.79	50.63	2.66
Pro27	6.73	42.18	11.95	Ala77	12.51	54.28	1.90
Asn28	4.67	44.45	9.70	Ser78	14.35	56.01	4.74
Phe29	6.68	47.00	7.72	Gln79	15.80	53.06	6.64
Pro30	8.47	45.99	4.53	Lys80	16.71	51.63	3.25
Lys31	6.66	42.65	4.57	Met81	19.25	54.46	3.20
Leu32	2.97	43.53	4.85	Ser82	21.52	53.82	6.18
Ala33	2.40	40.68	7.30	Val83	23.80	52.20	3.61
Gly34	1.34	38.87	10.47	Gly84	27.43	52.28	2.46
Gln35	-.83	41.77	11.64	Met85	29.59	54.07	5.03
Gly36	-2.85	41.61	8.43	Ala86	32.90	52.25	4.61
Glu37	-5.96	42.09	10.56	Asn/Asp87	32.42	49.11	2.51
Arg38	-6.13	45.66	9.28	Pro88	33.41	45.50	3.15
Tyr39	-5.76	45.01	5.55	Asn/Asp89	32.55	45.78	6.84
Leu40	-3.69	48.19	5.58	Leu90	30.07	48.65	7.13
Leu41	-6.65	50.49	6.18	Val91	27.22	50.65	8.66
Lys42	-7.39	53.56	8.30	Glu/Gln92	25.07	47.95	7.07
Gln43	-9.86	52.59	11.02	Ala93	22.70	45.80	5.02
Met44	-8.56	49.17	12.04	Gly94	20.19	48.63	5.40
His45	-5.16	50.85	12.37	Glu95	18.60	49.38	8.77
Asp46	-4.87	54.23	14.09	Ala96	19.18	45.76	9.79
Ile47	-4.91	57.43	16.14	Leu97	17.42	43.34	12.13
Lys48	-4.15	55.20	19.12	Phe98	16.42	39.87	13.29
Asp49	-3.54	51.45	19.10	Arg99	12.92	39.32	11.91
Gly50	-3.26	47.76	18.23	Gly100	14.12	41.27	8.87

Table 4.16 (contd..)

Residue	x	y	z
Gly101	16.71	40.11	6.34
Lys102	14.42	37.14	5.73
Ile103	11.63	39.23	4.21
Ala104	13.42	42.24	2.73
Glu105	15.66	42.72	-0.30
Gly106	18.53	41.28	1.73
Met107	19.55	37.83	2.95
Pro108	16.50	36.77	0.96
Ala109	16.05	33.13	-0.04
Cys110	14.60	32.57	3.43
Thr111	10.98	33.73	3.43
Gly112	10.68	31.99	0.06
Cys113	12.55	28.71	0.57
His114	11.31	28.62	4.16
Gly115	10.10	28.60	7.76
Ser116	9.48	31.01	10.64
Ser117	7.82	33.22	8.05
Pro118	6.19	30.85	5.56
Val119	6.49	28.39	2.68
Gly120	8.61	25.62	1.17
Ile121	11.50	23.61	-0.25
Ala122	13.38	23.80	3.05
Thr123	12.42	23.31	6.70
Ala124	12.92	25.05	10.04
Gly125	14.84	27.51	7.87
Phe126	18.04	27.51	5.82
Pro127	19.49	24.98	8.26
His128	19.01	21.51	9.73
Leu129	20.71	21.02	13.09
Gly130	24.36	20.01	12.73
Gly 131	26.25	20.98	9.58
Leu132	29.22	23.30	10.11
His133	30.37	25.61	12.90
Ala134	32.86	28.48	13.11
Gln135	35.30	31.04	11.74
Tyr136	32.66	33.10	9.94
Val137	32.44	30.16	7.55
Ala138	29.19	29.20	9.27
Lys139	25.51	29.72	8.48
Gln140	26.69	33.02	6.99

Residue	x	y	z
Leu141	29.73	33.35	4.74
Thr142	30.56	30.16	2.85
Asp143	26.88	29.33	3.29
Phe144	24.68	32.27	2.33
Arg145	26.77	35.01	0.72
Glu146	28.25	32.18	-1.34
Gly147	25.80	29.29	-1.55
Thr148	24.38	26.22	0.17
Arg149	25.15	22.59	-0.67
Thr150	26.01	19.42	1.24
Asn151	24.00	20.96	4.07
Asp152	20.20	20.89	4.05
Gly153	20.84	18.06	1.59
Asp154	20.05	20.82	-0.91
Thr155	19.34	20.50	-4.63
Lys156	21.46	23.64	-4.83
Ile157	20.24	26.60	-2.78
Met158	21.26	29.82	-4.50
Gln159	23.73	32.68	-4.93
Ser160	22.29	34.94	-2.23
Ile161	22.55	38.49	-3.56
Ala162	23.13	39.99	-0.12
Ala163	25.33	42.19	2.06
Lys164	28.25	40.38	3.69
Leu165	27.14	42.39	6.71
Ser166	23.51	41.27	6.80
Asn167	25.00	37.78	6.63
Lys168	26.70	38.53	9.95
Asp169	23.50	39.69	11.64
Ile170	21.01	37.63	9.64
Ala171	23.45	34.89	10.66
Ala172	23.77	35.22	14.43
Ile173	20.14	36.32	14.56
Ser174	18.81	33.75	12.10
Ser175	19.99	30.36	13.33
Tyr176	18.50	31.58	16.61
Ile177	15.67	34.07	16.06
Gln178	13.08	34.47	13.30
Gly179	14.34	33.07	10.00
Leu180	14.91	29.88	11.99
His181	13.96	29.31	15.63

Ala1	Ala5	4.84 Å			
Gly7	Lys10	4.29 Å;	Ala11	4.98 Å	
Gln8	Lys10	4.90 Å;	Ala11	4.98 Å	
Ala9	Ala11	4.98 Å			
Ala20	Gln79	4.96 Å			
Asn/Asp21	Pro30	4.98 Å;	Gly100	4.85 Å	
Gly22	Gly100	4.82 Å			
Ala93	Ser166	4.93 Å			
Gly101	Met107	4.97 Å			
Gly115	Gly125	4.86 Å			

Thr 123	Gly125	4.98 Å
Gly125	Leu180	4.75 Å
Asp143	Gly147	4.96 Å
Asn151	Gly153	4.95 Å
Asp152	Asp154	4.96 Å
Ala163	Leu165	4.99 Å
Asn167	Ile170	5.00 Å
Lys168	Ala171	4.93 Å
Asp169	Ala171	4.90 Å
Ala171	Ser 174	4.99 Å
Ser174	Gly179	4.98 Å

Figure 4.25A Projections of cytochrome c_4 along the z and x axes. Two c_{551} molecules have been shown in the same orientations as each half of cytochrome c_4. x is horizontal and y is vertical.

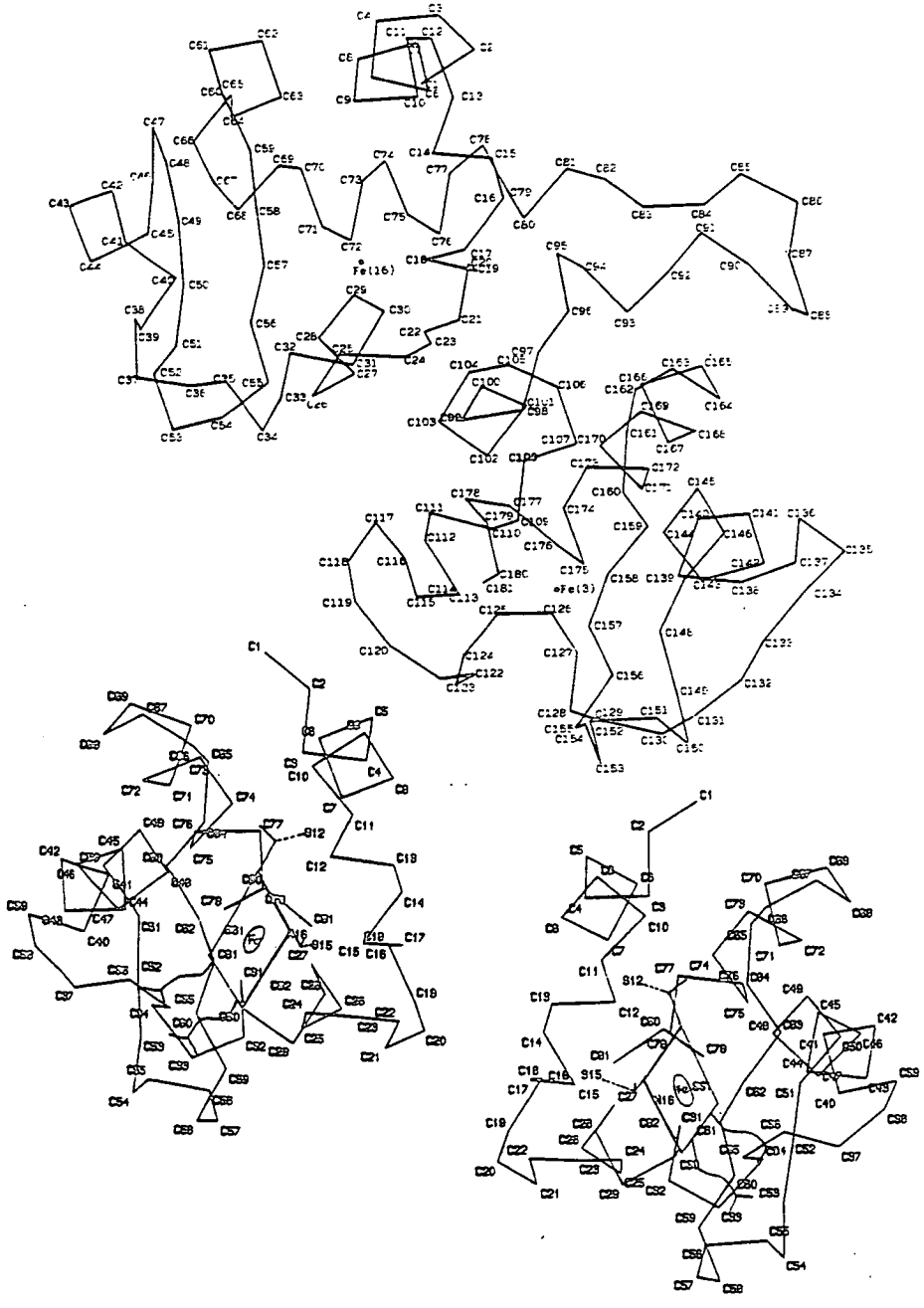

Figure 4.25B Projections of cytochrome c_4 along the z and x axes. Two c_{551} molecules have been shown in the same orientations as each half of cytochrome c_4. y is horizontal and z is vertical

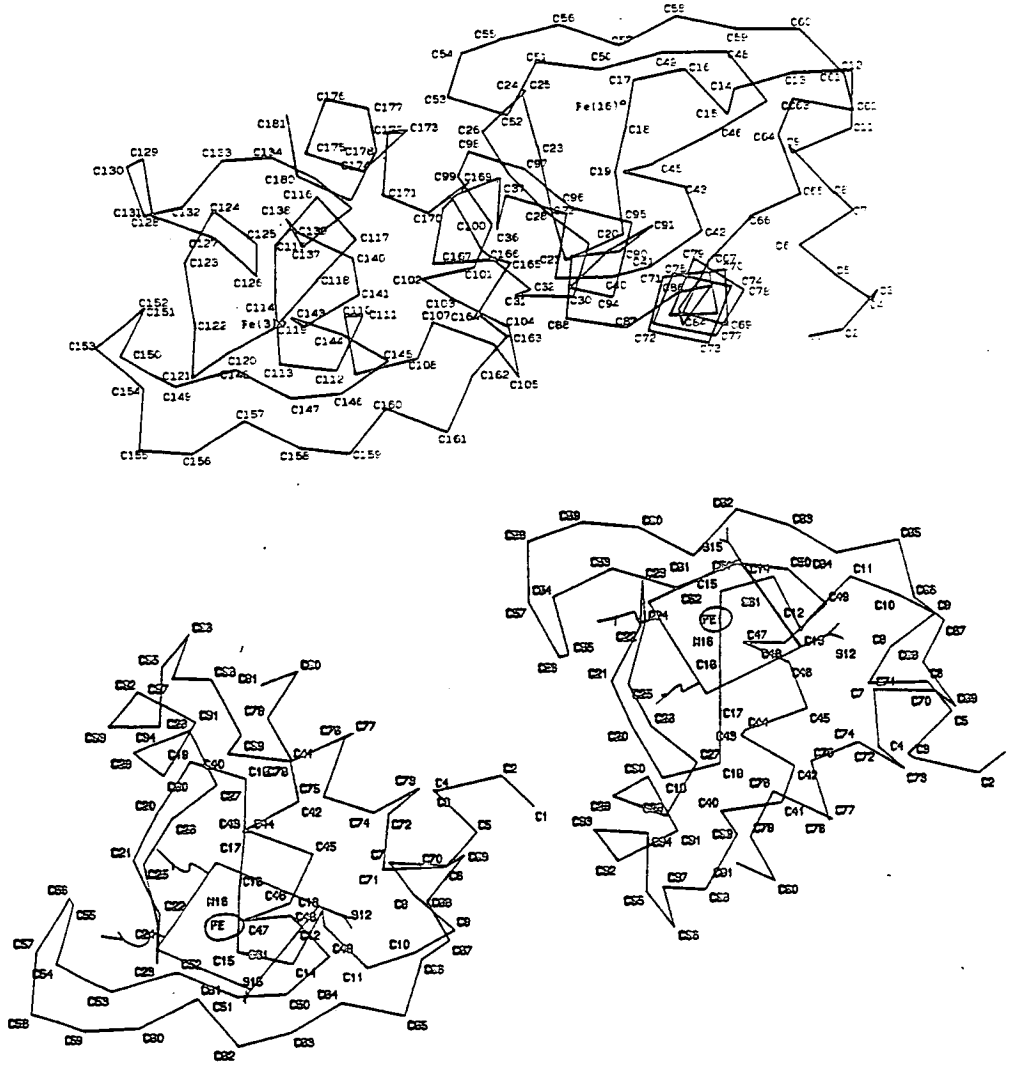

Figure 4.26 Ribbon diagram of the polypeptide chain in cytochrome c_4

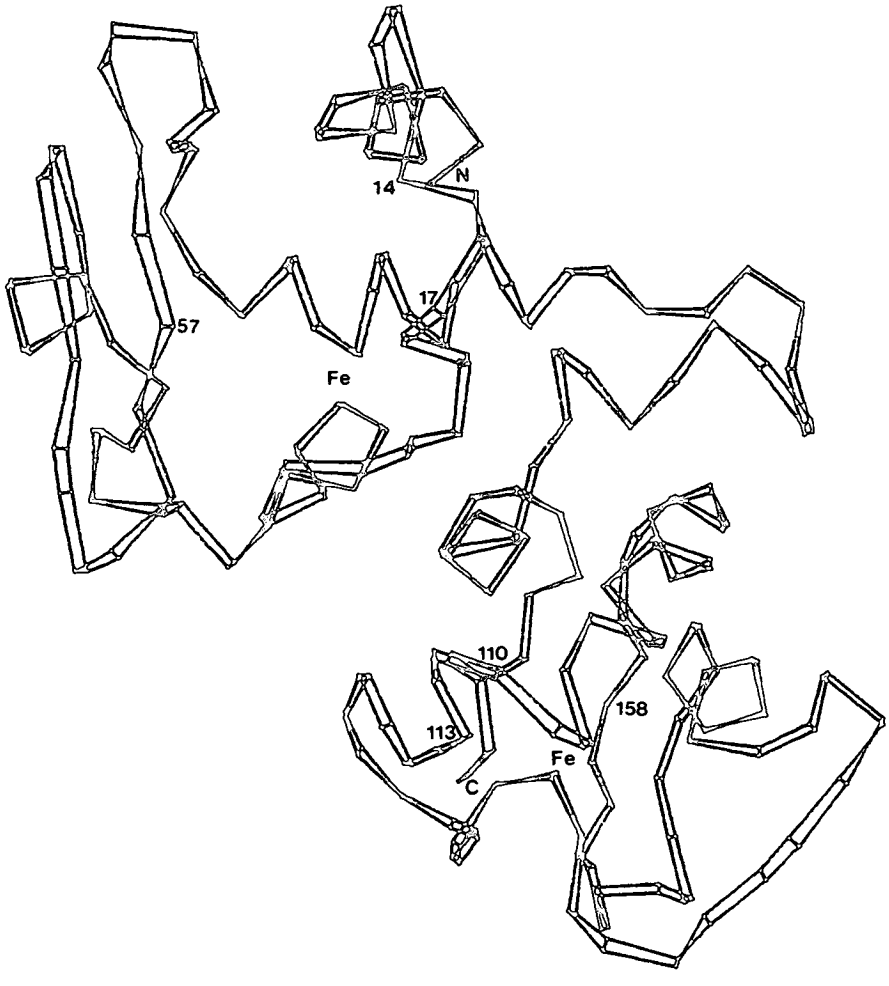

5. Heavy atom binding sites and the packing of the molecule

The uranyl ion, UO_2^{2+}, often binds carboxylate groups of aspartic acid or glutamic acid and occasionally the hydroxyl side chains of threonine or serine[6]. The principal uranium-binding site occurs near residue Arg52, but Thr53 is nearby.

The $(Pt(NO_2)_4)^{2-}$ has been reported to bind one methionine and one histidine[7]. In this case, however, the most heavily occupied platinum site occurs near Ala77 and Ser78. Another site is near His114 and Val 119 and the smaller site is near Ala4.

All these sites occur on the outside part of the molecule as was expected.

The overall shape of the molecule is roughly ellipsoidal, with dimensions 40 x 52 x 28 Å.

The molecular boundary is clearly defined for most of the molecule and agrees with the one found for the 5 Å map. The boundary has been indicated on the electron density map.

Figure 4.27 shows one unit cell with a diagram of the c_4 molecule occuring between sections z = -6/180 to z = 22/180 and its symmetry related by the two-fold axes present at z = 0 and z = 1/12. The part of the unit cell which has been presented on the electron density map is indicated.

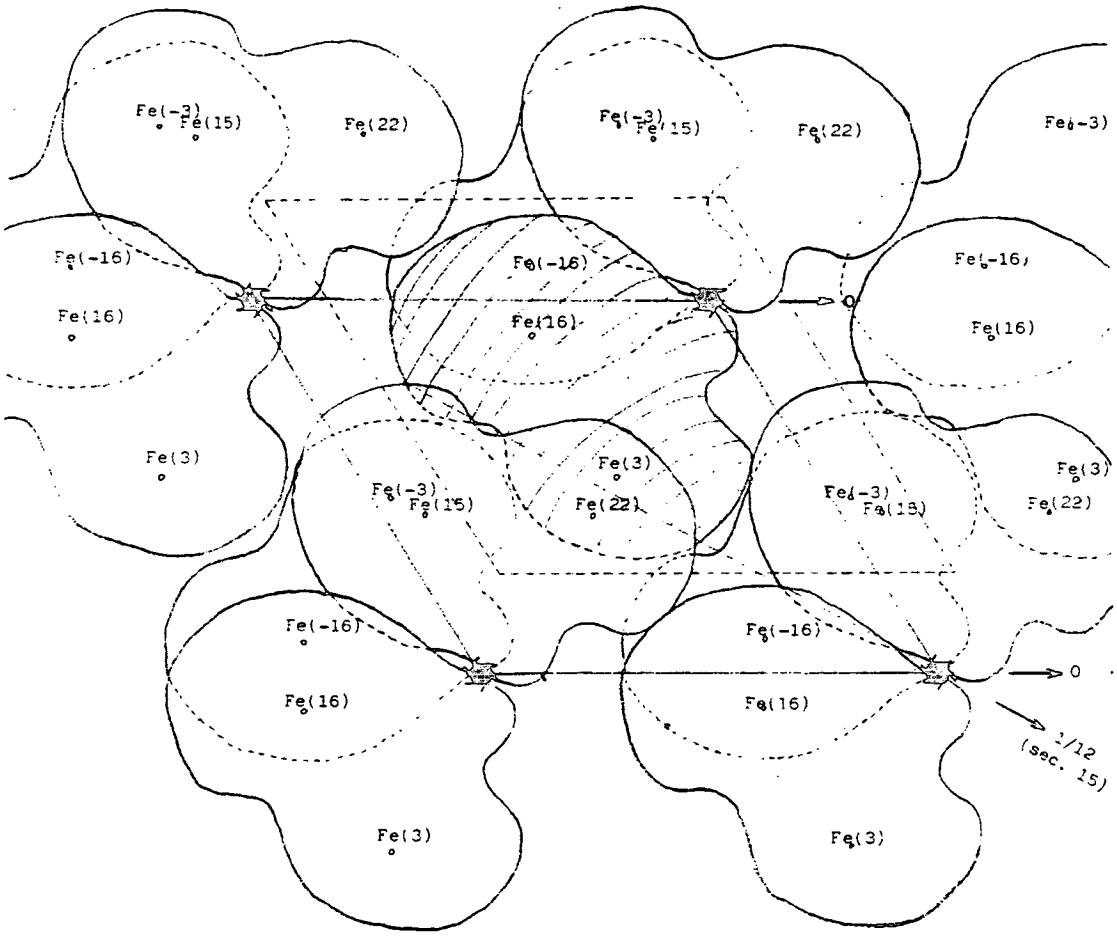

Figure 4.27 Projection of the unit cell along z showing the molecular packing in the unit cell between $z = -|c|/9$ and $z = +|c|/9$. The region in the unit cell which has been presented on the electron density mass is indicated by the dashed lines

6. Results

The structure determinations of Pseudomonas aeruginosa cytochrome c_{551} and Tuna c have provided a precise alignment of their amino acid sequences[2] showing that although Tuna cytochrome c has 21 more residues than c_{551} the basic molecular folding is the same.

It is apparent from the last sections that the overall cytochrome fold has been found twice in this di-haem molecule. An important aspect will be to know whether the structural similarity in these three molecules extends to more than the overall folding.

Azotobacter vinelandii cytochrome c_4 has an insertion of nine residues between residues 48 and 49. This is at the surface of the molecule, making an insertion of some residues possible without major modifications on the molecular outline, possibly giving more turns on the α-helix near that position.

6.1 Hydrophobic environment around the haem group

Table 4.17 compares the equivalent hydrophobic side chains packed around the haem group in cytochromes c and c_{551}[2] as well as in cytochrome c_4. The comparison with cytochrome c_4 was based on the amino acid sequence similarities and finally on the amino acid three dimensional positions.

It is apparent that there are many haem contacts in the other two cytochromes which are similar to those in cytochrome c_4.

Table 4.17 Hydrophobic haem contacts. The residues in brackets correspond to Azotobacter vinelandii cytochrome c_4

Cytochrome c		Cytochrome c_{551}		P.aeruginosa cytochrome c_4	
Tuna	60 Eukaryotes	P.aeruginosa	6 Prokaryotes	1st half	2nd half
Phe10	60Phe	Phe7	5Phe, 1Tyr	Ala9(Gly)	Ile103(Leu)
Pro30	60Pro	Pro25	6Pro	Pro27(Pro)	uncertain
Leu32	60Leu	Tyr27	3Phe, 2Leu, 1Tyr	Phe29(Phe)	Phe126(Tyr)
Leu35	51Leu, 5Ile, 2Val, 2Phe	Val30	6Val	Leu32(Leu)	uncertain
Leu64	57Leu, 2Met, 1Phe	Leu44	5Leu, 1Ile	uncertain	Phe144(Phe)
Tyr67	59Tyr, 1Phe	no haem contact		uncertain	
Leu68	60Leu	Ile48	6Ile	uncertain	Gly147(Gly)
Pro71	60Pro	Gly51	6Gly	uncertain	
no haem contact		Pro62	6Pro	uncertain	Ile157(Ile)
Phe82	60Phe	no haem contact		Leu55(Leu)	uncertain
Ile85	36Leu, 24Ile	Val66	6Val	Leu64(Phe)	uncertain
Leu94	58Leu, 2Ile	Leu74	6Leu	uncertain	Ile170(Ile)
Val95	55Ile, 4Val, 1Leu	Ala75	6Ala	Tyr75(Tyr)	uncertain
Leu98	57Leu, 3Met	Val78	4Val, 2Ile	Phe76(Phe)	uncertain

6.2 Aromatic residues

The aromatic side chains also show some degree of homology and conservatism in cytochromes c and c_{551}. A comparison between those two cytochromes and cytochrome c_4 is shown in Table 4.18.

It has been found in cytochromes c and c_{551}, that the haem groups seem to demand the nearby presence of aromatic residues, though their orientation does not seem critical.

From Table 4.18 it is apparent that most of the aromatic residues present in c_{551} are present in cytochrome c_4 and, looking at their position, apart from Tyr176 they all have been assigned to the interior of the molecule.

6.3 Charged side chains

The distribution of negatively and positively charged chains is very asymmetric in relation to the haem group but fairly similar in both halves of the molecule.

All those residues expect Arg99 are clearly outside or on the molecular surface. Figure 4.28 shows their distribution on the molecule. Residues Asp and Glu have been marked with a negative sign and Lys and Arg with a positive one.

It has been observed[2] that cytochromes c and c_{551} have the exposed haem edge surrounded by a ring of lysine residues which are believed to be important for the electron transfer. Cytochrome c_4 has a total of nine lysine and four arginine

Table 4.18 Aromatic sidechains in cytochromes c, c_{551} and c_4

Tuna c	P.aeruginosa c_{551}	cytochrome c_4 1st half P. aeruginosa	A. Vinelandii	2nd half P.aeruginosa	A. vinelandii
Phe 10	Phe 7	-		Phe98(13,14)	Tyr
Not aromatic	Tyr 27	Phe29(7,8)	Phe	Phe126(5,6)	Tyr
Phe 36	Not aromatic	-		-	
Not aromatic	Phe 34	Tyr39(6)	Tyr	Tyr136(7,8,9,10)	Tyr
Tyr 46	Deletion region	-		-	
Tyr 48	Deletion region	-		-	
Trp 59	Trp 56	-		Phe144(0,1,2)	Phe
Tyr 67	Not aromatic	-		-	
Tyr 74	Not aromatic	-		-	
Phe 82	Not aromatic			-	
Tyr 92	Trp 77	Tyr75(6,7)	Tyr	Tyr176(16)	Tyr
-	-	Phe76(3,4)	Phe	-	

The numbers in brackets indicate the amino acid position (section) in the electron density map

residues and cytochrome c_{551} has eight lysines and one arginine, of which six positive charged residues surround the exposed haem edge. Although the distribution of those residues is not the same in both molecules, cytochrome c_4 appears to have four positively charged residues around each exposed haem edge: Lys10, Lys48, Lys51, Arg52 and Arg145, Arg149, Lys156, Lys164.

Figure 4.28 The distribution of charged residues in the molecule

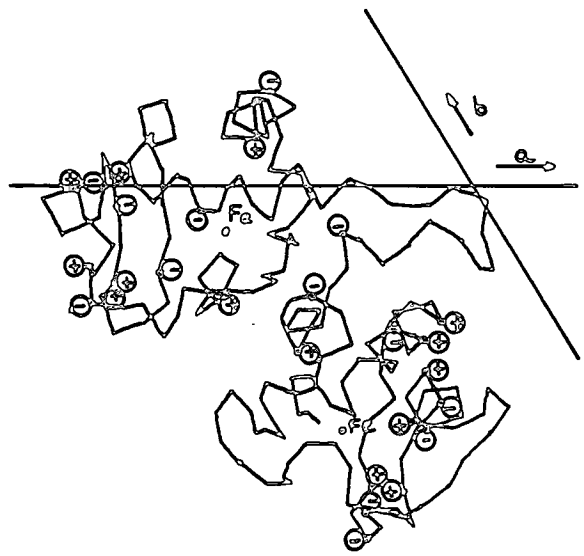

7. Conclusion

The comparison of cytochrome c_4 with c_{551} and Tuna c shows that although c_4 is approximately twice the size of the others, the folding of those cytochromes has been conserved and c_4 is essentially two cytochromes with the amino terminus of one connected to the carboxyl terminus of the other - a covalent dimer. It is thus likely that all cytochromes are a consequence of different developments from a common ancestor.

Although cytochrome c_4 resembles c_{551} in many regions, there are significant differences. Both halves of cytochrome c_4 have a haem group with its cavity open to the solvent, suggesting that both are functional.

This study is not complete, but it has provided information which will be very helpful in the interpretation of a high resolution electron density map for which data to 2.3 Å resolution have just been collected at an optimised wavelength for the Fe anomalous scattering, using the synchrotron radiation and the rotation camera at the S.E.R.C. Laboratory in Daresbury.

References

1. Adman, E.T., Biochim.Bioph.Acta., 549, 107-144, 1979.

2. Almassy, R.J., Dickerson, R.E., Proc.Natl.Acad.Sci., U.S.A., 75, 2674-2678, 1978.

3. Arndt, U.W. and Wonacott, A.J., The rotation method in crystallography, Elsevier/North-Holland Biomedical Press, 1977.

4. Azaroff, L.V., Acta Cryst., 8, 701-704, 1955.

5. Blundell, T.L. and Johnson, L.N., Protein Crystallography, Academic Press Inc. (London) Ltd., 1976, page 278

6. Reference 5, page 204.

7. Reference 5, page 224.

8. Dickerson, R.E., Takano, T., Eisenberg, D., Kallai, O.B., Samson, L., Cooper, A. and Margoliash, E., J.Biol.Chem., 246, 1511-1535, 1971.

9. "CONTOUR" program, available at E.R.C.C.

10. Fox and Holmes, Acta Cryst., 20, 886-891, 1966.

11. Harding, M.M., Gould, R.O., "FRP65", $P6_522$ Fourier program.

12. Hendrickson, W.A., Lattman, E.E., Acta Cryst., B26, 136-143, 1970.

13. Korszun, Z.R., Salemme, F.R., Proc.Natl.Acad.Sci, U.S.A., 74, 5244-5247, 1977.

14. Matthews, B.W., Klopfenstein, C.E., Colman, P.M., J.Phys.Sci. Instr., 5, 353-359, 1972.

15. Papiz, M., "MERGPHA". Merge phases program.

16. Protein Data Bank. The Brookhaven National Laboratory Protein Data Bank.

17. Salemme, F.R., Freer, S.T., Xuong, N.H., Alden, R.A., Kraut, J., J.Biol.Chem., 248, 3910-3921, 1973.

18. Sawyer, L., personal communication.

19. Stuart, D., Chapness, J., Wonacott, A., Nyborg, J., Levine, M., Stammers, D., Todd, R., Walker, M., "PDP11 Oxford" suite of programmes for processing Arndt-Wonacott oscillation camera data.

20. Timkovich, R., Dickerson, R.E., J.Biol.Chem., 251, 4033-4046, 1976.

21. Wittaker, E.J.W., Acta Cryst., 6, 218, 1953.

Appendix 1 Observed and calculated structure factors for the heterocyclic compounds

Observed and calculated structure factors for compound $C_9H_6NOSCl_3$

0,0,L

2	337	-382
4	722	-773
5	785	-839
6	134	-138
7	291	-293
8	85	-78
9	49	54
10	69	-71

0,1,L

2	592	-677
3	862	-1005
4	878	-1030
5	25	26
6	148	-152
7	213	-221
8	144	138
9	62	-69
10	46	-51
11	32	29

0,2,L

2	90	97
3	470	-510
4	258	-279
5	135	-138
6	73	-88
7	30	22
8	-25	-39
9	155	146
10	174	177
11	34	29

0,3,L

1	390	-441
2	266	-292
3	140	-169
4	365	-397
5	99	105
6	342	364
7	145	160
8	301	320
9	215	224
10	-29	30
11	33	25

0,4,L

1	48	-50
2	83	105
3	82	-89
4	239	273
5	324	356
6	73	75
7	160	170
8	105	109
9	113	-117
10	73	-85
11	58	-53

0,5,L

1	26	-22
2	374	-405
3	-16	4
4	70	66
5	216	-224
6	127	128
7	115	115
8	168	-171
9	44	-44
11	94	-94

0,6,L

1	349	-391
2	87	-94
3	76	82
4	81	91
5	240	249
6	136	141
7	47	-45
8	36	-9
10	72	-67

0,7,L

1	282	311
2	100	108
3	169	182
4	216	220
5	47	43
6	69	-73
7	39	-39
8	-19	-17
9	57	-58

0,8,L

1	60	64
2	-17	4
3	28	32
4	28	20
5	47	-50
7	33	-30
8	50	-41

0,9,L

1	-15	12
2	86	95
3	47	41
5	44	43
6	37	-39

0,10,L

1	69	84
2	47	48
3	28	-33
4	-20	22

1,1,L

-10	44	38
-9	56	-59
-8	101	-93
-7	54	-48
-6	-17	3
-5	182	-182
-4	61	69
-3	572	597
-2	428	-433
-1	111	104
2	128	123
3	48	46
4	399	414
5	159	167
7	164	173
8	91	-91
9	152	-154
10	81	-78
11	69	-64

1,2,L

-11	39	31
-10	-24	-13
-9	145	-141
-8	99	101
-7	63	61
-6	101	-103
-5	325	337
-4	80	77
-3	85	78
-2	280	288
-1	200	-192
2	39	-38
3	131	131
4	68	-55
5	255	-273
6	249	-261
7	127	-117
8	249	-251
9	86	-98
10	70	72
11	-29	-22

1,3,L

-11	-24	-21
-9	79	83
-8	47	-48
-7	69	-70
-6	136	147
-5	38	40
-4	77	-87
-3	163	166
-2	92	-99
-1	300	-300
0	77	-76
1	726	-723
2	389	-389
3	90	90
4	433	-455
5	33	-44
6	317	332
7	82	-85
8	75	73
9	221	230
11	33	29

1,4,L

-11	63	-63
-10	50	-44
-9	56	-57
-8	122	-124
-6	-19	12
-5	101	-112
-4	30	28
-3	69	-72
-2	426	-442
-1	182	-180
0	74	68
1	157	-143
2	261	277
3	562	594
4	121	134
5	231	253
6	198	203
7	92	-89
8	-19	-8
10	32	-29
11	-21	2

1,5,L

-10	77	-70
-9	39	-34
-8	38	32
-7	-21	7
-6	99	98
-5	116	118
-4	23	20
-3	148	165
-2	195	197
-1	218	228
0	178	178
1	279	273
2	262	251
3	157	-155
4	65	-70
5	31	-39
6	190	-183
7	80	-79
9	-17	-7
10	-23	5

1,6,L

-10	-34	21
-9	83	81
-8	103	97
-7	148	148
-6	149	155
-5	164	169
-4	123	132
-3	42	-37
-2	158	-165
-1	44	-51
0	146	-196
1	380	-395
3	21	-19
4	155	-157
5	71	70
6	-22	-1
7	-24	-23
9	76	-71

1,7,L

-9	31	13
-8	109	107
-7	89	93
-6	218	-217
-5	26	-28
-4	41	-39
-3	512	-537
-2	124	-131
-1	82	81
0	194	-264
1	113	124
2	198	201
3	71	-68
4	76	81
5	27	-22
6	127	-129
7	-20	21
8	-18	11
9	30	-19

1,8,L

-7	126	-121
-6	63	-72
-5	29	23
-4	253	-251
-3	64	55
-2	217	219
-1	237	-257
0	83	128
1	268	299
2	195	-194
3	23	16
4	174	167
5	44	-47
6	47	47
7	98	93
8	-28	13

1,9,L

-6	62	59
-5	36	-30
-4	92	-96
-3	64	65
-2	30	30
-1	47	-56
0	108	172
1	122	142
2	56	56
3	134	133
6	-17	7
7	103	-98

1,10,L

-3	37	36
-2	92	96
-1	99	127
0	35	59
1	-16	24
2	36	-39
3	109	-102
4	86	-84
5	106	-102

2,0,L

-11	132	-114
-10	158	-142
-9	197	191
-8	80	72
-7	221	226
-6	827	877
-5	27	-12
-4	134	123
-3	309	298
-1	252	-241
0	589	589
1	74	66
2	735	696
4	527	547
5	55	-50
6	71	75
7	360	-352
8	245	-246
9	165	-161
10	310	-296
11	-20	-3

2,1,L

-11	44	48
-10	173	172
-9	158	157
-8	121	126
-7	390	403
-6	-20	7
-5	621	-652
-4	365	369
-3	43	30
-1	1039	1062
0	922	932
1	606	-590
2	342	327
3	436	-432
4	506	-507
5	307	-301
6	580	-602
7	178	-190
8	41	6
9	125	-133
10	-27	-27
11	84	87

2,2,L

-10	89	86
-9	47	41
-8	-24	-8
-7	74	71
-6	78	-35
-5	268	-271
-4	251	-255
-3	293	-295
-2	676	-663
-1	615	-590
0	587	-556
1	312	-309

2,2,L

2	134	-118
3	-130	73
4	324	321
5	142	141
6	195	187
7	69	69
8	36	-32
9	79	79
10	48	47
11	45	47

2,3,L

-10	72	75
-8	67	-78
-7	138	-143
-6	254	-264
-5	425	-456
-4	498	-510
-3	236	-245
-2	200	-205
-1	353	339
0	868	847
1	614	603
2	1054	1091
3	710	722
4	144	-123
5	48	47
6	28	-28
7	269	-277
8	76	-89
9	80	87
10	-29	30
11	31	34

2,4,L

-9	130	-134
-8	75	-78
-7	-16	-13
-6	129	-133
-5	102	101
-4	313	324
-3	167	175
-2	580	599
-1	819	857
0	76	82
1	406	399
2	435	404
3	647	-652
4	340	-347
5	78	-89
6	420	-444
7	65	-70
8	103	110
9	75	-59
10	51	47
11	40	33

2,5,L

-9	50	49
-8	183	184
-7	38	38
-5	138	143
-4	116	-119
-3	54	-53
-2	150	153
-1	40	-45
0	156	144
1	-17	2
2	433	-410
3	174	-174
4	165	-158
5	402	-412
6	62	-60
7	164	167
8	72	-75
9	69	66
10	116	113
11	53	-51

2,6,L

-9	-29	7
-7	213	-213
-6	182	-185
-5	35	-38
-4	26	-18
-3	99	105
-2	225	219
-1	216	216
0	77	86
1	251	-244
2	327	-311
3	92	-91
4	257	-265
5	95	-90
6	211	219
7	41	44
8	79	80
9	122	119
10	-19	-2

2,7,L

-8	43	-43
-7	78	-80
-6	147	144
-5	117	122
-4	56	54
-3	249	255
-2	25	21
-1	139	-144
0	125	-135
1	200	-202
2	103	-109
3	90	-86
4	40	45
5	132	129
6	70	73
7	83	84
8	53	45
9	54	44

2,8,L

-6	51	47
-4	54	-53
-3	42	37
-2	44	-42
-1	116	-126
0	33	35
1	49	-58
2	80	-77
3	60	59
4	-14	2
5	34	37
6	91	88
7	42	46
8	-24	25

2,9,L

-6	33	30
-4	27	23
-3	59	57
-2	29	-31
-1	40	-30
0	27	-26
1	82	-89
2	-21	-5
3	-16	15
4	-20	14
5	117	121
6	67	63
7	-26	-10

2,10,L

-4	-20	24
-3	55	-47
-2	-17	11
-1	-17	-14
0	74	-86
1	26	25
2	51	48
3	-18	-18
4	93	84

3,1,L

-11	46	-45
-10	65	62
-9	44	39
-8	92	-93
-7	145	145
-6	29	-29
-5	179	-172
-4	392	393
-3	-15	4
-2	155	146
-1	563	539
0	101	-90
1	22	0
2	322	-296
3	569	-543
4	288	-282
5	-17	-18
6	101	-107
7	116	113
8	298	308
10	33	27
11	81	85

3,2,L

-11	81	75
-10	54	48
-8	80	79
-7	108	115
-6	-25	13
-5	37	-33
-4	190	182
-3	45	45
-2	229	-214
-1	488	-466
0	426	-404
1	50	-48
2	790	-765
3	54	-58
4	630	601
5	160	-154
6	255	258
7	358	363
8	163	-162
9	41	-40
10	41	-40
11	121	-118

3,3,L

-10	-22	-7
-9	53	49
-7	176	-179
-5	220	-220
-4	397	-411
-3	23	-12
-2	100	-104
-1	190	-187
0	134	136
1	174	153
2	46	-44
3	272	272
5	101	-107
6	198	205
7	74	-76
8	39	-47
9	123	126
10	36	-41
11	29	17

3,4,L

-10	34	-37
-9	55	-54
-8	139	-144
-7	144	-149
-6	42	-37
-5	98	-101
-4	147	144
-3	270	266
-2	149	-139
-1	409	396
0	165	150
1	607	-570
2	329	313
3	207	191
4	124	-106
5	376	377
6	241	249
7	50	52
8	90	90
9	41	-41
10	86	-84
11	35	-27

3,5,L

-9	-27	-30
-7	84	80
-6	47	53
-5	69	69
-4	218	213
-3	50	51
-1	169	159
0	70	77
1	113	114
2	327	300
3	179	172
4	45	44
5	61	53
6	154	-155
7	228	-226
8	161	-161
9	144	-145
10	82	-75
11	39	-41

3,6,L

-9	48	46
-8	63	-56
-7	60	56
-6	132	136
-5	69	-66
-4	143	145
-3	211	208
-2	33	-34
-1	91	93
0	43	-41
1	206	-205
2	180	-179
3	312	-295
4	267	-264
5	161	-155
6	76	-68
7	90	-87
9	115	112
10	-23	-11

3,7,L

-8	49	59
-7	32	28
-6	101	-95
-5	141	135
-4	50	57
-3	318	-309
-2	99	-111
-1	97	-92
0	411	-410
1	172	-174
2	44	48
3	-21	-2
4	150	149
5	150	150
6	63	65
7	155	152
8	-25	0
9	57	-51

3,8,L

-7	109	-100
-6	37	-40
-5	54	51
-4	130	-129
-3	51	-59
-2	102	90
-1	30	-30
0	90	95
1	225	222
2	52	54
3	141	141
4	131	127
5	75	-74
6	-23	16
7	-19	-9
8	54	-51

3,9,L

-5	45	48
-4	-24	18
-3	183	178
-2	-21	-9
-1	79	-79
0	49	54
1	46	-45
2	33	-29
3	-14	-14
4	36	-25
5	40	42
6	-23	-18

3,10,L

-3	62	-57
-2	85	-79
-1	84	-91
0	-18	-15
1	47	46
2	47	45
4	-22	17

4,0,L

-11	112	-101
-10	76	-58
-8	221	-212
-7	75	-64
-6	497	493
-5	519	507
-4	505	473
-3	1150	1162
-2	779	785
-1	102	-98
1	819	-803
2	565	-526
3	295	-278
4	773	-746
5	-18	-22
6	28	23

4,0,L

7	227	-223
9	34	-10
10	39	-39
11	43	-41

4,1,L

-11	-25	-13
-10	82	82
-9	79	79
-8	73	72
-7	398	397
-6	236	229
-5	60	56
-4	282	269
-3	367	-359
-2	762	-731
-1	643	-624
0	645	-630
1	647	-623
2	528	-509
3	135	-126
4	44	-45
5	75	-73
6	41	-36
7	64	64
8	168	166
9	29	-31
11	119	119

4,2,L

-10	-19	10
-9	89	-97
-8	79	-76
-6	311	-312
-5	190	-189
-4	66	58
-3	385	-356
-2	120	-100
-1	177	-158
0	263	-239
1	121	-106
2	470	-442
3	44	-48
4	352	322
5	302	291
6	209	199
7	326	323
8	287	289
9	34	-31
11	70	75

4,3,L

-10	63	-56
-9	45	-47
-8	88	-92
-7	136	133
-6	165	169
-5	69	-59
-4	322	326
-3	132	137
-2	535	-523
-1	50	-53
0	55	-63
1	410	-384
2	377	339
3	679	659
4	388	376
5	495	490
6	306	311
7	69	-71
8	-25	-31
9	126	-130
10	136	-142

4,4,L

-10	75	77
-9	-21	27
-8	61	60
-7	184	193
-6	29	29
-5	32	30
-4	95	95
-3	312	-313
-2	27	-34
-1	101	98
0	311	-298
1	432	409
2	640	631
3	34	-28
4	170	168
5	168	165
6	336	-337
7	209	-218
8	127	-134
9	189	-197
11	38	-29

4,5,L

-9	-20	5
-8	53	53
-7	51	50
-6	56	49
-5	52	51
-4	128	-128
-3	227	-218
-2	-19	-10
-1	211	-211
0	179	-167
1	382	361
2	47	-47
3	53	-37
4	182	179
5	328	-322
6	110	-107
7	26	-25
8	191	-190
9	47	46
10	44	43

4,6,L

-8	120	115
-7	48	-52
-6	77	-83
-5	87	-86
-4	270	-263
-3	180	-175
-2	154	-149
-1	31	23
0	353	343
1	58	56
2	96	95
3	306	293
4	99	-99
5	180	-190
6	63	60
7	30	-23
8	89	-85
9	62	64
10	53	48

4,7,L

-8	46	-44
-7	94	-91
-6	57	-55
-5	97	-99
-3	78	70
-2	111	106
-1	219	214
0	194	189
1	73	62
2	80	77
3	30	13
4	138	-138
5	52	-43
6	54	-50
7	125	-123
8	31	32
9	-23	-2

4,8,L

-6	44	45
-3	75	74
-1	50	47
0	68	66
2	24	-27
3	46	-46
4	110	-105
5	140	-136
6	38	-29
7	-23	-26
8	-29	-16

4,9,L

-5	92	-85
-4	-19	19
-3	54	50
-2	39	-39
-1	116	117
0	76	77
1	77	-82
2	27	25
3	67	-63
4	170	-163
5	31	29

4,10,L

-2	58	52
-1	67	66
0	37	-37
2	38	-31
3	149	-137

5,1,L

-10	43	46
-8	-25	31
-7	76	73
-6	64	-62
-5	51	54
-4	56	-54
-3	289	-282
-2	112	102
-1	319	297
1	491	460
2	716	685
3	314	-270
4	-18	-9
5	-19	-15
6	677	-659
7	188	-190
8	54	-51
9	185	-182
10	105	110
11	108	112

5,2,L

-10	52	57
-9	52	-55
-8	70	76
-7	57	58
-6	172	-183
-5	92	97
-4	54	49
-2	324	320
-1	39	-44
0	77	76
1	162	163
2	751	-722
3	592	-569
4	148	-142
5	535	-514
6	221	-224
7	331	325
8	151	144
9	107	101
10	256	260
11	67	70

5,3,L

-10	-19	-7
-9	32	-31
-6	-21	-17
-5	57	-61
-4	258	-258
-3	47	48
-2	160	-160
-1	618	-603
0	246	241
1	90	-95
2	313	-291
3	407	393
4	70	62
5	124	123
6	338	330
7	58	53
8	121	122
9	116	117
10	43	-45
11	-18	-18

5,4,L

-9	39	28
-8	126	-129
-7	-24	-20
-6	28	-23
-5	229	-234
-4	49	42
-3	114	119
-2	112	110
-1	445	433
0	380	386
1	132	134
2	187	181
3	58	58
4	251	-256
5	29	-30
7	64	-65
8	126	134
9	-22	-6
11	41	53

5,5,L

-9	-31	21
-8	40	40
-7	36	39
-6	65	63
-5	180	176
-4	253	248
-3	96	101
-2	131	130
-1	148	141
0	255	-241
1	286	-270
2	200	-196
3	224	-212
4	-23	-4
5	59	-57
6	85	83
7	211	208
8	99	-95
9	29	-29
10	-29	33

5,6,L

-8	-26	-10
-7	98	97
-6	-23	-11
-5	141	-130
-4	31	-32
-3	147	-135
-2	209	-209
-1	98	-95
0	90	-80
1	84	-89
2	42	38
3	25	27
4	98	-94
5	119	116
6	-18	6
7	175	-161
8	95	98
10	97	-91

5,7,L

-7	37	-40
-6	151	-143
-5	91	-89
-4	54	52
-3	50	-49
-2	31	25
-1	143	137
0	64	-62
1	47	-42
3	97	-96
4	25	19
5	102	97
6	83	85
7	100	93
8	85	75
9	-23	21

5,8,L

-6	-26	-14
-5	98	95
-4	34	32
-3	-25	-18
-2	73	70
-1	-17	20
1	-28	22
2	57	59
3	158	150
4	123	106
5	45	40
6	90	81
7	-28	16
8	103	-101

5,9,L

-4	32	31
-3	81	74
-2	66	65
-1	37	42
0	52	50
2	31	-37
4	70	-67
5	81	-75
6	-31	-28

5,10,L

-1	92	-80
0	126	-116
1	50	-48
2	63	-55
3	74	-70

6,0,L

-10	72	73
-9	150	144
-8	100	92
-7	79	-73
-6	-22	25
-5	53	49
-4	110	-105
-3	123	110
-2	477	444
-1	323	302
0	-16	31
1	337	323
2	69	69
3	441	-399
4	248	-242
5	351	-337
6	269	-253
7	327	-311
8	293	-281
9	43	29
10	81	-80
11	48	-44

6,1,L

-10	64	66
-8	98	-97
-6	38	37
-5	117	-116
-4	25	-6
-3	72	69
-2	229	-216
-1	168	-153
0	290	-281
1	475	-460
2	141	-133
3	277	-269
4	438	-414
5	24	-23
6	28	-13
7	82	-83
8	142	141
9	164	165
10	74	79
11	126	127

6,2,L

-9	77	-90
-8	43	-40
-7	134	-139
-6	171	-169
-5	177	-174
-4	312	-314
-3	71	-67
-2	64	-54
-1	57	49
0	313	300
1	227	226
2	210	203
3	-35	-18
4	116	115
5	147	139
6	28	-26
7	250	245
8	222	220
9	32	26
10	70	67
11	-20	17

6,3,L

-9	96	-96
-8	99	-93
-7	40	-38
-6	109	-113
-5	29	25
-4	324	326
-3	389	394
-2	360	357
-1	508	500
0	374	379
1	101	-93
2	178	-167
3	159	-157
4	73	-72
5	-19	10
6	117	-114
7	139	141
8	99	92
9	200	-211
10	-23	-14
11	-29	16

6,4,L

-8	57	54
-7	138	145
-6	32	38
-5	236	236
-4	364	370
-3	74	70
-2	71	69
-1	32	32
0	466	-462
1	340	-342
2	222	-223
3	409	-410
4	64	57
5	42	38
6	127	-129
7	158	156
8	-26	-17
9	78	-83
10	73	72
11	-27	-22

6,5,L

-8	-22	-4
-7	-31	30
-6	-23	-19
-5	134	128
-4	83	-82
-3	118	-114
-2	81	79
-1	459	-447
0	371	-359
1	49	46
2	213	-209
3	83	-83
4	217	215
5	142	145
6	44	45
7	114	115
8	33	30
10	53	46

6,6,L

-7	-18	-4
-6	77	74
-5	59	56
-4	50	-49
-3	-19	-2
-2	112	-109
-1	216	-213
0	48	44
1	39	-38
2	73	-68
3	330	325
4	68	68
5	34	-29
6	274	266
8	74	-76
9	80	80

6,7,L

-5	-31	-6
-3	60	-60
-2	140	-141
-1	26	26
0	-16	3
1	106	-110
2	134	133
3	131	126
4	29	21
5	136	133
6	52	41
7	-24	-10

6,8,L

-5	29	-25
-4	40	-38
-3	39	-30
-2	77	-75
-1	70	-71
0	31	30
1	27	26
2	65	65
3	188	182
4	76	75
5	-25	-2
6	-21	6
7	81	-83

6,9,L

-3	49	-47
-2	85	-81
-1	63	66
0	59	61
1	-27	17
2	170	165
3	83	75
4	85	-85

7,1,L

-8	-24	30
-7	58	57
-6	74	73
-5	156	157
-4	118	112
-3	175	-172
-2	49	-45
-1	119	-112
0	645	-651
1	79	-90
2	192	178
3	129	-123
4	361	349
5	430	423
6	60	65
7	27	26
8	28	-24
9	159	-162
10	126	-135
11	54	-55

7,2,L

-9	-24	5
-8	96	97
-7	-21	-23
-6	88	-87
-5	59	56
-4	271	-264
-3	393	-375
-2	-25	11
-1	257	-257
0	80	-77
1	582	565
2	128	126
3	181	178
4	492	477
5	274	-257
6	289	-283
7	-23	17
8	307	-305
9	171	-164
10	125	125
11	33	32

7,3,L

-7	147	-150
-5	58	-58
-4	132	-139
-3	198	190
-2	-26	-16
-1	93	-97
0	314	304
1	154	152
2	165	-166
3	162	159
4	124	126
5	208	-206
6	64	64
7	50	51
8	46	-54
9	121	120
10	-23	2
11	-23	15

7,4,L

-7	78	75
-6	77	74
-5	-25	-27
-3	86	90
-2	104	-106
-1	69	70
0	201	199
1	185	186
2	389	395
3	39	33
4	91	90
5	155	154
6	352	-360
7	125	-132
8	-22	-20
9	186	-188
10	-29	-7

7,5,L

-7	35	35
-4	28	22
-3	55	61
-2	135	135
-1	146	140
0	183	181
1	-25	27
2	201	-191
3	105	-99
4	327	-316
5	484	-464
6	94	-91
7	66	-58
8	131	-123
9	108	110
10	149	147

7,6,L

-4	36	-34
-3	45	-42
-2	141	-134
-1	121	-118
0	136	-137
1	278	-270
2	104	-95
3	51	-56
4	140	-130
5	43	42
6	127	118
7	60	58
8	116	108
9	149	142

7,7,L

-5	110	-109
-4	67	-63
-3	98	-94
-2	36	-40
-1	73	72
0	78	76
1	130	127
2	175	164
3	-20	-1
4	43	37
5	124	116
6	71	-69
7	55	52
8	132	122

7,8,L

-4	95	93
-3	40	35
-2	136	132
-1	141	139
0	-26	16
1	39	35
2	46	-37
3	107	-96
4	-20	-6
5	39	-35
6	-20	10

7,9,L

0	34	-25
1	82	-75
2	36	-32
4	47	-48

8,0,L

-8	201	193
-7	90	84
-6	169	158
-5	215	206
-4	87	-82
-3	90	-87
-2	38	-40
-1	382	-380
0	240	-227
1	218	-210
2	508	-496
3	46	-40
4	121	-123
5	222	-221
6	174	177
7	38	-42
8	87	-81
9	140	141
10	45	-35
11	38	-30

8,1,L

-7	97	-106
-6	87	-93
-5	132	-131
-4	278	-279
-3	222	-216
-2	210	-215
-1	290	-286
0	158	-154

8,1,L

1	128	-132
2	65	74
3	191	187
4	30	22
5	256	253
6	173	176
7	60	-55
8	122	125
9	30	31
11	88	90

8,2,L

-8	85	-90
-7	49	-49
-6	-18	-6
-5	102	-97
-4	62	-64
-3	115	-112
-1	76	64
0	29	10
1	383	373
2	442	437
3	161	155
4	168	170
5	202	198
7	86	-85
8	84	86
10	-27	-23
11	-29	30

8,3,L

-7	56	49
-6	41	40
-5	54	-54
-3	45	44
-2	94	94
-1	249	247
0	230	234
1	325	332
2	172	173
3	129	-127
4	58	59
5	113	-115
6	222	-223
7	34	37
8	54	-59
9	109	-114
10	42	-45

8,4,L

-6	90	-88
-5	37	-36
-4	75	77
-3	32	-21
-2	63	70
-1	170	177
0	62	62
1	33	-31
2	200	-200
3	119	-116
4	95	-98
5	269	-276
6	131	-132
7	-23	15
8	75	-85
9	97	-93
10	39	44

8,5,L

-6	90	-87
-4	75	-71
-2	162	156
-1	54	-55
0	128	-127
1	144	137
2	202	-202
3	242	-243
4	173	166
5	148	-144
6	69	-61
7	183	183
8	-30	-13
9	83	85

8,6,L

-5	-25	13
-4	58	-54
-3	186	184
-2	75	75
-1	84	-89
0	150	149
2	98	-101
3	75	71
4	32	-27
5	32	-27
6	94	91

8,7,L

-4	73	70
-3	68	58
-2	-19	21
-1	76	78
1	103	-106
2	46	-43
3	97	-93
4	126	-125
7	36	17

8,8,L

-2	-25	-20
-1	40	-35
0	72	-71
1	149	-148
2	110	-106
3	30	-21
4	-27	25
5	64	65

9,1,L

-6	50	-50
-5	41	30
-4	121	122
-3	42	47
-2	213	216
-1	194	183
0	137	-133
1	131	-134
2	162	-160
3	439	-438
4	312	-320
5	29	34
6	34	-29
7	51	50
8	252	257
9	107	109
10	42	42
11	47	45

9,2,L

-7	45	-49
-5	176	176
-4	53	-59
-3	117	-117
-2	99	101
-1	319	-319
0	487	-487
1	61	-63
2	230	-229
3	144	-141
4	380	378
5	240	233
6	230	223
7	367	361
8	36	24
9	44	-44
10	34	36

9,3,L

-7	83	-85
-6	-22	-7
-4	120	-120
-3	38	34
-1	116	-118
0	245	247
1	65	64
3	448	449
4	93	93
5	-18	-9
6	224	229
7	39	-39
8	108	-110
9	38	-22
10	62	-61

9,4,L

-6	91	98
-5	76	80
-4	131	136
-3	151	152
-2	89	92
-1	62	-63
0	73	-74
1	65	69
2	163	-162
3	68	-63
4	203	207

9,4,L

5	-19	20
6	-20	-7
9	99	-99

9,5,L

-4	61	-56
-3	46	-41
-2	167	-163
-1	240	-235
0	40	-31
1	-22	22
2	68	-59
3	139	131
4	170	168
5	77	-72
6	47	-45
7	47	-42
8	189	-183
9	79	-75

9,6,L

-4	62	-63
-3	57	-58
-2	85	-91
-1	-28	21
0	45	36
1	48	-50
2	91	85
3	117	117
4	98	-93
6	50	47
7	117	-116

9,7,L

-2	34	-38
-1	75	65
0	-26	-16
1	57	59
2	201	193
3	-40	32
4	74	71
5	99	89
6	65	-70

9,8,L

0	59	59
1	148	139
2	-33	19
3	-27	-23
4	-26	9

10,0,L

-6	-28	17
-5	55	49
-4	49	-48
-2	35	-20
-1	180	-181
0	-22	-10
1	167	-176
2	303	-305
3	71	-75
4	279	-296
5	212	-208
6	34	39
7	160	-164
9	147	147
10	-31	-23

10,1,L

-6	45	-46
-5	104	-102
-4	100	-108
-3	56	-50
-2	163	-166
-1	35	-43
0	36	-29
1	239	-247
3	104	103
4	46	-50
5	181	185
6	227	231
7	83	80
8	152	154
9	97	103
10	-27	24

10,2,L

-5	40	47
-4	74	72
-3	82	80
-2	63	65
-1	115	117
0	50	46
1	31	26
2	290	292
3	142	146
4	90	90
5	220	222
6	-19	-38
7	39	-43
8	42	-45
9	89	-96
10	-20	12

10,3,L

-5	150	151
-4	-30	32
-3	45	44
-2	132	134
-1	124	-127
0	74	-79
1	176	184
2	78	-78
3	140	-144
4	41	-45
5	119	-125
6	137	-144
7	108	-107
9	34	43

10,4,L

-5	45	-44
-4	56	-54
-3	107	-108
-2	169	-171
-1	107	-105
0	75	-75
1	123	-127
2	51	-52
3	44	-38
5	45	43
6	-28	29
7	93	101
8	68	71

10,5,L

-4	101	-95
-3	126	-124
-2	37	30
-1	58	-52
0	36	36
1	145	149
3	130	130
4	166	164
5	-24	-24
6	-21	-5
7	63	58
8	47	-40

10,6,L

-3	82	79
-2	52	47
-1	44	-39
0	123	122
1	100	101
2	48	-48
3	102	99
4	31	28
5	94	-87
6	41	43

10,7,L

-1	-20	7
0	68	64
1	48	43
2	42	42
3	34	36
4	51	-46

11,1,L

-5	70	-71
-4	35	-36
-3	110	-109
-2	107	-108
-1	107	113
0	64	69
1	71	76
2	273	281
4	79	-81
5	-26	19
6	211	-217
7	162	-166
8	-24	-21
9	44	-51

11,2,L

-5	-27	5
-4	82	-87
-2	241	242
-1	54	53
0	-23	23
1	214	213
2	114	-116
3	237	-248
4	64	-66
5	158	-159
6	116	-113
7	85	89
8	71	70
9	97	95

11,3,L

-3	78	83
-2	70	69
-1	60	54
0	55	59
1	38	-27
3	38	37
4	-19	-19
5	60	-63
6	135	135
7	77	74
8	55	-56

11,4,L

-3	106	113
-2	115	123
-1	57	52
0	88	95
1	49	-55
2	81	-87
3	96	-102
4	197	-208
5	72	-68
6	65	-57
7	33	-37

11,5,L

-2	52	-50
-1	172	-177
0	59	-62
1	192	-187
2	293	-293
3	79	-83
4	37	-30
6	112	117

11,6,L

0	47	34
1	93	-90
3	155	151
4	76	74

12,0,L

-4	120	-123
-3	69	-74
-2	176	-171
-1	210	-213
0	82	-79
1	81	-78
2	81	-86
3	-23	15
4	58	53
5	49	56
6	115	118
7	52	57
8	-24	31

12,1,L

-4	96	-95
-2	37	-42
-1	47	51
0	141	151
1	56	53
2	148	156
3	128	136
5	155	161
6	54	56
7	-29	-35
8	63	65

12,2,L

-3	45	50
-2	98	98
-1	255	262
0	-19	10
1	-31	-13
2	98	109
4	-23	24
5	-32	27
7	-27	0
8	77	-84

12,3,L

-2	38	40
-1	62	-64
0	41	-52
1	49	-43
4	65	-68
5	48	-49
6	71	-79
7	161	-177

12,4,L

-1	46	-55
0	45	-57
1	34	-42
3	107	-114
4	108	-111

12,5,L

0	-32	-15
1	-22	5
2	-22	-12
4	118	117

13,1,L

-1	-29	-26
0	164	-170
1	94	-101
2	-21	26
4	81	90
5	134	141
6	74	71

13,2,L

-1	39	-35
1	160	172
2	169	176
3	84	83
4	195	196
5	72	70
6	61	-60

13,3,L

1	103	112
2	-22	12
3	73	81
4	-21	-27

Observed and calculated structure factors for compound $C_{16}H_{12}NO_2SF_3$

0,0,L

3	734	-731
4	301	-310
5	114	-104
6	65	64
7	290	-285
8	-49	58
9	418	416
10	348	-350
11	246	-243
12	465	463
13	255	-265
14	159	176
15	369	-362
16	155	-161
17	-66	52

0,1,L

1	761	752
2	348	356
3	829	-835
4	816	-829
6	256	-263
7	314	-310
8	72	69
9	97	-94
10	-47	-53
12	-45	59
13	94	-90
14	232	233
15	-39	3
17	-44	-2

0,2,L

1	380	379
2	754	-758
3	782	-787
4	-50	59
5	233	227
6	57	-64
7	59	-58
8	327	318
10	112	-101
11	94	-96
12	152	149
13	323	334
14	-55	-18
15	88	-86
16	-52	-35
18	-94	-42

0,3,L

1	930	945
2	35	32
3	501	-490
4	53	49
5	93	-98
6	348	342
7	207	206
8	185	-179
9	415	415
10	113	115
11	223	-223
12	233	-238
13	108	120
14	79	-66
15	-51	48
16	97	-86
17	-51	-56
18	92	65

0,4,L

1	52	-61
2	199	190
4	247	251
6	196	185
7	83	-94
8	-54	-25
9	184	-181
10	-71	-69
11	113	-111
12	-47	-28
13	118	131
15	87	63
17	-74	-78

0,5,L

1	47	-35
2	60	-56
3	157	-162
4	105	-108
5	60	64
6	115	109
7	-75	-64
9	133	130
10	121	130
11	86	-96
12	98	-91
14	-65	59

0,6,L

1	116	127
2	64	-81
3	-46	48
4	143	-148
5	85	77
7	140	136
8	87	-90
10	-58	36
11	84	57
12	95	-89
13	-83	-30

0,7,L

1	-28	-13
2	93	104
3	67	-74
4	-36	-24
5	-58	62
6	-65	-48
9	-59	-33
10	80	-54

0,8,L

3	72	-70
4	-56	-52
5	-61	-10
6	-49	40

1,1,L

-17	-56	31
-15	113	-115
-14	143	139
-13	138	-146
-12	131	-140
-11	117	123
-10	235	238
-9	123	-124
-8	137	-129
-7	239	234
-6	145	145
-5	142	137
-4	823	-831
-3	522	-525
-2	451	449
-1	666	-658
0	61	67
1	385	368
2	423	417
3	183	-180
6	71	-64
7	300	280
8	226	-221
9	89	83
10	169	168
12	-53	-45
13	149	-158
14	93	77
15	79	80
17	-43	-59

1,2,L

-18	-60	75
-17	-72	52
-14	307	-320
-13	190	187
-12	122	-122
-11	179	-187
-10	178	175
-9	-58	51
-8	-55	-48
-7	-50	-62
-6	285	271
-5	-43	-35
-4	547	-560
-3	776	-786
-2	385	-385
-1	1575	1612
0	327	-323
1	832	826
2	669	663
3	183	-187
4	288	-289
5	118	-114
6	165	-158
7	-44	42
8	191	183
9	297	-305
10	176	-166
11	287	294
12	-52	43
13	127	120
14	215	-223
15	84	-86
17	-76	-21
18	-66	-60

1,3,L

-17	91	-69
-16	84	-50
-15	110	104
-14	86	-99
-13	-47	-70
-12	-48	-21
-10	123	109
-9	218	-213
-8	119	-118
-7	198	-192
-6	379	375
-5	695	688
-4	660	655
-3	99	-91
-2	614	-609
-1	239	234
0	445	-440
1	46	-44
2	208	205
3	148	144
4	158	155
5	293	-286
6	-50	-40
7	83	-80
8	89	91
9	-44	-70
10	134	-140
11	218	-229
12	223	-228
13	335	337
14	83	85
16	-40	28

1,4,L

-17	-57	9
-16	94	-93
-14	134	141
-13	141	133
-12	-74	-55
-10	142	144
-9	144	148
-7	149	142
-6	200	-197
-5	164	156
-3	95	-92
-2	204	-203
-1	114	119
1	130	-131
2	356	-343
3	-36	40
5	68	-85
6	-59	-42
7	172	178
8	90	-105
11	140	150
15	145	129
16	-63	-25

1,5,L

-13	-59	56
-12	133	154
-11	-61	66
-10	-51	-16
-9	71	41
-8	278	-291
-7	207	-211
-5	62	54
-4	119	119
-3	91	-82
-2	328	-323
-1	149	-140
0	259	257
2	72	70
3	107	111
4	131	-125
5	85	64
6	87	-87
7	-61	45
8	308	311
9	152	147
10	132	-121
11	-59	-62
13	112	-82
14	-62	70

1,6,L

-12	-60	-62
-11	-52	-28
-10	-72	-62
-9	74	62
-7	115	-108
-6	101	-105
-5	-48	50
-4	79	80
-3	139	138
-2	-33	-22
-1	-45	-39
1	-30	16
3	93	107
4	68	57
5	153	151
6	77	-67
7	91	-94
8	119	-98
9	-44	-8
11	-71	6
13	-74	-73

1,7,L

-10	-57	-22
-7	-47	-26
-5	-41	22
-3	-37	29
0	76	65
1	159	158
2	120	-111
4	120	-120
5	94	-111
6	-56	-62
8	-69	53
10	-69	31

1,8,L

-6	-58	-7
-3	59	35
-2	-32	-25
-1	82	-74
1	-40	-37
2	-38	39
5	-55	-4

2,0,L

-17	84	80
-16	-61	14
-15	-64	47
-14	131	-138
-13	112	119
-12	104	94
-11	77	-83
-10	264	263
-9	776	769
-7	860	-848
-6	176	-195
-5	389	387
-4	-34	23
-2	648	660
-1	393	379
0	693	-718
1	1414	-1469
2	563	-569
3	562	565
4	379	385
5	470	-484
6	996	-977
7	119	-114
8	695	674
9	570	565
10	171	-159
11	104	-104
12	211	218
13	113	-108
14	240	-251
16	213	204
17	116	115

2,1,L

-17	79	72
-16	120	-110
-15	371	377
-14	275	-287
-12	152	158
-11	-51	-37
-10	179	-176
-9	209	209
-8	348	342
-7	218	-210
-6	138	129
-5	820	-815
-4	587	-589
-2	1485	-1534
-1	940	943
0	571	573
1	62	-60
2	335	-340
3	147	145
5	194	202
6	515	497
7	740	-727
8	135	129
9	305	302
10	136	132
11	88	83
13	-54	61
15	157	-154
16	-70	-68
17	75	72

2,2,L

-18	-78	-16
-17	92	80
-16	86	55
-15	-52	65
-14	-69	-71
-13	-54	41
-12	219	-222
-11	175	-171
-10	206	219
-9	100	80
-8	442	-425
-7	155	-149
-6	489	-471
-5	319	315
-4	408	414
-3	512	505
-2	767	-773
-1	1035	1047
0	402	-397
1	130	-138

2,2,L

2	90	89
3	586	583
4	324	306
5	-59	-42
6	464	-461
7	80	68
8	194	204
10	221	-231
11	188	187
12	154	-157
13	-75	47
14	128	-141
17	-82	72
18	-69	-27

2,3,L

-18	75	-34
-14	77	-54
-13	-59	-61
-12	73	51
-11	143	-130
-10	261	-262
-9	107	107
-8	456	462
-7	141	151
-6	-51	-49
-5	128	-137
-4	119	113
-3	254	260
-2	189	-184
-1	133	133
0	364	352
1	57	64
2	509	-505
3	355	-353
4	196	196
5	360	356
6	-54	-61
7	363	-371
8	82	-87
9	201	204
10	-57	-39
12	83	-65
13	172	166
15	-60	-64
17	-97	92

2,4,L

-17	-67	-2
-14	127	111
-13	152	-146
-12	-46	-41
-11	170	176
-8	-41	-16
-7	73	-66
-6	149	147
-5	-39	35
-3	151	-156
-2	134	125
-1	492	-479
0	198	195
1	78	-74
3	-39	43
5	106	-93
6	128	142
7	86	100
8	95	-89
9	-53	-45
10	102	102
12	95	82
14	-73	84
15	-72	-23

2,5,L

-13	133	149
-10	206	-217
-9	-58	38
-8	73	-50
-6	90	-91
-4	188	188
-3	168	172
-2	58	48
-1	302	-309
0	60	-42
1	125	125
2	337	-344
3	87	85
4	129	131
5	206	215
6	-62	54
8	-48	43
9	-69	-62
11	228	-231
12	89	95
14	-60	1

2,6,L

-13	112	-90
-12	-65	42
-11	85	86
-6	74	65
-5	-63	-12
-4	181	-193
-3	63	56
-2	192	198
-1	-44	-27
0	67	-59
1	-42	34
2	-36	19
3	-49	10
4	115	-113
8	-62	-62
10	-54	33
11	-52	-59

2,7,L

-10	-49	35
-7	-45	-23
-5	83	82
-3	94	-93
-2	92	-100
-1	-43	32
0	-42	57
1	69	-63
2	-39	21
3	-44	-69
4	-57	24
9	-65	61

2,8,L

-5	117	-124
-4	124	137
-3	85	-90
-2	-38	40
-1	-47	-44
0	-62	-67
1	-53	40
2	86	87
4	78	81
6	-47	13

3,1,L

-17	88	-75
-16	135	-131
-15	315	316
-14	-58	-74
-13	285	-292
-12	-36	10
-11	322	325
-10	-38	-19
-9	179	-175
-8	52	44
-7	74	-63
-6	285	282
-5	243	-240
-4	526	-513
-3	854	847
-2	52	33
-1	42	-35
0	424	-425
1	146	153
2	386	391
3	290	286
4	349	-354
5	239	-239
6	464	458
7	156	-146
8	212	-204
9	157	150
11	72	-59
12	142	-143
13	-56	44
14	88	86
16	95	-90

3,2,L

-18	115	109
-16	180	-188
-14	144	151
-13	-78	-71
-12	229	-231
-11	-64	60
-10	410	423
-9	92	104
-8	230	213
-7	152	-150
-6	-40	28
-5	239	-250
-4	200	-204
-3	51	-59
-2	82	88
-1	399	399
0	161	152
1	184	-190
2	257	249
3	222	230
4	117	-109
5	716	-709
6	122	-125
7	72	-61
8	-43	44
9	-64	-35
10	238	245
11	311	314
12	109	-114
13	222	-232
15	-76	10
17	-62	-19

3,3,L

-18	-56	-38
-16	171	161
-15	-54	-60
-12	119	-122
-10	86	83
-7	465	436
-5	361	-345
-4	334	-325
-3	287	-277
-2	318	304
-1	151	-150
0	347	-337
1	251	242
2	-44	40
3	71	-76
4	180	177
5	-52	51
6	216	-217
7	103	107
8	-46	-41
9	232	-246
10	75	61
11	182	182
12	117	127
14	87	-87

3,4,L

-17	92	-78
-16	-73	67
-15	-72	-61
-14	159	163
-12	154	-149
-11	88	68
-10	93	74
-9	-42	2
-8	259	-253
-7	354	-346
-6	-50	63
-5	246	254
-3	418	-407
-2	669	664
-1	160	-160
0	177	-188
2	-48	47
3	184	183
4	87	78
5	169	-153
6	73	-42
7	221	220
8	92	66
9	86	-83
10	80	86
11	185	-194
12	106	104
15	-55	34

3,5,L

-15	-56	-33
-14	-59	59
-11	125	-121
-10	-55	-62
-9	126	126
-8	108	109
-6	94	-97
-5	64	-70
-4	-50	52
-2	285	281
-1	117	116
0	204	195
1	329	-321
2	148	-138
3	109	100
4	-44	25
5	-54	22
6	-55	-54
8	-66	-40
9	-49	22
10	-76	-30
11	-68	-68
12	132	140
13	115	-106

3,6,L

-14	-73	-47
-13	100	103
-11	-57	3
-10	86	94
-9	74	-77
-8	86	-85
-6	141	140
-4	85	93
-3	108	-110
-2	94	-92
-1	160	174
0	94	-98
1	-50	-63
3	79	-81
8	155	166
9	110	-83
10	-52	-23

3,7,L

-11	106	-96
-7	79	-59
-6	88	-90
-5	-41	30
-4	-50	28
-1	102	111
0	-49	-41
1	133	-130
2	-48	4
3	-57	-57
4	130	127
5	81	54

3,8,L

-5	-57	46
-4	-68	-61
-2	-49	-56
0	149	153

4,0,L

-17	150	160
-16	215	-212
-15	112	-104
-14	283	283
-13	232	233
-12	-66	-63
-11	148	-133
-10	-41	-47
-9	705	-680
-8	342	321
-7	438	-427
-6	121	118
-5	279	278
-4	486	481
-3	173	-176
-2	278	268
-1	57	-53
1	619	-614
2	222	-223
3	65	-56
4	246	231
5	586	-556
6	617	585
7	626	607
8	217	218
9	483	-490
10	230	-230
12	-82	97
13	140	-137
15	81	53
16	97	105
17	-67	16

4,1,L

-17	105	90
-15	80	-85
-14	159	-171
-12	-47	43
-11	88	-91
-9	129	128
-8	-44	-18
-7	111	101
-6	96	92
-5	244	-256
-4	182	-177
-3	307	293
-2	201	-204
-1	111	-123
0	119	117
1	286	279
3	-41	-47
4	210	201
5	290	-290
6	320	-322
7	133	-124
8	342	336
9	108	106
10	93	-89
17	-51	3

4,2,L

-17	-59	-60
-16	-76	58
-15	92	-79
-13	119	133
-12	-47	36
-11	115	-112
-10	-45	-27
-9	69	61
-8	123	-119
-7	269	268
-6	267	262
-5	127	115
-4	182	-181
-3	376	-374
-2	-37	34
-1	289	294
0	284	-276
1	72	-76
2	74	68
3	69	72
5	-52	10
6	-44	-32
7	115	115
9	130	-136
10	95	-88
11	97	99

4,2,L

12	-67	34
14	98	-94
16	-66	68

4,3,L

-18	-66	78
-17	-70	-48
-16	241	255
-15	175	-184
-14	91	-51
-13	-47	-21
-12	93	91
-10	-57	19
-9	-57	44
-6	120	-122
-5	60	-61
-4	520	517
-3	480	-470
-2	126	-136
-1	428	-405
0	408	412
2	160	156
3	199	181
4	-48	62
5	110	109
6	354	-351
7	-60	-17
8	169	174
9	87	104
10	97	-92
11	166	-163
12	94	119
14	-76	45
15	89	-53

4,4,L

-16	-71	54
-14	119	-124
-13	96	-61
-11	-46	17
-10	-49	-20
-7	107	96
-6	149	150
-5	314	-307
-3	180	-178
-2	251	255
0	-53	-68
1	152	139
2	222	231
3	-40	40
4	89	-84
6	149	-148
7	205	-201
10	193	187
11	-56	-34
13	-69	-40

4,5,L

-15	-53	44
-13	-52	-56
-12	87	21
-10	-53	41
-9	-62	67
-8	-43	26
-7	111	-114
-5	188	197
-4	170	176
-3	90	-85
-2	216	-215
-1	-37	40
0	-49	-27
1	86	-90
3	-63	47
7	121	-124
8	-65	37
9	-66	-53
10	-51	-3
11	-79	-57

4,6,L

-13	83	-70
-12	90	87
-11	-67	45
-10	-49	-5
-7	89	64
-6	235	-239
-4	132	-143
-3	361	367
-2	80	-88
-1	151	-148
0	-43	10
2	-59	22
4	74	-63
7	121	121
8	137	-127
9	196	193
10	-81	-46

4,7,L

-11	77	-29
-10	-71	61
-8	-51	6
-7	84	-105
-6	94	77
-5	117	-116
-4	-49	-73
-3	82	85
-2	-44	36
-1	85	81
1	87	-81
3	71	58
4	-72	61
5	-61	-40
6	-51	-12
7	-52	-33

4,8,L

0	-51	35

5,1,L

-17	85	-74
-16	130	131
-14	63	-65
-13	-47	-64
-12	251	260
-11	139	146
-10	122	-142
-9	303	-299
-8	86	92
-7	217	203
-6	104	-93
-5	692	-684
-4	64	68
-3	808	800
-2	564	548
-1	598	-594
0	80	66
1	66	72
2	231	-226
3	374	-380
4	73	-75
5	255	258
6	262	261
7	135	-142
8	150	-150
9	87	87
10	91	84
11	94	-99
12	-52	12
13	-63	-54
14	-63	43
16	-59	-49
17	-61	38

5,2,L

-18	-52	15
-17	166	-167
-15	164	177
-14	82	86
-13	-47	-52
-12	-59	-34
-11	-45	60
-9	149	143
-8	501	-488
-7	-42	-11
-6	505	512
-5	-45	-37
-4	438	-453
-3	-48	55
-2	396	401
-1	224	221
0	272	-258
1	228	-227
4	441	-445
5	118	112
6	188	190
7	119	125
8	-48	55
10	-70	-35
12	-57	-57
13	-80	-64
15	88	82
16	-55	-17

5,3,L

-18	-74	99
-17	77	-60
-16	-65	35
-14	84	-87
-12	92	54
-11	-57	-48
-10	146	-148
-9	113	113
-8	197	196
-7	152	150
-6	122	-126
-5	287	-275
-4	215	210
-3	256	-248
-2	245	-230
-1	207	193
1	148	141
2	262	262
3	57	47
4	207	-195
5	151	152
7	243	-246
8	-51	6

5,3,L

10	194	203
11	115	109
12	-95	-92
14	-64	-22

5,4,L

-17	-58	-5
-14	163	162
-13	112	-105
-12	114	-106
-11	172	168
-10	73	-46
-9	223	-233
-8	126	-129
-7	280	287
-6	85	92
-5	135	135
-4	230	-233
-3	94	-93
-2	348	344
-1	137	-131
0	126	-124
3	97	98
4	-59	-53
6	77	87
7	308	304
8	291	-292
9	159	-167
10	105	102

5,5,L

-16	-76	-93
-14	-52	-6
-9	-43	6
-8	-49	39
-7	179	-181
-6	-55	71
-5	225	228
-4	141	-134
-3	-61	62
-2	160	-158
-1	-49	-56
1	78	75
2	-55	-24
3	90	70
4	75	69
5	170	-169
7	-49	44
8	-48	-10
10	82	-73
12	-80	37

5,6,L

-13	-63	-62
-11	-68	-29
-9	-58	-21
-7	-47	1
-5	-42	-18
-4	150	-157
-3	212	226
1	71	-65
2	74	49
3	-63	53
4	-58	-3
5	105	-87
6	104	102
7	-66	-72
8	-57	-47
9	-75	65
10	-84	-55

5,7,L

-10	92	62
-9	-58	10
-8	108	-108
-7	102	104
-6	98	-105
-5	170	171
-3	-41	-11
0	-51	-61
1	-65	-72
4	-48	45
6	92	-85

5,8,L

-5	82	-87
-2	-66	69
0	-68	-74

6,0,L

-16	-53	-52
-15	-52	-60
-14	91	94
-13	82	84
-12	136	-143
-11	124	-121
-10	142	147
-9	283	268
-8	190	-195
-7	556	-555
-6	95	90
-5	402	403
-4	185	-187
-3	390	-374
-2	255	244
-1	-50	28
0	80	-79
1	140	-137
2	-53	-37
3	122	133
4	185	186
5	159	164
6	140	134
7	-62	40
8	-73	-64
9	152	-157
10	-80	-77
12	136	140
13	103	-91
14	-71	-44
15	-70	75

6,1,L

-17	-42	15
-16	91	-81
-14	69	-55
-13	77	76
-11	-38	12
-10	235	-229
-9	214	213
-8	85	101
-7	245	-246
-6	405	-405
-5	105	108
-4	233	230
-3	365	358
-2	221	-205
-1	604	585
0	64	66
1	104	-107
2	-40	-9
3	125	-124
4	192	-166
5	64	74
6	140	138
7	80	-87
8	104	103
10	124	-137
11	-52	38
12	83	-93
13	-58	34
15	84	-53
16	-54	37
17	-72	56

6,2,L

-18	94	85
-15	-58	-87
-14	95	97
-13	-70	11
-12	146	-160
-10	85	-79
-9	230	236
-7	216	220
-6	135	-135
-5	-47	42
-4	-56	-40
-3	117	-105
-2	133	116
0	-50	-30
2	-64	-61
3	133	139
4	137	-131
6	194	-190
7	194	194
8	152	-151
9	106	-104
10	-49	52
11	111	109

6,3,L

-18	-75	-56
-16	-65	-20
-15	-51	-73
-13	153	166
-12	75	62
-11	-66	-77
-10	99	-77
-9	102	107
-8	143	146
-6	218	-219
-5	61	-45
-4	101	104
-3	-62	-68
-2	-37	4
-1	165	165
0	103	95
1	81	-91
2	310	-314
3	68	-59
4	-53	61
5	141	127
6	132	-130
9	-83	21
10	-70	-47
11	-64	11
12	-68	67
13	-49	31

6,3,L

14 -66 -66

6,4,L

-17 -64 52
-16 -53 -51
-15 102 60
-12 -64 64
-11 -61 -69
-10 -59 -24
-9 173 -183
-8 278 271
-7 74 84
-5 184 -197
-4 79 -107
-3 -58 71
-2 150 -142
0 113 108
1 78 69
2 -42 10
3 133 -121
5 110 -106
6 242 234
7 105 -96
8 -50 9
12 -81 5

6,5,L

-15 -67 -60
-14 -74 10
-8 -69 -99
-7 312 308
-6 164 -160
-5 104 120
-4 268 -259
-3 75 -77
-2 -62 -39
-1 91 95
1 -52 19
3 -72 -23
4 155 159
6 196 -209
7 -51 87
8 -65 -45
11 -57 70

6,6,L

-12 -53 51
-10 81 -56
-9 -65 -70
-8 -52 -27
-7 -56 -8
-6 -65 34
-5 75 86
-4 -46 -31
-3 -59 61
-2 -58 -52
-1 -54 28
0 78 79
1 -64 65
2 -68 -61
3 169 -169
4 -50 -7
5 150 148
6 82 86
8 -74 -57

6,7,L

-9 -66 -35
-8 -47 55
-6 102 98
-5 -63 -43
-1 -53 11
0 -54 -11
1 80 55
3 -53 -1
4 90 -98
5 -77 -72

7,1,L

-17 70 61
-15 -48 -34
-14 171 -167
-13 88 103
-12 221 227
-11 96 91
-10 328 -335
-9 90 -83
-8 110 108
-7 95 92
-6 185 -193
-5 230 227
-4 340 346
-3 -46 54
-2 607 -598
-1 263 -261
0 180 181
1 320 317
2 -50 -51
3 249 -262
4 135 -130
5 272 270
6 72 62
7 69 -78
9 162 158
10 -64 -70
11 133 -130
12 -45 -53
13 99 106
14 -69 64
15 -52 -27

7,2,L

-18 -65 2
-16 -64 -63
-15 142 144
-14 77 -42
-13 200 -218
-12 81 72
-11 272 283
-10 -48 74
-9 266 -282
-8 81 -71
-7 100 -96
-6 -48 60
-5 229 -240
-4 143 -144
-3 624 614
-1 192 -198
0 165 -172
2 120 125
3 130 111
4 124 -129
5 183 -189
6 434 440
7 -65 54
8 75 -87
9 -50 17
11 -57 25
12 99 -105
13 -54 -33
14 -80 40

7,3,L

-16 -72 36
-15 82 -63
-14 -54 -5
-13 -62 43
-12 73 -47
-11 81 -92
-10 -53 75
-9 88 74
-8 262 -263
-7 99 102
-6 -50 -44
-5 -53 -32
-4 151 147
-2 79 -71
0 221 228
1 95 91
3 69 -70
4 -57 -16
6 219 -229
7 -69 73
8 161 159
10 -73 -87
11 -79 -75
13 -70 9

7,4,L

-15 -56 37
-14 -73 -58
-13 96 -85
-11 -64 -49
-10 98 90
-9 -62 -45
-8 -77 36
-7 191 183
-6 -62 67
-5 -62 -55
-3 106 107
-2 94 93
-1 206 -207
0 201 -205
1 -62 71
2 267 259
3 83 -94
4 -64 -68
5 -60 86
7 121 -126
8 112 -110
10 100 88

7,5,L

-14 -83 78
-10 -77 90
-9 98 -97
-8 149 147
-7 141 -128
-6 78 61
-5 139 146
-4 127 -136
-3 130 -130
-2 71 45
-1 77 60
0 -50 -51
2 -44 -36
3 -46 -45
4 130 131

7,5,L

5 166 -162
6 95 98
7 -66 64

7,6,L

-12 -51 43
-10 91 -80
-7 -64 75
-6 -62 19
-5 -59 -57
-4 -58 -28
-3 -65 -9
-2 89 -78
-1 84 -95
0 84 77
1 -53 42
2 -65 74
6 -75 5
7 -76 -24

7,7,L

-7 -68 -76
-6 127 130
-5 -59 -68
-3 -73 -73
-1 -73 25
0 -57 35

8,0,L

-17 105 109
-16 251 -267
-14 134 136
-13 153 -174
-12 118 -114
-11 -61 71
-10 191 191
-9 210 -210
-8 85 80
-7 79 -86
-6 404 402
-5 389 383
-4 485 -473
-3 78 58
-2 -45 16
-1 88 95
1 234 -239
2 -59 61
3 296 300
4 173 175
5 641 -657
6 144 136
8 172 -177
11 -65 66
12 -53 32
13 -61 -27

8,1,L

-17 -60 52
-15 94 -95
-13 114 119
-12 -43 36
-11 -51 56
-10 116 124
-9 74 77
-8 189 -189
-7 66 -61
-6 61 44
-5 164 158
-3 -46 26
-2 205 -212
0 133 154
1 150 -145
2 275 -282
3 124 -126
4 134 127
5 -45 -17
6 -44 -15
7 72 66
8 139 140
10 111 -111
12 -47 19
13 -73 -30
14 -61 15
15 -49 11
16 -57 17

8,2,L

-18 110 78
-16 -56 6
-13 -54 -2
-12 -60 -37
-11 -62 80
-10 130 134
-9 150 155
-8 318 -321
-7 189 -187
-5 67 55
-4 -54 -40
-3 141 -140
0 75 -54
2 146 152
3 115 118
4 190 -193
5 -57 51
6 92 -99
7 83 83
8 81 71
11 -62 34
12 -78 -47

8,3,L

-17 82 92
-15 90 -115
-14 -71 32
-13 -50 46
-12 -52 57
-11 166 -159
-10 148 141
-9 161 -173
-8 151 149
-7 349 -356
-6 -78 -55
-5 202 194
-4 235 227
-3 190 -188
-1 -78 89
0 86 76
2 -84 -85
3 98 -102
4 256 249
5 182 -184
6 -65 -54
7 -66 71
8 109 114
9 81 -63
11 -73 -71

8,4,L

-13 93 -70
-12 -73 63
-11 -49 7
-10 79 81
-9 103 104
-8 161 -160
-7 127 -118
-6 -67 -72
-4 233 237
-3 103 106
-1 137 -139
2 -66 76
3 116 -117
4 -74 -23
6 -72 -46
7 -74 -61
8 107 88
9 -54 59

8,5,L

-10 84 -71
-9 128 115
-8 113 84
-7 -68 -62
-6 98 -92
-5 -64 62
-4 -64 64
-1 -67 -32
2 -79 66
3 78 73
5 -69 -47
8 -58 10

8,6,L

-11 -79 70
-9 -75 -83
-8 -73 82
-4 101 107
-3 -57 53
-2 79 -79
0 113 -114
3 93 92
4 -74 73
5 -53 5

8,7,L

-3 -49 17

9,1,L

-17 -72 69
-16 103 111
-12 101 -98
-11 269 -270
-10 99 109
-9 -56 -28
-8 329 340
-6 239 -240
-4 115 130
-2 103 -115
0 -56 39
2 104 -97
3 68 -67
4 535 544
5 81 68
6 190 -189
7 184 -187
9 -58 45
11 -68 -14

9,1,L

13	-62	54

9,2,L

-18	-62	26
-17	109	-107
-14	-66	-71
-13	-45	8
-12	99	84
-11	-50	-12
-10	115	-124
-9	-63	44
-7	186	189
-6	146	150
-5	231	-234
-3	-56	76
-1	86	-76
1	166	179
2	68	65
3	227	-214
4	169	-169
5	266	258
6	87	85
7	154	-162
8	-77	-82
10	-74	42
11	-49	24

9,3,L

-17	-54	-33
-16	-60	39
-12	-70	71
-11	85	93
-10	-86	-53
-9	199	198
-7	129	-115
-4	76	82
-3	80	-68
-2	109	110
-1	-52	62
1	145	-151
2	83	-87
3	94	85
4	154	-160
5	-62	36
6	-64	16
7	-56	2
8	-72	49

9,4,L

-15	-67	75
-14	-74	-57
-13	-71	-11
-12	-70	49
-11	-49	17
-10	103	95
-9	187	-182
-8	85	74
-7	114	110
-6	94	-73
-5	226	-211
-2	131	-142
0	-49	25
1	104	119
2	-80	83
3	97	-89
7	-62	-36

9,5,L

-13	-51	-32
-12	-64	-84
-11	-54	44
-9	-77	32
-8	113	-118
-7	87	-74
-6	-55	21
-4	-80	-68
-3	-65	89
-2	90	97
0	-70	-22
3	87	97
4	-62	-11

9,6,L

-9	-51	-8
-5	-53	31
-4	-62	46
-2	-49	25
-1	-78	-13
2	-67	-64
3	-61	-9

10,0,L

-17	-86	-85
-15	157	163
-14	165	171
-13	-51	-33
-12	-52	-56
-11	122	-126
-10	123	118
-8	127	-130
-7	-50	-21
-6	196	204
-5	-72	-73
-4	270	-274
-3	118	118
-2	207	227
-1	134	-133
0	274	-266
1	81	-95
2	324	314
3	-68	-49
4	-47	-34
5	-75	-45
6	169	169
7	84	42
8	-69	-74
9	-56	-47
10	-73	29

10,1,L

-17	-46	6
-16	-42	-12
-12	106	-111
-11	-59	49
-10	374	-377
-9	246	252
-8	-42	-19
-7	104	-106
-6	71	79
-5	-60	60
-4	76	-65
-3	-46	-51
-2	81	89
1	113	-102
2	123	-117
3	384	385
4	-63	-65
5	-53	32
10	-58	-62
11	-58	-53
12	77	79

10,2,L

-17	114	-115
-15	112	108
-13	-79	-50
-12	-62	-49
-11	-64	-25
-10	-49	64
-9	95	-94
-8	-50	-65
-7	-116	118
-6	181	183
-5	177	-179
-3	73	68
-2	102	98
-1	171	187
0	78	-69
1	93	-104
4	146	-160
6	85	81
9	-69	-58

10,3,L

-16	-64	-57
-14	-98	91
-13	-57	47
-12	92	-81
-11	76	-88
-9	162	161
-8	-60	59
-7	112	-105
-6	94	101
-5	121	119
-4	-71	-54
-3	146	-136
-1	-68	61
0	-60	-34
1	130	-140
2	-83	-86
3	173	173
4	-62	52
5	-59	-52
9	-71	-56

10,4,L

-14	-61	37
-11	-58	66
-10	105	-85
-9	85	-74
-8	86	96
-7	-74	89
-6	-66	-71
-5	-66	-43
-4	112	-86
-3	-64	-88
-2	85	94
-1	-66	59
0	110	108
2	120	-115
3	-79	-76
5	-72	17
6	-57	47

10,5,L

-12	96	-80
-10	99	-105
-9	79	-83
-8	-77	59
-7	72	74
-6	119	-110
-5	-68	-71
-4	175	181
-1	127	-133
0	92	-100
1	113	100
2	100	-95
3	-66	82
5	-60	48
7	-60	-76

10,6,L

-6	-62	-47
-4	-62	-32
-3	-50	-16

11,1,L

-17	-64	61
-16	-48	-19
-15	90	-97
-14	-53	-71
-13	92	101
-12	68	73
-11	103	107
-10	194	-193
-9	-62	60
-8	94	81
-7	107	-120
-6	-40	-18
-5	162	166
-3	135	-134
-2	122	-116
-1	-44	17
0	120	120
1	107	112
2	105	-107
3	-63	83
5	91	-85
6	-57	-67
8	77	57
10	-80	-79
11	-59	-41
12	86	91
13	-59	57

11,2,L

-16	129	106
-12	114	-122
-11	198	211
-10	99	-105
-9	79	-83
-8	-77	59
-7	72	74
-6	119	-110
-5	-68	-71
-4	175	181
-1	127	-133
0	92	-100
1	113	100
2	100	-95
3	-66	82
5	-60	48
7	-60	-76

11,3,L

-15	-63	-15
-11	92	-93
-10	84	56
-9	-69	-32
-8	90	-66
-7	-72	42
-6	-52	12
-4	-72	-43
-2	-50	-68
-1	102	75
4	-76	39
5	-58	27
6	-77	-16
7	-51	40

11,4,L

-12	-78	49
-9	-62	-17
-7	-77	57
-6	150	-143
-3	102	104
-1	-50	-38
0	-52	7
1	-68	87
3	130	-144
4	-61	15

11,5,L

-7	88	77
-6	-75	50
-4	-52	-35
-3	-62	-40
-2	-67	41
0	-54	-33
1	-78	-55

12,0,L

-14	-81	-82
-12	207	-211
-11	318	322
-9	191	-196
-8	101	-92
-7	198	187
-5	-72	-60
-4	86	60
-3	90	-102
-2	98	97
0	-128	-121
1	158	152
3	-74	-36
4	94	-98
6	-77	81

12,1,L

-16	84	-73
-14	-54	40
-13	70	64
-12	108	-107
-9	78	78
-8	86	-80
-7	-50	-33
-6	107	99
-2	72	-75
0	-47	-35
1	-70	43
2	-53	-37
3	84	96
5	-53	-41
9	99	-78
10	-62	3

12,2,L

-14	-70	-47
-12	-54	59
-9	-68	-64
-8	76	-60
-7	110	80
-5	-59	-47
-4	-57	-54
-3	105	114
-1	103	-74
0	118	-119
1	86	61
2	-62	64
3	-57	-8
4	-52	-75
5	-64	60

12,3,L

-14	-79	78
-13	-71	-52
-12	-56	6
-11	147	-134
-10	159	154
-8	112	-119
-7	-58	-29
-6	112	112
-4	-72	-10
-3	112	-119
-2	-50	16
-1	-62	54
0	-52	33
1	136	-139
2	124	150
3	-66	34

12,4,L

-9	-78	56
-8	-72	12
-6	88	-45
-5	-68	32
-4	-60	36
-1	91	-107
0	-83	38

13,1,L

-15	-50	-50
-13	86	83
-11	85	-90
-9	130	121
-7	115	-120
-6	-53	-30
-4	71	76
-3	-54	-43
-2	-48	-21
-1	81	81
0	98	100
1	-44	-52
2	103	-96
5	-68	-44
8	-55	52
9	-72	-23

13,2,L

-12	161	161
-10	104	-106
-8	-70	59
-7	-58	15

13,2,L

-6	-52	11
-5	-65	-2
-3	102	96
-2	-72	-27
-1	134	-133
0	-74	72
2	-61	-5

13,3,L

-9	-52	30
-7	-54	-15
-5	93	92
-4	-65	-34
-3	-71	-13
1	-87	-100

14,0,L

-10	-58	3
-9	-71	-75
-8	-68	57
-7	97	67
-6	-71	27
-5	154	-153
-4	-63	-67
-3	-64	76
-2	120	105
-1	124	-116
0	-78	-43

14,1,L

-14	-46	11
-12	-52	-23
-11	-50	43
-8	-58	-57
-5	93	95
-4	105	-107
-3	-62	-43
-2	-55	52
-1	86	81
0	-57	-43
3	-50	39
4	-63	-44
5	-55	-8

14,2,L

-8	81	51
-7	-66	39
-3	-69	42
-2	-51	-23

15,1,L

-15	-61	-22
-14	-65	31
-11	-70	-61
-10	-68	52
-9	102	64
-8	83	-50
-7	74	-63
-5	101	111
-4	-49	-10
-3	85	-68
-1	-66	65
1	100	-83
3	-59	53
5	-53	-25

16,1,L

-13	-59	4
-8	-57	-29
-7	-73	53
-5	-53	-40
-4	-50	-47
0	-56	-41
1	-57	20
2	-67	5

17,1,L

-9	-58	-11
-6	106	58
-5	-57	1
-4	-48	-25

Observed and calculated structure factors for compound $C_9H_7NO_3S$

0,0,L

4	115	113
5	64	61

0,1,L

-5	25	-27
-4	29	-26
-3	196	-187
-2	62	65
-1	169	-164
1	317	-323
2	65	-63
3	74	74
4	56	-58
5	28	-26

0,2,L

-5	46	43
-4	105	105
-3	19	-16
-2	160	-165
-1	165	160
0	141	129
1	50	48
2	153	-157
4	90	90
5	48	47

0,3,L

-5	-16	-16
-4	80	-77
-3	79	77
-2	195	196
-1	30	-22
0	151	143
1	305	-308
3	-17	-22
4	40	-44
5	42	-42

0,4,L

-4	76	73
-3	-19	-12
-2	39	-41
-1	90	-94
0	100	89
1	291	296
2	44	42
3	136	-137
4	-16	9
5	41	36

0,5,L

-4	85	-81
-3	59	-59
-1	38	43
0	415	-383
1	111	-115
2	44	44
3	87	90
4	69	69
5	51	-50

0,6,L

-4	-15	16
-3	270	267
-1	192	-199
0	27	29
1	228	223
2	75	75
3	123	-124
4	-20	-16

0,7,L

-4	53	-49
-2	30	-29
-1	56	62
0	49	-46
1	48	-51
3	72	-71
4	-16	-1

0,8,L

-3	55	54
-2	82	-83
-1	95	-100
0	34	35
1	142	146
2	82	85
3	33	-32

0,9,L

-1	29	25
0	31	29
1	88	-93
2	40	-40
3	43	43

0,10,L

-1	-15	-12
0	88	-86
1	32	33
2	-24	27

0,11,L

-1	70	71
0	44	35

1,-10,L

-2	-18	19
0	49	-44
1	35	30
2	69	71

1,-9,L

-3	36	-36
-2	65	-64
-1	39	-41
0	-16	-23
1	-13	9
2	61	-64
3	-16	-16

1,-8,L

-3	157	156
-2	52	53
-1	-19	23
0	92	-87
1	44	51
2	45	48
3	40	38

1,-7,L

-4	-18	18
-3	79	82
-2	170	-171
-1	43	-46
0	82	83
1	76	80
2	36	-35
3	174	-174
4	-20	7

1,-6,L

-4	37	-36
-3	94	-92
-2	76	79
-1	47	-46
0	20	-21
1	54	-55
2	115	117
3	131	130

1,-5,L

-4	91	91
-3	61	61
-2	59	-61
-1	179	-185
0	27	-22
1	172	178
2	102	-107
4	58	-59

1,-4,L

-5	-14	-1
-4	58	-57
-3	26	25
-2	128	129
-1	230	234
0	327	-303
1	35	-40
2	55	58
4	83	-78

1,-3,L

-5	23	-26
-4	36	38
-3	108	-104
-2	24	-22
-1	200	-200
0	165	152
1	326	332
2	41	38
3	60	-62
4	53	-53
5	34	29

1,-2,L

-5	-20	15
-4	41	-43
-3	167	-163
-2	252	249
-1	142	142
0	103	-87
1	19	-19
2	77	-76
3	217	212
4	38	37

1,-1,L

-5	60	-60
-4	-16	14
-3	166	170
-2	84	88
1	16	-15
2	97	94
3	134	-136
4	114	-112
5	30	28

1,0,L

-1	335	358
1	82	-87
2	152	-154
3	71	71
4	76	73
5	27	-23

1,1,L

-5	27	-26
-4	-13	-10
-3	123	121
-2	120	126
-1	232	-241
1	213	213
2	173	175
3	20	21
4	31	-32

1,2,L

-5	66	63
-3	224	-215
-2	191	-177
-1	190	187
0	60	-55
1	783	-892
2	-9	-12
3	72	73
4	80	82
5	-13	-10

1,3,L

-5	45	-43
-4	20	19
-3	76	75
-2	361	359
-1	179	-183
0	11	6
1	72	-71
2	153	154
3	109	111
4	80	-79

1,4,L

-5	56	54
-4	23	24
-3	145	-144
-2	53	-56
-1	71	67
0	307	287
1	57	56
2	144	-144
3	-13	11
4	51	-52
5	-15	11

1,5,L

-4	-21	-15
-3	41	-38
-2	27	-24
-1	23	25
0	49	-52
1	180	-174
2	216	222
3	54	56

1,6,L

-4	68	68
-3	116	-115
-2	44	-45
-1	98	-105
0	207	199
1	59	-60
2	132	-138
3	42	-46
4	67	64

1,7,L

-4	-22	-25
-3	38	33
-2	192	195
-1	101	101
0	68	-62
1	57	56
3	31	33
4	66	-65

1,8,L

-4	-22	22
-3	-15	-3
-2	268	-271
0	113	108
1	52	54
2	78	-78
3	112	-108
4	53	51

1,9,L

-2	43	43
-1	50	53
0	27	26
1	56	-55
2	38	40
3	28	27

1,10,L

-2	29	-34
-1	52	-52
0	34	31
1	25	-26
2	53	-52
3	52	-46

1,11,L

-2	-17	-8
-1	78	79
0	-15	8
1	48	-46
2	27	26

2,-10,L

-1	55	-56
0	25	26
1	53	50

2,-9,L

-1	52	50
0	20	20
1	84	-90

2,-8,L

-2	-18	18
-1	70	-70
0	100	-97
1	46	45
2	-21	12
3	-15	-18

2,-7,L

-3	53	53
-2	25	-26
-1	129	133
0	160	149
1	22	28
2	78	-80
3	-19	-24

2,-6,L

-4	43	-40
-2	139	-137
-1	50	-50
0	48	-48
2	36	40
3	56	-51

2,-5,L

-4	67	67
-3	59	-60
-2	186	-193
-1	169	174
0	255	228
2	140	-144
3	26	23
4	183	178

2,-4,L

-5	-21	3
-4	78	-76
-3	122	120
-2	110	111
0	125	-118
1	256	-247
2	47	47
3	-20	-19
4	59	-58

2,-3,L

-5	-19	19
-4	58	59
-3	29	-31
-2	156	-158
-1	129	130
0	376	361
1	28	29
2	80	-84
5	44	41

2,-2,L

-5	33	-34
-4	64	-63
-3	49	-46
-2	46	-39
-1	31	-32
0	433	-413
1	182	184
2	-11	11
3	95	92
5	27	-23

2,-1,L

-5	83	81
-4	83	87
-3	139	138
-1	136	-136
0	88	78
1	122	125
2	22	-26
3	73	-75
5	50	50

2,0,L

-5	94	-99
-4	47	-52
-3	34	-33
-2	193	198
-1	244	-245
0	372	-360
1	193	-195
2	56	-54
3	47	49
4	117	-119
5	-22	-20

2,1,L

-5	97	-95
-4	138	143
-3	132	131
-2	116	-119
-1	222	-233
0	11	9
2	69	-72
3	79	-77
5	71	71

2,2,L

-5	43	44
-4	61	-62
-3	-12	6
-2	233	-222
-1	23	23
0	292	-285
1	67	-67
2	125	-120
3	27	31
4	-18	15
5	43	-42

2,3,L

-5	44	-42
-4	100	97
-3	154	151
-2	115	-115
-1	228	-233
0	288	268
1	27	30
3	92	-94
4	-14	9
5	38	40

2,4,L

-5	30	-24
-4	44	-42
-3	132	-133
-2	194	183
-1	253	260
0	63	-51
1	59	60
2	54	-58
3	27	22
4	-15	-9
5	30	-28

2,5,L

-4	-14	-2
-3	85	84
-2	40	-41
-1	81	-80
0	35	-38
1	124	127
2	143	145
3	-12	-11
4	84	-86

2,6,L

-4	45	-47
-3	117	-117
-2	-12	-13
-1	27	27
0	31	33
1	314	-318
2	66	-65
3	47	49
4	47	46

2,7,L

-3	34	36
-2	292	295
-1	27	-31
0	166	-158
1	38	38
2	144	141
4	60	-59

2,8,L

-4	-21	-14
-3	83	-82
-2	51	51
-1	-14	17
0	61	59
1	71	-72
2	37	-37
4	37	-34

2,9,L

-3	45	44
-2	46	47
-1	138	-140
0	88	-84
1	37	37
2	84	86
3	33	32

2,10,L

-3	34	-34
-2	23	-17
-1	59	63
0	24	23
1	-14	2
2	62	-61
3	-21	-10

2,11,L

-2	45	42
0	29	-30
1	52	-56
2	26	26

2,12,L

0	84	78

3,-9,L

-2	79	78
1	23	-23

3,-8,L

-3	-20	-6
-2	70	-67
-1	60	-61
0	-12	-6
1	22	-25
2	-16	-12

3,-7,L

-3	-17	-16
-2	196	194
-1	57	59
0	18	-13
1	78	-82
2	59	60
3	-25	28

3,-6,L

-4	-17	11
-2	92	95
-1	173	-183
0	-13	15
1	82	88
2	31	35
3	41	-38

3,-5,L

-4	-14	-18
-3	50	-53
-2	98	-99
-1	97	100
0	95	-87
1	69	-73
2	29	-31
3	87	87
4	63	61

3,-4,L

-4	-20	10
-3	157	158
-2	19	20
-1	27	-22
0	145	-136
1	34	39
2	90	94
3	71	-74
4	29	27

3,-3,L

-5	58	57
-4	38	-34
-3	117	-117
-2	103	100
-1	193	195
0	123	118
1	287	-282
2	23	-26
3	43	47
4	-22	6

3,-2,L

-5	72	-69
-3	80	80
-2	163	-153
-1	75	-73
0	146	-134
1	137	144
2	211	212
3	-13	-5
4	40	-37

3,-1,L

-5	129	130
-3	84	-87
-2	245	-232
-1	317	317
0	21	20
1	126	-125
2	26	-31
3	-16	-16
4	100	98

3,0,L

-5	69	69
-4	55	-52
-3	61	63
-2	234	226
-1	54	48
0	24	-21
1	259	-257
3	-19	21
4	69	-71
5	44	-45

3,1,L

-5	-14	-13
-4	37	-39
-3	146	-145
-2	233	-231
-1	143	140
0	321	318
1	18	20
2	100	-107
3	51	-52
4	36	38
5	31	32

3,2,L

-4	22	-23
-3	29	31
-2	120	121
-1	118	117
0	165	-159
1	183	184
2	171	173
3	67	67

3,3,L

-5	41	42
-4	115	115
-3	78	-81
-2	303	-294
-1	127	-124
0	211	197
1	44	-40
2	511	-542
4	46	44
5	25	26

3,4,L

-5	54	-58
-4	58	-59
-3	63	65
-2	108	111
-1	381	385
0	161	-149
1	49	48
2	36	-35
3	102	102
4	26	31
5	25	-27

3,5,L

-5	27	-25
-4	73	74
-2	217	-217
-1	25	22
0	89	84
1	127	131
3	67	-70
5	29	-28

3,6,L

-4	-13	18
-2	36	39
-1	68	-64
0	33	-30
1	48	-50
2	58	-58
3	117	118
4	-14	11

3,7,L

-4	51	51
-3	77	74
-2	145	-151
-1	64	-68
0	60	-60
1	114	120
2	63	-61
3	73	-72
4	-18	-17

3,8,L

-4	25	-25
-2	66	67
-1	186	195
0	35	33
1	49	-52
2	81	80
3	-22	20

3,9,L

-3	-17	25
-2	24	-24
-1	284	-294
0	28	23
1	85	90
2	-19	22
3	68	-64

3,10,L

-3	32	-33
-2	33	33
-1	22	19
0	40	37
3	31	34

3,11,L

-1	40	-39
0	-16	-14
1	39	36
2	-23	-27

3,12,L

0	59	55

4,-9,L

0	57	-51

4,-8,L

-2	60	-64
-1	23	15
0	58	53
2	62	-64

4,-7,L

-3	47	44
-2	-20	13
-1	32	-28
0	78	-70
1	59	-66
2	38	37

4,-6,L

-2	57	55
-1	-17	6
0	144	137
1	90	95
2	-22	25
3	48	-43

4,-5,L

-4	32	-33
-3	27	-27
-2	43	42
-1	192	-192
0	76	-71
1	24	-26
2	26	27
3	-15	9

4,-4,L

-4	89	92
-3	84	86
-2	98	-99
-1	198	-204
0	223	211
1	138	140
2	31	-33
3	75	-71
4	-24	25

4,-3,L

-3	68	-69
-2	158	157
-1	93	95
0	46	-43
1	81	-83
2	94	-91
3	27	28
4	-18	-21

4,-2,L

-5	37	-31
-4	50	48
-3	57	58
-2	93	-100
-1	109	-113
0	148	136
1	225	232
2	21	-21
3	48	-50
4	-17	10

4,-1,L

-4	103	-103
-3	51	-53
-2	29	-27
-1	64	-59
0	99	-93
1	245	-255
2	140	140
3	28	23
4	35	34

4,0,L

-4	132	133
-3	106	101
-2	110	110
-1	31	25
0	47	-46
1	69	72
2	59	61
3	64	-65
4	-20	-13

4,1,L

-5	23	27
-4	164	-167
-3	74	-74
-2	31	33
-1	282	278
0	279	-259
1	168	-169
2	94	-95
3	-13	3
4	27	27
5	64	-65

4,2,L

-5	22	-20
-4	156	-153
-3	216	216
-2	86	85
-1	153	-151
0	147	-137
1	80	87
2	509	529
3	44	-49
4	27	-31

4,3,L

-5	59	56
-4	35	36
-3	83	-81
-2	75	76
-1	116	-107
0	-8	-7
1	218	-223
2	-16	-8
3	32	-36
4	34	28

4,4,L

-5	52	-48
-4	27	-22
-3	143	144
-2	146	141
-1	176	-178
0	183	-173
1	164	168
2	31	-31
3	27	-27
4	43	-42

4,5,L

-5	58	53
-4	48	-53
-3	64	-66
-2	123	-126
-1	253	249
0	188	180
1	59	-60
3	43	45

4,6,L

-4	-18	13
-2	48	49
-1	66	-68
0	119	-113
1	-15	7
2	82	83
3	49	48
4	23	-20

4,7,L

-4	74	74
-3	87	-91
-2	111	-113
-1	34	36
0	24	23
1	-18	15
2	176	-180
3	-21	-21
4	29	33

4,8,L

-4	51	-49
-2	34	39
-1	209	213
0	48	-44
1	61	-66
2	31	29
3	69	71

4,8,L

4	-24	-20

4,9,L

-3	43	-40
-2	93	-94
-1	88	90
0	46	46
1	38	39
2	54	-56
3	-17	-13

4,10,L

-3	-20	-24
-2	50	54
-1	-17	16
0	154	-143
1	40	-42
2	34	33
3	32	28

4,11,L

-2	35	-38
0	93	89

4,12,L

-1	23	25
0	19	-9
1	31	-31

5,-8,L

-1	88	90
0	39	-33

5,-7,L

-2	-16	-6
-1	80	-80
0	39	-36
1	23	23
2	27	-27

5,-6,L

-3	96	-91
-2	-17	9
-1	174	176
0	41	41
1	34	-34
2	46	-50

5,-5,L

-3	35	32
-1	78	80
0	130	-124
1	47	48
2	60	64

5,-4,L

-4	30	-33
-3	50	-50
-2	53	-56
-1	76	-79
0	68	65
1	86	-88
2	65	-69
3	-14	-18

5,-3,L

-4	-14	17
-3	35	35
-2	178	180
-1	41	-42
0	30	30
1	51	-55
2	51	52
3	30	30
4	42	-34

5,-2,L

-4	78	79
-3	85	-91
-2	141	-149
-1	138	138
0	195	180
2	174	-175
4	29	26

5,-1,L

-5	-16	-13
-4	84	-83
-3	-16	14
-2	91	95
-1	162	-153
0	91	-84
1	22	-27
2	86	90
3	105	106
4	-17	-14

5,0,L

-4	154	157
-3	49	-52
-2	97	-101
-1	197	-188
0	259	236
1	30	-33
2	79	-80

5,1,L

-5	29	-34
-4	92	90
-3	-14	2
-2	107	108
-1	186	184
0	27	25
1	-14	-14
2	42	-37

5,2,L

-3	71	-74
-2	195	-193
-1	197	-199
0	102	99
1	146	152
2	27	-31
3	66	-64

5,3,L

-5	39	40
-4	26	-30
-3	23	20
-2	78	81
-1	66	68
0	18	18
1	65	-61
2	133	133
3	93	90

5,4,L

-5	40	-36
-4	76	77
-3	152	153
-2	170	-174
-1	245	-244
0	44	-42
1	102	103
2	31	-33
3	256	-270

5,5,L

-5	45	39
-4	91	-93
-3	51	-50
-2	94	95
-1	84	88
0	225	204
1	72	-75
2	38	43
4	49	55

5,6,L

-3	62	64
-2	61	-58
-1	198	-203
0	93	81
1	58	62
2	40	39
3	-14	-4
4	-20	-19

5,7,L

-3	-14	22
-2	-15	15
-1	77	80
0	80	-71
1	50	-52
2	-21	-19
3	-19	-8
4	47	40

5,8,L

-4	25	-22
-3	67	65
-2	45	47
-1	121	-126
0	49	-47

5,9,L

2	45	48
3	43	-40

5,9,L

-3	47	-47
-2	33	31
-1	84	85
0	140	133
2	30	-30
3	61	62

5,10,L

-3	34	31
-2	-17	18
-1	33	-35
0	233	-217
1	30	31
2	47	47

5,11,L

-2	-22	-24
-1	56	53
0	21	-16
1	-16	17

5,12,L

0	27	-27

6,-7,L

-1	29	-26
0	23	21

6,-6,L

-2	66	65
0	68	-60
1	39	-43
2	25	-32

6,-5,L

-3	29	29
-2	-20	-23
-1	47	48
0	37	35
1	88	94
2	29	34

6,-4,L

-3	32	-28
-1	48	47
0	206	-188
1	53	-53
2	-13	-5
3	32	27

6,-3,L

-4	-15	8
-3	101	102
-2	63	66
-1	101	-101
0	162	-150
1	161	165
2	55	56
3	27	-31

6,-2,L

-4	35	-30
-3	-13	-2
-2	-20	-25
-1	138	139
0	71	66
1	44	-44
2	33	-32
3	-20	-14

6,-1,L

-3	68	67
-2	-14	21
-1	123	-129
0	32	-29
1	83	90
2	95	98
3	31	-34
4	29	-21

6,0,L

-4	-19	-1
-3	157	-158
-1	-17	19
0	53	-48
1	89	-91
2	99	-104
3	84	85
4	-22	11

6,1,L

-5	28	-25
-4	-21	20
-3	161	162
-2	77	74
-1	28	31
0	38	30
2	30	33
3	-16	15
4	48	-47

6,2,L

-5	48	46
-3	200	-202
-2	59	-59
-1	78	82
0	225	203
1	159	-162
2	83	-81
3	38	-36
4	-14	5

6,3,L

-5	24	-21
-4	24	-13
-3	189	-187
-2	201	204
0	131	-125
1	51	-52
2	64	65
3	176	183
4	29	-23

6,4,L

-4	68	65
-2	56	-55
-1	95	96
2	116	-118
3	-23	21

6,5,L

-4	81	-79
-3	25	18
-2	122	126
-1	66	63
0	158	-144
1	71	-72
2	84	86
3	37	-41
4	-22	-27

6,6,L

-4	75	72
-3	79	-84
-2	73	-75
-1	50	-52
0	219	206
1	77	83
2	32	-31
3	-16	-12
4	66	56

6,7,L

-4	41	-39
-3	31	34
-2	30	34
0	58	-54
1	78	-81
2	23	24
3	35	33

6,8,L

-4	57	54
-3	75	81
-2	97	-103
-1	60	-62
0	53	51
3	81	-82

6,9,L

-3	43	-44
-1	29	26
0	105	97
1	32	-32
2	-15	-10
3	-14	11

6,10,L

-3	31	32

6,10,L

-2	53	-54
-1	72	-74
0	100	92
1	35	36

6,11,L

-2	-14	-11
-1	35	38
0	24	-17
1	96	-103

6,12,L

-1	30	-29
0	-14	5

7,-6,L

0	71	-64

7,-5,L

-2	102	-100
-1	35	32
0	119	110
1	-15	16

7,-4,L

-2	46	43
-1	-20	-15
0	55	51
1	46	-49
2	41	42

7,-3,L

-3	50	-52
-2	63	-63
-1	34	-38
0	54	-49
1	-19	18
2	58	-56
3	34	-36

7,-2,L

-4	35	-34
-3	41	42
-2	47	52
-1	132	136
0	73	-69
1	62	62
3	35	31

7,-1,L

-3	73	75
-2	118	-126
-1	101	-108
0	123	115
1	119	121
2	48	-49
3	86	-85

7,0,L

-3	61	-64
-2	40	37
-1	66	70
0	130	-114
1	62	-66
3	36	38

7,1,L

-4	44	43
-3	128	128
-2	81	-85
-1	70	-75
0	96	-88
1	114	117
2	39	-41
3	35	-32

7,2,L

-4	59	-60
-3	96	94
-2	59	62
-1	90	93
0	84	78
2	-13	-4
3	-16	12

7,3,L

-4	22	16
-2	97	-101
-1	157	-163
0	92	-86
1	35	38
2	61	58
4	-25	-25

7,4,L

-4	27	29
-3	48	-48
-2	67	67
-1	83	86
0	24	24
1	31	-32
2	-14	-4
3	78	83
4	41	38

7,5,L

-4	31	-27
-3	92	92
-2	146	146
-1	172	-176
0	134	-122
2	46	41
3	-21	-21

7,6,L

-4	30	28
-3	106	-106
-2	-18	-19
-1	84	86
0	47	44
1	59	64
2	35	-31
3	-23	28

7,7,L

-4	-20	-22
-3	25	14
-2	34	33
-1	71	-74
0	121	-115
1	80	83
2	26	26

7,8,L

-3	36	-36
-2	23	28
-1	29	27
0	64	59
1	56	-59
2	42	-42

7,9,L

-2	52	51
-1	-17	8
0	75	-71
1	-19	-23
2	-15	14

7,10,L

-2	56	-55
-1	48	47
0	74	68
1	62	64
2	-17	-14

7,11,L

-2	37	35
-1	-19	7
0	31	-28
1	113	-116

7,12,L

0	53	49

8,-4,L

-1	24	-17
0	41	38
1	43	41

8,-3,L

-3	65	-67
-1	35	31
0	34	32
1	127	-131
2	29	-25

8,-2,L

-3	-19	23
-2	74	77
-1	24	25
0	73	-68

8,-2,L

1	88	-88
2	91	91

8,-1,L

-3	53	-49
0	89	81
1	37	38
2	24	-24
3	-16	-5

8,0,L

-4	46	-39
-3	-17	11
-2	51	55
-1	25	-25
0	111	-103
1	-19	15
2	29	34
3	28	29

8,1,L

-4	44	45
-2	148	-155
-1	28	31
0	32	33
1	35	-38
2	59	-57
3	28	-24

8,2,L

-4	-21	-27
-3	36	38
-2	128	131
-1	30	29
0	20	-19
1	34	38
2	30	25
3	-16	8

8,3,L

-4	76	72
-2	164	-169
-1	-19	-17
0	92	77
1	107	108
2	78	-82
3	33	-31

8,4,L

-4	35	-32
-2	165	-164
-1	122	122
0	42	-40
1	61	-64
2	-21	-15
3	37	30

8,5,L

-4	44	48
-3	57	52
-2	-16	-19
0	79	75
1	24	25
3	51	-50

8,6,L

-4	46	-42
-3	83	-82
-2	50	53
-1	62	63
1	89	-89
2	22	-18
3	-21	32

8,7,L

-3	65	64
-2	84	-88
-1	62	-65
1	111	114
2	-22	24
3	-15	-10

8,8,L

-3	39	-38
-2	41	46
-1	30	31
0	32	-29
1	28	-28
2	37	-38

8,9,L

-3	55	51
-2	54	59
-1	74	-78
0	-17	-16
1	28	33
2	-16	-13

8,10,L

-2	-15	-21
1	28	30

8,11,L

-1	44	-43
0	41	-39
1	63	65

9,-3,L

-1	36	36
0	28	-21

9,-2,L

-2	54	-57
-1	43	-48
0	24	-18
1	29	-32

9,-1,L

-3	-18	-20
-2	49	53
-1	45	44
0	73	67
1	56	-58
2	60	60

9,0,L

-2	43	46
-1	105	-111
0	46	-46
1	68	70
2	69	70

9,1,L

-3	-14	-21
-2	-22	-26
-1	32	32
0	36	33
1	64	-64
2	32	-35

9,2,L

-3	65	62
-2	62	63
-1	71	-73
0	31	-29
1	-21	-18
2	44	42
3	31	-25

9,3,L

-3	65	-67
-2	76	78
-1	77	81
0	55	53
1	-19	18

9,4,L

-3	26	22
-1	88	-93
0	93	-89
1	25	-19
3	-18	13

9,5,L

-2	49	-47
-1	75	78
0	58	53
1	-16	0
2	31	-34

9,6,L

-2	69	70
-1	105	105
0	130	-119
1	39	-45
2	-19	21

9,7,L

-2	85	-85
0	47	45

9,8,L

-2	28	24
0	57	-54
1	35	-38
2	54	57

9,9,L

-2	41	-40
-1	29	32
0	25	24
1	-21	25
2	33	-35

9,10,L

-1	-19	22
0	-13	-10
1	-22	-24

10,-1,L

-1	33	37

10,0,L

-2	41	-45
-1	-21	24
0	36	31
1	31	35

10,1,L

-1	26	26
0	40	-36
1	55	-56
2	28	26

10,2,L

-3	34	32
-1	100	-103
0	44	41
1	26	18
2	-17	-29

10,3,L

-3	-18	-15
-2	45	45
-1	71	72
1	26	-27
2	-19	31

10,4,L

-3	75	73
-2	23	-25
-1	95	-98
1	38	38
2	42	44

10,5,L

-3	26	-28
-2	-19	16
-1	109	-111
0	54	44
1	30	-33
2	26	-23

10,6,L

-3	47	48
-2	24	28
-1	-23	-22
0	31	29
1	41	43

10,7,L

-2	59	-57
-1	58	57
0	-17	13
2	41	-41

10,8,L

-2	34	35
-1	59	-62
0	49	-43
1	30	29

10,9,L

-2	24	-23
-1	38	41
1	30	-25

11,1,L

-1	-15	19
0	76	-66

11,2,L

0	-13	10

11,3,L

-2	54	54
0	47	-43

11,4,L

-2	42	-49
-1	51	52
0	63	59
1	-18	18

11,5,L

-1	-20	-18
0	65	-61
1	35	-33

11,6,L

-2	-18	-10
-1	29	-30
0	60	57
1	25	22

11,7,L

-1	35	35
0	73	67

11,8,L

-1	48	-48
0	-12	12

Observed and calculated structure factors for compound $C_{13}H_{13}NO_3S$

0,0,L

2	520	-489
4	509	483
6	-95	85
8	-120	122
10	-113	41

0,1,L

1	155	169
2	386	421
3	285	-308
5	155	157
7	229	-220
8	-82	-53
9	274	269

0,2,L

0	668	600
1	130	130
2	470	-502
3	324	357
4	298	323
5	-71	65
6	225	-228
7	204	210
8	175	-177
9	-93	-92
10	179	157
11	173	180

0,3,L

2	128	146
3	121	117
4	-70	-45
5	-55	64
6	90	113
8	194	-215
9	-68	-52

0,4,L

0	173	-162
1	108	134
2	169	167
3	-52	26
4	-78	-50
10	-76	-14

0,5,L

2	144	142
3	114	110
4	-86	80
7	256	259
8	154	147

0,6,L

5	-98	43

0,7,L

6	-112	-88

1,0,L

-8	128	-117
-6	396	375
-4	371	-373
-2	461	432
0	868	-775
2	1663	-1557
6	1059	-961
8	369	352
10	304	-301

1,1,L

-11	139	152
-10	194	177
-9	152	-123
-7	100	102
-3	241	233
-2	166	166
0	191	186
1	152	-171
2	442	-523
3	212	210
5	135	-150
6	237	-244
7	177	168
8	-84	103
11	232	-232

1,2,L

-9	145	127
-6	254	267
-5	-80	100
-4	-71	20
-3	-72	-88
-2	936	1021
-1	1810	1930
0	341	312
1	317	-379
2	286	-340
3	136	156
4	305	336
5	-57	39
6	222	-216
7	-80	83
8	146	138
10	105	-114
11	-85	-85

1,3,L

-9	200	197
-8	308	-298
-5	-81	70
-4	248	-253
-3	81	-84
-2	-56	-64
-1	123	112
0	235	229
3	101	-102
4	129	143
6	215	-222
8	220	224

1,4,L

-8	-102	-102
-5	-74	64
-3	140	-136
-1	145	140
1	-66	81
2	-73	-42
3	262	284
5	121	-112
9	227	223
10	134	129

1,5,L

-7	158	-160
-6	138	155
-5	-166	-16
-3	108	-97
-2	225	214
-1	203	-199
0	-90	94
2	94	93
3	105	-76
4	99	-80
5	121	106
7	173	-183
8	127	-115

1,6,L

-5	-74	-101
-3	-122	120
0	139	101
4	109	-56

1,7,L

1	-107	122
2	-67	97
5	-72	88
6	148	150

2,0,L

-10	-100	-128
-8	-79	61
-6	193	186
-4	-68	-27
-2	767	-748
0	425	-424
2	892	859
4	547	-517
6	171	173
12	-87	-74

2,1,L

-10	220	-214
-9	127	117
-5	101	95
-4	-85	87
-3	88	-77
-2	103	-107
-1	172	-163
0	88	77
1	227	229
2	490	538
3	134	-136
4	171	-180
5	235	245
6	93	91
7	221	-217
8	180	167
9	163	-167
10	106	-111
11	131	131

2,2,L

-9	-74	-89
-7	161	169
-5	337	-342
-4	92	-93
-3	319	314
-1	611	-627
0	1451	-1360
1	316	-331
2	280	-309
3	129	-149
4	168	-164
5	466	-477
6	-89	-87
7	336	332
8	100	-122
9	257	-261

2,3,L

-9	117	-108
-8	237	240
-7	195	-193
-5	91	67
-4	219	214
-3	280	-292
-2	452	451
-1	-55	31
0	142	-123
1	321	-325
2	99	102
3	196	205
4	187	-205
5	210	-208
6	197	211
9	-82	-102
10	181	-183

2,4,L

-8	-102	69
-6	154	159
-3	495	495
-2	559	543
-1	-80	-43
0	276	-242
3	120	124
5	-144	-159
8	-91	76
9	174	-179

2,5,L

-6	-68	-73
-3	100	-79
-2	-86	51
-1	246	229
0	106	-96
1	126	-101
3	134	130
5	159	-163
6	-97	71
7	-105	94

2,6,L

-6	-96	42
-4	140	-131
-2	123	102
0	107	-104
5	-97	-76
8	151	153

2,7,L

2	-80	-90
6	-74	-78

3,0,L

-10	-113	121
-8	148	-141
-6	209	206
-4	394	-385
-2	123	-139
0	493	-509
2	813	791
4	180	175
6	275	-267
8	173	190
10	-114	87
12	-111	7

3,1,L

-10	133	164
-9	200	-198
-8	157	153
-5	194	-168
-4	270	266
-3	322	-303
-1	87	90
0	-65	50
1	615	-632
2	298	-285
3	369	378
4	228	228
5	345	-314
6	246	-246
7	137	-136
8	173	-181
9	215	219
10	143	137

3,2,L

-8	125	128
-7	-98	13
-5	98	101
-4	175	-192
-3	225	-231
-2	-73	-56
-1	148	-150
0	198	191
1	806	824
2	250	261
3	594	-643
4	138	143
5	370	374
6	293	283
7	218	-227
8	107	95
10	-77	-26

3,3,L

-7	176	177
-2	410	-408
-1	268	266
0	113	123
1	205	204
2	216	-217
4	214	220
6	-74	-85
7	149	160
8	101	-123
9	115	-125
10	167	181
11	128	114

3,4,L

-8	-92	130
-7	107	-94
-6	323	-328
-5	-94	99
-4	124	136
-3	195	-189
-2	504	-488
-1	378	-357
0	313	-300
2	80	97
3	291	-306
6	135	149
7	180	-196

3,5,L

-3	169	164
-1	142	-151
1	113	104
2	-92	-102
8	-84	-72
9	104	-125

3,6,L

-6	-89	-28
-4	175	178
-2	-128	-68
1	128	-124
2	119	117
4	-106	-114
7	-83	37
8	135	-127

3,7,L

3	-86	-32
5	-76	7
6	-92	1

4,0,L

-6	186	-182
-4	191	186
-2	118	109
0	222	-234
2	1159	1116
4	444	-391
6	657	607
8	212	-201

4,1,L

-8	213	-217
-7	119	108
-6	-62	-31
-5	171	-173
-4	289	-276
-3	510	502
-2	214	-215
-1	100	-111
0	403	-400
1	372	342

4,1,L

2	458	458
3	222	-227
4	179	-169
5	190	185
6	189	-190
7	364	339
8	318	318
9	150	-142
10	-87	-55
11	113	121
12	-71	-52

4,2,L

-9	135	-137
-7	248	260
-6	161	-163
-5	205	-209
-4	-84	69
-3	-46	-2
-2	160	-158
0	370	356
1	143	143
2	237	229
3	133	-145
5	136	-150
6	143	148
8	-62	-47
9	176	163

4,3,L

-4	204	-201
-3	-85	50
-2	147	146
-1	215	-208
0	393	-389
1	161	168
2	-73	61
3	111	-123
4	121	-118
5	-55	5
6	170	-172
8	181	187
9	200	208
10	121	-117

4,4,L

-5	119	-120
-2	109	-99
-1	186	187
0	761	735
1	96	-87
2	231	-234
3	247	254
4	166	185
5	228	237
6	152	-159
10	-105	-127

4,5,L

-1	114	100
2	-79	36
4	-74	37
5	112	88
7	129	-131
9	175	163

4,6,L

-3	233	-224
-2	139	-141
0	-97	27
2	145	-120
6	-101	-70

4,7,L

-2	-74	-77
0	-78	22

5,0,L

-8	310	-283
-6	182	185
-2	-86	-27
0	196	194
2	-72	-64
4	221	215
6	257	-250
8	341	-305
10	180	186
12	230	-207

5,1,L

-8	111	104
-5	306	295
-4	256	236
-3	-75	-51
-2	220	202
-1	289	289
1	214	-209
2	81	85
3	132	106
5	388	383
6	274	272
7	337	-308
8	333	-335
9	153	168
10	-126	129
11	134	-121
12	-97	32

5,2,L

-8	-86	-82
-6	166	172
-3	126	117
-2	190	179
-1	459	-435
0	387	381
1	534	522
2	450	-430
4	137	-127
5	386	385
6	-66	-32
7	-49	-54
8	149	-140

5,3,L

-6	-93	-70
-4	91	113
-2	143	-149
0	197	194
1	130	121
2	242	238
3	151	-163
4	108	-126
5	89	82
6	403	420
7	-92	94
8	142	-160
9	-94	46
11	212	-207

5,4,L

-7	-71	-33
-5	-65	-60
-2	145	147
1	92	83
2	157	-156
8	-74	97

5,5,L

-1	139	-159
0	128	108
1	-74	-32
4	-70	-62
9	-81	-32

5,6,L

-2	-92	113
-1	286	278
1	102	-93
2	125	113
3	145	124
7	-90	57

5,7,L

-2	-87	62

6,0,L

-8	135	142
-6	-78	55
-2	594	559
0	636	-613
2	403	-384
4	271	-238
6	175	-171
10	179	-173
12	160	146

6,1,L

-8	-68	-57
-5	112	-91
-4	114	-108
-3	132	-126
1	471	-440
2	-75	85
3	291	271
4	186	177
5	565	-549
6	146	-128
7	279	297
9	289	-280
10	-110	73
11	-99	-89
12	-89	-74

6,2,L

-3	167	-169
-2	89	91

6,2,L

-1	252	242
0	349	-355
3	-55	41
4	110	102
5	324	-299
6	93	-98
7	168	-167
8	118	121
11	258	-257

6,3,L

-6	-97	95
-5	144	166
-2	190	198
-1	-77	-93
2	135	-138
3	199	193
4	247	262
5	91	-68
6	167	-173
7	209	-196

6,4,L

-3	-108	102
-2	116	-125
-1	132	94
1	151	-152
2	98	-90
8	-75	-46

6,5,L

-3	160	-143
-2	-88	55
-1	-97	104
0	119	136
5	184	170

6,6,L

-3	-107	118
2	130	-132
8	-88	-14

6,7,L

0	-88	-43
3	-70	67

7,0,L

-6	185	-195
-4	212	200
-2	470	-446
0	-130	-111
2	209	191
4	459	426
6	180	175
8	-127	144
10	315	306

7,1,L

-6	-93	-90
-5	-95	-34
-3	-107	-64
-2	128	116
-1	-75	-74
0	228	-220
1	202	202
3	320	-327
4	117	-108
6	123	125
8	177	-171
9	179	-176
10	-85	-39
11	221	226

7,2,L

-3	218	221
-2	120	-105
-1	196	-203
0	112	-112
1	157	-144
4	104	-104
7	177	174
9	166	-161
11	245	243

7,3,L

-6	-72	-51
-5	102	-107
-3	-63	-46
-2	-83	-36
0	143	-147
1	-82	-55
2	125	106
3	-86	92
4	251	-243
5	167	-168
6	130	117
10	120	-133

7,4,L

-4	156	-179
-3	-86	73
-1	141	-145
0	144	-134
1	162	156
2	-80	91
3	115	-102
7	-87	44
8	145	141
9	118	-115

7,5,L

-2	-94	-72
-1	-108	81
0	-88	-87
2	-88	-55
3	211	195
5	187	-178
6	110	-99

7,6,L

-2	-73	70
7	-65	-54

7,7,L

4	153	132

8,0,L

-6	-110	-76
-4	162	-169
-2	-82	65
0	230	229
2	138	-127
6	221	-206
8	118	104
10	436	-424
12	-107	28

8,1,L

-2	-67	-66
-1	124	127
0	218	224
1	-85	97
2	205	-205
4	145	138
5	-94	86
7	-104	49
9	279	295

8,2,L

-5	184	184
-3	268	-276
-1	-64	64
0	-85	-4
2	304	297
3	130	128
5	100	104
6	113	102
7	107	-101
8	176	165
9	100	122

8,3,L

-3	183	178
-2	145	-126
1	-73	81
2	288	-308
4	157	158
5	-74	65
6	145	-119
10	126	137

8,4,L

-3	174	-173
0	-65	-74
1	-79	-38
2	194	181
3	107	-90
4	163	-148
5	-97	101
6	199	204
7	111	-124
8	-118	-119
9	100	91

8,5,L

-2	-78	-33
-1	-106	-90
2	124	136
3	262	-235
9	-117	-112

8,6,L

1	-91	44

8,6,L

3	-95	-87
5	-62	0
7	-78	-8

9,0,L

-4	206	219
-2	-112	1
0	-121	127
2	-79	18
6	319	319
8	126	-100
10	184	188

9,1,L

-3	136	126
-1	-99	-100
1	220	231
3	133	-141
4	-94	83
5	149	147
7	-95	102
8	180	178
11	-73	-109

9,2,L

-4	124	132
-1	146	136
0	131	132
1	244	-235
3	-82	106
4	149	-156
5	269	-262
7	-98	114
8	270	-257
9	136	-139

9,3,L

-2	118	124
1	223	-225
2	162	160
6	-86	-11
8	292	308
10	-68	-81

9,4,L

-1	139	132
3	104	83
6	-63	0
7	141	132

9,5,L

3	121	127
4	-85	-67

10,0,L

-2	-108	-58
0	172	167
2	307	-319
4	282	281
6	265	-261
8	-100	-82

10,1,L

-3	144	-149
0	228	234
1	113	-113
3	-114	8
4	-94	-42
5	-106	5
6	149	140
7	266	-284
10	155	-122
11	157	-177

10,2,L

-3	133	121
0	-93	60
2	141	-136
3	-75	-4
4	180	183
5	165	178
6	124	-124
9	-107	63
10	131	142

10,3,L

2	121	-151
3	155	166

10,4,L

4	121	-120
5	-73	22
7	-84	-53

10,5,L

7	-112	111

11,0,L

-2	-100	71
0	195	-183
2	-106	85
4	-116	-119
6	-99	-99
8	175	173
10	-87	-7

11,1,L

0	125	-128
2	-71	-95
3	128	119
5	215	-227
6	155	-151
7	-88	94

11,2,L

1	-86	-11
3	155	118
4	-65	-13
5	-96	-86
6	127	-105
7	-83	-80
8	-73	57
10	-74	-96

11,3,L

0	-76	-3
3	-113	-138
4	-90	71
9	132	-134

11,4,L

4	174	176

12,0,L

4	-98	-42
6	153	174

12,1,L

-1	-137	58
0	-89	104
2	194	203
4	-106	-110
5	-76	85
6	134	121
7	-114	21
8	-84	61

12,2,L

2	120	121
3	161	-163
6	-66	81
7	-65	31
8	-87	75

12,3,L

4	123	-153
6	-80	47

12,4,L

4	-111	-65

13,0,L

2	152	165

13,1,L

1	127	-146
2	-83	-72
3	135	137
5	-74	-32
7	-90	23

13,2,L

5	103	120

Appendix 2

The electron density map for Pseudomonas aeruginosa cytochrome c_4. The sections are perpendicular to c and include z = -6/180 to z = 23/180. The a axis is horizontal, with $-5/6 \leq x \leq 1/6$, and b makes an angle of 120° with a, $-11/15 \leq y \leq 4/15$. The molecular boundary is indicated by a dashed line. The Fe and C_{α} positions have been indicated on the map. The top page shows the polypeptide chain as it has been traced on the map.

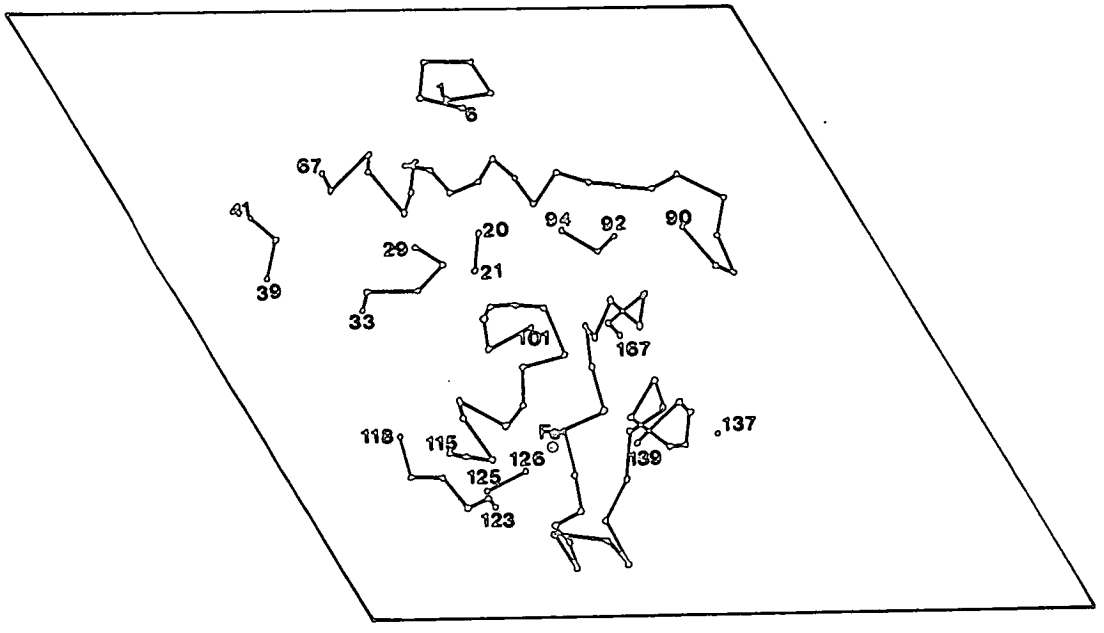
1
6
67
41
20
94
92
90
29
21
39
33
101
167
118
115
126
137
125
139
123

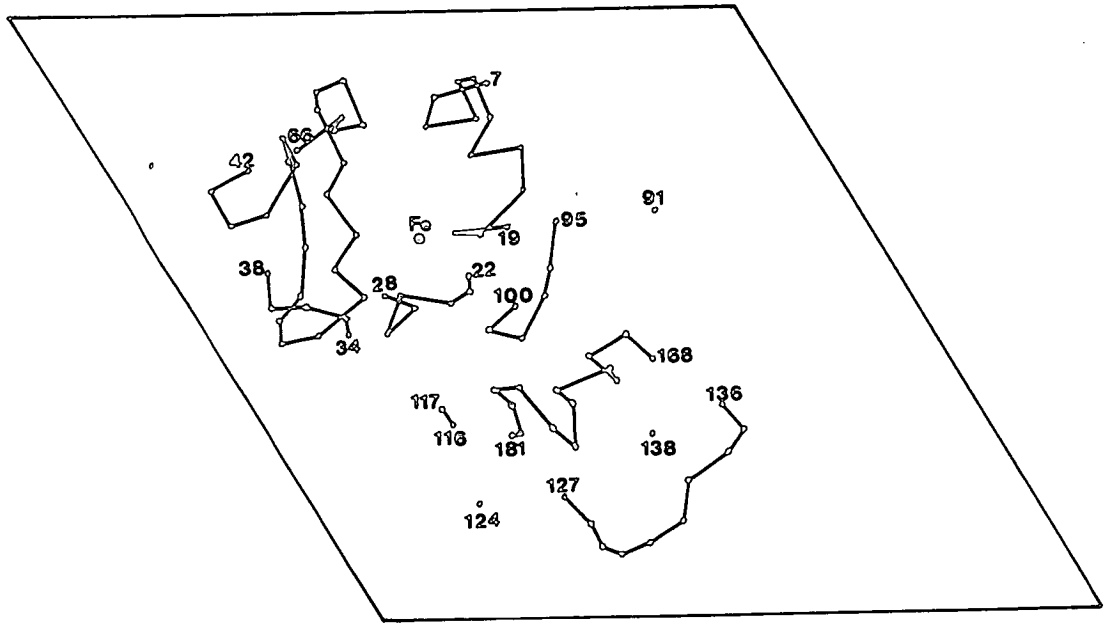
7
66
42
91
19
95
38
28
22
100
34
168
117
136
116
181
138
127
124

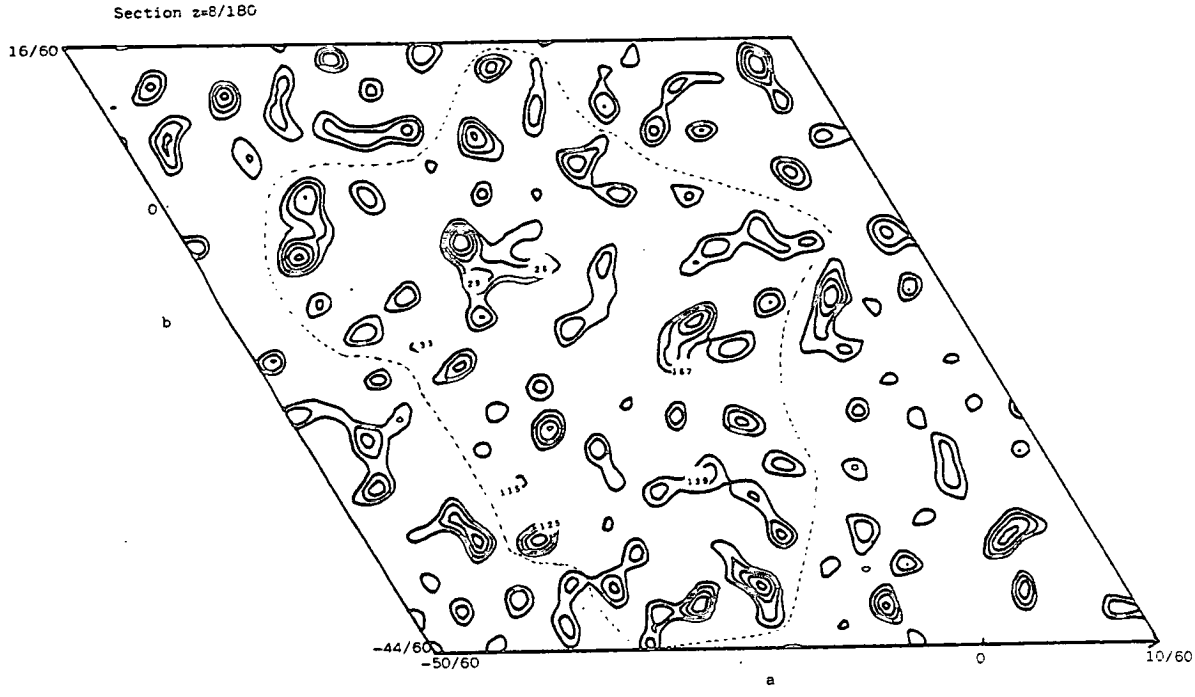
Section z=8/180
16/60
0
b
-44/60
-50/60
0
10/60
a

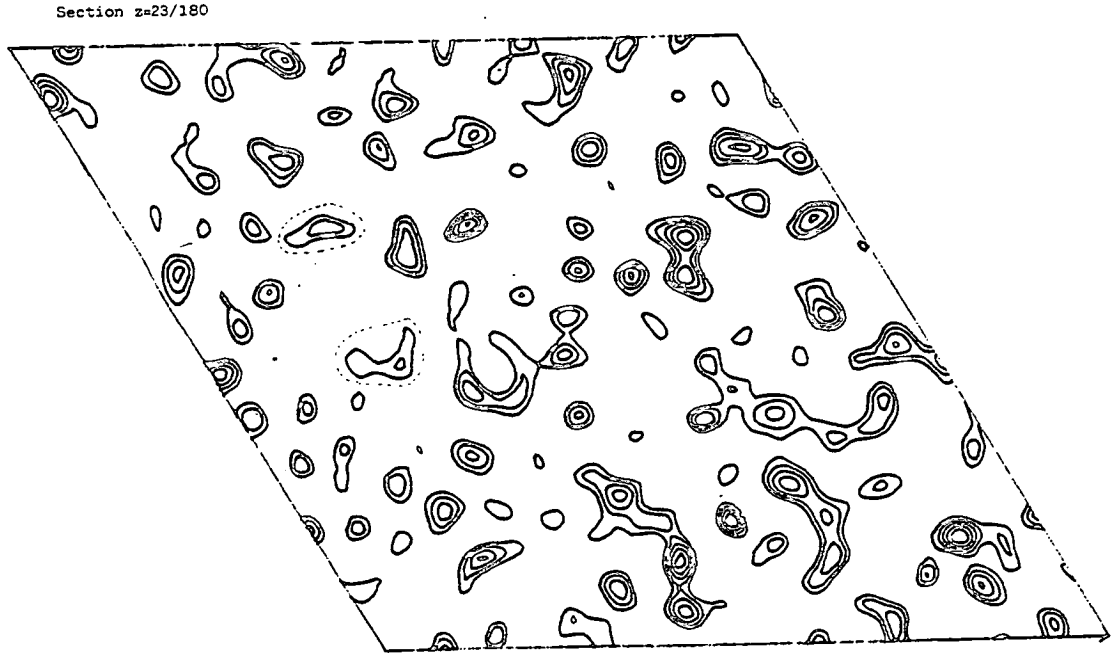
Section z=23/180

Section z=7/180

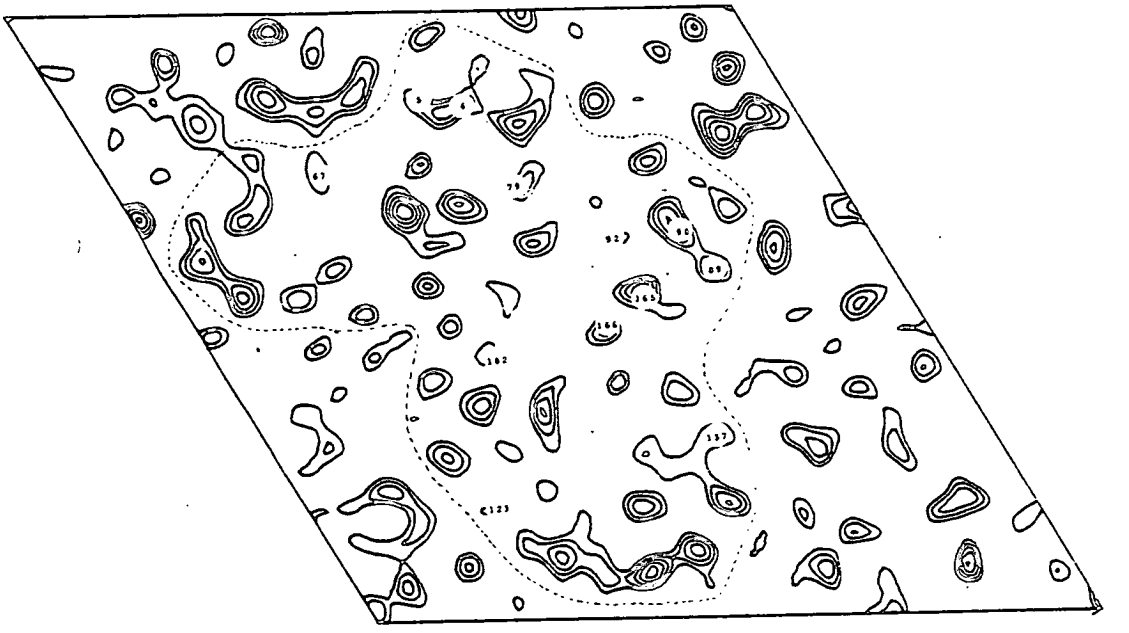

Section z=22/180

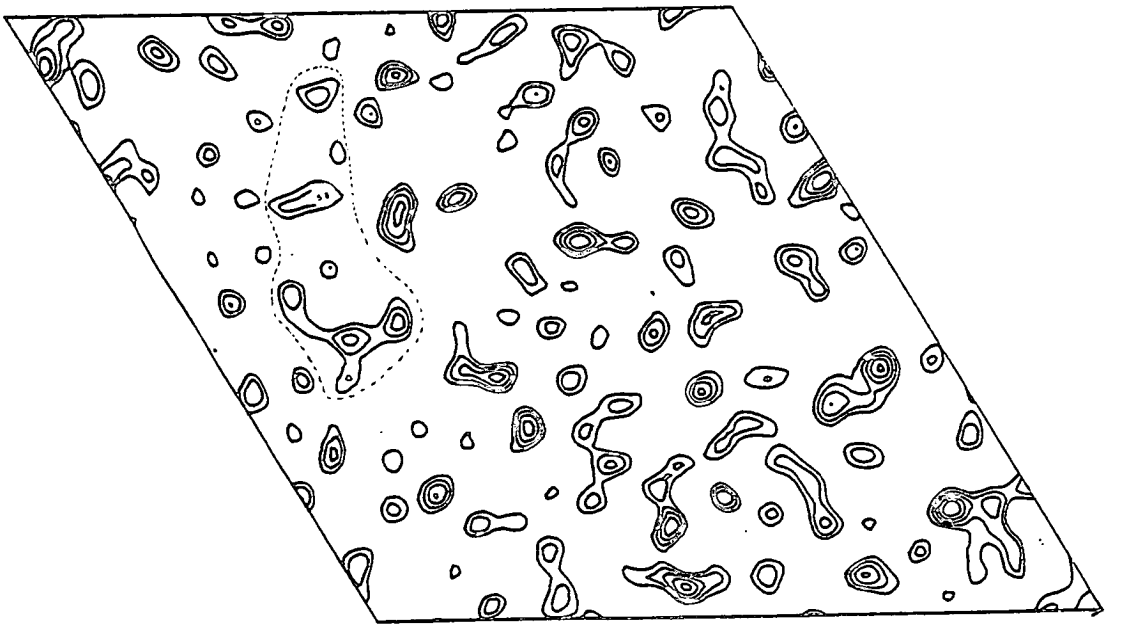

Section z=6/180

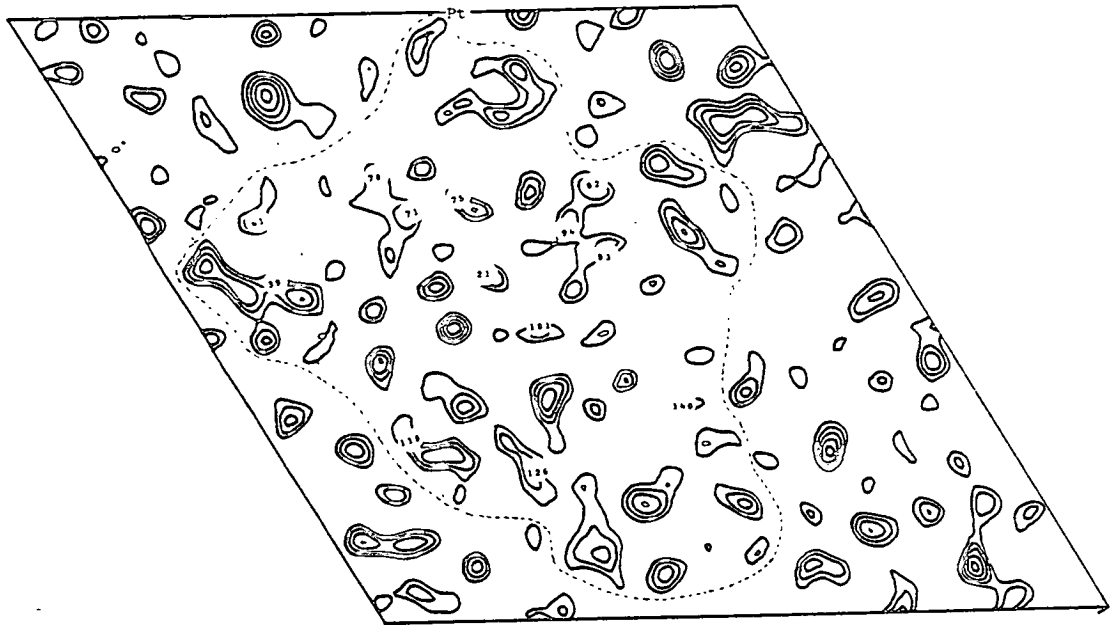

Section z=21/180

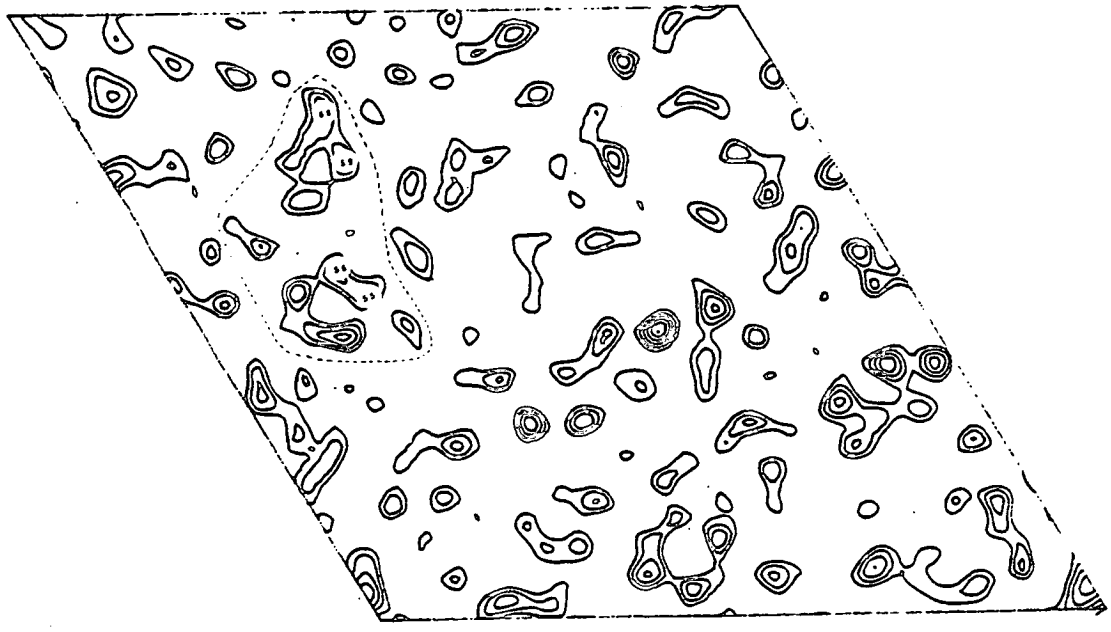

Section z=5/180

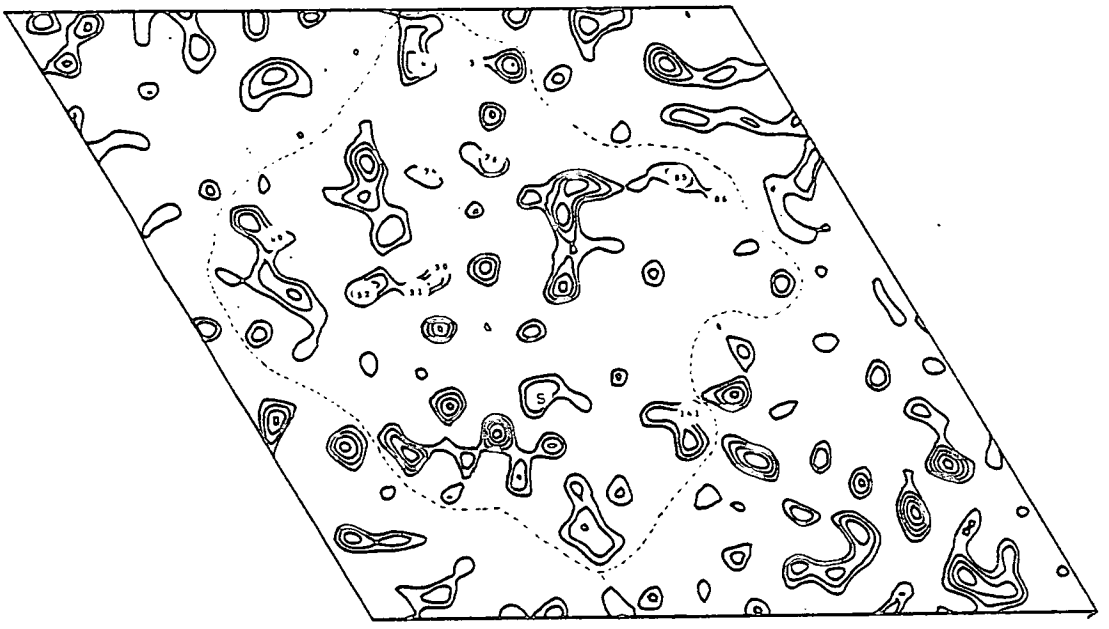

Section z=20/180

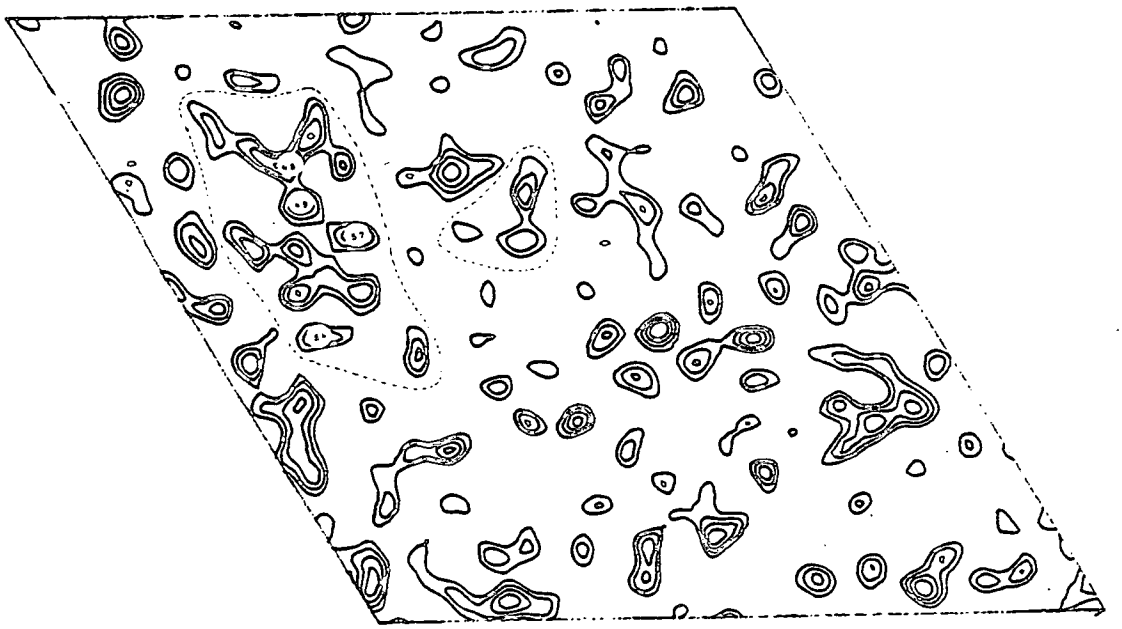

Section z=4/180

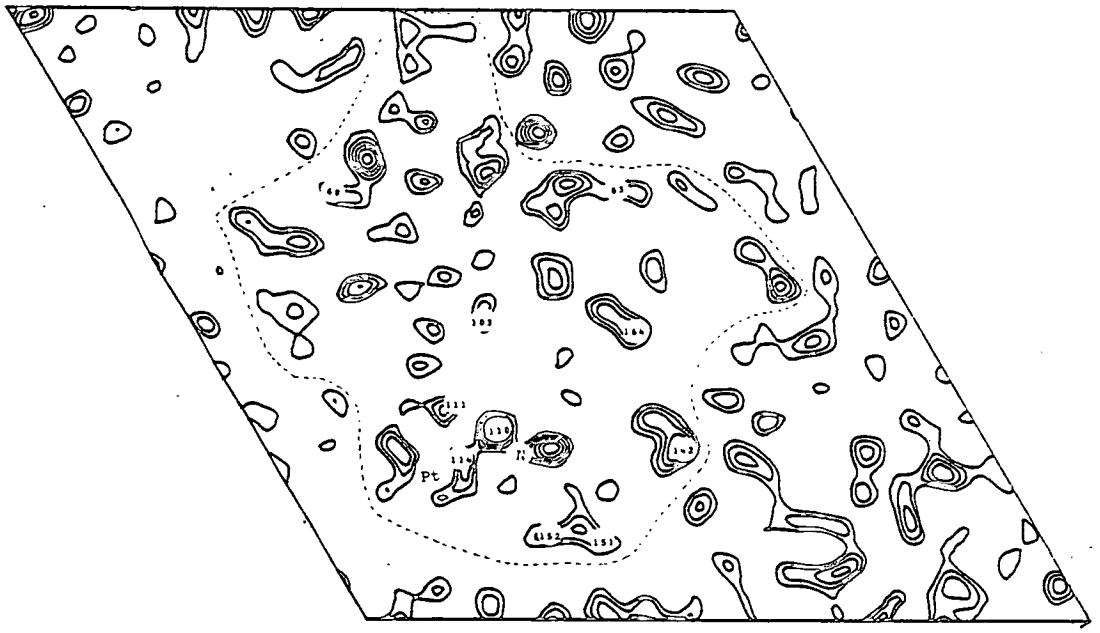

Section z=19/180

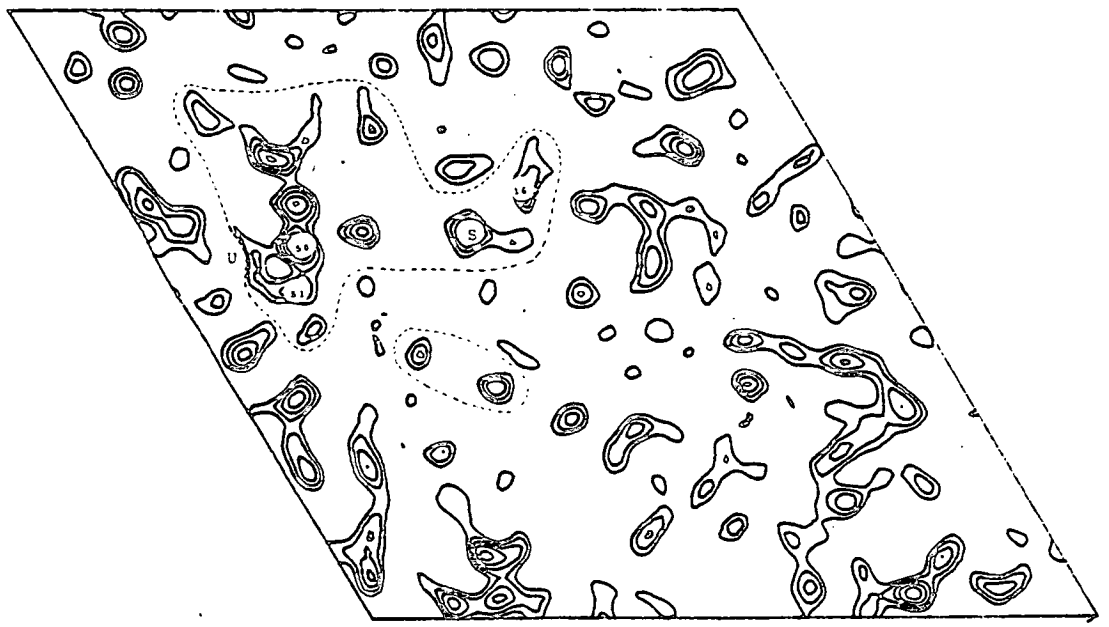

Section z=3/180

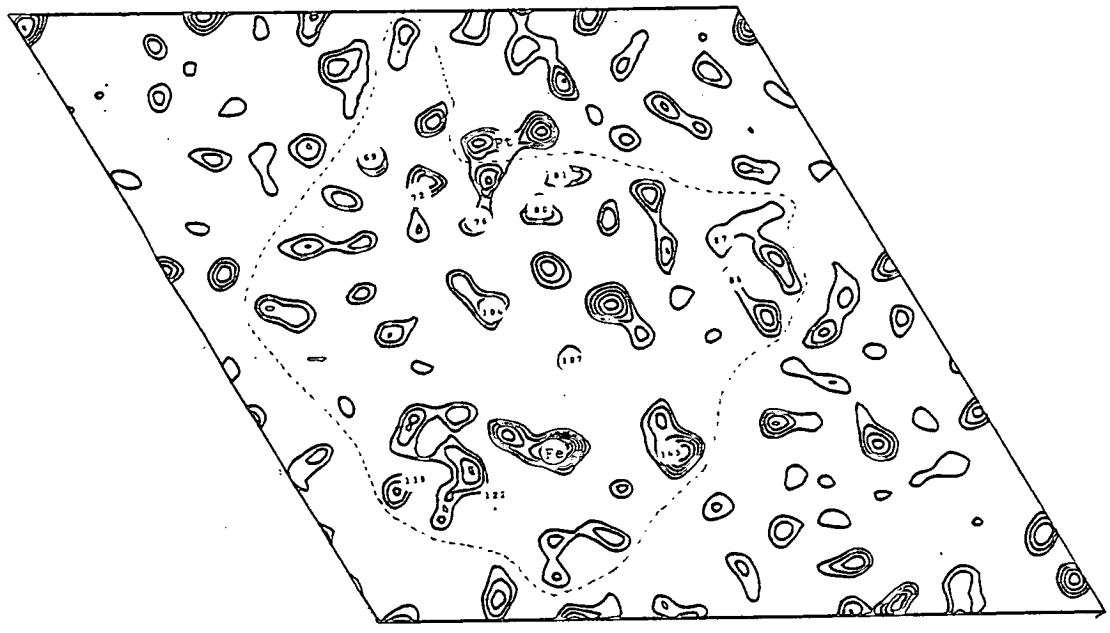

Section z=18/180

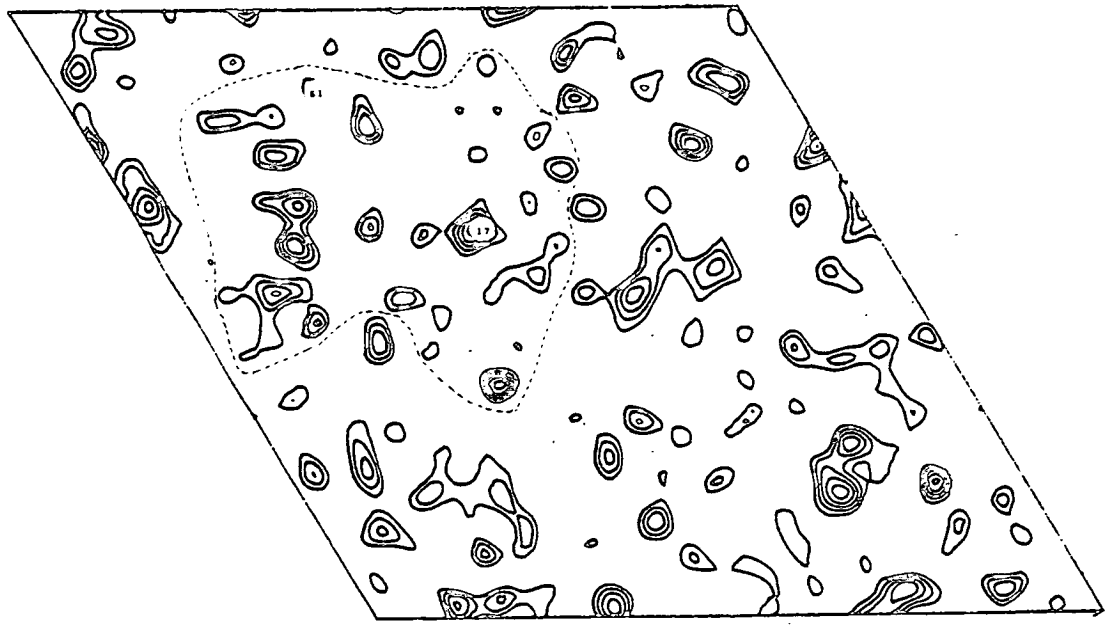

Section z=2/180

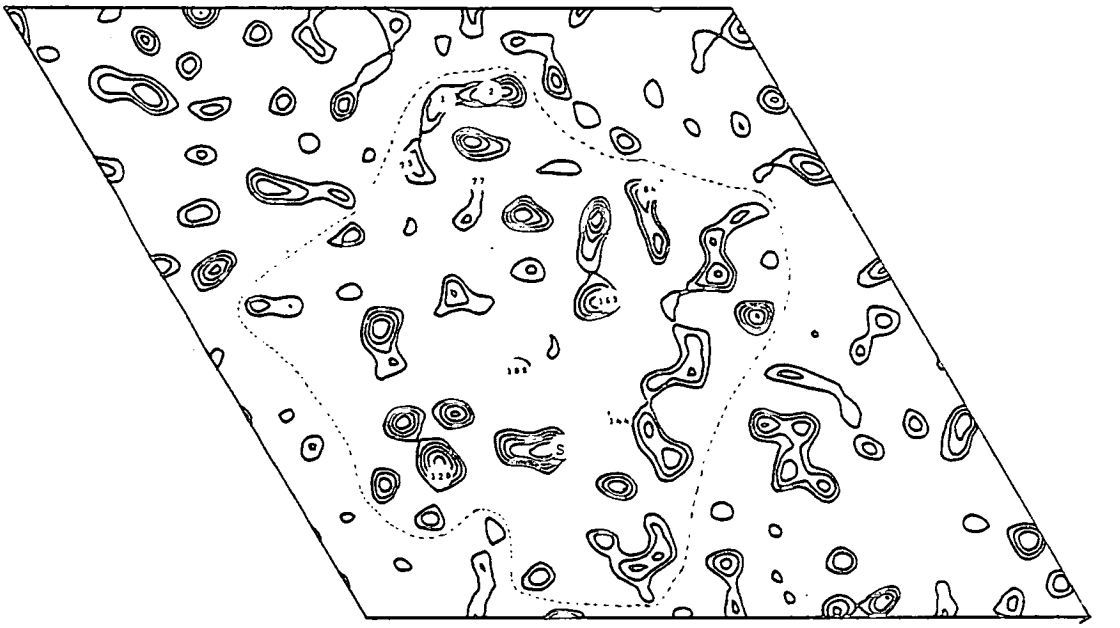

Section z=17/180

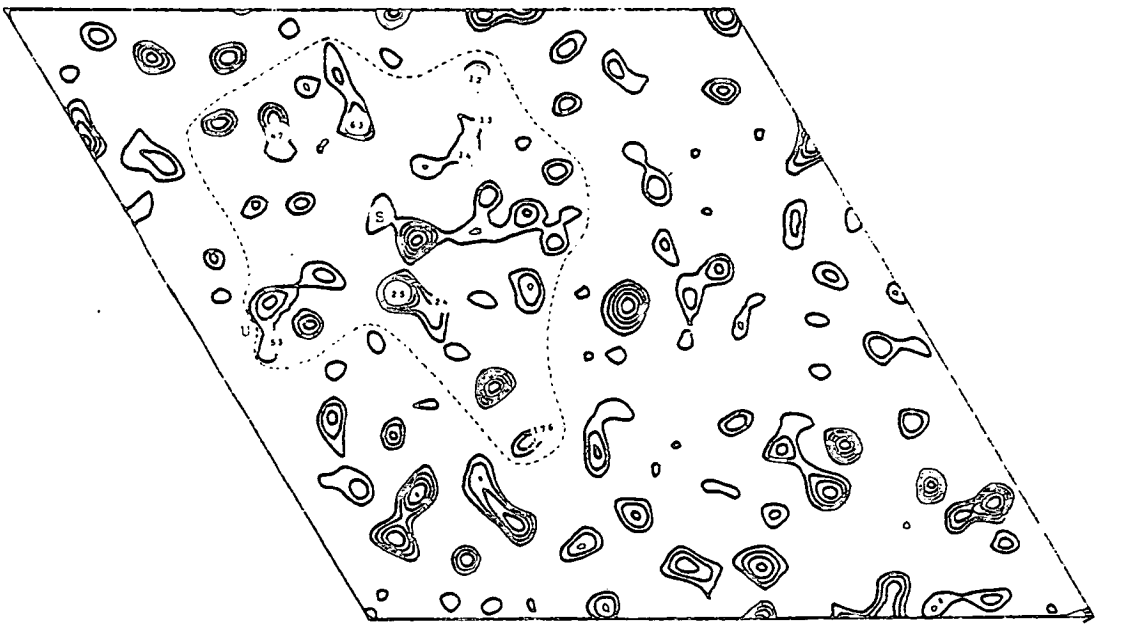

Section z=1/180

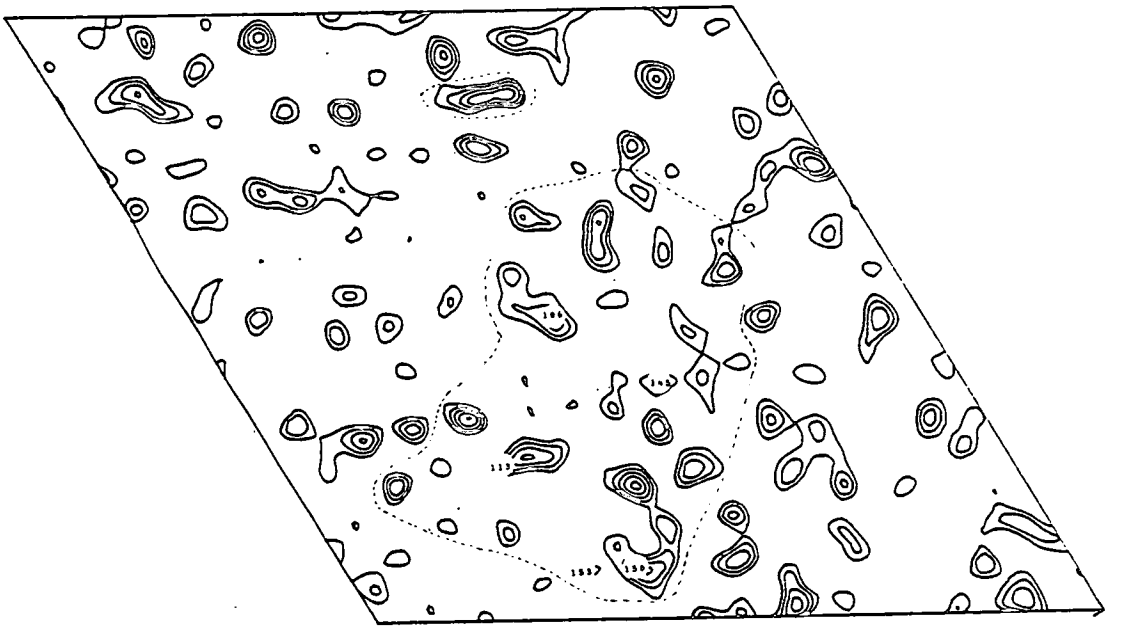

Section z=16/180

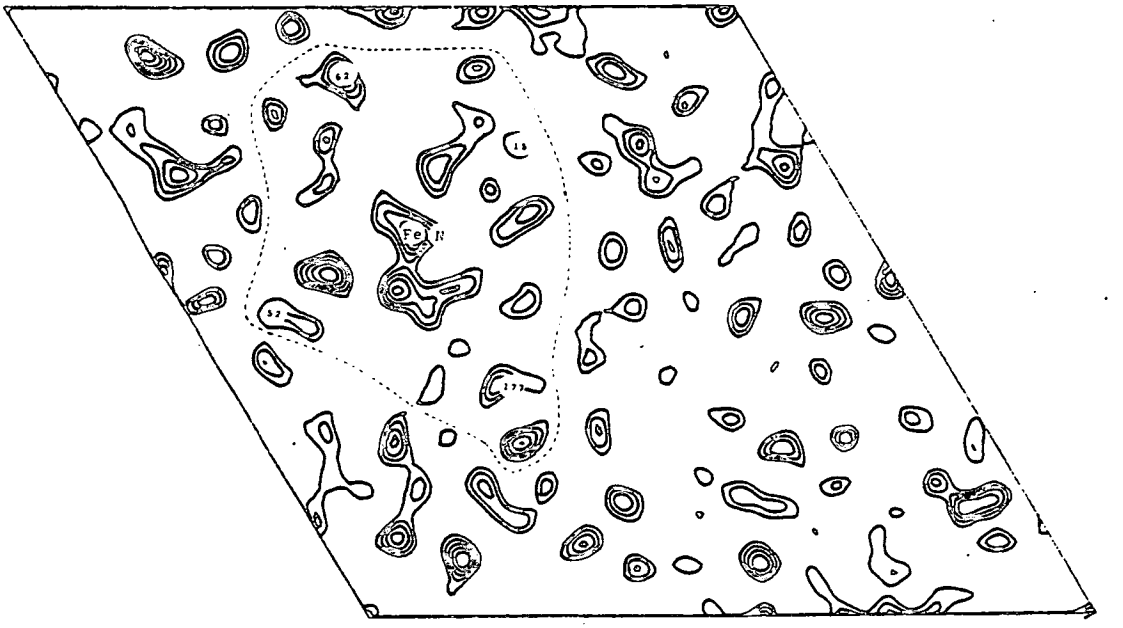

Section z=0

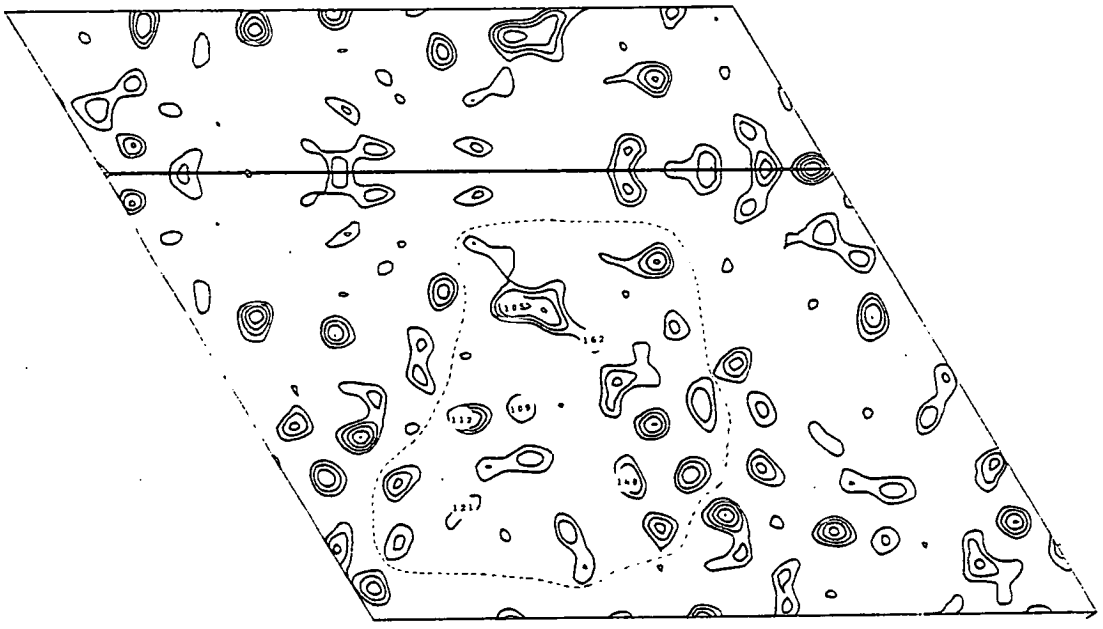

Section z=15/180

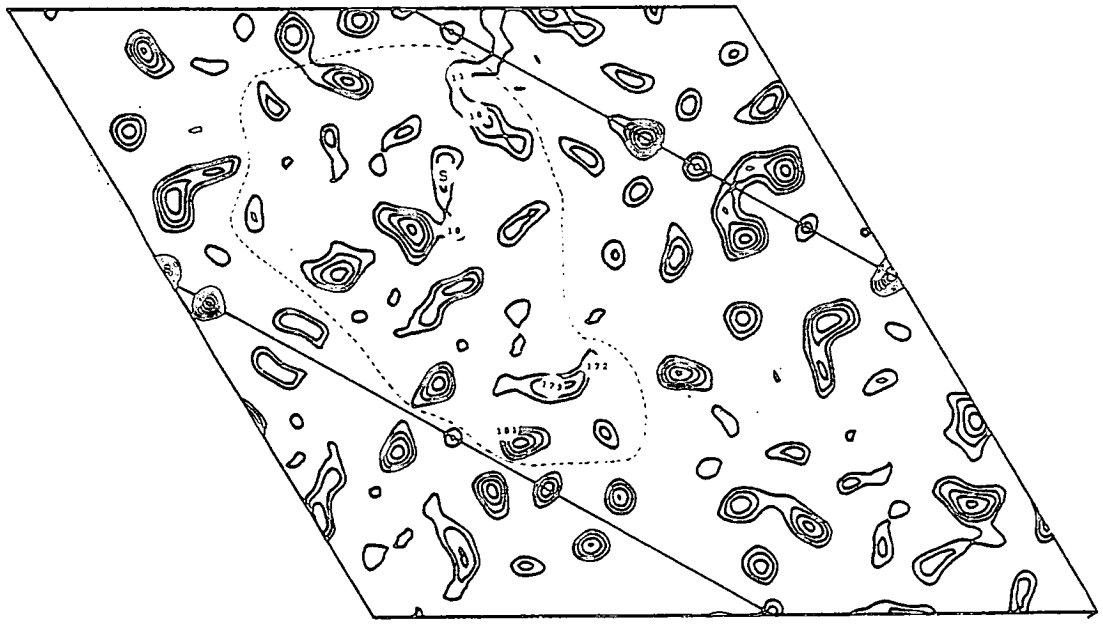

Section z=-1/180

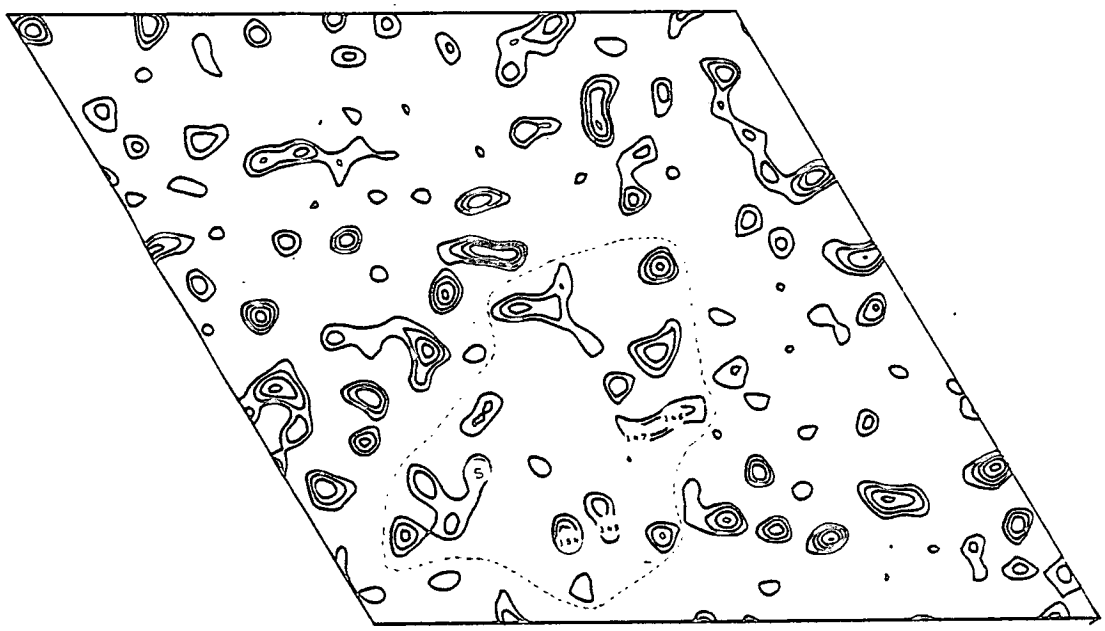

Section z=14/180

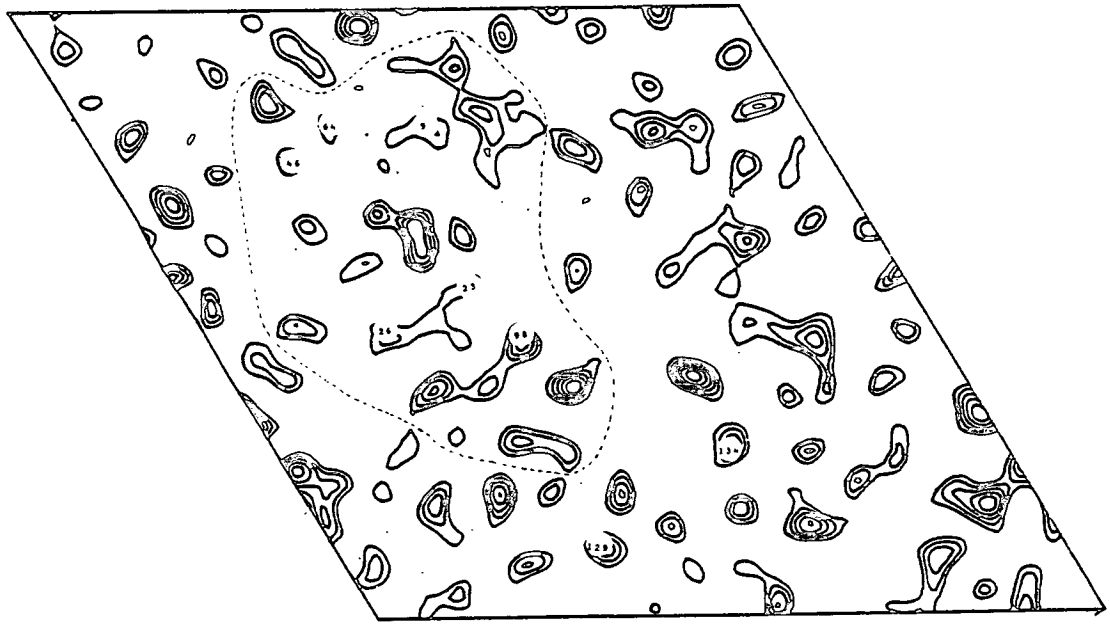

Section z=-2/180

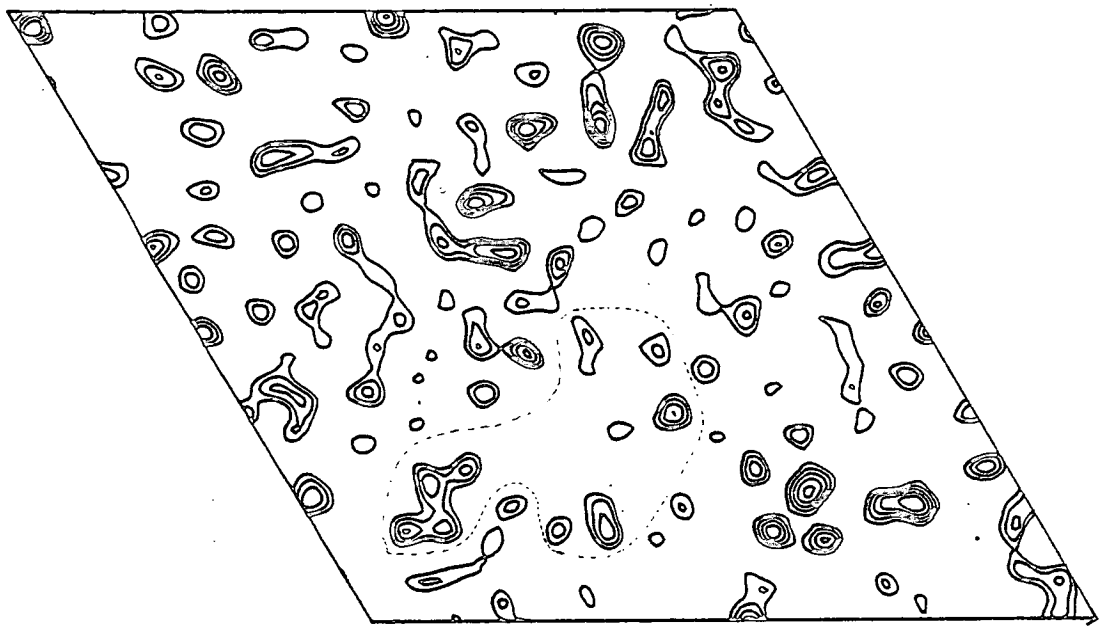

Section z=13/180

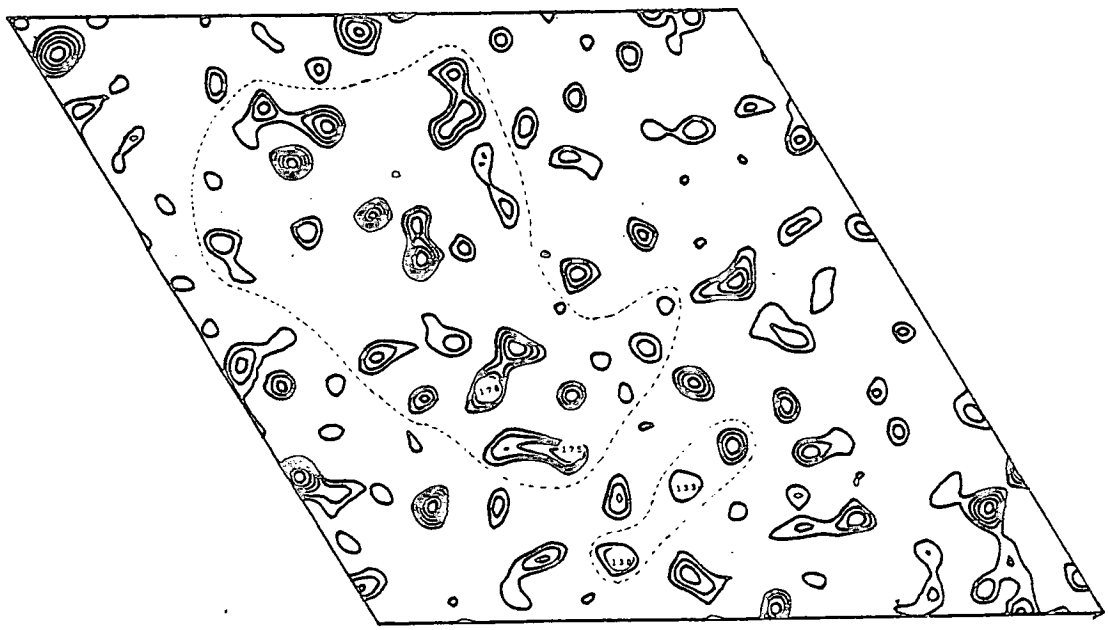

Section z=-3/180

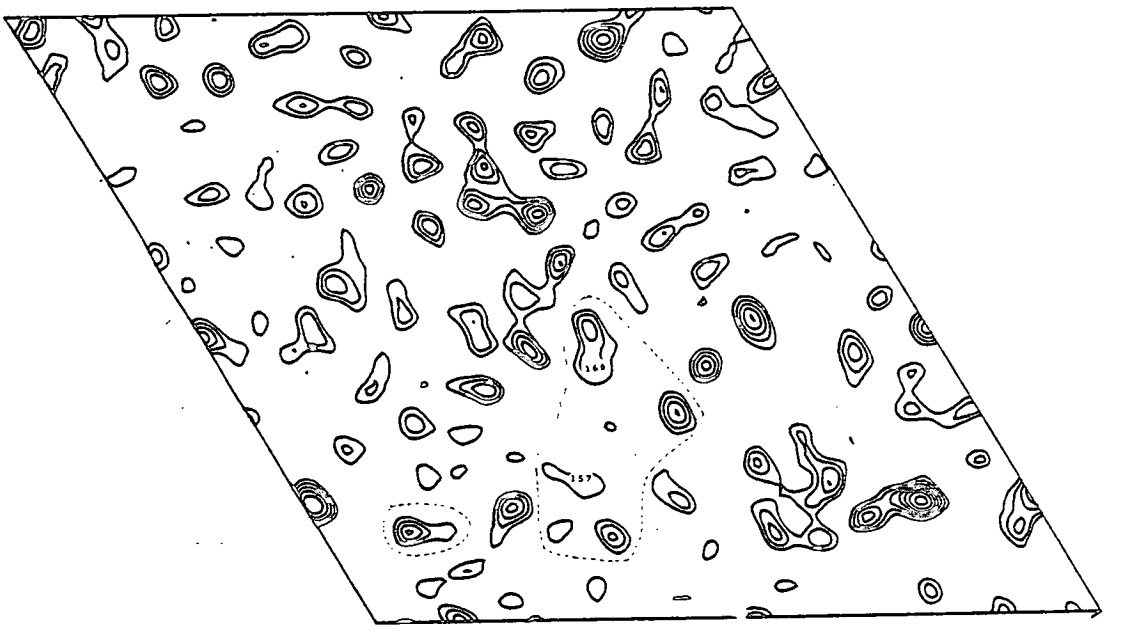

Section z=12/180

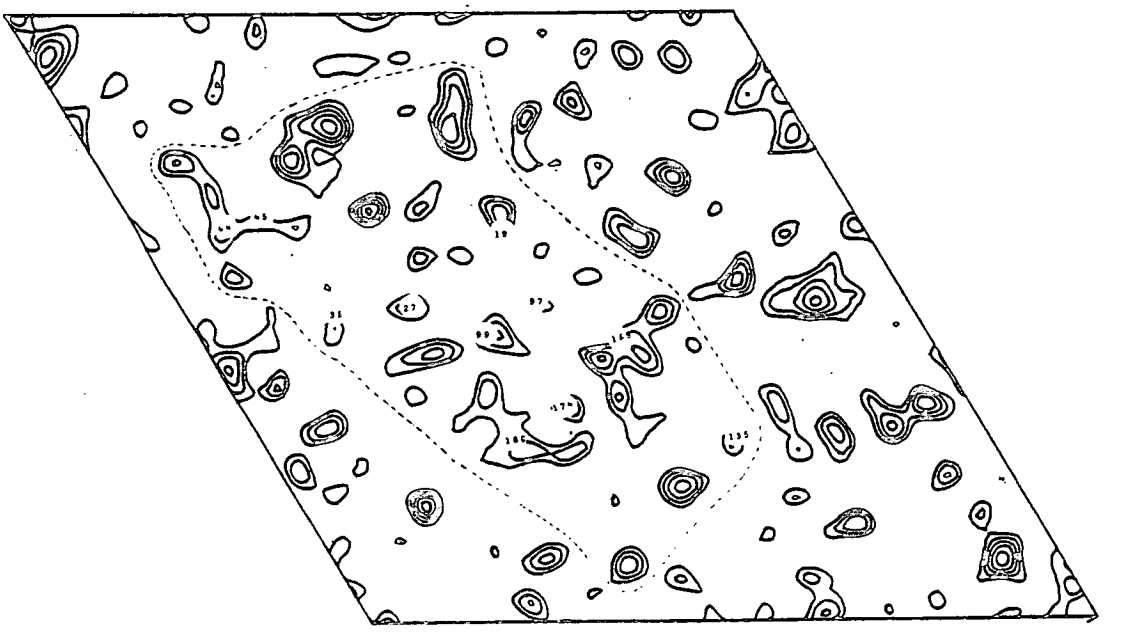

Section z=-4/180

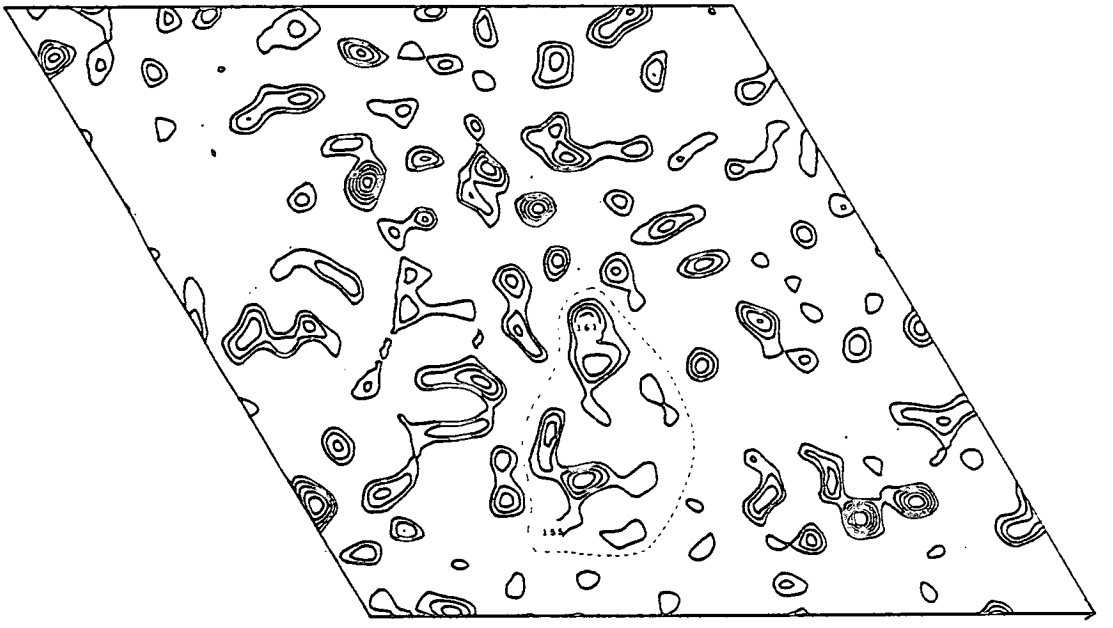

Section z=11/180

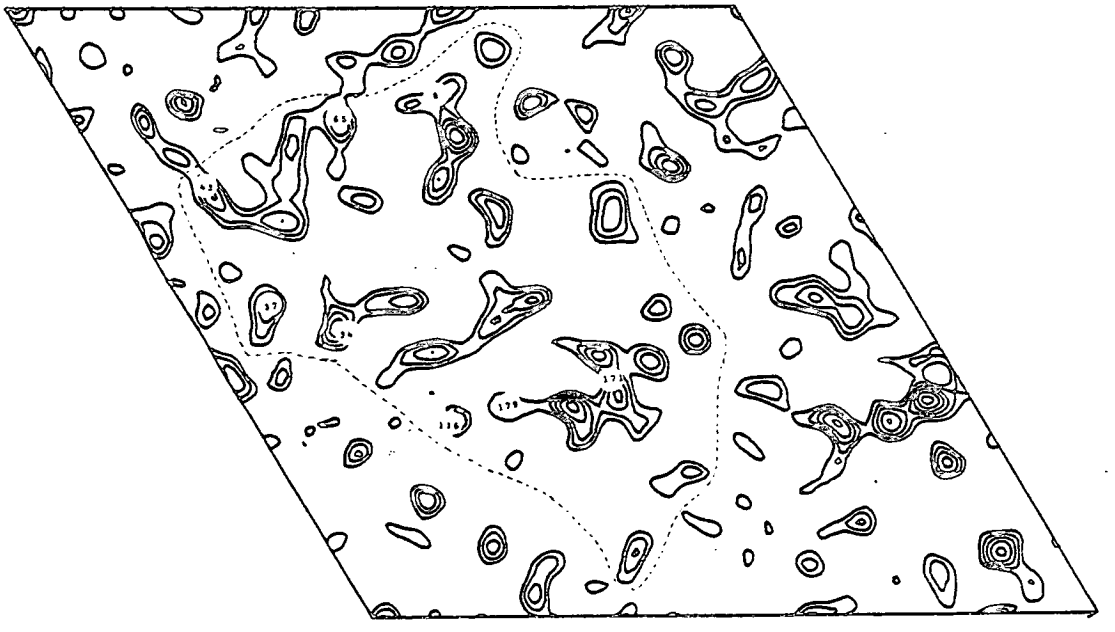

Section z=-5/180

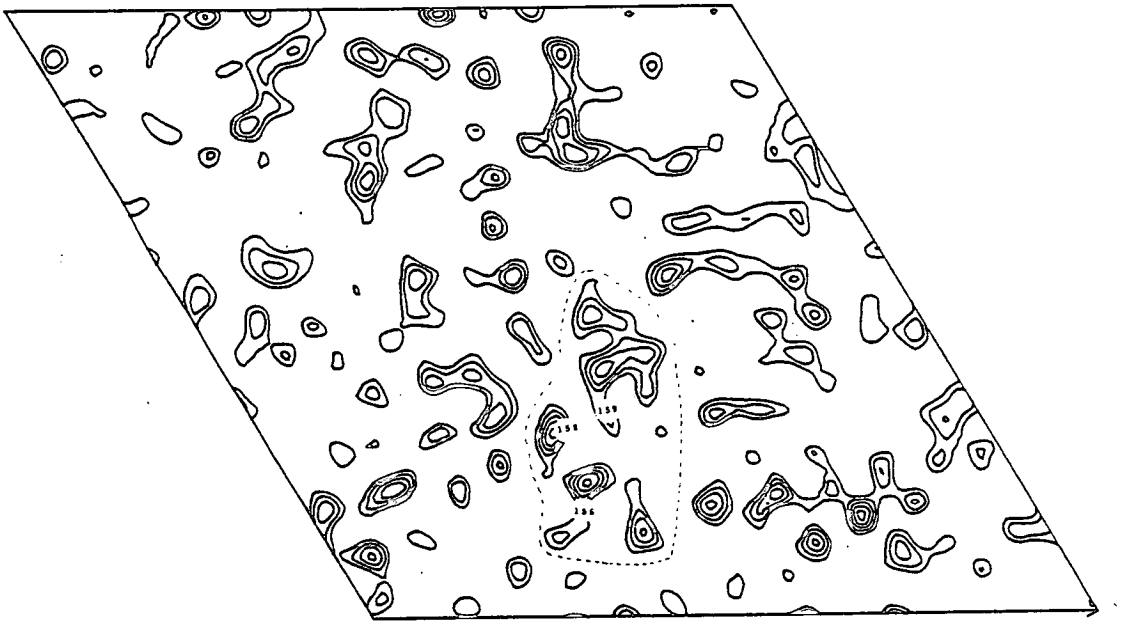

Section z=10/180

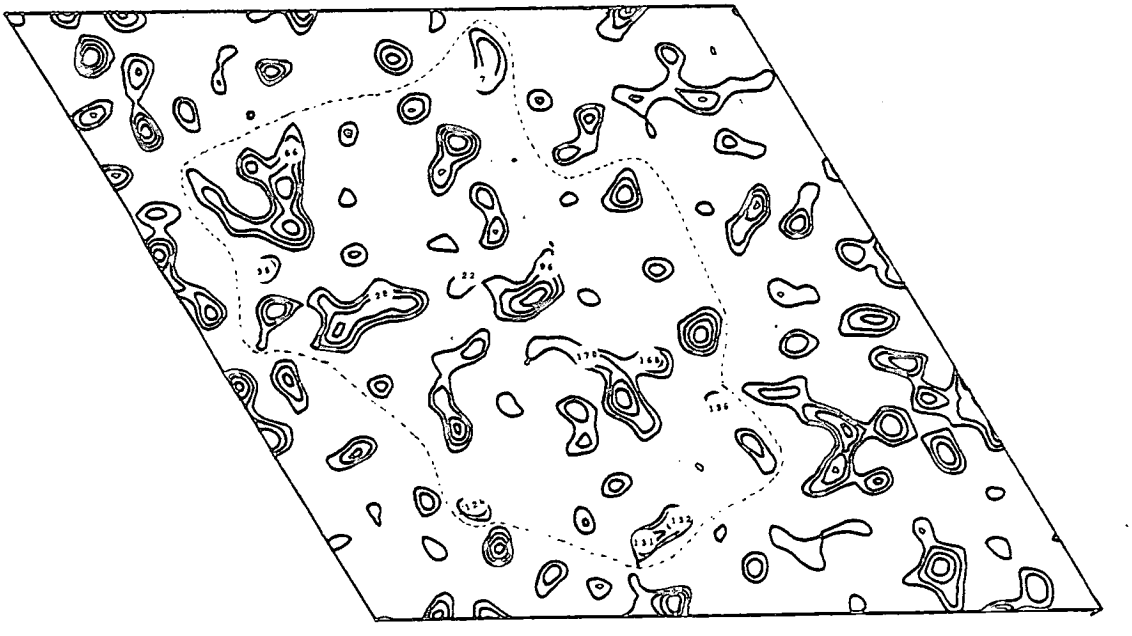

Section z=-6/180

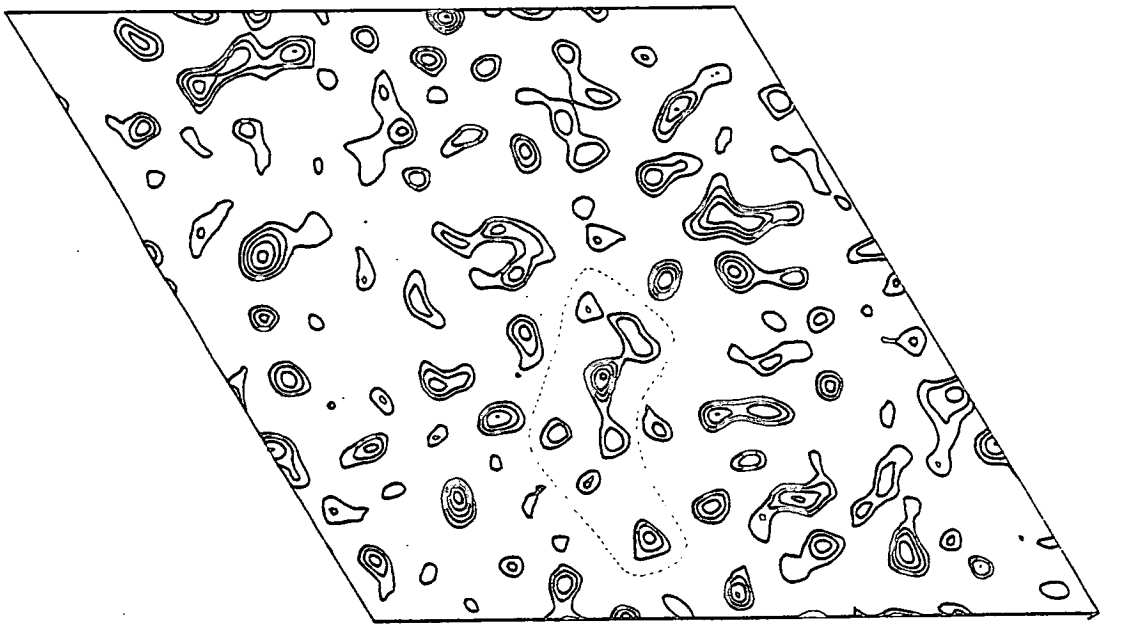

Section z=9/180

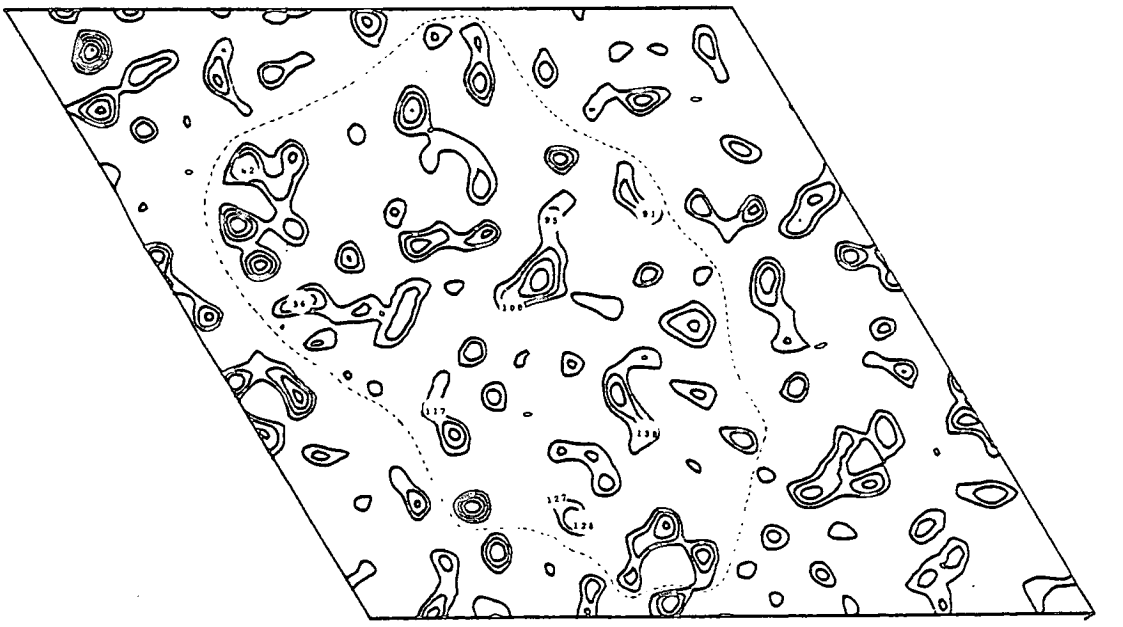

REPRINTS

Nitrile Sulphides. Part 1.[1] 1,3-Dipolar Cycloaddition to Carbonyl Groups activated by Trihaloalkyl Substituents; Synthesis and Crystal Structure of 1,3,4-Oxathiazoles

By A. Margarida Damas, Robert O. Gould, Marjorie M. Harding, R. Michael Paton,* and John F. Ross, Chemistry Department, University of Edinburgh, West Mains Road, Edinburgh EH9 3JJ, Scotland
John Crosby,* Imperial Chemical Industries Ltd., Organics Division, P.O. Box 42, Hexagon House, Blackley, Manchester M9 3DA

Nitrile sulphides, generated by the thermal decarboxylation of 1,3,4-oxathiazol-2-ones, undergo 1,3-dipolar cycloaddition to the carbonyl group in chloral, hexachloroacetone and α,α,α-trifluoroacetophenone to yield 2,2,5-trisubstituted 1,3,4-oxathiazoles (18—76%). Characterisation of the products is based on analytical and spectroscopic evidence, and is confirmed for 5-phenyl-2-trichloromethyl-1,3,4-oxathiazole and 5-(*p*-methoxyphenyl)-2-phenyl-2-trifluoromethyl-1,3,4-oxathiazole by *X*-ray crystal structure analyses. The oxathiazole rings are planar, with a localised C=N double bond.

THE synthesis of heterocycles *via* the 1,3-dipolar cycloaddition reactions of nitrile oxides (1) has been the subject of intensive study [2] over the last 20 years, the value of the method being well illustrated [3] by their reaction with carbonyl compounds yielding 1,3,4-dioxazoles (2), a group of compounds for which there are few preparative methods.[4] In contrast, the corresponding nitrile sulphides (3) have received much less attention, their reported cycloadditions being restricted to alkyne,[5] alkene,[6] and nitrile [7] dipolarophiles. We have examined their reaction with carbonyl compounds with a view to establishing a new route to 1,3,4-oxathiazoles (4), a rare class of heterocycles accessible only with difficulty by other means.[8]

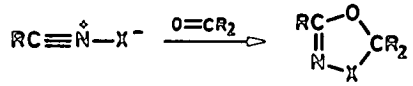

(1) X = O (2) X = O
(3) X = S (4) X = S

RESULTS AND DISCUSSION

For this investigation the nitrile sulphides were generated by the thermal decarboxylation of 1,3,4-oxathiazol-2-ones (5), while chloral, hexachloroacetone, and α,α,α-trifluoroacetophenone were selected as dipolarophiles in view of the established preference [3] of nitrile oxides for carbonyl groups which are activated by electron-withdrawing substituents.

The oxathiazolones were heated in xylene under reflux in the presence of an excess of the carbonyl compound [5 mol per mol of (5)] until h.p.l.c. analysis indicated their complete consumption. Removal of the solvent and excess of dipolarophile afforded the corresponding 1,3,4-oxathiazoles (4), (18—76%), together with sulphur and nitrile by-products which were separated by distillation and/or recrystallisation.

The identification of the products as 1,3,4-oxathiazoles follows from their analytical and spectroscopic data. The i.r. spectra are similar to those of the oxathiazolone precursors, but lack their carbonyl stretching band at 1 735—1 765 cm^{-1}; a new characteristic C=N peak appears at 1 615—1 655 cm^{-1}. The 1,3,4-oxathiazoles also have mass, ^1H, and ^{13}C n.m.r. spectra consistent with their structures. Comparison of the ^{13}C n.m.r. chemical shifts (Table 1) with those for the corresponding oxathiazol-2-ones (Table 2) supports the assignment of a

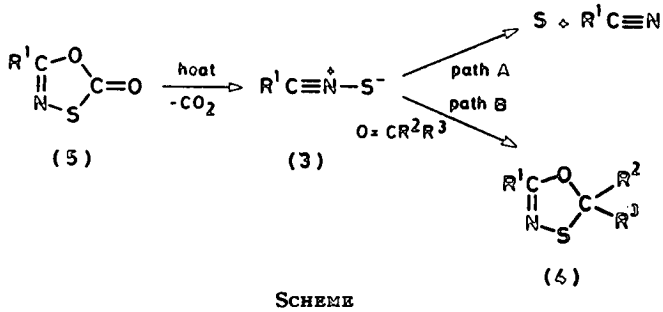

SCHEME

1,3,4-oxathiazole ring structure. The peaks attributable to the carbon at ring-position 5 and its substituent (R^1) show little or no variation; on the other hand significant shifts are observed for the carbon at position 2, consistent with replacement of the carbonyl group of (5) by CR^2R^3 in (4). The precise position of the C-2 absorption is also dependent on the nature of the C-2 substituents, being 95.6—95.9 p.p.m. for the oxathiazoles derived from chloral and trifluoroacetophenone, while those from hexachloroacetone lie between 111.9 and 112.2 p.p.m., thus reflecting the presence of the second trihaloalkyl group.

The mass spectra of the oxathiazoles showed, in addition to the parent ion, peaks corresponding to R^1CNS and R^1CN fragments, thus suggesting a major fragmentation pathway involving retro-1,3-dipolar cycloaddition to dipolarophile and 1,3-dipole and its subsequent cleavage to nitrile and sulphur. Similar behaviour is exhibited by compound (5) and the corresponding, nitrile oxide derived, 1,3,4-dioxazoles (2).[9]

The structures of 5-phenyl-2-trichloromethyl-1,3,4-oxathiazole (4A) and 5-(*p*-methoxyphenyl)-2-phenyl-2-trifluoromethyl-1,3,4-oxathiazole (4B) have been determined by *X*-ray analysis.

These appear to be the first crystal-structure determinations of the 1,3,4-oxathiazole ring. The molecular shapes found are illustrated in Figure 1 and important bond lengths and angles are compared in Figure 2.

TABLE 1

^{13}C N.m.r. data (p.p.m. from Me_4Si; $CDCl_3$ solvent) for 1,3,4-oxathiazoles (4)

R^1	R^2	R^3	C-2	C-5	C or R^1	C of R^2 and R^3
Ph	CCl_3	H	95.9	157.1	131.4, 128.4, 127.9 (5 Ph ring CH); 125.9 (Ph ring C)	99.7 (CCl_3)
Ph	CCl_3	CCl_3	112.2	156.1	131.8, 128.6, 128.0 (5 Ph ring CH); 125.5 (Ph ring C)	100.3 (2 CCl_3)
4-$MeOC_6H_4$	CCl_3	H	95.9	157.3	162.3, 118.9 (Ar ring C); 129.9, 114.1 (4 Ar ring CH); 55.4 (OMe)	100.1 (CCl_3)
4-$MeOC_6H_4$	CCl_3	CCl_3	112.1	156.1	162.4, 118.1 (Ar ring C); 129.9, 114.1 (4 Ar ring CH); 55.4 (OMe)	100.4 (2 CCl_3)
4-$MeOC_6H_4$	CF_3	Ph	95.6 (J_{C-C-F} 33 Hz)	156.0	162.2, 118.7 (Ar ring C); 129.7, 113.9 (4 Ar ring CH); 55.2 (OMe)	134.9 (Ph ring C) 129.7, 128.6, 126.0 (5 Ph ring CH); 123.7 (CF_3, J_{C-F} 284 Hz)
4-ClC_6H_4	CCl_3	CCl_3	112.4	155.2	138.3, 124.0 (Ar ring C); 129.3, 129.1 (4 Ar ring CH)	100.2 (2 CCl_3)
4-ClC_6H_4	CF_3	Ph	96.2 (J_{C-C-F} 33 Hz)	155.2	137.9, 124.6 (Ar ring C); 129.2, 128.9 (Ar ring CH)	134.6 (Ph ring C); 129.9, 128.7, 126.0 (5 Ph ring CH); 123.5 (CF_3, J_{C-F} 284 Hz)
Me	CCl_3	H	95.9	157.6	15.0 (CH_3)	99.9 (CCl_3)
Me	CCl_3	CCl_3	112.1	156.5	15.0 (CH_3)	100.4 (2 CCl_3)
$CH_3(CH_2)_2$	CCl_3	CCl_3	111.9	159.8	31.0, 19.1 (CH_2); 13.5 (CH_3)	100.3 (2 CCl_3)
$CH_3(CH_2)_{10}$	CCl_3	H	95.7	161.0	31.8, 29.4, 29.3, 29.2, 29.0, 28.8, 25.7, 22.5 (10 CH_2); 14.0 (CH_3)	99.8 (CCl_3)
$CH_3(CH_2)_{10}$	CCl_3	CCl_3	112.0	160.0	31.8, 29.5, 29.3, 29.2, 29.0, 28.8, 25.5, 22.6 (10 CH_2); 14.0 (CH_3)	100.4 (2 CCl_3)

There are no significant differences in the oxathiazole ring between the two compounds, and bond lengths are consistent with a localised C=N double bond. The oxathiazole rings are nearly planar, with a very slight fold across S · · · O; in (4A) the maximum deviation from the best plane of the five ring atoms is 0.08 Å and in (4B), 0.01 Å. The aryl groups at C(5) are not coplanar with the five-membered rings; in (4A) the torsion angle C(7)–C(6)–C(5)–N(4) is −16.7° and in (4B), −12.0°. [For atom numbering see Figure 1]. Bond lengths and angles in other parts of the molecule are in agreement with those in similar compounds. There are no intermolecular contacts between non-hydrogen atoms less than 3.3 Å in either compound.

TABLE 2

^{13}C N.m.r. data (p.p.m. from Me_4Si; $CDCl_3$ solvent) of 1,3,4-oxathiazol-2-ones (5).

R^1	C-2	C-5	C of R^1
Ph	173.7	157.4	132.6, 129.0, 127.4 (5 Ph ring CH); 125.8 (Ph ring C)
4-$MeOC_6H_4$	174.1	157.3	163.3, 118.5 (Ar ring C); 129.3, 114.5 (Ar ring CH); 55.5 (OMe)
4-ClC_6H_4	173.3	156.5	139.1, 124.3 (Ar ring C); 129.5, 128.7 (Ar ring CH)
Me	174.2	158.7	16.4 (CH_3)
$CH_3(CH_2)_2$	174.4	161.8	32.3, 18.6 (CH_2); 13.4 (CH_3)
$CH_3(CH_2)_{11}$	174.0	161.7	31.6, 30.2, 29.4, 29.1, 28.9, 28.6, 25.1, 22.4 (10 CH_2); 13.8 (CH_3)

The formation of nitrile and sulphur by-products is a common feature of nitrile sulphide chemistry and is attributed [7] to fragmentation (Scheme, path A) competing with cycloaddition (path B). As has been observed for other nitrile sulphide cycloadditions, we find that the balance between the two pathways, and consequently the yield of the cycloadduct, is dependent on the reactivity of the nitrile sulphide and on the nature of the dipolarophile. Electron-donating substituents in the dipole favour cycloaddition; thus the adduct yield rises from 35% for R^1 = 4-ClC_6H_4 to 57% for R^1 = 4-$MeOC_6H_4$ for reaction with hexachloroacetone. Electron-withdrawing groups in the dipolarophile also favour cycloadduct formation, but the slightly greater yields obtained for chloral compared with hexachloroacetone, in spite of the presence of two electron-withdrawing trihalogenoalkyl groups in the latter, suggest that steric factors may also play an important role.

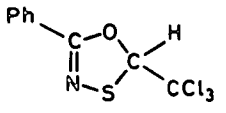

(4A)

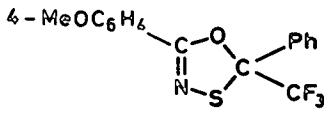

(4B)

EXPERIMENTAL

Mass spectra (70 eV ionisation potential) were measured using an AEI MS902 instrument. Varian HA 100 and CFT 20 spectrometers were used to record ^{1}H and ^{13}C n.m.r. spectra respectively. I.r. spectra were recorded with a Perkin-Elmer model 257 spectrophotometer. The reactions were followed and the yields of the products determined by high-performance liquid chromatography (h.p.l.c.) analysis, utilising a 15 × 0.5 cm alumina column (25% water deactivated) with 80% hexane–20% dichloromethane (25% water saturated) as eluant.

Preparation of the 1,3,4-*Oxathiazol*-2-*ones* (5).—The

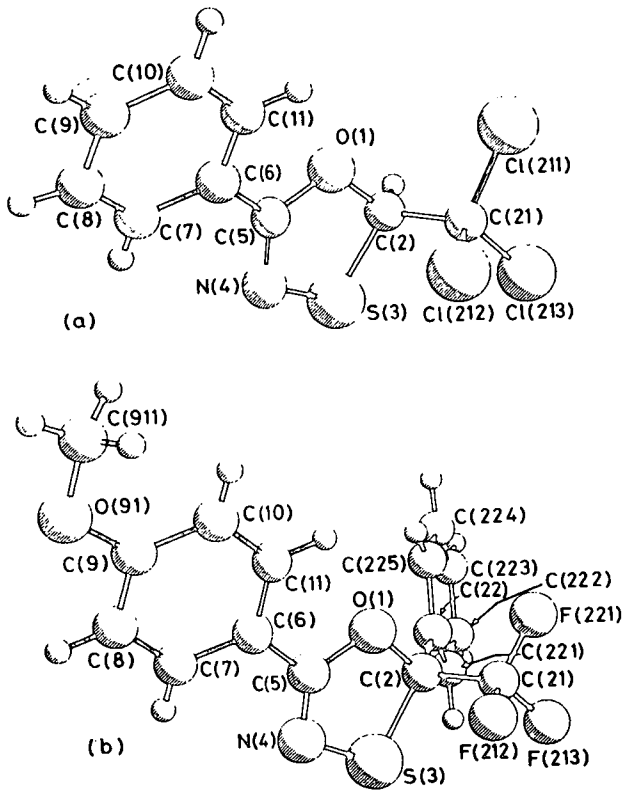

FIGURE 1 One molecule of compound (4A) (a) and compound (4B) (b) as found in the crystals and showing the atom numbering used in the crystallographic tables

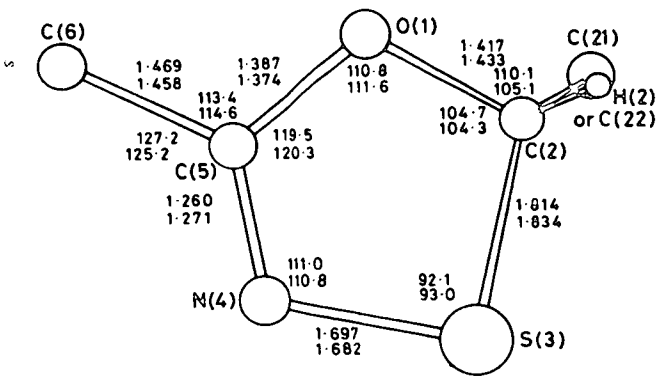

FIGURE 2 Bond lengths (in Å) and angles (in degrees) in the 1,3,4-oxathiazole ring in (4A) (above) and (4B). Estimated standard deviations range from 0.004 Å for the N–S bond to 0.006 Å for the C–C bonds in both compounds, and from 0.3° for the angle at sulphur to 0.6° for angles at carbon

following were prepared from chlorocarbonylsulphenyl chloride and the appropriate amide as described in the literature and had correct characteristics: 5-phenyl-1,3,4-oxathiazol-2-one,[10] 5-(*p*-chlorophenyl)-1,3,4-oxathiazol-2-one,[10] 5-methyl-1,3,4-oxathiazol-2-one.[11]

5-(p-Methoxyphenyl)-1,3,4-oxathiazol-2-one. This compound was prepared (54%) from *p*-methoxybenzamide and ClCOSCl by the same route and the product recrystallised from ethanol; it had m.p. 112 °C (Found: C, 51.4; H, 3.3; N, 6.5. $C_9H_7NO_3S$ requires C, 51.7; H, 3.4; N, 6.7%); $\nu_{max.}$ (Nujol) 1 750 cm^{-1} (C=O); *m/e* 209 (M^+), 165 ($MeOC_6H_4CNS^+$), 135 ($MeOC_6H_4CO^+$), and 133 ($MeOC_6H_4CN^+$).

5-Propyl-1,3,4-oxathiazol-2-one. This compound was similarly prepared in 59% yield from ClCOSCl and butanamide; it had b.p. 69—70 °C at 12 mmHg (Found: C, 41.1; H, 4.8; N, 9.9. $C_5H_7NO_2S$ requires C, 41.4; H, 4.9; N, 9.7%); $\nu_{max.}$ (film) 1 760 cm^{-1} (C=O); *m/e* 145 (M^+), 71 ($C_3H_7CO^+$), and 43 (C_3H_7).

5-Undecyl-1,3,4-oxathiazol-2-one. This compound was prepared in 75% yield from dodecanamide and ClCOSCl; it had m.p. 37—38.5 °C (Found: C, 60.9; H, 9.2; N, 5.0. $C_{13}H_{23}NO_2S$ requires C, 60.7; H, 9.0; N, 5.4%); $\nu_{max.}$ (Nujol) 1 765 cm^{-1} (C=O); *m/e* 257 (M^+), 213 ($C_{11}H_{23}CNS^+$), and 183 ($C_{11}H_{23}CO^+$).

Synthesis of 1,3,4-Oxathiazoles (4).—The general method was to heat under reflux a solution of the 1,3,4-oxathiazol-2-one and the carbonyl compound (5 mol per mol of oxathiazolone) in dry xylene, as described below for 5-(*p*-chlorophenyl)-2-phenyl-2-trifluoromethyl-1,3,4-oxathiazole. The reaction was continued until h.p.l.c. analysis showed that all the starting material had been consumed. After evaporation under reduced pressure to remove the solvent and excess dipolarophile, the oxathiazole was separated from nitrile and sulphur by-products by distillation and/or recrystallisation.

5-(p-Chlorophenyl-2-phenyl-2-trifluoromethyl-1,3,4-oxathiazole. A mixture of 5-(*p*-chlorophenyl)-1,3,4-oxathiazol-2-one (2.0 g, 9.4 mmol) and α,α,α-trifluoroacetophenone (8.2 g, 47 mmol) in dry xylene (50 ml) was heated under reflux until h.p.l.c. analysis indicated complete consumption of the oxathiazolone (12.5 h). The solvent and excess trifluoroacetophenone were removed under reduced pressure to leave a yellow oil, from which 4-chlorobenzonitrile (0.52 g, 65%) was isolated by vacuum distillation (80 °C, 0.003 mmHg). On dissolving the residue in hexane and cooling, a pale yellow solid was formed which, after treatment with charcoal and recrystallisation from hexane, afforded 5-(*p*-chlorophenyl)-2-phenyl-2-trifluoromethyl-1,3,4-oxathiazole (0.30 g, 18%) as white crystals, m.p. 77 °C (Found: C, 52.4; H, 2.6; N, 4.0. $C_{15}H_9ClF_3NOS$ requires C, 52.4; H, 2.6; N, 4.1%); $\nu_{max.}$ (Nujol) 1 625 cm^{-1} (C=N); δ_H ($CDCl_3$, Me_4Si) 7.84 (d, 2 H, *J* 8.5 Hz, ArH), 7.2—7.5 (m, 7 H, ArH); *m/e* 345 and 343 (M^+), 276 and 274 ($[M - CF_3]^+$), 171 and 169 ($ClC_6H_4CNS^+$), 139 and 137 ($ClC_6H_4CN^+$).

2,2-Bis(trichloromethyl)-5-(p-chlorophenyl)-1,3,4-oxathiazole. After a reaction period of 28 h this compound (35%), together with 4-chlorobenzonitrile (58%), was obtained as white crystals, m.p. 104.5 °C (from hexane, charcoal) (Found: C, 27.5; H, 0.9; N, 3.2. $C_{10}H_4Cl_7NOS$ requires C, 27.6; H, 0.9; N, 3.2%); $\nu_{max.}$ (Nujol) 1 625 cm^{-1} (C=N); δ_H ($CDCl_3$, Me_4Si) 7.84 (d, 2 H, *J* 8.5 Hz, ArH), and 7.40 (d, 2 H, *J* 8.5 Hz, ArH); *m/e* 433, 431, 429 and 427 (M^+), 314, 312 and 310 [(M — CCl_3)$^+$], and 165 ($ClC_6H_4CN^+$).

5-Phenyl-2-trichloromethyl-1,3,4-oxathiazole. After a reaction period of 26 h this compound was obtained (59%) as white crystals, m.p. 67—68 °C (from hexane, charcoal) (Found: C, 38.1; H, 2.1; N, 5.0. $C_9H_6Cl_3NOS$ requires C, 38.3; H, 2.1; N, 5.0%); $\nu_{max.}$ (Nujol) 1 615 cm^{-1} (C=N); δ_H ($CDCl_3$, Me_4Si) 7.3—8.2 (m, 5 H, PhH) and 6.44 (s, 1 H, $CHCCl_3$); *m/e* 285, 283 and 281 (M^+), 166 and 164 ([M — CCl_3]$^+$), 135 ($PhCNS^+$), 105 ($PhCO^+$), 103 ($PhCN^+$), and 77 (Ph^+).

2,2-Bis(trichloromethyl)-5-phenyl-1,3,4-oxathiazole. After a reaction period of 8 h this compound was obtained (64%) as white needles, m.p. 53—54 °C (from hexane) (Found: C,

29.8; H, 1.2; N, 3.4. $C_{10}H_5Cl_6NOS$ requires C, 30.0; H, 1.3; N, 3.5%); $\nu_{max.}$ (Nujol) 1 630 cm^{-1} (C=N); δ_H ($CDCl_3$, Me_4Si) 7.4—8.1 (m, 5 H, PhH); *m/e* 403, 401, 399 and 397 (M^+), 284, 282 and 280 ($[M - CCl_3]^+$), 135 ($PhCNS^+$), 105 ($PhCO^+$), 103 ($PhCN^+$), and 77 (Ph^+).

5-(p-Methoxyphenyl)-2-trichloromethyl-1,3,4-oxathiazole. After a reaction period of 5 h this compound was obtained (76%) as white crystals, m.p. 82—83 °C (from hexane) (Found: C, 38.5; H, 2.6; N, 4.4. $C_{10}H_8Cl_3NO_2S$ requires C, 38.4; H, 2.6; N, 4.5%); $\nu_{max.}$ (Nujol) 1 615 cm^{-1} (C=N); δ_H ($CDCl_3$ Me_4Si) 7.83 (d, 2 H, *J* 9 Hz, ArH), 6.88 (d, 2 H, *J* 9 Hz, ArH), 6.43 (s, 1 H, $CHCCl_3$), and 3.80 (s, 3 H, OMe); *m/e* 315, 313 and 311 (M^+), 194 ($[M - CCl_3]^+$), 165 ($MeOC_6H_4CNS^+$), 135 ($MeOC_6H_4CO^+$), and 133 ($MeOC_6H_4CN^+$).

2,2-Bis(trichloromethyl)-5-(p-methoxyphenyl)-1,3,4-oxathiazole. After a reaction period of 5 h this compound was obtained in 57% yield and purified by chromatography (silica–hexane), m.p. 87—88 °C (from hexane) (Found: C, 31.0; H, 1.7; N, 3.2. $C_{11}H_7Cl_6NO_2S$ requires C, 30.7; H, 1.6; N, 3.3%); $\nu_{max.}$ (Nujol) 1 620 cm^{-1} (C=N); δ_H ($CDCl_3$, Me_4Si) 7.86 (d, 2 H, *J* 9 Hz, ArH), 6.92 (d, 2 H, *J* 9 Hz, ArH), and 3.82 (s, 3 H, OMe); *m/e* 433, 431, 429 and 427 (M^+), 314, 312 and 310 ($[M - CCl_3]^+$), 165 ($MeOC_6H_4CNS^+$), 135 ($MeOC_6H_4CO^+$), and 133 ($MeOC_6H_4CN^+$).

5-(p-Methoxyphenyl)-2-phenyl-2-trifluoromethyl-1,3,4-oxathiazole. After a reaction period of 4 h this compound (28%), together with 4-methoxybenzonitrile (59%), was obtained as white crystals, m.p. 86—87 °C (from hexane) (Found: C, 56.4; H, 3.5; N, 4.0. $C_{16}H_{12}F_3NO_2S$ requires C, 56.6; H, 3.6; N, 4.1%); $\nu_{max.}$ (Nujol) 1 620 cm^{-1} (C=N); δ_H ($CDCl_3$, Me_4Si) 7.89 (d, 2 H, *J* 9 Hz, ArH), 7.3—7.5 (m, 5 H, PhH), 6.91 (d, 2 H, *J* 9 Hz, ArH), and 3.81 (s, 3 H, OMe); *m/e* 339 (M^+), 270 ($[M - CF_3]^+$), 165 ($MeOC_6H_4CNS^+$), 135 ($MeOC_6H_4CO^+$), and 133 ($MeOC_6H_4CN^+$).

5-Methyl-2-trichloromethyl-1,3,4-oxathiazole. After a reaction period of 5 h this compound was obtained (62%) as white crystals, m.p. 44.5—50 °C (from hexane, charcoal) (Found: C, 21.5; H, 1.7; N, 6.2. $C_4H_4Cl_3NOS$ requires C, 21.8; H, 1.8; N, 6.3%); $\nu_{max.}$ (Nujol) 1 650 cm^{-1} (C=N); δ_H ($CDCl_3$, Me_4Si) 6.30 (s, 1 H, $CHCCl_3$), and 2.12 (s, 3 H, Me); *m/e* 223, 221 and 219 (M^+), 102 ($[M - CCl_3]^+$), 73 ($MeCNS^+$), 43 ($MeCO^+$), and 41 ($MeCN^+$).

2,2-Bis(trichloromethyl)-5-methyl-1,3,4-oxathiazole. After a reaction period of 6 h this compound was obtained (56%) as white needles, m.p. 70 °C (from hexane) (Found: C, 17.5; H, 0.9; N, 3.9. $C_5H_3Cl_6NOS$ requires C, 17.8; H, 0.9; N, 4.1%); $\nu_{max.}$ (Nujol) 1 655 cm^{-1} (C=N); δ_H ($CDCl_3$, Me_4Si) 2.23 (s, 3 H, Me); 341, 339, 337 and 335 (M^+), 218 ($[M - CCl_3]^+$), 73 ($MeCNS^+$), 43 ($MeCO^+$), and 41 ($MeCN^+$).

2,2-Bis(trichloromethyl)-5-propyl-1,3,4-oxathiazole. After a reaction period of 5 h this compound was obtained (44%) as a colourless oil, b.p. 135 °C at 0.003 mmHg (Found: C, 22.7; H, 1.6; N, 3.7. $C_6H_7Cl_6NOS$ requires C, 23.0; H, 1.9; N, 3.8%); $\nu_{max.}$ (film) 1 655 cm^{-1} (C=N); δ_H ($CDCl_3$, Me_4Si) 2.43 (t, 2 H, CH_2), 1.6—1.9 (m, 2 H, CH_2), and 1.00 (t, 3 H, Me); *m/e* 339, 337, 335 and 333 (M^+), 101 ($PrCNS^+$).

2-Trichloromethyl-5-undecyl-1,3,4-oxathiazole. After a reaction period of 6.5 h this compound was obtained as a pale yellow oil (60%) and purified by chromatography (silica–hexane) (Found: *m/e* 359.065 016. $C_{16}H_{26}{}^{35}Cl_3NOS$ requires *M*, 359.064 412); $\nu_{max.}$ (film) 1 650 cm^{-1} (C=N); δ_H ($CDCl_3$, Me_4Si) 6.28 (s, 1 H, $CHCCl_3$), 2.40 (t, 2 H, CH_2), 1.6—1.8 (m, 2 H, CH_2), 1.1—1.6 (m, 16 H, CH_2), and 0.87 (t, 3 H, Me); *m/e* 363, 361 and 359 (M^+), 242 ($[M - CCl_3]^+$). An attempted distillation of the product at 175 °C/0.003 mmHg yielded a pale yellow oil; i.r. spectroscopy indicated that it contained some nitrile, $\nu_{max.}$ (film) 2 210 cm^{-1} (C=N), arising from the thermal fragmentation of the oxathiazole.[7]

2,2-Bis(trichloromethyl)-5-undecyl-1,3,4-oxathiazole. After a reaction period of 7 h this compound was obtained as a pale yellow oil (31%) and purified by chromatography (silica–hexane) (Found: *m/e* 474.963 078. $C_2H_2{}^{35}Cl_6NOS$ requires *M* 474.963 146); $\nu_{max.}$ (film) 1 655 cm^{-1} (C=N); δ_H ($CDCl_3$, Me_4Si) 2.50 (t, 2 H, CH_2), 1.9—1.6 (m, 2 H, CH_2), 1.1—1.5 (m, 16 H, CH_2) and 0.87 (t, 3 H, Me); *m/e* 481, 479, 477 and 475 (M^+), 362 and 360 ($[M - CCl_3]^+$). An attempted distillation of the product at 170—180 °C/0.003 mmHg yielded a yellow oil; i.r. spectroscopy indicated that it contained some nitrile, $\nu_{max.}$ (film) 2 210 cm^{-1} (C=N), arising from the thermal fragmentation of the oxathiazole.[7]

X-Ray Crystal Structure Analysis of 5-Phenyl-2-trichloromethyl-1,3,4-oxathiazole (4A) *and 5-(p-Methoxyphenyl)-2-phenyl-2-trifluoromethyl-1,3,4-oxathiazole* (4B).—Crystallisation of (4A) from hexane gave monoclinic needles, elongated along *c*, and of (4B) from hexane gave monoclinic prisms.

Crystal Data for (4A).—$C_9H_6Cl_3NOS$, $M = 282.6$, monoclinic, $a = 11.507(8)$, $b = 9.356(2)$, $c = 10.560(9)$ Å, $\beta = 78.54(1)°$, $U = 1\,114.2$ Å^3, $D_m = 1.65$ g cm^{-3}, $Z = 4$, $D_c = 1.68$ g cm^{-3}, space group $P2_1/c$ (by systematic absences), Mo-K_α radiation (graphite monochromatised) $\lambda = 0.710\,69$ Å, μ(Mo-K_α) = 9.7 cm^{-1}. Dimensions of crystal used for intensity data 0.2 × 0.2 × 0.7 mm.

Crystal Data for (4B).—$C_{16}H_{12}F_3NO_2S$, $M = 339.3$, monoclinic, $a = 12.282(5)$, $b = 7.311(2)$, $c = 17.181(7)$ Å, $\beta = 105.89(3)°$, $U = 1\,483.8$ Å^3, $D_m = 1.52$ g cm^{-3}, $Z = 4$, $D_c = 1.52$ g cm^{-3}, space group $P2_1/c$ (by systematic absences), Mo-K_α radiation (graphite monochromatised), $\lambda = 0.710\,69$ Å, μ(Mo-K_α) = 2.6 cm^{-1}. Dimensions of crystal used for intensity data 0.15 × 0.20 × 0.25 mm.

After preliminary oscillation and Weissenberg photographs each crystal was mounted on the Stadi-2 diffractometer with *b* along the spindle; cell dimensions were refined and the intensity data recorded using an ω scan and $\theta_{max.} = 25°$. In each case two unique sets of reflections were recorded and subsequently averaged after Lp correction.

Both structures were solved by direct methods using the MULTAN system [12] and refined by least-squares using the XRAY system; [13] difference Fourier maps confirmed the presence of hydrogen atoms at the stereochemically expected positions. In the final cycles, positional parameters were refined for hydrogen atoms but their thermal parameters were fixed at $U = 0.06$ Å^2; positional and anisotropic thermal parameters were refined for all other atoms. Unit weights were used in (4B) and a weighting scheme dependent on both $|F_{obs.}|$ and sin θ in (4A).

The atomic scattering factors in the XRAY system were used. *R* Converged to 0.044 for 1 588 reflections with $I > 2\sigma(I)$ for (4A) and 0.043 for 1 223 reflections for (4B).

Positional parameters for atoms other than hydrogen are given in Table 3. The molecules (and atom numbering) are illustrated in Figure 1 (drawn by the programme PLUTO [14]), and selected bond lengths and angles in Figure 2. All positional and thermal parameters are deposited as supplementary publication No. SUP No. 23145 (28 pages).*

* For details of the Supplementary Publications Scheme see Notice to Authors No. 7, *J. Chem. Soc., Perkin Trans. 1*, 1980, Index issue.

TABLE 3

Fractional co-ordinates for atoms other than hydrogen, with their standard deviations.

Atom	*x*	*y*	*z*
(*a*) for compound (4A)			
O(1)	0.438 1(2)	0.410 7(3)	0.297 8(3)
C(2)	0.396 4(3)	0.273 3(4)	0.273 6(4)
S(3)	0.488 8(1)	0.148 8(1)	0.340 0(1)
N(4)	0.583 8(3)	0.280 8(4)	0.359 7(4)
C(5)	0.545 4(3)	0.401 8(4)	0.334 4(3)
C(6)	0.605 2(3)	0.539 4(4)	0.335 5(3)
C(7)	0.699 9(3)	0.552 0(5)	0.398 0(4)
C(8)	0.760 9(4)	0.677 7(7)	0.392 0(5)
C(9)	0.731 3(5)	0.792 2(7)	0.325 5(5)
C(10)	0.638 2(5)	0.782 8(6)	0.263 2(5)
C(11)	0.574 9(4)	0.656 8(5)	0.270 0(4)
C(21)	0.402 4(3)	0.255 0(4)	0.130 0(4)
Cl(211)	0.308 9(1)	0.384 4(1)	0.080 6(1)
Cl(212)	0.545 7(1)	0.280 7(1)	0.042 6(1)
Cl(213)	0.352 8(1)	0.082 0(1)	0.102 2(1)
(*b*) for compound (4B)			
O(1)	0.738 6(2)	0.335 7(5)	0.715 4(2)
C(2)	0.825 1(4)	0.350 4(8)	0.790 4(3)
S(3)	0.951 2(1)	0.421 1(3)	0.760 7(1)
N(4)	0.882 6(3)	0.418 9(7)	0.661 4(2)
C(5)	0.779 6(4)	0.374 3(7)	0.650 5(3)
C(6)	0.696 0(4)	0.360 4(6)	0.571 9(3)
C(7)	0.719 8(4)	0.429 1(7)	0.502 8(3)
C(8)	0.643 6(4)	0.411 4(9)	0.428 8(3)
C(9)	0.540 8(4)	0.324 2(7)	0.421 0(3)
C(10)	0.514 7(4)	0.257 4(7)	0.489 2(3)
C(11)	0.592 3(4)	0.277 6(7)	0.564 3(3)
C(21)	0.838 7(5)	0.159 4(8)	0.825 2(3)
F(211)	0.746 5(3)	0.099 1(5)	0.841 5(2)
F(212)	0.865 7(3)	0.040 0(5)	0.775 3(2)
F(213)	0.923 0(3)	0.153 2(5)	0.893 8(2)
C(22)	0.789 7(4)	0.479 6(7)	0.847 2(3)
C(221)	0.870 6(5)	0.570 5(9)	0.905 9(3)
C(222)	0.838 7(7)	0.688 4(10)	0.957 3(4)
C(223)	0.726 0(7)	0.718 4(9)	0.950 8(4)
C(224)	0.645 6(6)	0.627 9(9)	0.893 3(4)
C(225)	0.677 2(5)	0.506 7(8)	0.841 5(3)
O(91)	0.471 6(3)	0.311 8(5)	0.344 5(2)
C(911)	0.370 0(6)	0.212 7(9)	0.332 7(4)

We are grateful to the Edinburgh Regional Computing Centre for their co-operation, the S.R.C. for research and maintenance (J. F. R.) grants, and INVOTAN, Portugal for a research studentship (A. M. D.).

[1/743 *Received*, 11*th May*, 1981]

REFERENCES

[1] Preliminary report, R. M. Paton, J. F. Ross, and J. Crosby, *J. Chem. Soc., Chem. Commun.*, 1979, 1146.
[2] C. Grundmann and P. Grünanger, 'The Nitrile Oxides,' Springer-Verlag, West Berlin and Heidelberg, 1971, Ch. 5, p. 85.
[3] T. Sasaki and T. Yoshioka, *Bull. Chem. Soc. Jpn.*, 1968, **41**, 2206; R. Huisgen and W. Mack, *Chem. Ber.*, 1972, **105**, 2805.
[4] H. Nohira, K. Inoue, H. Hattori, T. Okawa, and T. Mukaiyama, *Bull. Chem. Soc. Jpn.*, 1967, **40**, 664; E. Schmitz and S. Schramm, *Chem. Ber.*, 1967, **100**, 2593.
[5] R. K. Howe, T. A. Gruner, L. G. Carter, L. L. Black, and J. E. Franz, *J. Org. Chem.*, 1978, **43**, 3736.
[6] J. R. Grunwell and S. L. Dye, *Tetrahedron Lett.*, 1975, 1739; R. K. Howe and J. E. Franz, *J. Org. Chem.*, 1978, **43**, 3742; M. J. Sanders and J. R. Grunwell, *J. Org. Chem.*, 1980, **45**, 3753; R. M. Paton, J. F. Ross, and J. Crosby, *J. Chem. Soc., Chem. Commun.*, 1980, 1194.
[7] R. K. Howe and J. E. Franz, *J. Org. Chem.*, 1974, **39**, 962.
[8] M. Haake, B. Eichenauer, and K. H. Ahrens, *Z. Naturforsch.* (*B*), 1974, **29**, 284; E. M. Burgess and H. R. Penton, *J. Org. Chem.*, 1974, **39**, 2885.
[9] A. Selva, A. Citterio, E. Pella, and R. Tonani, *Org. Mass. Spectrom.*, 1974, **9**, 1017.
[10] A. Senning and P. Kelly, *Acta Chem. Scand.*, 1967, **21**, 1871.
[11] B.P. 1 079 348/1967.
[12] P. Main, L. Lessinger, M. M. Woolfson, G. Germain, and J. P. Declercq, 'MULTAN. A System of Computer Programs for the Automatic Solution of Crystal Structures from X-Ray Diffraction Data,' Univs. of York, England, and Louvain, Belgium, 1977.
[13] J. M. Stewart, P. A. Machin, C. Dickinson, H. L. Ammon, H. Heck, and H. Flack, 'The X-RAY '76 System,' Tech. Rep. TR-446. Computer Science Center, University of Maryland, U.S.A., 1976.
[14] 'PLUTO, A Program for Plotting Molecular and Crystal Structures,' W. D. S. Motherwell, University Chemical Laboratory, Cambridge, England.

Reprinted from *J.Mol. Biol.* (1981) **153**, 831–835

Cytochrome c_4 from *Pseudomonas aeruginosa*

L. Sawyer, C. L. Jones, A. M. Damas, M. M. Harding
R. O. Gould and R. P. Ambler

J. Mol. Biol. (1981) **153**, 831–835

Cytochrome c_4 from *Pseudomonas aeruginosa*

The dihaem cytochrome c_4 from *Pseudomonas aeruginosa* has been crystallized in space group $P6_522$ with cell dimensions $a = b = 62{\cdot}4$ Å, $c = 174{\cdot}2$ Å, and one molecule per asymmetric unit. Two heavy-atom derivatives, $UO_2(NO_3)_2$ and $K_2Pt(NO_2)_4$, which substitute at one and three sites, respectively, have allowed a low-resolution electron density map to be obtained. This shows clearly the two domains of the molecule.

Cytochromes *c*, proteins with a covalently bound haem prosthetic group, are found widely distributed in nature, are easy to isolate and, as a consequence, have been a prime subject for comparative investigations of both amino acid sequence and tertiary structure. The comparisons that have been made have provided evidence for the classification of the many varied cytochromes *c* of bacterial origin (Ambler, 1981). and the fact that the sequence variation of eukaryotic cytochrome *c* from many organisms correlates well with the phylogeny derived from morphological evidence (Fitch & Margoliash, 1970) has led to the use of both sequence and three-dimensional structural information to propose a bacterial phylogenetic tree based on the prokaryotic cytochromes *c* of class I (Dickerson, 1980). High-potential cytochrome *c* is involved in electron transport both in respiration and in photosynthesis but, whereas in mitochondrial respiration the electrons are used to reduce oxygen to water with the concomitant production of ATP, bacteria are less specialized and some can utilize nitrate, for example, in place of oxygen. One such nitrate respiring bacterium is *Pseudomonas aeruginosa*, which is capable of producing at least five distinct cytochromes *c*, although not all are members of class I (Ambler, 1981). Of these, cytochrome c_{551} has had its tertiary structure determined (Almassy & Dickerson, 1978) and has been sequenced from many bacterial sources (Dayhoff, 1979). The cytochrome *cd* that is also known as nitrite reductase and cytochrome oxidase, has been crystallized and is now the subject of X-ray crystallographic analysis (Takano *et al.*, 1979). Cytochrome *c* peroxidase has also been purified (Soininen *et al.*, 1973; Coulson & Oliver, 1979), although no real structural information is available other than molecular weight and amino acid composition. A cytochrome c_5 has been partially sequenced (Ambler & Taylor, 1973) and an X-ray analysis of the protein isolated from another denitrifying bacterium, *Azotobacter vinelandii*, is currently in progress (Stout, 1978). Whilst no cytochrome *c'* has yet been found in *P. aeruginosa* it occurs in *A. vinelandii*, which appears to have a similar complement of electron transport proteins; it may also be present in *P. aeruginosa*. We report here the crystallization and low-resolution structure of another cytochrome from *P. aeruginosa*.

Cytochrome c_4 is a dihaem, high-potential cytochrome of molecular weight 19,000, which was characterized first by Neumann & Burris (1959) from *A.*

0022–2836/81/350831–05 $02.00/0

vinelandii and by Kodama & Shidara (1969) from *Pseudomonas stutzeri*. Ambler (1981) has reported the near-complete sequence of 181 residues, from which it can be seen that the protein appears to be two "short" (Dickerson, 1980) molecules joined covalently. The cytochrome c_4 is closely related to that from *A. vinelandii* (R. P. Ambler, unpublished results) and also each "half" is similar in sequence to that of c_{554} from the halotolerant bacterium *Paracoccus* ATCC12084 (see Dickerson, 1980). There is, indeed, more homology between c_{554} and c_4 than there is between the two halves of the latter protein. Although the exact function of c_4 is unknown, it is produced in significant but variable quantities together with c_{551} and azurin when *P. aeruginosa* is grown anaerobically. These observations led us to wonder if there was some subtle yet significant difference between the c_4 and c_{551} structures, between the two halves, and if there was some interaction between the two haems. The redox potentials of the two proteins are similar (Lemberg & Barrett, 1973) and, although there is a small difference in the α-band, the binding of the haems must be very similar. In order to seek the answer to these questions, together with the extra insight into the "cytochrome fold" afforded by *two* structures, which should help in limiting the search for the mechanism of electron transfer (Winfield, 1965; Takano *et al.*, 1973; Salemme *et al.*, 1973; Salemme, 1976; Poulos & Kraut, 1980), we began a study of the crystal structure of cytochrome c_4 from *Pseudomonas aeruginosa*.

The protein from the neotype strain of *P. aeruginosa*, NCTC 10332, was isolated from acetone-dried cells by the procedure of Ambler & Wynn (1973) as modified by Coulson & Oliver (1979). A solution of the cytochrome was concentrated to about 1 mg ml^{-1} by elution from CM-cellulose equilibrated in 50 mM-ammonium acetate (pH 5·01), with a 0·1 M solution of the same buffer, pH 7·0. This concentrated solution was precipitated by the addition of finely divided $(NH_4)_2SO_4$ to 80% saturation. After spinning down the precipitate, it was resuspended in a minimum quantity of 50 mM-ammonium acetate (pH 6·0), from which suspension hexagonal bipyramidal crystals grew at 4°C over a period of one to three days. The crystals were transferred to a stock solution of 2 M-$(NH_4)_2SO_4$, 50 mM-ammonium acetate (pH 6), in which they are quite stable at temperatures from 4 to 22°C.

X-ray diffraction spectra recorded by precession camera revealed 6-fold symmetry for both *hk*0 and *hk*1 zones, establishing a 6-fold rotation axis whilst the 0*kl* and *hhl* zones showed mm symmetry. Further, the 00*l* reflections were only present for $l = 6n$ and, in consequence, the space group was determined as $P6_122$ ($P6_522$). The cell dimensions are $a = b = 62{\cdot}4(1)$ Å, $c = 174{\cdot}2(1)$ Å, $\gamma = 120°$. The molecular weight calculated from the sequence is about 19,000, and this gives a value of 2·57 $Å^3$/dalton (Matthews, 1968) for 12 molecules per unit cell. Since this is well within the range found for proteins of similar size, we felt confident that there is one molecule per asymmetric unit. The next permissible number, 2, yields a highly improbable V_M value, which is not consistent with the observed density of the crystals of 1·22 g cm^{-3}.

Space group $P6_122$ possesses three centric zones, two of which, the 0*kl* and *hhl*, allow all three co-ordinates of an atom to be obtained from a Patterson synthesis. The structure of thermolysin (Colman *et al.*, 1972) was successfully determined in this way, and so a similar procedure was tried here. Crystals were soaked in heavy

metal complex solutions; the diffraction spectra of those showing unaltered cell dimensions and small intensity changes at medium resolution were scanned on an Optronix P-1000 scanner and syntheses with coefficients $(|F_{PH}|-|F_P|)^2$ were calculated. The various vector sets obtained were never totally convincing, and all failed to refine satisfactorily either by the method of Hart (1961) or by least-squares (Lipscomb *et al.*, 1966). Three-dimensional data for both native and the more promising derivatives were collected to 5 Å resolution on an Enraf-Nonius CAD4 diffractometer with a crystal to counter aperture distance of 368 mm. At this distance the peaks along the *c*-axis were adequately resolved by an ω-scan. The crystal decay was no more than 10% during data collection, which routinely measured some 3500 reflections per set. After correction for Lorentz and polarization effects and absorption (North *et al.*, 1968), there were about 1650 unique reflections, of which 85% had $I > 3\sigma(I)$. Of the six derivative sets collected from crystals soaked for 24 hours in 1 mM solutions of $K_2Pt(NO_2)_4$, $KAu(CN)_2$, dimercury acetic acid, *p*-chloromercuribenzene sulphonic acid, mersalyl and $UO_2(NO_3)_2$, the UO_2^{2+} was solved from an $|F_{HLE}|^2$ synthesis (Harding, 1962: Blundell & Johnson, 1976) yielding a single site close to the dyad at $z = \pm 1/12$. Phases calculated from the refined UO_2^{2+} position allowed a different Fourier of the $Pt(NO_2)_4^{2-}$ derivative to be interpreted in terms of three sites, each consistent with the $(F_{HLE})^2$ synthesis, although some peaks in the latter map remained unexplained. The refined sites are shown in Table 1. The cross-difference Fourier technique (see Blundell & Johnson, 1976) showed slightly but consistently higher peaks for the heavy atoms in $P6_522$ as compared to $P6_122$, thus indicating the former as the more probable space group. Figure 1 shows the electron density map plotted on plastic sheets perpendicular to the *z*-axis at a separation of 1·45 Å. The zero and negative contours have been omitted, and the Figure shows clearly the two-domain structure of cytochrome c_4 occupying a volume of about 60 Å × 30 Å × 35 Å, which compares very favourably with the size expected from two monohaem cytochromes. The haem group in the upper lobe is shown clearly, that in the lower lobe (below and to the left) is less distinct. Data collection is in progress and a medium-resolution map should be available in the near future.

TABLE 1

Heavy-atom parameters for cytochrome c_4

Derivative	Site	*x*	*y*	*z*	Occupancy	*R*(%)†	Slope‡
$UO_2(NO_3)_2$	1§	0·480	0·225	−0·077	0·32	53·9	0·32
$K_2Pt(NO_2)_4$	1	0·701	0·977	0·022	0·42		
	2	0·807	0·338	0·037	0·15	56·5	0·27
	3	0·383	0·489	0·027	0·11		

The temperature factors were held constant at 15 $Å^{-2}$. The overall figure of merit was $m = 0·74$.

† The *R* factor is defined as $\Sigma||F_{HLE}|-|F_{Hcalc}||/\Sigma|F_{HLE}|$.

‡ The slope is the slope of $[<F_H^{calc}>^2]^{1/2}$ *versus* $|(k|F_{PH}|-|F_P|)|$ (Dodson, 1976).

§ The uranium site is that for an atom in a general position just off the dyad axis, and the occupancy refers to this general position.

metal complex solutions; the diffraction spectra of those showing unaltered cell dimensions and small intensity changes at medium resolution were scanned on an Optronix P-1000 scanner and syntheses with coefficients $(|F_{PH}|-|F_P|)^2$ were calculated. The various vector sets obtained were never totally convincing, and all failed to refine satisfactorily either by the method of Hart (1961) or by least-squares (Lipscomb *et al.*, 1966). Three-dimensional data for both native and the more promising derivatives were collected to 5 Å resolution on an Enraf-Nonius CAD4 diffractometer with a crystal to counter aperture distance of 368 mm. At this distance the peaks along the *c*-axis were adequately resolved by an ω-scan. The crystal decay was no more than 10% during data collection, which routinely measured some 3500 reflections per set. After correction for Lorentz and polarization effects and absorption (North *et al.*, 1968), there were about 1650 unique reflections, of which 85% had $I > 3\sigma(I)$. Of the six derivative sets collected from crystals soaked for 24 hours in 1 mM solutions of $K_2Pt(NO_2)_4$, $KAu(CN)_2$, dimercury acetic acid, *p*-chloromercuribenzene sulphonic acid, mersalyl and $UO_2(NO_3)_2$, the UO_2^{2+} was solved from an $|F_{HLE}|^2$ synthesis (Harding, 1962: Blundell & Johnson, 1976) yielding a single site close to the dyad at $z = \pm 1/12$. Phases calculated from the refined UO_2^{2+} position allowed a different Fourier of the $Pt(NO_2)_4^{2-}$ derivative to be interpreted in terms of three sites, each consistent with the $(F_{HLE})^2$ synthesis, although some peaks in the latter map remained unexplained. The refined sites are shown in Table 1. The cross-difference Fourier technique (see Blundell & Johnson, 1976) showed slightly but consistently higher peaks for the heavy atoms in $P6_522$ as compared to $P6_122$, thus indicating the former as the more probable space group. Figure 1 shows the electron density map plotted on plastic sheets perpendicular to the *z*-axis at a separation of 1·45 Å. The zero and negative contours have been omitted, and the Figure shows clearly the two-domain structure of cytochrome c_4 occupying a volume of about 60 Å × 30 Å × 35 Å, which compares very favourably with the size expected from two monohaem cytochromes. The haem group in the upper lobe is shown clearly, that in the lower lobe (below and to the left) is less distinct. Data collection is in progress and a medium-resolution map should be available in the near future.

TABLE 1

Heavy-atom parameters for cytochrome c_4

Derivative	Site	*x*	*y*	*z*	Occupancy	*R*(%)†	Slope‡
$UO_2(NO_3)_2$	1§	0·480	0·225	−0·077	0·32	53·9	0·32
$K_2Pt(NO_2)_4$	1	0·701	0·977	0·022	0·42		
	2	0·807	0·338	0·037	0·15	56·5	0·27
	3	0·383	0·489	0·027	0·11		

The temperature factors were held constant at 15 $Å^{-2}$. The overall figure of merit was $m = 0·74$.

† The *R* factor is defined as $\Sigma||F_{HLE}|-|F_{Hcalc}||/\Sigma|F_{HLE}|$.

‡ The slope is the slope of $[<F_H^{calc}>^2]^{1/2}$ *versus* $|(k|F_{PH}|-|F_P|)|$ (Dodson, 1976).

§ The uranium site is that for an atom in a general position just off the dyad axis, and the occupancy refers to this general position.

Department of Chemistry
Edinburgh University
Edinburgh, EH9 3JJ, U.K.

A. M. DAMAS
M. M. HARDING†
R. O. GOULD

Department of Molecular Biology
Edinburgh University
Edinburgh, EH9 3JJ, U.K.

R. P. AMBLER

Received 17 July 1981

REFERENCES

Almassy, R. J. & Dickerson, R. E. (1978). *Proc. Nat. Acad. Sci., U.S.A.* **75**, 2674–2678.
Ambler R. P. (1981). In *From Cyclotrons to Cytochromes* (Robinson, A. B. & Kaplan, N. O., eds), Academic Press, New York in the press.
Ambler, R. P. & Taylor, E. (1973). *Biochem. Soc. Trans.* **1**, 166–168.
Ambler, R. P. & Wynn, M. (1973). *Biochem. J.* **131**, 485–498.
Blundell, T. L. & Johnson, L. N. (1976). *Protein Crystallography*, Academic Press, London.
Colman, P. M., Jansonius, J. N. & Matthews, B. W. (1972). *J. Mol. Biol.* **70**, 701–724.
Coulson, A. F. W. & Oliver, R. K. (1979). *Biochem. J.* **181**, 159–169.
Dayhoff, M. O. (1979). Editor of *Atlas of Protein Sequence and Structure*, vol. 5, suppl. 3, Nat. Biomed. Res. Found., Washington.
Dickerson, R. E. (1980). *Sci. Amer. (March)*, 99–110.
Fitch, W. M. & Margoliash, E. (1970). *Evol. Biol.* **4**, 67–109.
Dodson, E. J. (1976). In *Crystallographic Computing Techniques* (Ahmed, F. R., ed.), pp. 259–268, Munksgaard, Copenhagen.
Harding, M. M. (1962). D.Phil. thesis, University of Oxford.
Hart, R. G. (1961). *Acta Crystallogr.* **14**, 1194–1196.
Kodama, T. & Shidara, S. (1969). *J. Biochem. (Tokyo)*, **65**, 351–360.
Lemberg, R. & Barrett, J. (1973). *Cytochromes*, Academic Press, London.
Lipscomb, W. N., Coppola, J. C., Hartsuck, J. A., Ludwig, M. L., Muirhead, H., Searl, J. & Steitz, T. A. (1966). *J. Mol. Biol.* **19**, 423–441.
Matthews, B. W. (1968). *J. Mol. Biol.* **33**, 491–497.
Neumann, N. P. & Burris, R. H. (1959). *J. Biol. Chem.* **234**, 2386–2390.
North, A. C. T., Phillips, D. C. & Mathews, F. S. (1968). *Acta Crystallogr. sect. A*, **24**, 351–355.
Poulos, T. L. & Kraut, J. (1980). *J. Biol. Chem.* **255**, 10322–10330.
Salemme, F. R. (1976). *J. Mol. Biol.* **102**, 563–568.
Salemme, F. R., Freer, S. T., Xuong, N. H., Alden, R. A. & Kraut, J. (1973). *J. Biol. Chem.* **248**, 3910–3921.
Soininen, R., Ellfolk, N. & Kalkkinen, W. (1973). *Acta Chem. Scand.* **27**, 1106–1107.
Stout, C. D. (1978). *J. Mol. Biol.* **126**, 105–108.
Takano, T., Kallai, O. B., Swanson, R. & Dickerson, R. E. (1973). *J. Biol. Chem.* **248**, 5234–5255.
Takano, T., Dickerson, R. E., Schichman, S. A. & Meyer, T. E. (1979). *J. Mol. Biol.* **133**, 185–188.
Winfield, M. E. (1965). *J. Mol. Biol.* **12**, 600–611.

Edited by A. Klug

† Present address: I.P.I. Chemistry Department, Liverpool University, P.O. Box 147, Liverpool L69 3BX, U.K.

FIG. 1. The electron density map at 5 Å resolution of cytochrome c_4 showing the 2 "halves" of the molecule. The parallel lines represent the dyad axes at $z = 1/12$, which are 31·2 Å apart ($a/2$). The 6_5 screw axis is seen as a series of circles to the right. The UO_2^{2+} site is shown as a square on the dyad. Only 1 asymmetric unit has been plotted in order to emphasize the molecular boundary which, for the most part, is well-defined. The electron density contours are at equal, arbitrary intervals.

We would like to thank Professor R. A. Cowley, Physics Department, Edinburgh University for the use of diffraction and computing facilities and Drs H. Watson and H. Muirhead, Bristol and Dr Mike Elder, Science Research Council Microdensitometer Service for help with film scanning. This work was supported by Science Research Council grant GR/A/0934.2 (to L.S.). One author (A.M.D.) is grateful to INVOTAN, Portugal for a studentship.

Department of Chemistry
Napier College
Edinburgh EH10 5DT, U.K.

L. SAWYER
C. L. JONES